AD-A285 496

Final Scientific Report

"INTERACTION OF ELECTROMAGNETIC FIELDS WITH MAGNETIZED PLASMAS"

Covering the Period
April 1, 1989 to March 31, 1994

by

J. Reece Roth, Principal Investigator
UTK Plasma Science Laboratory

AFOSR Contract 89-0319
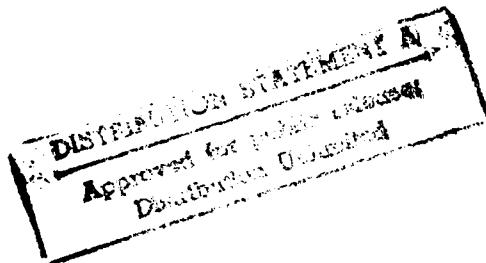
DTIC
ELECTE
OCT. 0 5 1994
S
B

94-31608

Dist: A

REPORT DOCUMENTATION PAGE

Form Approved
OMB No. 0704-0188

1a. REPORT SECURITY CLASSIFICATION	1b. RESTRICTIVE MARKINGS
Unclassified	None

2a. SECURITY CLASSIFICATION AUTHORITY	3. DISTRIBUTION/AVAILABILITY OF REPORT
N/A	Distribution unlimited
2b. DECLASSIFICATION/DOWNGRADING SCHEDULE	Approved for public release
N/A	A

4. PERFORMING ORGANIZATION REPORT NUMBER(S)	5. MONITORING ORGANIZATION REPORT NUMBER(S)
UTK-PSL 94-3	AFOSR-TR- 94 0594

6a. NAME OF PERFORMING ORGANIZATION	6b. OFFICE SYMBOL (If applicable)	7a. NAME OF MONITORING ORGANIZATION
UTK Plasma Science Laboratory	ECE Dept.	AFOSR/NE (Dr. Robert J. Barker)

6c. ADDRESS (City, State, and ZIP Code)	7b. ADDRESS (City, State, and ZIP Code)
Room 101 Ferris Hall Department of Electrical Engineering 37996- University of Tennessee, Knoxville, TN 2100	110 Duncan Avenue Bolling Air Force Base, Bldg. 410, Rm B115 Washington, DC 20332-0001

8a. NAME OF FUNDING/SPONSORING ORGANIZATION	8b. OFFICE SYMBOL (If applicable)	9. PROCUREMENT INSTRUMENT IDENTIFICATION NUMBER
AFOSR	NE	Grant AFOSR-89-0319

8c. ADDRESS (City, State, and ZIP Code)	10. SOURCE OF FUNDING NUMBERS			
110 Duncan Ave. Bolling Air Force Base, Bldg. 410, Rm B115 Washington, DC 20332-0001	PROGRAM ELEMENT NO.	PROJECT NO.	TASK NO	WORK UNIT ACCESSION NO.
	61102F	2301	A7	----

11. TITLE (Include Security Classification)
"Interaction of Electromagnetic Fields with Magnetized Plasmas" - UNCLASSIFIED

12. PERSONAL AUTHOR(S)
J. Reece Roth, Principal Investigator

13a. TYPE OF REPORT	13b. TIME COVERED	14. DATE OF REPORT (Year, Month, Day)	15. PAGE COUNT
Final Scientific	FROM 4/1/89 TO 3/31/94	1994, September 7	

16. SUPPLEMENTARY NOTATION

17. COSATI CODES			18. SUBJECT TERMS (Continue on reverse if necessary and identify by block number)
FIELD	GROUP	SUB-GROUP	physics, plasma, plasma turbulence, RF plasma interactions,
20	.09		plasma absorption, radar absorption, RF plasma absorption,
			RF plasma emission, plasma cloaking, one atmosphere plasma

19. ABSTRACT (Continue on reverse if necessary and identify by block number)

This Final Scientific Report describes research at the UTK Plasma Science Laboratory which was supported by the Air Force Office of Scientific Research, contract AFOSR #89-0319, with Dr. Robert J. Barker, Program Manager. Eight archival scientific papers were published, 19 oral or poster conference papers were presented at the annual APS and IEEE plasma meetings, and one patent was obtained and two additional patents were filed for. This contract also supported three graduate theses, including partial support for one Ph.D. dissertation, and two Master of Science in Electrical Engineering theses. This contract additionally supported approximately eight person-years of half time GRA research and training, and the preparation of nine routine reports to the Air Force. This contract also supported Professor Shenggang Liu, UTK's first Visiting Distinguished Professor, for a period of one year.

The contract has supported several major research activities. These include: 1) The writing up for archival publication results from the previous Air Force contract, relating

20. DISTRIBUTION/AVAILABILITY OF ABSTRACT	21. ABSTRACT SECURITY CLASSIFICATION
☐ UNCLASSIFIED/UNLIMITED ☒ SAME AS RPT ☐ DTIC USERS	UNCLASSIFIED-Distribution Unlimited

22a. NAME OF RESPONSIBLE INDIVIDUAL	22b. TELEPHONE (Include Area Code)	22c. OFFICE SYMBOL
Dr. Robert J. Barker	(202) 767-5011	AFOSR/NE

DD Form 1473, JUN 86   Previous editions are obsolete.

Block No. 19

to plasma turbulence and plasma heating by collisional magnetic pumping; 2) Theoretica,
computational, and experimental investigation of the interaction of microwave radiation with
cylindrical plasmas, particularly in the vicinity of the electron cyclotron frequency;
3) investigation of cyclotron damping near the electron gyrofrequency of magnetized plasmas
as a method for plasma cloaking of earth satellites and spacecraft; 4) development of a
parallel plate one atmosphere glow discharge plasma reactor, allowing the production of a
uniform plasma at one atmosphere; and 5) development of a method for covering the surface
of an aircraft or other body in the atmosphere with a thin layer of plasma for cloaking or
boundary layer control.

Accession For

NTIS G &I ☑
DTIC TAB ☐
Unannounced ☐
Justification

By
D

A-1

Final Scientific Report

INTERACTION OF ELECTROMAGNETIC FIELDS WITH MAGNETIZED PLASMAS

Submitted to

THE AIR FORCE OFFICE OF SCIENTIFIC RESEARCH

by

Prof. J. Reece Roth, Principal Investigator
UTK Plasma Science Laboratory
Department of Electrical & Computer Engineering
University of Tennessee
Knoxville, Tennessee 37996-2100

for

Dr. Robert J. Barker
NE Program Manager
Air Force Office of Scientific Research
110 Duncan Ave, Room B115
Bolling Air Force Base
Washington, D.C. 20332-0001

UTK Plasma Science Laboratory
Report No. PSL 94-3
Submitted September 8, 1994

Duration of Effort: April 1, 1989 to March 31, 1994

PRINCIPAL INVESTIGATOR: J. Reece Roth
Phone: (615) 974-4446 (Office)
(615) 974-6223 (Lab)
FAX: 615-974-5492

BUSINESS CONTACT: Mrs. Chris Cox
Phone: (615) 974-8159

Dr. J. Reece Roth
Principal Investigator

TABLE OF CONTENTS

ABSTRACT

This Final Scientific Report describes research at the UTK Plasma Science Laboratory which was supported by the Air Force Office of Scientific Research, contract AFOSR #89-0319, with Dr. Robert J. Barker, Program Manager. Eight archival scientific papers were published, 19 oral or poster conference papers were presented at the annual APS and IEEE plasma meetings, and one patent was obtained and two additional patents were filed for. This contract also supported three graduate theses, including partial support for one Ph.D. dissertation, and two Master of Science in Electrical Engineering theses. This contract additionally supported approximately eight person-years of half time GRA research and training, and the preparation of nine routine reports to the Air Force. This contract also supported Professor Shenggang Liu, UTK's first Visiting Distinguished Professor, for a period of one year.

The contract has supported several major research activities. These include: 1) The writing up for archival publication results from the previous Air Force contract, relating to plasma turbulence and plasma heating by collisional magnetic pumping; 2) Theoretical, computational, and experimental investigation of the interaction of microwave radiation with cylindrical plasmas, particularly in the vicinity of the electron cyclotron frequency; 3) investigation of cyclotron damping near the electron gyrofrequency of magnetized plasmas, as a method for plasma cloaking of earth satellites and spacecraft; 4) development of a parallel plate one atmosphere glow discharge plasma reactor, allowing the production of a uniform plasma at one atmosphere; and 5) development of a method for covering the surface of an aircraft or other body in the atmosphere with a thin layer of plasma for cloaking or boundary layer control.

EXECUTIVE SUMMARY

This Final Scientific Report describes a recently completed five year program of research at the University of Tennessee's Plasma Science Laboratory, which is located on the Knoxville campus, and affiliated with the Electrical and Computer Engineering Department. Our laboratory specializes in the experimental investigation of interactions between electromagnetic radiation and plasma; and in research on electric field dominated steady state plasmas, both magnetized and unmagnetized. In the last three years covered by this report, we have expanded our interest in the latter topic to include the generation and study of unmagnetized uniform glow discharge plasmas operating at one atmosphere of pressure in air and other gases. These electric field dominated plasmas exhibit several characteristics which make them interesting for potential Air Force applications: very high levels of plasma turbulence; broad-band radio frequency emission; ability to strongly absorb incident electromagnetic radiation near the electron cyclotron frequency; and the ability to maintain a uniform glow discharge plasma on the surface of an aircraft or other body in the atmosphere with a power input density on the order of 10 milliwatts/cubic centimeter.

The research described in this report was supported entirely or in part by the Air Force Office of Scientific Research, contract AFOSR 89-0319, of which Dr. Robert J. Barker, AFOSR/NP, is the program manager. Also, one patent on magnetized plasma cloaking of spacecraft and earth satellites was applied for, granted, and assigned to the Secretary of the Air Force, and two additional patents have been disclosed and filed, which the Air Force will have the right to use without the payment of royalties, as a result of its support of the research. This contract also supported three graduate theses, and eight person-years of half-time GRA research and training, which included one Ph.D. dissertation and two Master's theses for the degree of Master of Science in Electrical

2

Engineering. This contract also supported the preparation of 9 routine reports to the Air Force.

The technical accomplishments of this contract have included a patented method for plasma cloaking of satellites and space vehicles, a method for generating a uniform glow discharge plasma in one atmosphere of air, and a method to generate a thin layer of plasma on the surface of aircraft at one atmosphere, also in air. The latter is a very recent accomplishment. Since the end of this contract period, we have demonstrated that the thin layer of plasma generated on the surface of a simulated aircraft fuselage will not blow away under the action of an air jet of modest velocity from the laboratory air supply. These accomplishments may have direct and far-ranging applications for the Air Force, including plasma cloaking of military targets and drag reduction by electrostatic boundary layer control. In addition, the one atmosphere uniform glow discharge plasma is potentially useful for a wide range of industrial plasma surface treatment processes which require active species from a plasma, but are uneconomic when the surface treatment must be accomplished in expensive vacuum systems at low pressure, and with batch processing. There has been intense industrial interest in licensing related technologies made possible by the one atmosphere uniform glow discharge plasma, and the University of Tennessee's Research Corporation (UTRC) is now negotiating with several Fortune-500 companies.

RESULTS OF RESEARCH PROGRAM

In this section we will briefly summarize, in the approximate order in which the research was performed, the results of major research efforts made during the five year duration of this research program. In each case, the results will not be described in detail, but the reader wil be referred to the archival and conference abstracts, included in the appendices, in which more detail can be found.

Previous Research Funded by AFOSR

Our previous contract AFOSR-86-0100 supported research on plasma turbulence and collisional magnetic pumping, the winding-up and documentation phases of which were carried over into the current research program. Some new and interesting results were obtained from the application of a commercial software program based on chaos theory to electrostatic plasma turbulence. This work formed the basis of Mr. Scott A. Stafford's Master' thesis, and was published in paper #4 appearing in Appendix A, in the Journal of Applied Physics. Some experimental results on plasma heating by collisional magnetic pumping in a modified Penning discharge were presented at conferences, the abstracts of which are in items #1 and 4 in Appendix B, and in two archival papers in the Physics of Fluids which are papers #2 and 3 included in Appendix A. These papers both indicated a measurable effect of collisional magnetic pumping in increasing the plasma electron temperature by an amount predicted by the theoretical and computational results published in the Physics of Fluids.

Interaction of Electromagnetic Waves with Plasmas

During the first three years of this research program, our efforts were focused primarily on the interaction of electromagnetic radiation with a magnetized plasma in the vicinity of the electron cyclotron frequency. This regime was considered interesting

4

because of its potential application to magnetized plasma cloaking, in which a magnetized plasma absorbs very strongly in the vicinity of the electron cyclotron frequency. Such absorption can be used to protect a military target against radar interrogation or directed microwave energy weapons. We used our microwave network analyzer, a very expensive and specialized piece of equipment which was purchased in the mid 1980's with AFOSR University Research Instrumentation funds, to measure the attenuation across the diameter of a Penning discharge plasma. As expected, very strong absorption was observed. A plasma about 12 centimeters in diameter, with number densities in the high 10^9 particles per cubic centimeter range, was capable of providing up to 40 dB of attenuation near the electron cyclotron frequency. Some computational and analytical studies of this interaction were made by Dr. Mounir Laroussi, and published in papers #5 and 7 included in Appendix A. Other analytical and computational work on this problem were reported in conference presentations, the abstracts of which are included as items 10 and 13 in Appendix B. Experimental measurements of the interaction of microwave radiation with our magnetized plasma were reported in conference publications, the abstracts of which are included in Appendix B as items #2, 5, 6, and 13.

Magnetized Plasma Cloaking

The large attenuation observed near the electron cyclotron frequency in a magnetized plasma indicated that this physical process could be used for plasma cloaking of spacecraft and earth satellites, which operate in a vacuum, or in an environment in which a magnetized plasma could be maintained around the target. A United States patent on this concept was applied for, and granted in January, 1991. A copy of this patent is included in Appendix C as item 1. This concept is based on the operation of a target vehicle, whether a spacecraft or a earth satellite, in a vacuum environment. The vehicle would carry on board a superconducting magnetic field coil capable of generating a dipolar

5

magnetic field strong enough to trap a plasma. The electrons in the plasma would resonate with the electromagnetic radiation incident on the target at the local electron cyclotron frequency, and the radiation would be absorbed at that point. The magnitude of the dipolar magnetic field would be adjusted in such a way that all likely probing frequencies would be covered as electromagnetic radiation propagated toward the surface of the vehicle.

Development of a Notch Microwave Filter

While associated with the UTK Plasma Science Laboratory, Dr. Mounir Laroussi independently conceived the idea of using electron cyclotron resonance in magnetized plasmas as a basis for a tunable notch filter of microwave radiation. This invention was described in a conference paper, the abstract of which is listed as item 15 in Appendix B, and also in an archival journal article which appeared in the Journal of Infrared and Millimeter Waves, which is included as item 6 in Appendix A.

This concept is based on inserting a magnetized plasma in a microwave waveguide, or in a microwave circuit, and adjusting the notched absorption frequency by altering the parallel magnetic field in the plasma-filled microwave cavity. Absorption occurs at the electron gyrofrequency. An attempt was made to apply for a patent for this idea, but the University of Tennessee's Research Corporation declined to apply for such a patent on grounds that the concept did not appear to possess sufficient commercial licensing potential.

Microwave Tube Theory

We were extremely fortunate to have Dr. Liu, Shenggang, President of the University of Electronic Science and Technology in Chengdu, China as a Distinguished Visiting Professor. While here, he gave an excellent graduate course on microwave tube theory, and had time to write papers on microwave tube theory, including one with the Principal Investigator. Abstracts of the four conference papers which Professor Liu gave

while in the United States are included in Appendix B as items 7, 8, 11, 12. The abstract of a fifth conference paper, which extended some previous work done for the Air Force by the Principal Investigator in the early 1980's, is included in item #9 in Appendix B. This paper describes the relativistic theory of the two interpenetrating beam-plasma interaction. This paper carried the previous work of Prof. Igor Alexeff and the Principal Investigator into the relativistic charged particle regime.

Generation of a Uniform Glow Discharge Plasma at One Atmosphere

One of the limitations of the magnetized plasma cloaking concept described previously is that there appears to be no obvious way in which that approach could be applied to aircraft in the atmosphere. To have any kind of plasma cloaking in the atmosphere, one must generate a uniform glow discharge plasma over the surface of the aircraft in atmospheric air. The generation of corona discharges and filamentary discharges at one atmosphere of pressure in air is well known, but there was no well-known way to generate a uniform glow discharge plasma under these conditions at the time that we started our research program with this objective in the summer of 1991.

For reasons that are outlined in the ball lightning preprint which is included as item 8 in Appendix A, (this paper has been accepted for publication in the Journal Fusion Technology), the Principal Investigator recognized that ball lightning was a real natural phenomenon, even though no one has yet been able to understand it well enough to reproducibly generate ball lightning in the laboratory for scientific study. Ball lightning, among other things, is a glow discharge plasma, which has been observed to last for durations as long as 90 seconds in air at one atmosphere. This phenomenon gives some encouraging indication that it should be possible to generate a uniform glow discharge plasma at one atmosphere, and perhaps even on the surface of aircraft to provide plasma cloaking.

7

We began a research program with this objective in the summer of 1991, and in January, 1992 achieved our first uniform glow discharge in helium gas at one atmosphere. This plasma is shown in Figure 1. These results were reported at the IEEE and APS plasma meetings, and the abstracts of these papers are included as items 14, 16, 17, and 18 of Appendix B. The industrial and military applications of this one atmosphere glow discharge are so far-reaching that, while we have presented our results at meetings (after filing patent applications), we have been too busy writing up patent disclosures to get these results written up for the archival literature as yet. We intend to get them well-documented in the archival literature in the future. Because of this delay in publication, I have included more background on the uniform glow discharge plasma in this report than the other accomplishments mentioned above which are represented only by their archival publications and by their abstracts.

The generation of plasma at one atmosphere is not a recent development. Electrical arcs have been used at one atmosphere since the early 19th Century for various industrial processes, as has the more recently developed plasma torch (ref. 6, 7). The generation of low power density plasmas at one atmosphere also is not new. Filamentary discharges between parallel plates in air at one atmosphere have been used in Europe to generate ozone in large quantities for the treatment of public water supplies since the late 19th century. Such filamentary discharges, while useful for ozone production, are of limited utility because of their nonuniformity, since the plasma filaments tend to puncture exposed materials or the electrode surface insulation, or lead to arcs. The properties of a glow discharge plasma at high pressures, including one atmosphere in air and hydrogen, was reported by von Engel et al. in 1933 (Ref. 8). These discharges were initiated at low pressure (thus requiring a vacuum system), required temperature control of the electrodes, and appear too unstable for routine industrial use. More recently, a group affiliated with Sofia University in Japan (refs. 9-11) has reported the generation of both filamentary and

8
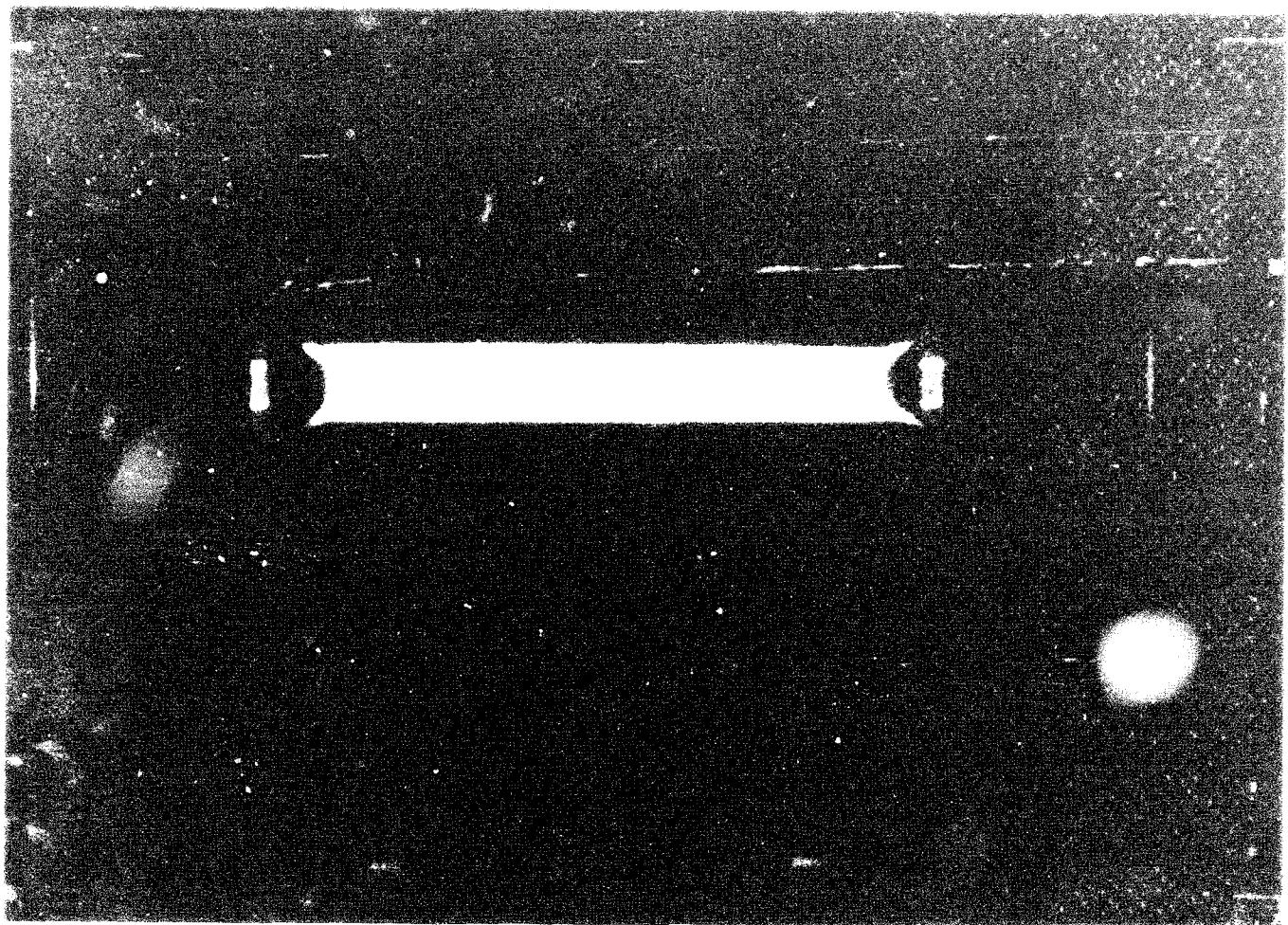
FIGURE 1 - Original one atmosphere glow discharge plasma reactor
operating with helium gas. Plasma volume approximately
2.8 liters, electrodes 25 cm square, frequency 3 kHz.

steady state glow discharge plasmas at one atmosphere of pressure in gases which include helium and argon with an admixture of acetone, but not atmospheric air. Similar work later originated independently in the UTK Plasma Science Laboratory at the University of Tennessee in Knoxville (refs. 1-5).

The "MOD-I" one atmosphere glow discharge plasma reactor was developed at the UTK Plasma Science Laboratory with AFOSR support (refs. 1-3), and is shown in Figure 1. This reactor consists of two 25 cm square, water-cooled copper plates covered with approximately 1 mm of the tough, rubberized material used on the walls of electroplating baths. The approximately 2.0 liter helium plasma shown in Figure 1 was energized at 30 kHz.

A schematic of the "MOD-II" one atmosphere glow discharge plasma reactor system developed at the UTK Plasma Science Laboratory is shown in Figure 2. The reactor volume is bounded by two plane, parallel plates across which an RF electric field is imposed. This voltage has an amplitude of kilovolts per centimeter, and frequencies in the kilohertz range. The electric fields must be strong enough to electrically break down the gas used, and are much lower for helium and argon than for atmospheric air. The RF frequency must be in the right range, discussed below, since if it is too low, the discharge will not initiate, and if it is too high, the plasma forms filamentary discharges between the plates. Only in a relatively limited frequency band will the atmospheric glow discharge plasma reactor form a uniform plasma without filamentary discharges.

The parallel electrode plates consitituting the reactor are enclosed in a plexiglass container, shown in the photographs of Figure 3. The principal function of this container is to control the composition of the operating gas used during operation at one atmosphere, and to act as a barrier to toxic gases, such as ozone. As indicated in Figure 2, the reactor has a metal median screen, which may be grounded through a current choke, located midway between the two parallel electrode plates. The top and bottom half of the box in
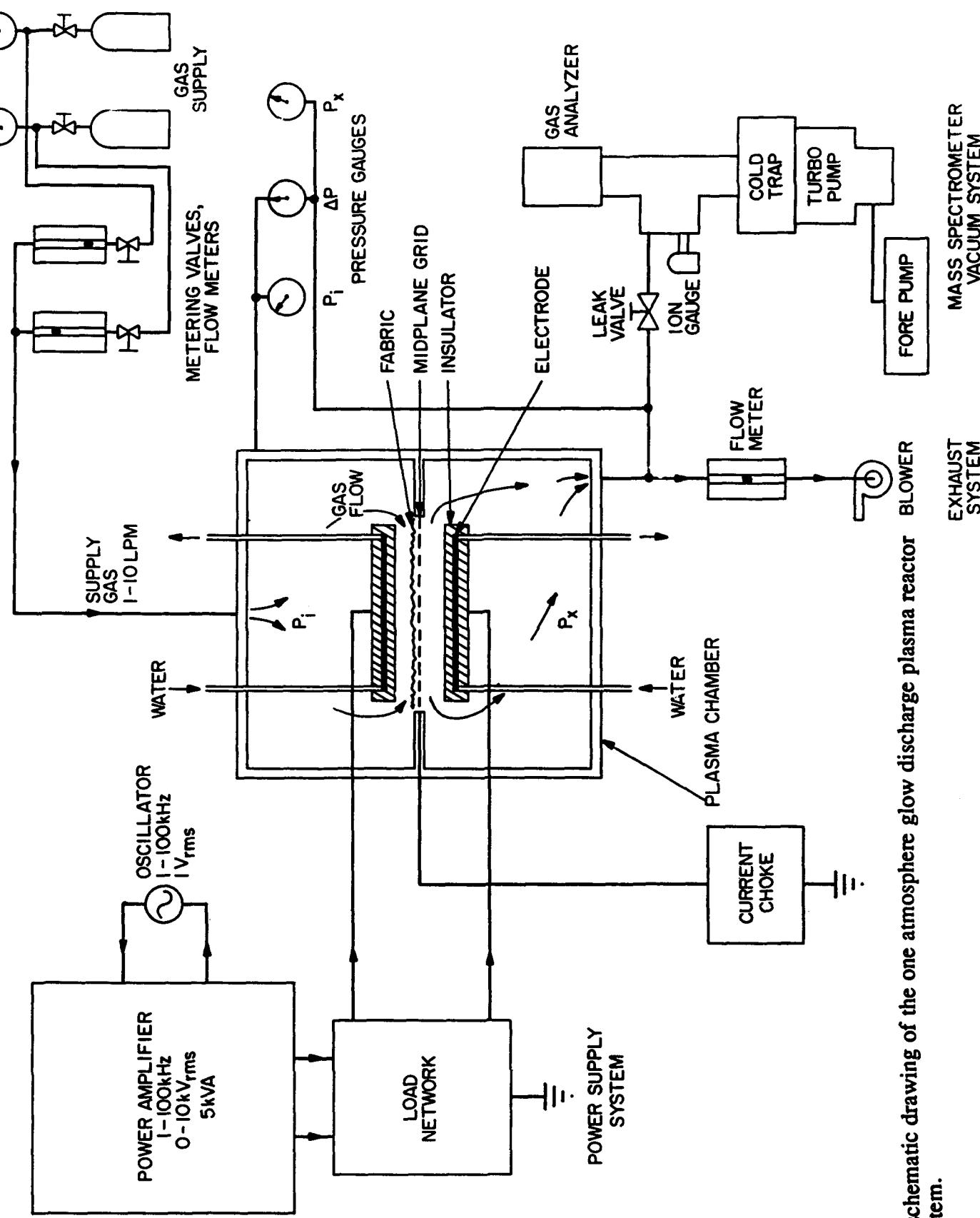
Figure 2. A schematic drawing of the one atmosphere glow discharge plasma reactor system.

FIGURE 2

11

the MOD-II reactor are divided by a horizontal partition which supports the metal screen and bisects the volume of space defined by the two parallel plates. The holes in the metal screen provide the only route by which gas fed into the top half of the chamber can flow to the bottom half. This flow of gas through the experimental volume is intended to enhance the contact of active species from the plasma with the surface exposed on the midplane screen, and to make the plasma more stable and uniform.

The two parallel electrode plates shown on Figure 2 are driven by a power amplifier capable of operation from 0 to 10 kilovolts RMS, over frequencies from less than one kHz to 100 kHz. This amplifier is capable of producing 5 kW of RF power, far beyond the requirements of the test plasma, which rarely exceed 100 watts. The supply gas is sampled from the exhaust line and leaked into a vacuum system with a mass spectrometer. The two copper electrode plates of the MOD-II reactor are 21.6 cm square, and the surfaces in contact with the plasma are covered with a 3.2 mm thick Pyrex insulating plate. The median screen is an uninsulated electrical conductor, and may be grounded or allowed to float electrically. Operating the plasma reactor with the median screen grounded (either directly or through a current choke) makes it possible to reduce the maximum voltage in the plasma reactor chamber to half that which would otherwise be required if one of the two electrode plates were grounded. In addition, keeping the median screen at ground potential also allows treated materials to remain at ground potential.

Figure 3a shows a photograph of the MOD-II one atmosphere glow discharge plasma reactor system as it is currently set up in the UTK Plasma Science Laboratory. This photograph shows, from left to right, the RF power amplifier and power supply; the chiller for the cold trap; the mass spectrometer system and vacuum system for analysis of the gas composition in the one atmosphere glow discharge plasma; the gas flow monitoring and control panel; and the one atmosphere glow discharge plasma reactor. The equipment rack containing the oscilloscope, signal generator, and other diagnostic equipment is out of sight

12
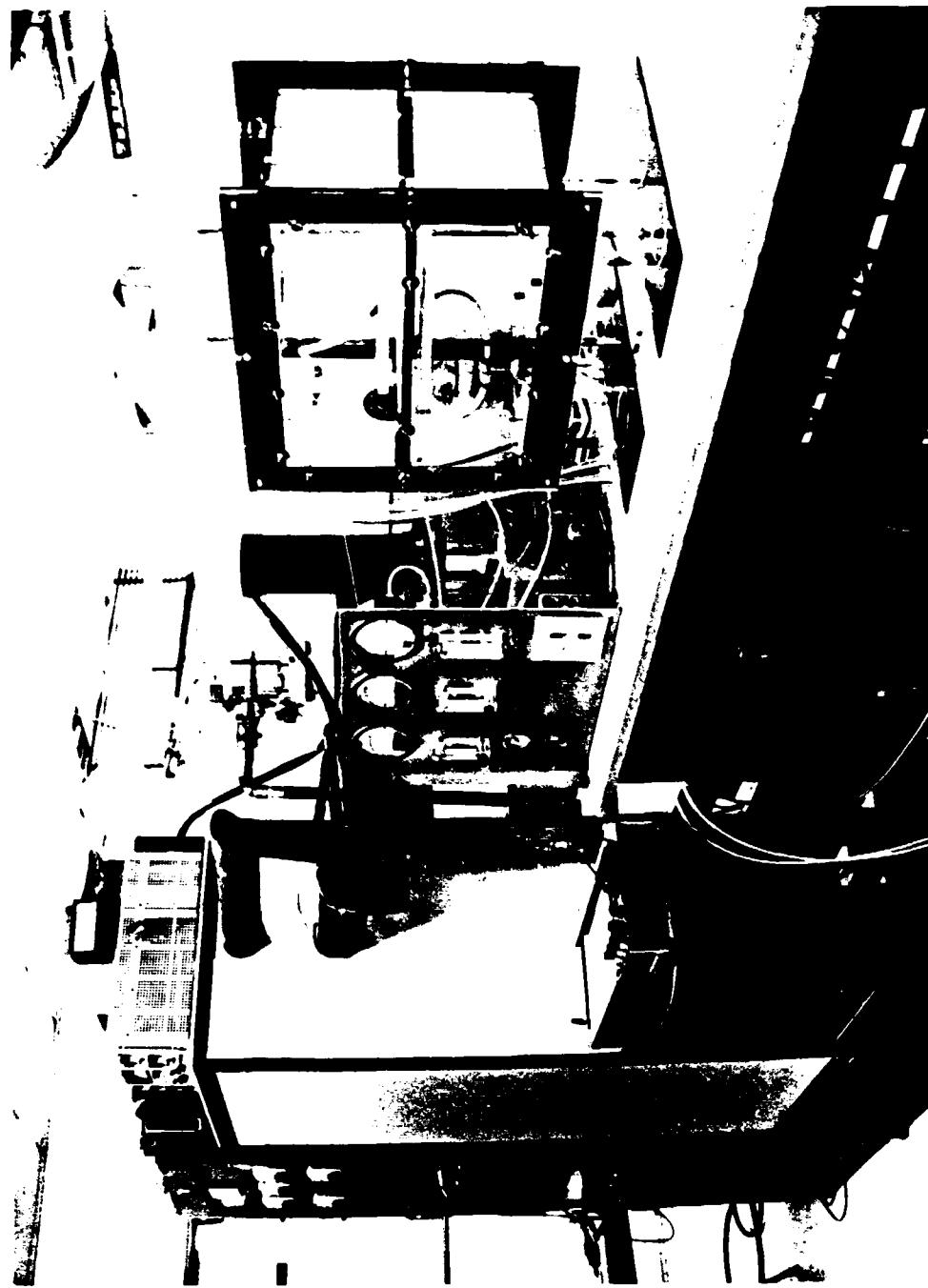
Figure 3a. Photograph of the complete *One Atmosphere Glow Discharge Plasma Reactor System.* Green equipment rack on left is the RF amplifier; next to right is cold trap chiller and vacuum system for the mass spectrometer; next is the gas flow and pressure monitoring panel; and the plexiglass enclosure on the right contains the plasma reactor.

beyond the RF power amplifier to the far left. Figure 3b shows a photograph of the plasma reactor chamber, with the two electrodes occupying the center of the chamber volume to the right, and the gas flow and monitoring panel on the left. The plexiglass cover nearest the camera may be removed for installation and removal of individual samples of treated materials. Figure 3c shows the back aspect of the plasma reactor chamber, with the impedance matching network and current choke in the box to the lower right.

Figure 4 is a photograph of the glow discharge plasma reactor with the electrode plates withdrawn to shown the Pyrex glass covers of the electrode plates, and the metal screen in the median plane between the electrodes.

Figure 5a shows the uniform plasma created in the one atmosphere glow discharge plasma reactor using one atmosphere of helium gas. The line running horizontally through the center of the plasma is the plexiglass support in the median plane, which contains the metal screen. In this photograph, helium gas flows from the upper chamber downward through the plasma and median plane, then to the lower chamber where it is drawn out by a blower which maintains a slight negative pressure. The gas flow through the plasma is driven by a pressure differential of a few hundred pascals (a few inches of water). The plasma in Figure 5a was generated with an RF voltage of 3 kV RMS, an RF frequency of 3.0 kHz, and a plate separation of d = 1.27 cm, which produces a uniform plasma. Figure 5b shows a close-up of the plasma reactor operating with helium in the uniform discharge regime under the same conditions as 5a, but with a voltage of 2.3 kV RMS.

Figure 6 shows the one atmosphere glow discharge plasma reactor operating at the same voltage and other conditions as Figure 5a, but at a higher frequency of 8.0 KHz, which produces a filamentary discharge. Such filamentary discharges are useful as ozonizers and for other plasma-chemical applications, but they are not desirable for the surface treatment of materials, since they treat the sample materials nonuniformly, and their

14
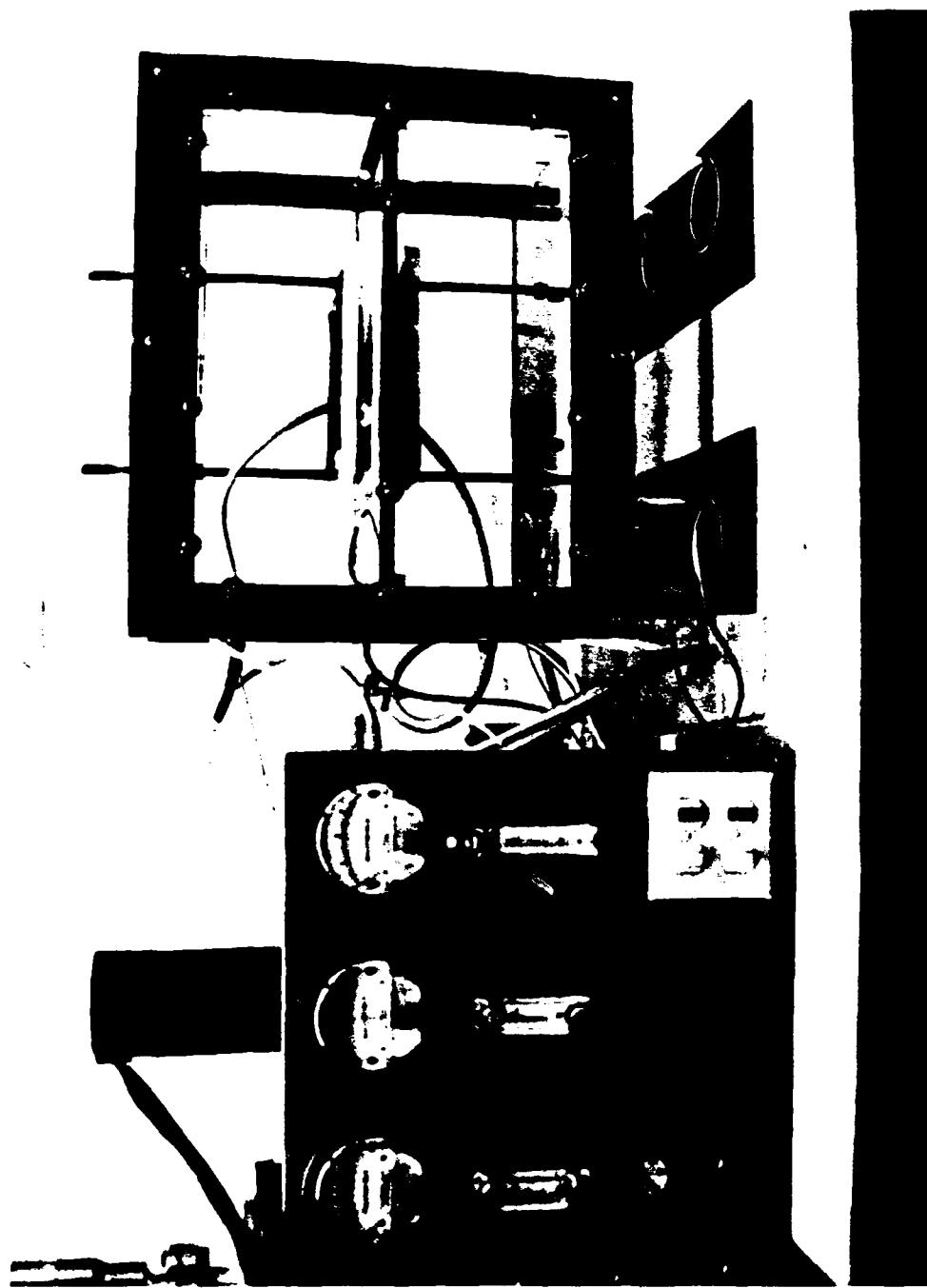
Figure 3b. Photograph of the *One Atmosphere Glow Discharge Plasma Reactor* with its plexiglass enclosure which controls gas purity and flow.
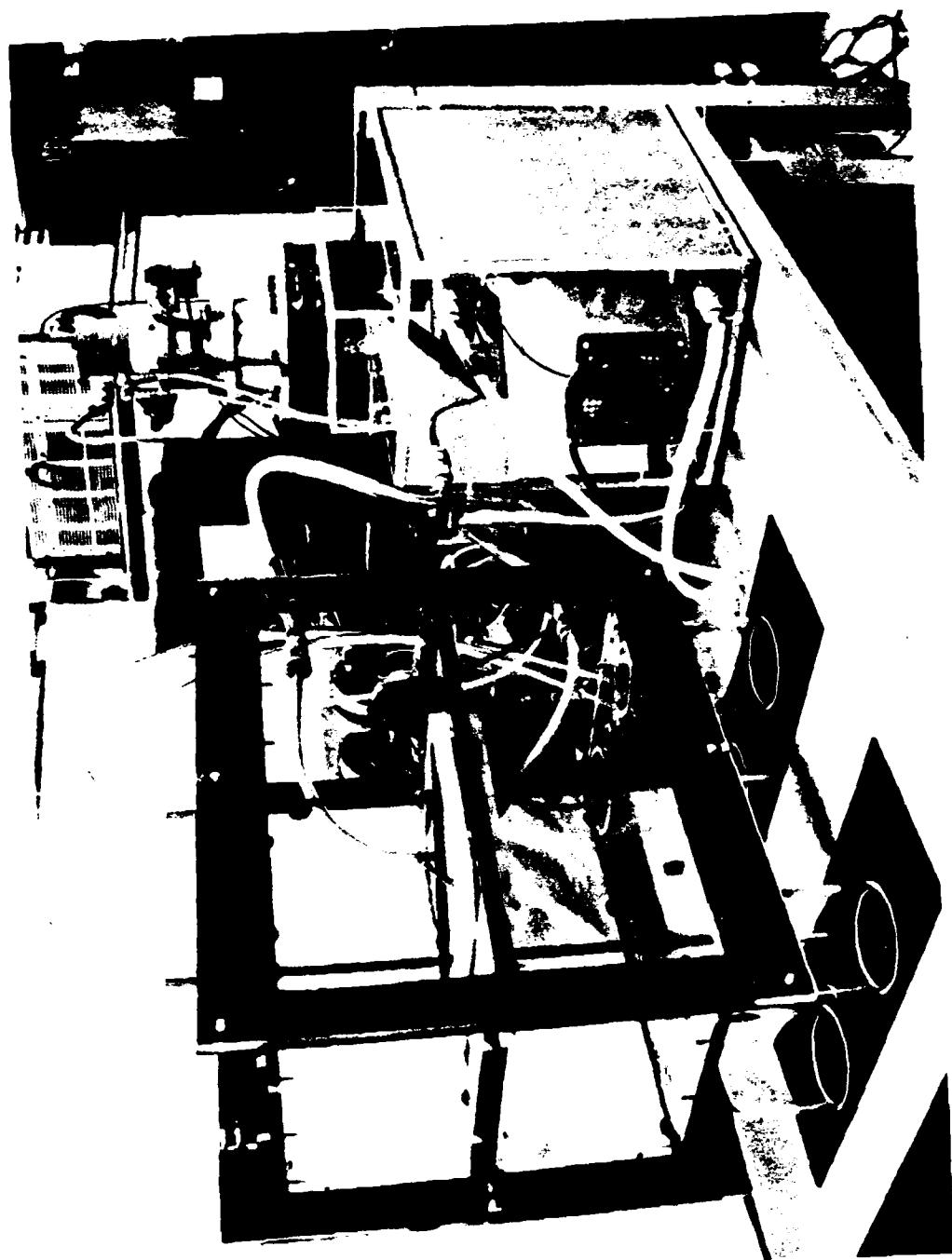
Figure 3c. Photograph of the back aspect of the plasma reactor showing the impedance matching network on the lower right.
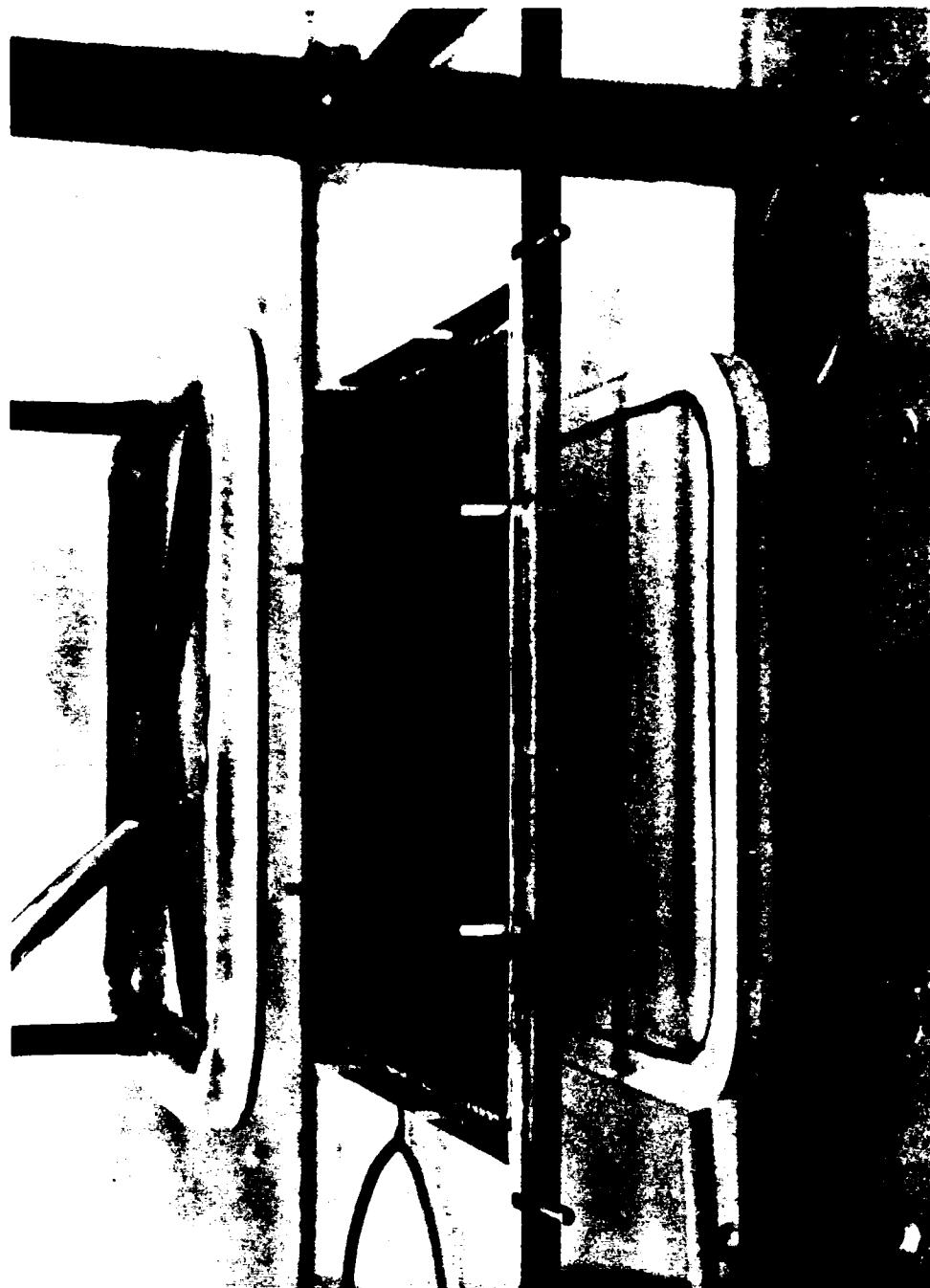
Figure 4. Photograph of the *One Atmosphere Glow Discharge Plasma Reactor* with the electrode plates withdrawn to show the Pyrex glass cover of the electrode plates, and the metal screen in the median plane between the electrodes.

Figure 5a. A photograph of the one atmosphere glow discharge plasma operated in helium with a RMS voltage of 3.0 KV, an RF frequency of v_0=3.0 KHz, and a plate separation d=1.27 cm, taken in the uniform plasma regime.

18
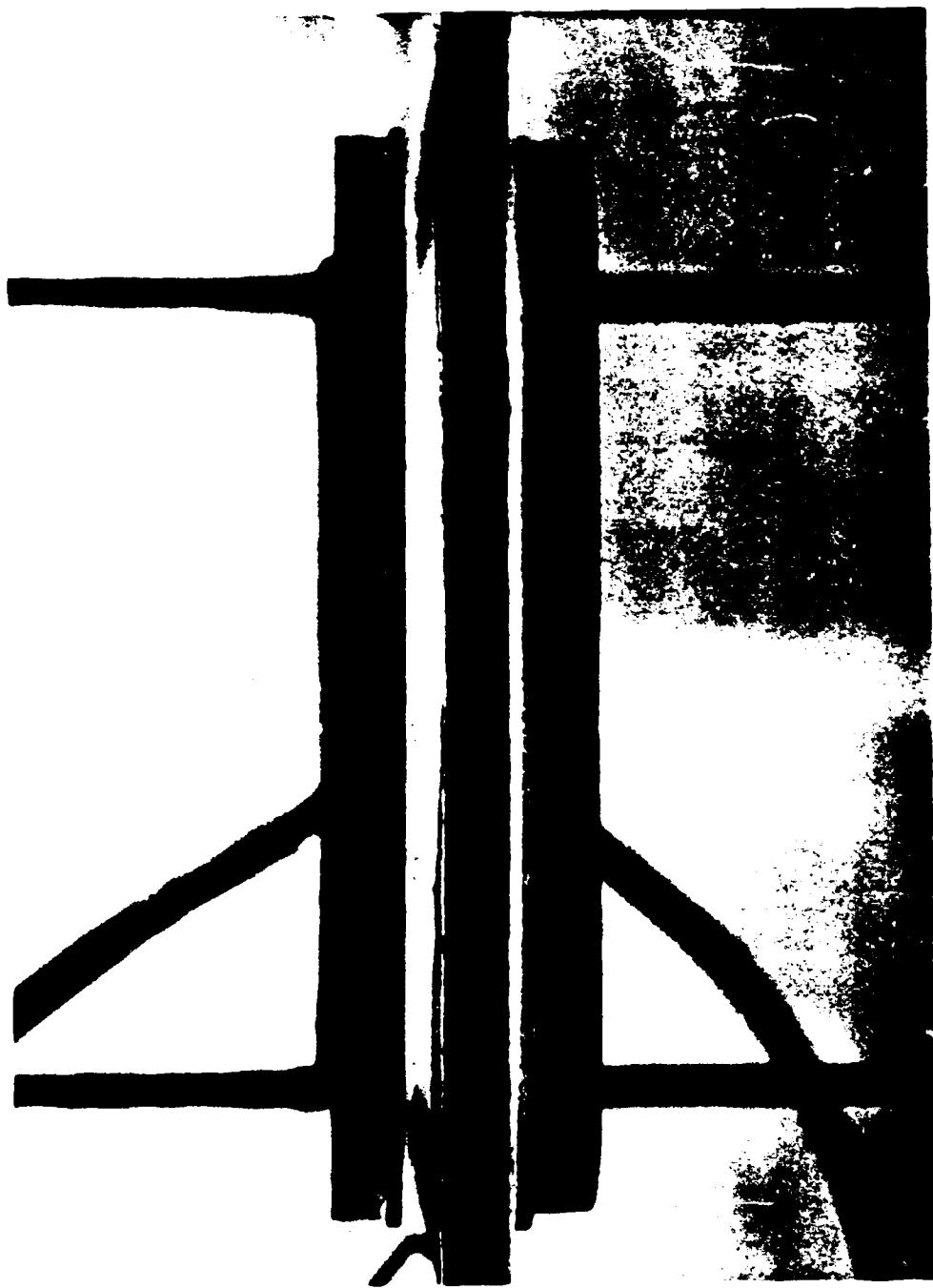
Figure 5b. Close-up of plasma reactor operating with helium gas, an RMS electrode voltage of 2.3 KV; a plate separation d=1.27 cm; and an RF frequency of ν_0=3.0 KHz. The reactor is in the uniform discharge regime.
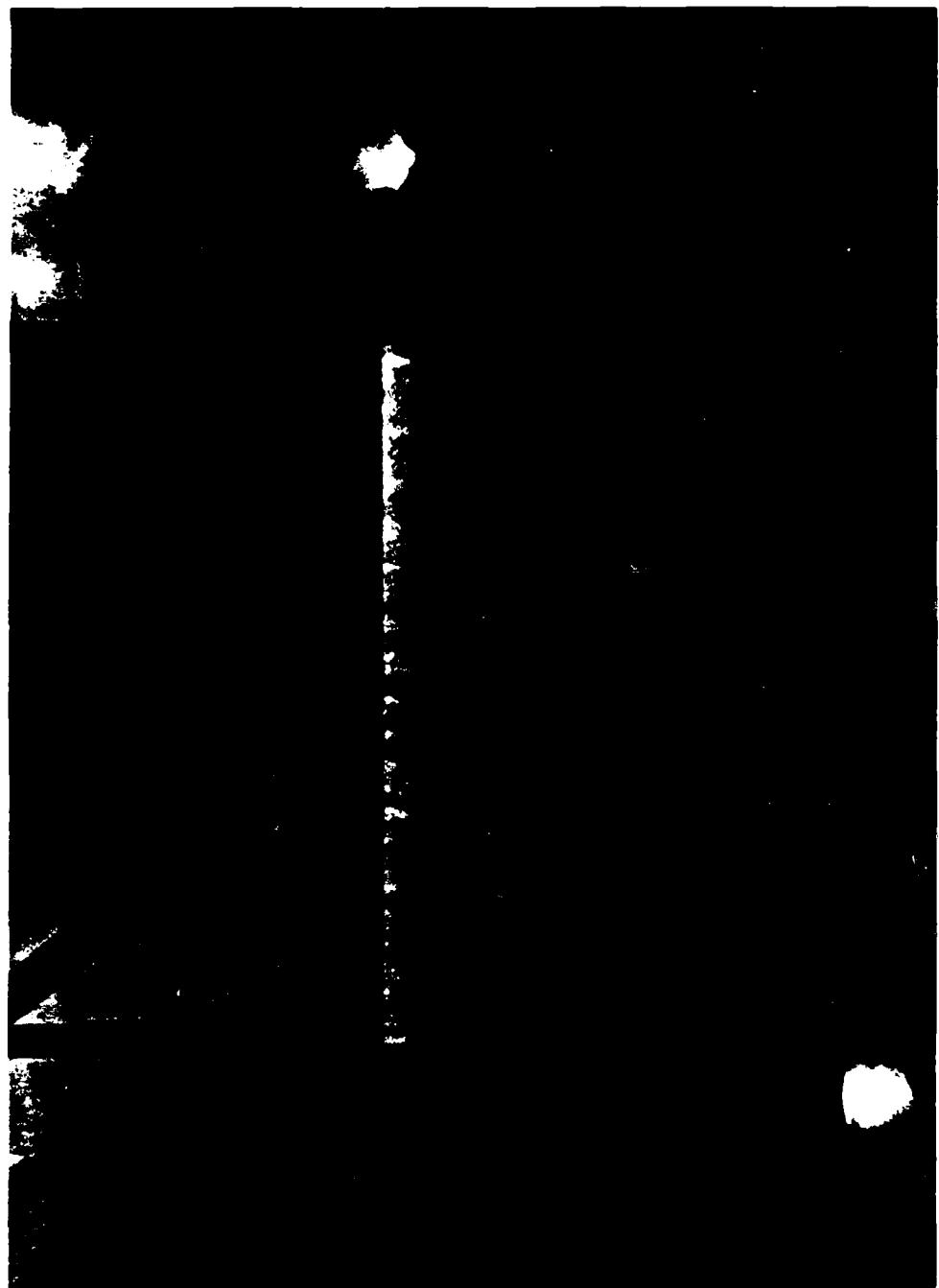
**Figure 6.** Photograph of the one atmosphere glow discharge plasma using helium gas, taken with an RF frequency v_0=8.0 KHz, and an RMS electrode voltage of 3.0 KV, a plate separation d=1.27 cm, operated in the *filamentary* plasma regime.

attachment points on the grounded screen in the median plane may produce small holes or pits in or on the treated material.

The plasma diagnostics utilized thus far include a mass spectrometer, which draws a sample from the exhaust gas of the plasma reactor through a needle valve and into a vacuum system, where the gas composition is monitored by a quadrupole mass spectrometer. Additional diagnostics include monitoring the floating potential of the median screen, the power and power density absorbed by the plasma, and monitoring the voltage and current waveforms on the electrodes with a digital oscilloscope.

The electric fields normally employed in the one atmosphere glow discharge plasma reactor are only a few kilovolts per centimeter, values usually too low to electrically break down the background gas. Gases such as helium and argon will break down under such low electric fields, however, if the positive ion population is trapped between the two parallel plates, shown in Figure 7, while at the same time the electrons are free to travel to the insulated electrode plates where they recombine or build up a surface charge. The most desirable uniform one atmosphere glow discharge plasma is therefore created when the applied frequency of the RF electric field is high enough to trap the ions between the median screen and an electrode plate, but not so high that the electrons are also trapped.

If the RF frequency is so low that both the ions and the electrons can reach the boundaries and recombine, the plasma will either not initiate or form a few coarse filamentary discharges between the plates. If the applied frequency is in a narrow band in which the ions oscillate between the median screen and an electrode plate, they do not have time to reach either boundary during a half period of oscillation. If the more mobile electrons are still able to leave the plasma volume and impinge on the boundary surfaces, then the desirable uniform plasma is produced. If the applied RF frequency is still higher so that both electrons and ions are trapped in the discharge, then the discharge forms the filamentary plasma illustrated in Figure 6. A patent disclosure for the one atmosphere

21
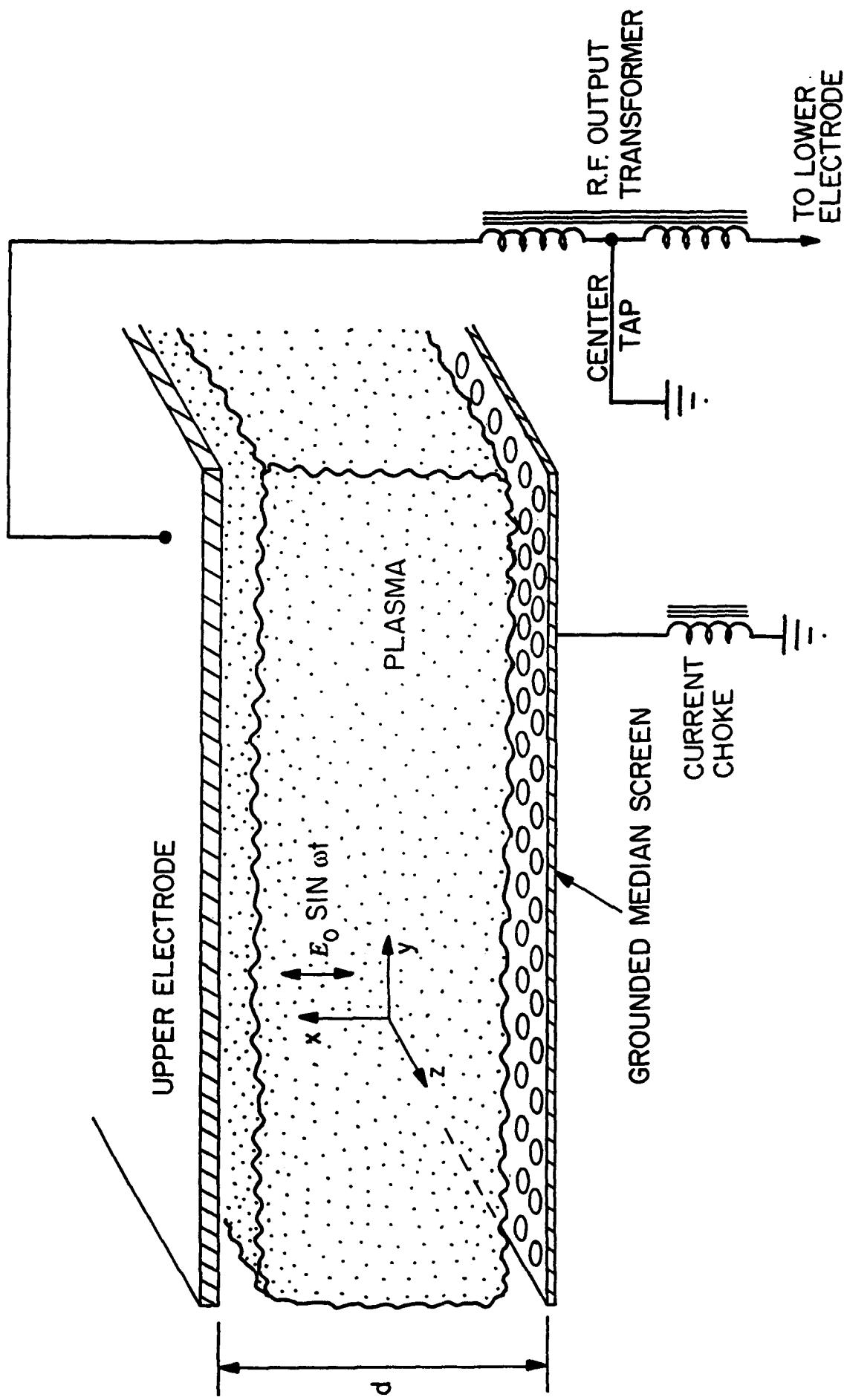
Figure 7. A schematic of the one atmosphere glow discharge helium plasma reactor, with RF electrical connections between the RF transformer secondary, the matching network, and the reactor electrodes.

22

uniform glow discharge plasma reactor has been written and filed with the U.S. Patent Office. The original version of this patent filing is included as item 2 in Appendix C. That patent disclosure contains a quantitative theory of the ion trapping mechanism discussed above, and other information about the many possible variations of the parallel plate one atmosphere uniform glow discharge plasma reactor.

Generating a Plasma on The Surface of Aircraft

After producing a uniform one atmosphere glow discharge plasma in a parallel plate configuration in gases ranging from helium to air, it was desirable to get from the parallel plate configuration to one which could arguably be installed on the surface of aircraft. As an intermediate step between these two configurations, we tested a number of geometrical configurations, including the two parallel insulated rods shown in Figure 8. These two rods generated a plasma between them in helium gas when the rods were energized with several kilovolts rms of RF at frequencies of several kilohertz. The plasma generated between the two rods was approximately 14 centimeters long, and the gap between the rods was approximately one centimeter. The experiment of Figure 8, and similar experiments, led us to expect that if we installed a series of strip electrodes on the insulated surface of an aircraft or solid body, that the ions might be trapped along the arched electric field lines between the individual electrodes, thus generating a plasma above a planar surface. We tested this approach by wrapping two bifilar helical wires around a two inch diameter cylinder, and energizing the adjacent wires with opposite RF phase. Figure 9 shows one of our first experiments of this kind. A very thin layer of plasma is generated on the surface of the cylinder covered with these wires. The blob of material running along the axis is some epoxy that was used to hold the wire coil in place. The cylindrical plasma generated in Figure 9 was in helium gas at one atmosphere, with an excitation frequency of 2 kilohertz, and an excitation voltage of two to three kilovolts rms.

Figure 8

24
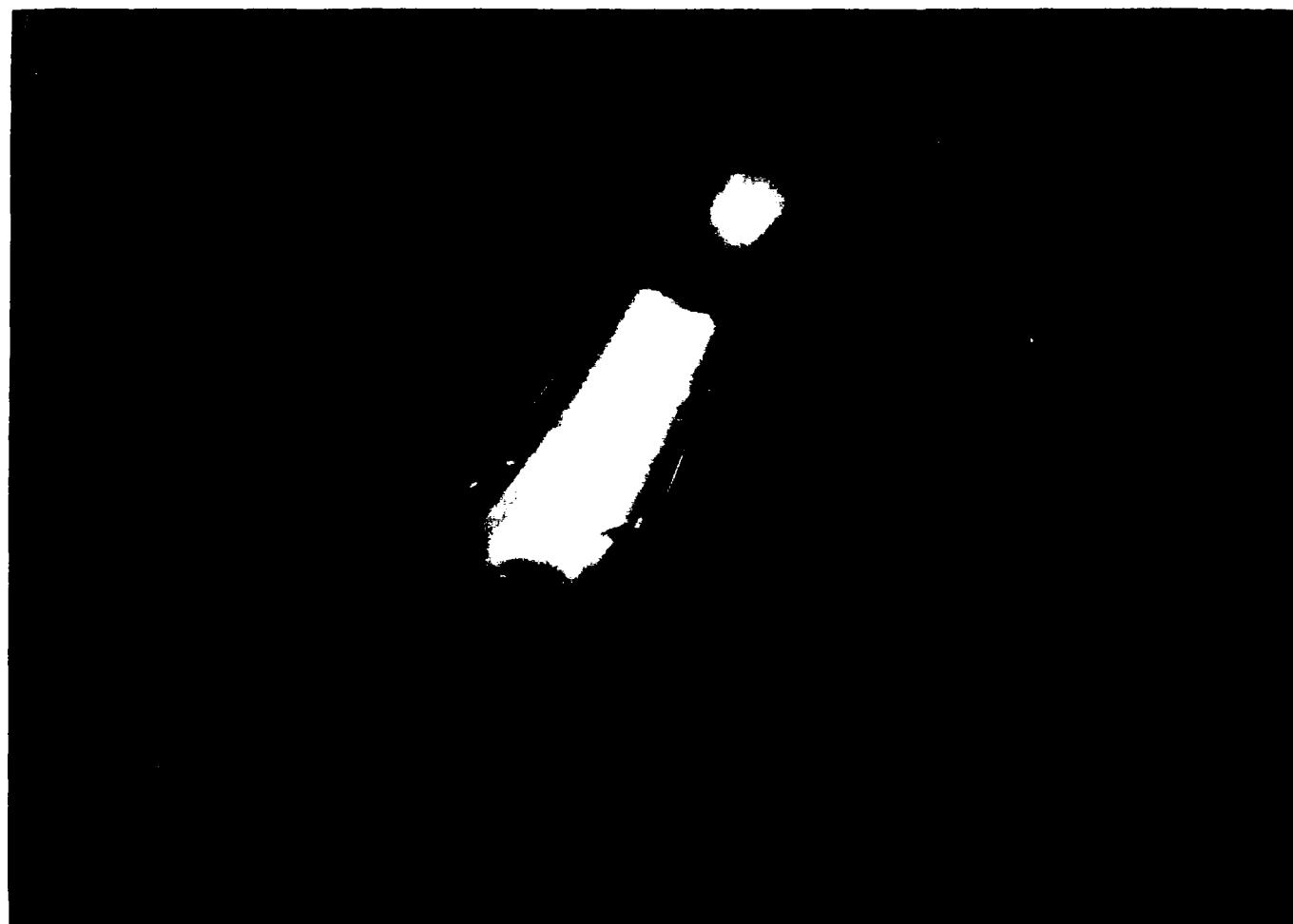
Upon achieving the results photographed in Figure 9, the Principal Investigator wrote up a patent disclosure for this method of generating a plasma on the surface of aircraft or other bodies in the atmosphere, and that disclosure has been filed with the U.S. Patent Office on June 6, 1994. A preliminary copy of this patent filing is included as item 3 in Appendix C of this report. This document has a great deal more information about operating conditions and range of performance for this concept. This work also was reported at a plasma conference in June, 1994. Item 19 of Appendix B contains the abstract of that poster paper.

Plasma-Based Boundary Layer Control and Drag Reduction for Aircraft

Once a plasma has been generated on the surface of an aircraft or other body in the atmosphere using the RF electric field ion trapping mechanism discussed above, the presence of an electrodynamic body force on the plasma provides a mechanism with which one might achieve boundary layer control. It might be possible to achieve acceleration or deceleration of the boundary layer, or to prevent the formation of turbulent vortices and vortex shedding from the trailing edge of aerodynamic bodies. If one considers Figure 9, and imagines that the surface of an aircraft is covered by a series of parallel electrode strips at right angles to the flow velocity, then perhaps instead of operating the alternate strips exactly in phase with one another, one can arrange to sequence the application of the RF electric fields in such a way that a peristaltic wave propagates normal to the electrode strips along the surface of the plasma, much like the sequenced lights on a theater marquee. The velocity of this propagating wave can be adjusted by changing the relative phase of the signal applied to alternate electrode strips; the propagating electric field should drag with it the plasma layer and the fluid dynamic boundary layer with which it will interact on the surface of the body. This then may provide a mechanism by which the boundary layer can be accelerated, decelerated, and maintained in a laminar state during the process.
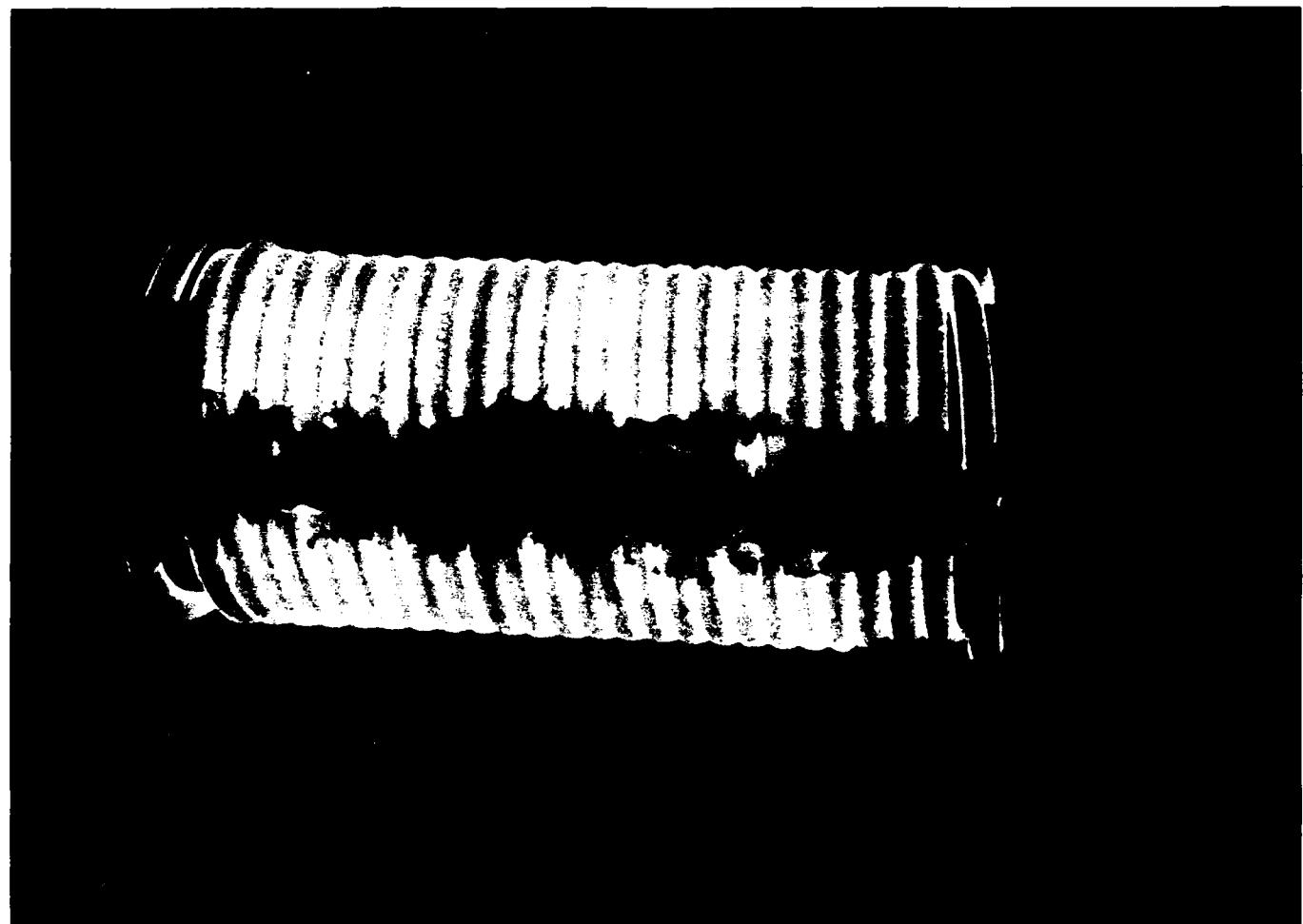
Figure 9

We have generated such a surface plasma not only in helium (shown in Figure 9), but also in air. The plasma surrounding the cylinder in air has not been blown away by a relatively low velocity jet of gas from the laboratory air supply. This method of aerodynamic boundary layer control was put forward in a paper the abstract of which is listed as item 19 in Appendix B, and it was also included in the patent filing which is included as item 3 in Appendix C.

POTENTIAL UTILITY OF RESEARCH TO THE AIR FORCE

The research described in the previous section has several potential Air Force applications, including the plasma cloaking of military radar targets, covering aircraft with plasma in the atmosphere, and plasma-based boundary layer control and drag reduction for aircraft. The range of some of these applications is discussed at length in the claims to the three patents and patent filings included in Appendix C, but they will be reviewed briefly here.

Magnetized Plasma Cloaking

Magnetized plasma cloaking for military radar and directed microwave energy targets was an outgrowth of our research on the interaction of electromagnetic radiation with magnetized plasmas, which led to the concept described in U.S. Patent #4,989,006. This concept will work only when it is possible to surround the target with a magnetized plasma, such as a dipolar magnetic field. This would appear to rule out operation within the atmosphere and restrict its application to protecting earth satellites and space vehicles against radar probing, radar guided missiles, and possibly directed microwave energy weapons. According to Mr. William Auton, the Air Force patent lawyer, he was not aware of any patent like it in the entire field of electronic warfare, and, in the event, it went through the U.S. Patent Office in less than 15 months, presumably because of its novelty.

27

Covering Aircraft with A Plasma Layer

The technology disclosed in the patent application included as item #3 in Appendix C may have stealth implications, if the plasma layer can be made thick enough, or have the right properties to absorb incoming radar pulses. The disclosed method of generating a plasma on the surface of an aircraft has a number of potential advantages. One is that the required power density is not large. A uniform glow discharge plasma in air requires only power inputs on the order of 10 to perhaps hundreds of milliwatts per cubic centimeter under the conditions for which they have been operated in our laboratory. Secondly, the method of generating the plasma with strip electrodes of various configurations is one that might be retrofitted to existing aircraft, simply by coating them with an insulating layer, and imbedding on the outer surface of this layer the strip electrodes which are required to generate the plasma. One of our future research topics is going to be to irradiate this plasma layer at one atmosphere and see what degree of attenuation is experienced by electromagnetic radiation reflected off it. Its behavior will not be the same as that which we observe at low pressures (in the experiments described above on the interaction of electromagnetic radiation with low pressure plasmas) since, at one atmosphere, the electron collision frequencies are on the order of gigahertz, and there is little opportunity for cyclotron damping to occur near the electron cyclotron frequency. On the other hand, the very high electron collision frequencies may lead to much higher levels of attenuation than are experienced by low pressure, less collisional plasmas.

Plasma-Based Boundary Layer Control and Drag Reduction

If the electrodynamic body force on the plasma and on the boundary layer is sufficiently strong, there is a good possibility that by phasing the voltage applied to strip electrodes on the surface of an aircraft, one can accelerate, decelerate, and otherwise manipulate the boundary layer flowing over the surface of an aircraft in flight. We have

28

already observed in the laboratory that the plasma surface layer generated in the way discussed above and shown in Figure 9 does not blow away when a gas jet of modest velocity is directed on it from the laboratory air supply. We do not have a wind tunnel available to us in the UTK Plasma Science Laboratory, and I hope to interest someone at the NASA Lewis Research Center, Wright-Patterson AFB, or perhaps at the University of Tennessee's Space Institute in Tullahoma, in collaborating with me on a series of measurements to see whether a phased operation of these electric fields on the surface of an aerodynamic body will alter the drag coefficient and permit boundary layer control.

One of the most exciting possibilities which such electrodynamic boundary layer control opens up, is the possibility of imitating on the surface of aircraft the boundary layer control which allows dolphins in the ocean to swim at velocities of more than 50 miles an hour, while exerting no more than a few horsepower of power output. The ability of dolphins and other marine mammals to swim so swiftly with so little power input has been of interest to the U.S. Navy for a long time. Research on this phenomenon appears to show that the dolphins do this by twitching their skin in such a way as to discourage the formation of turbulent vortices and turbulence which leads to drag and power dissipation. If something similar could be done to the plasma boundary layer surrounding an aircraft, very large reductions in drag and motive power might be possible.

RESULTS OF OTHER CONTRACT ACTIVITIES

Development of The UTK Plasma Science Laboratory

During the five year period covered by this report, a major parallel contract with the Office of Naval Research was terminated at the beginning of this five year period. The UTK Plasma Science Laboratory began a transition from basic research oriented to the Department of Defense, to the general field of industrial plasma engineering, and basic and applied research in the field of industrial plasmas. In aid of this transition, the UTK

29

Plasma Science Laboratory held a three and a half year research contract with the Army Research Office, which terminated at the end of September, 1993 and which allowed us to develop the UTK Microwave Plasma Facility, and the ability to implant metals with nitrogen ions using plasma ion implantation. At present, the UTK Plasma Science Laboratory is one of no more than four or five university laboratories in the United States which can do plasma ion implantation, and it is probably the only one whose research program in this area is aimed specifically at improving the corrosion resistance of metals, rather than improving their hardness and wear characteristics, which is also an outcome of plasma ion implantation.

The one atmosphere glow discharge plasma reactor is of interest to industrial organizations within which the surface treatment of materials and other plasma processing applications have been held back by the requirement for the purchase and operation of vacuum systems, and the batch processing which vacuum systems make necessary. With a uniform one atmosphere glow discharge plasma like that shown in Figure 1 or Figure 8, it is possible to treat the surface of materials at one atmosphere in a continuous way, and much more cheaply than processing applications that require vacuum systems.

SUPPORT OF GRADUATE STUDY AND RESEARCH AT UTK

During the five year history of this contract, 8 person-years of GRA time were supported. Also during that five year period, three students received their degrees from UTK, some of which were in the pipeline when the contract started. Abstracts of the theses and dissertation of these students are included in Appendix E.

PUBLICATIONS AND INTERACTIONS WITH OTHER RESEARCH PROGRAMS

Archival Publications

During the five year history of this research program, eight archival papers were published in journals, and reprints or preprints of these are included in Appendix A. These cover the range of activities researched during this five year period, except for the one atmosphere uniform glow discharge plasma, which is sufficiently new that archival papers have not yet been written and published.

Patents

The novelty and wide potential range of industrial applications of the uniform glow discharge reactor technology has made it advisable to seek patents for the basic ideas behind generating the one atmosphere glow discharge reactor plasma, and also for the basic ideas behind the use of the one atmosphere glow discharge plasma for aerodynamic boundary layer control and drag reduction. The patent disclosures on these topics have been filed with the U.S. Patent Office, and copies of them are included in Appendix C. The patent on the magnetized plasma cloaking concept for earth satellites and spacecraft also has been written up, has been granted, and is included also in Appendix C.

Conference Presentations

During the five year history of this contract, we have had at least one paper at each IEEE and APS plasma meeting, most of which have been progress reports on our work at the time of the meeting. The abstracts for these conference presentations are included in Appendix B, and copies of the poster materials to which these abstracts refer have been included for the most part in previous annual reports that are listed in Table 1 of the introduction. During the period covered by this contract, we have given eighteen

conference presentations, many of which attracted a great deal of interest at the meetings with, in some cases, more than fifty reprint requests for copies of our poster materials.

Media Coverage

During the five year history of this contract, the media have covered our activities Most of this conference has been in the Knoxville area or the university community. Clippings from the media coverage are included as Appendix D.

Support of Visiting Scholars

We have been very fortunate to have Prof. Liu, Shenggang with us during the academic year 1990-1991. He was UTK's first Visiting Distinguished Professor, and contributed substantially to the intellectual life of the University and the UTK Plasma Science Laboratory. Prof. Igor Alexeff and the Principal Investigator as well as our graduate students sat in on his two semester course on microwave tube theory, which was a remarkably complete and clear coverage of the subject of microwave tubes, including a number of configurations that were the invention of Prof. Liu and which are only now under development at the University of Electronic Science and Technology of China in Chengdu. In addition to his technical interactions, Prof. Liu gave some general seminars attended by faculty from the School of Liberal Arts on the current state of higher education in China, as well as other plasma seminars on microwave tube theory to our students.

Lectures

During the five year history of this research program, the Principal Investigator has several times lectured at other Air Force related installations, including at least two lectures at the Polytechnic University in Farmingdale, on some of our activities here. Prof. Spencer Kuo from Polytechnic University also has been to the University of Tennessee to give lectures at our plasma seminar.

STAFFING

Faculty

The Principal Investigator was supported by this AFOSR contract for three months per year during the initial years of this five year program. When funding constraints became more stringent toward the end of the five year program, this support was reduced to one month per academic year. In addition to supporting Prof. Roth, this contract also supported Prof. Liu, Shenggang who spent approximately one year at UTK on sabbatical leave from the University of Electronic Science and Technology of China in Chengdu, during academic year 1991-1992.

Postdoctoral Associates

During various times in this five year period, two postdoctoral associates were supported for AFOSR-related work. One of these was Dr. Paul Spence, who did some work on the interaction of microwaves with DC plasmas for plasma generation and heating, and Dr. Mounir Laroussi, who made contributions to the development of our one atmosphere uniform glow discharge plasma and its power supply, and also to the computational and analytical study of the interaction of electromagnetic radiation with magnetized plasmas. An outgrowth of Dr. Laroussi's work on the latter subject was a new concept for the tunable notch microwave filter discussed previously.

Graduate Research Assistants

During the five year history of this contract, eight graduate research assistants were supported at some stage of their academic programs. Mr. Wu, Stafford, Ghannadian, Crowley and Kamath all received their Master of Science degree in Electrical Engineering from the ECE Department at UTK, although some of them were supported during this five year period only for a few months after they received their Master's degree and so are not

listed among those students who received their degrees during the five year period supported by this contract. Mr. Combs withdrew from his graduate program at UTK before completing his degree requirements; as did Mr. Jiang, a physics student who took a job in private industry before completing his doctoral studies at UTK. Mr. Liu is still affiliated with the AFOSR contract, and should complete his studies at UTK in a year to a year and a half.

REFERENCES

1. Roth, J. R.; Liu, C.; and Laroussi, M.: Experimental Generation of a Steady-State Glow Discharge at Atmospheric Pressure. Paper 5P-21, Proc. 1992 IEEE International Conference on Plasma Science, Tampa, FL, IEEE Catalog No. 92-TH0460-6, ISBN 0-7803 0716-X (1992). pp. 170-171.

2. Liu, C.; Chen, D.; and Roth, J. R.: Characteristics of a Steady-State, Low-Power Glow Discharge at Atmospheric Pressure. APS Bulletin Vol. 37, No. 6 (1992) p. 1563.

3. Liu, C.; Tsai, P.P.-Y.; and Roth, J. R.: Plasma Related Characteristics of a Steady-State Glow Discharge at Atmospheric Pressure. Paper 2P-18, Proc. 1993 IEEE International Conference on Plasma Science, Vancouver, B. C. IEEE Catalog No. 93-CH3334-0, ISBN 0-7803-1360-7 (1993) p. 129.

4. Roth, J. R.; Spence, P. D.; and Liu, C.: Preliminary Measurements of the Plasma Properties of a One Atmosphere Glow Discharge Plasma. APS Bulletin Vol. 38, No. 10 (1993) p. 1901.

5. Roth, J. R.; Wadsworth, L. C.; Spence, P. D.; Tsai, P. P.-Y; and Liu, C.: A One Atmosphere Glow Discharge Plasma for Surface Treatment of Nonwoven Fabrics. Proc. 3rd Annual Tandec Conference, Nov. 1-3, 1993 Knoxville, TN.

6. Roth, J. R.: Industrial Plasma Engineering: Volume I-Principles. Institute of Physics Press, Bristol, U.K. (1994) ISBN 0-7503-0317-4 (to be published April, 1994).

7. Roth, J. R.: Industrial Plasma Engineering: Volume II-Applications. Institute of Physics Press, Bristol, U.K. (to be published April, 1996).

8. Von Engle, A.; Seeliger, R.; and Steenbeck, M.: On the Glow Discharge at High Pressure. Zeit. fur Physik, Vol. 85 (1933) pp. 144-160.

9. Kanazawa, S; Kogoma, M.; Moriwaki, T.; and Okazaki, S.: Stable Glow Plasma at Atmospheric Pressure, J. Physics D., Vol. 21 (1988) pp. 838-840.

10. Yokoyama, T.; Kogoma, M.; Moriwaki, T.; and Okazaki, S.: The Mechanism of the Stabilization of Glow Plasma at Atmospheric Pressure, J. Physics D., Vol. 23 (1990) pp. 1125-1128.

11. Kanda, N.; Kogoma, M.; Jinno, H.; Uchiyama, H.; and Okazaki, S.: Atmospheric Pressure Glow Plasma and its Application to Surface Treatment and Film Deposition Paper 3.2-20, Proc. 10th International Symposium on Plasma Chemistry, Vol. 3 (1991) pp. 3.2-201 to 3.2-204.

APPENDIX A

ARCHIVAL PUBLICATIONS

SPACE APPLICATIONS OF FUSION ENERGY

OVERVIEW

FUSION REACTORS

J. REECE ROTH *University of Tennessee*
Department of Electrical and Computer Engineering
Room 409 Ferris Hall, Knoxville, Tennessee 37996-2100

When more than a few hundred kilowatts of steady-state power are required for space applications, the only feasible choices appear to be nuclear fission or nuclear fusion. Space application places different and usually more stringent constraints on the choice of fusion reactions and fusion confinement systems than do ground-based electric utility applications. In space, the dominant constraint is a minimum mass per unit of power output; for ground-based utilities, the cost of electricity is the dominant constraint. Forseeable applications of fusion reactors to space-related power and propulsion systems appear to require thermal power levels ranging from 10 MW up to 1 GW. There appears to be no mission for the multigigawatt reactors currently of interest to the electrical utilities.

Desirable characteristics of fusion reactors for space include avoidance of tritium-fueled reactions; an operation that is as nearly aneutronic as possible; a steady-state operation; an operation at high beta, with a plasma stability index greater than $\beta = 0.20$; the use of direct conversion or direct production of thrust to minimize the power flows that must be handled by heavy energy conversion equipment; and a value of the system-specific mass below $\alpha = 5$ kg/kW(electric), to be competitive with fission systems for space applications. Only the deuterium-tritium reaction appears feasible for magnetic fusion reactors having large recirculating power flows; for reactors with little recirculating power, the best all-around fusion reaction for space applications appears to be D^3He.

I. INTRODUCTION

It is very probable that only nuclear fission or nuclear fusion energy will be capable of satisfying space-related requirements for more than a few hundred kilowatts of steady-state electrical power. Early work at the National Aeronautics and Space Administration (NASA) Lewis Research Center on fusion propulsion systems between 1958 and 1978 (Refs. 1 and 2) examined the application of steady-state fusion reactors, generating several hundred megawatts of thermal power, to direct fusion rockets for manned interplanetary missions. More recent design studies of fission and fusion space electrical power systems[3-6] have addressed the long-term needs of the strategic defense initiative (SDI) program, for which a requirement of 1 to 10 MW of steady-state electrical power is anticipated, with a further possible requirement of up to several hundred megawatts of "burst" electrical power for periods of hours. A preliminary report on advanced fusion power for space applications of interest to the U.S. Department of Defense (DOD) has recently been published by the National Academy of Sciences, under the sponsorship of the Air Force Studies Board.[7] The data in this report indicate that fusion power and propulsion systems may have a lower specific mass (kilograms per kilowatt of electrical power) than that anticipated for fission electric systems.

The above-mentioned studies[1-6] described several ways in which fusion energy may be applied to space power and propulsion systems. Figure 1 shows a fusion electric propulsion system with a heat cycle, in which the fusion energy appears as the enthalpy of a working fluid, which is processed through a conventional energy conversion system characterized by very large radiators. This system radiates the waste thermal energy into space and produces electrical power from a generator driven by shaft horsepower. A modified fusion electric propulsion system may be possible, in which the energy of charged particles from the plasma is transformed into electrical power by a direct converter, operating like an inverse Van de Graaff generator. In either case, the electrical power can be used for SDI applications, to supply the needs of an orbiting space station or as input into some form of electrical propulsion.

ENERGY FORM:

HEAT   MECHANICAL   ELECTRICAL   JET KINETIC
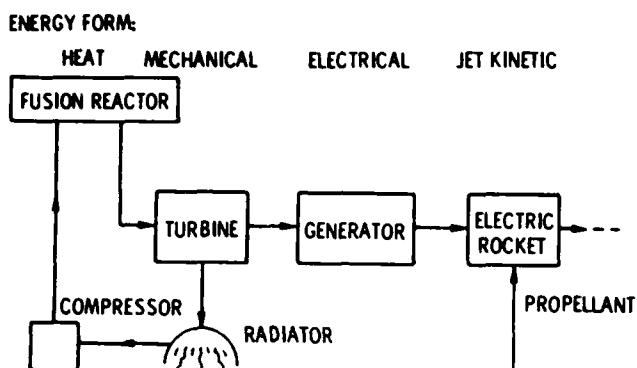
Fig. 1. Fusion electric space propulsion system.

ENERGY FORM:

PARTICLE KINETIC   JET KINETIC
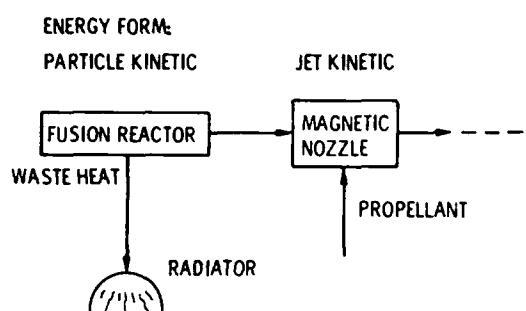
Fig. 2. Direct fusion rocket.

The most effective propulsion system, which minimizes the size of the radiator required and the total mass, is the direct fusion rocket shown in Fig. 2. In this propulsion system, the escaping unreacted fuel and reaction products are expanded in a magnetic nozzle, where they are mixed with cold propellant to achieve a unidirectional plasma jet with a spread of velocities, but an optimum mean exhaust velocity.[8] If an aneutronic fusion reaction (one which produces few neutrons from all sources, including side reactions) is used, and if all the unburned reaction products appear in the exhaust jet, relatively little heat energy remains on board the spacecraft to be disposed of by massive radiators. This direct propulsion system may either require a very high burnup fraction or waste what might be a scarce or expensive fuel.

Design studies have been made of both magnetic and inertial fusion power plants for space applications. Figure 3 is a schematic of the major subsystems of a direct fusion rocket based on a toroidal reactor with a magnetic nozzle consisting of a magnetic divertor.[2] This magnetic nozzle removes the outwardly diffusing unburned fuel and reaction products from the plasma and injects cold propellant to lower the average jet velocity to values appropriate to the mission of interest. The equipartitioned energy of the unburned fuel

and reaction products is converted, by conservation of the magnetic moment, into virtually unidirectional motion when the exhaust jet is expanded to weaker magnetic fields.

Figure 4 shows one of many schemes suggested for space propulsion using inertial fusion. In this concept, a laser or charged-particle beam is fired at a deuterium-tritium (D-T) pellet that explodes, after which the propellant and some of the filler material bounce off a pusher plate, located at a sufficient distance so that significant ablation does not occur. This pusher plate is connected to the vehicle by springs and dashpots, which absorb and transmit momentum to the spacecraft. Sometimes a magnetic field, which "catches" the charged reaction products, replaces the pusher plate in this concept. The repetitive explosion of these fusion microbombs can yield high accelerations and short interplanetary round trip times. In most inertial fusion schemes, 14-MeV neutrons, 3.5-MeV ^{4}He ions, radiation, and other materials are emitted isotropically (except those that intercept the pusher plate) into space.

I.A. Scope

This paper examines some of the constraints on fusion reactions, plasma confinement systems, and fusion reactors that are imposed by such space-related missions as manned or unmanned operations in near earth orbit, interplanetary missions, or requirements of the SDI program. The principal performance parameter used to compare various power plant options for space application is the specific mass, the kilograms of power plant mass per unit of electrical or thermal power generated by the power plant. Minimization of this parameter should reduce to a minimum the initial mass in earth orbit of the power plant and also minimize the cost, to the extent that the cost of the power plant is proportional to its mass. Fusion propulsion systems should, in addition, be capable of operating over a wide range of specific impulse (exhaust velocity), including the optimum for a particular mission, but this appears to be relatively easy to accomplish with direct fusion rockets.

Of the many constraints on space power and propulsion systems, those arising from safety and environmental considerations are emphasized in this paper, since these considerations place severe constraints on some fusion systems and have not been adequately treated in previous studies. This paper first examines the literature of space applications of fission and fusion energy to summarize the performance of such systems in tabular form. Then, the factors that affect the selection of fusionable fuels are discussed, followed by a consideration of factors that affect the choice of confinement concept. Finally, some conclusions are drawn on the basis of currently available information about the choice of fission versus fusion power for space applications, the choice of magnetic
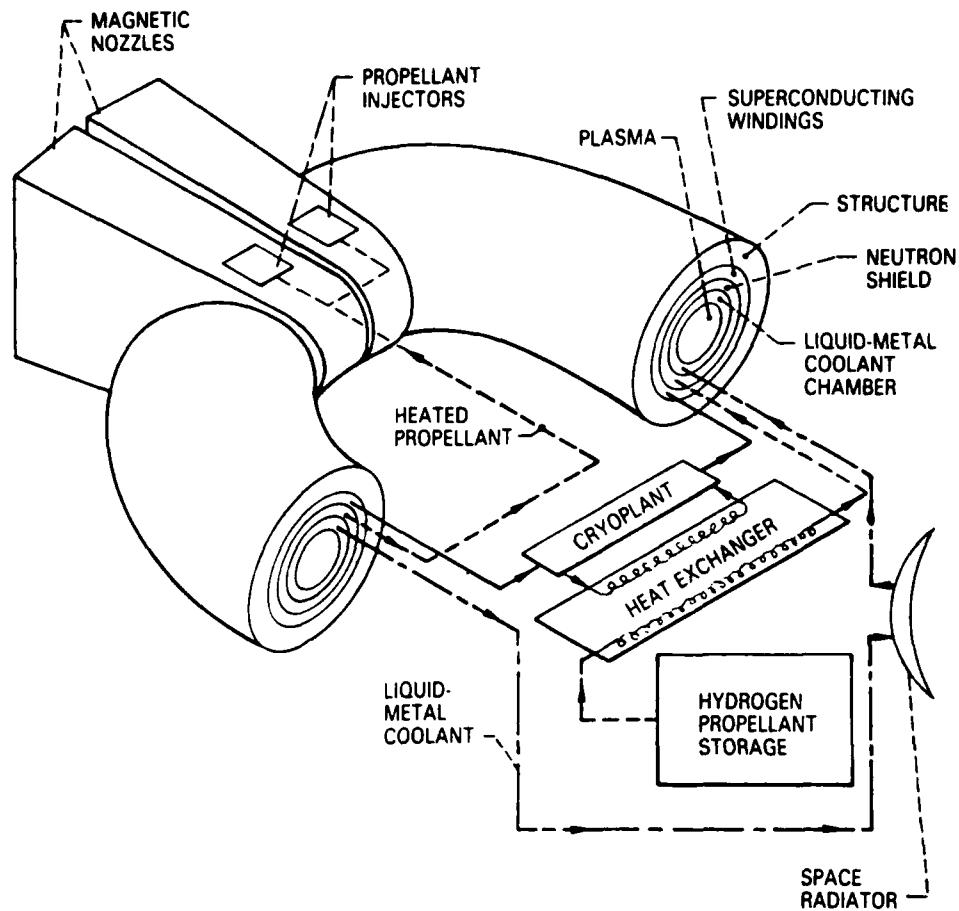
Fig. 3. Major subsystems of toroidal fusion rocket propulsion system.

versus inertial fusion, the best apparent choice of fusion reaction, and the constraints that magnetic containment concepts must satisfy for space applications.

II. PERFORMANCE OF SPACE POWER AND PROPULSION SYSTEMS

Mission studies of space power and propulsion systems go back at least 30 yr. An early focus of such effort was at the NASA Lewis Research Center, where fusion-related research and development totaling several hundred person-years was conducted from 1958 to 1978. A present long-term concern of NASA, the Air Force, and the SDI program is the generation of electrical power in space over extended periods of time (>1 d····) at the multimegawatt level. The performance param···er relevant to this application is the electrical-specific mass, measured in kilograms per kilowatt of electrical power produced. A further long-term concern of NASA, and possibly the Air Force, is direct nuclear space propulsion systems in which thrust is provided either by heated hydrogen propellant, in the case of fission propulsion systems, or energetic fusion

reaction products and unburned fuel mixed with additional propellant, in the case of direct fusion propulsion systems. The performance parameter relevant to such direct propulsion applications is the thermal-specific mass, measured in kilograms per kilowatt of thermal power produced.

II.A. Performance of Fission Systems for Space Applications

Table I lists the specific masses of fission electric and direct fission rocket propulsion systems taken from selected studies made over the past 20 yr (Ref. 7). These are consistent in predicting specific masses of 25 to 30 kg/kW(electric) for space systems operating at a level of a few hundred kilowatts of electrical power and 4 to 9 kg/kW(electric) for multimegawatt systems.

II.B. Performance of Space Fusion Propulsion Systems

Figure 5 shows the distribution of specific mass in a direct fusion rocket based on the concept illustrated in Fig. 3 (Ref. 2). This was a relatively detailed parametric study in which the mass of the propulsion system was obtained as a function of the strength of the
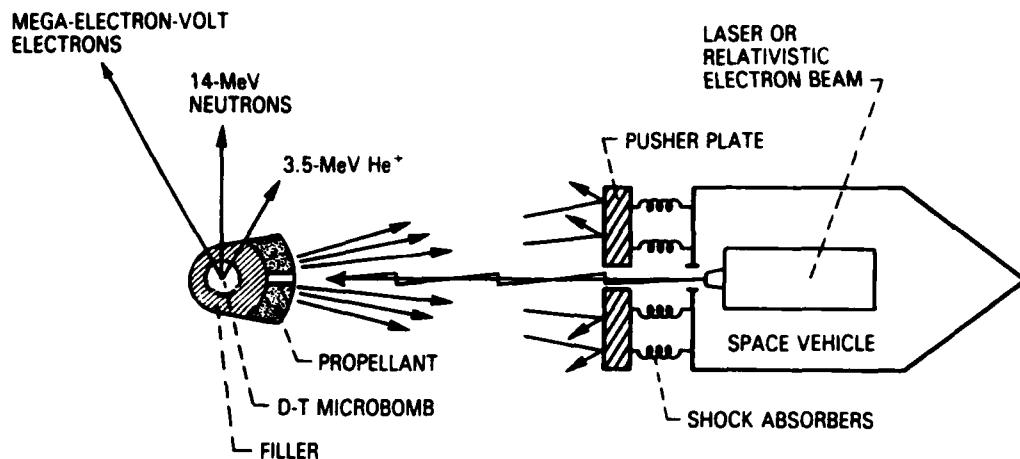
Fig. 4. Inertial fusion propulsion system.

TABLE I

Specific Masses of Fission Power Systems

| Item	System	Direct Rocket [kg/kW(thermal)]	Electrical Power [kg/kW(electric)]	Total Power Level	Reference
1	Direct fission rocket	0.0025	---	50 to 70 MW(thermal)	7
2	Fission electric system	---	4.0	7.5 to 15 MW(electric)	7
3	Fission electric system	---	5.0	5 to 10 MW(electric)	5
4	Goal of DOD fission electric system	---	30.0	100 kW(electric)	7
5	NASA SNAP studies 1965 through 1970 fission electric systems	---	7.0 to 9.0	10 MW(electric)	1 and 2
6	Small fission electric systems	---	25.0	0.1 to 1.0 MW(electric)	6
7	Large fission electric systems	---	5.0	1.0 to 10 MW(electric)	6
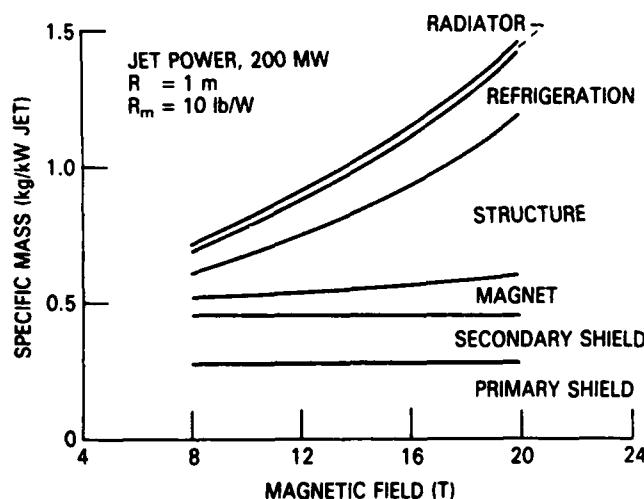
Fig. 5. Distribution of the system-specific mass in a D^3He direct fusion rocket in which 200 MW appears in charged-particle energy.[2]

magnetic induction in the plasma. This direct fusion rocket employed the D^3He reaction and had a plasma radius of 1 m. As is evident, the largest contribution to the mass of the overall system is shielding, and, at higher magnetic inductions, structure required to bear the magnetic forces.

The distribution of specific mass in Fig. 5 is characteristic of direct fusion rockets in that the radiator is a small fraction of the overall mass. In aneutronic direct fusion rockets, it is possible to "dump overboard" thermal energy in the form of reaction products and unburned fusion fuel with the propellant, rather than having to dispose of this thermal energy through massive energy conversion systems and radiators. In design studies of fusion electric systems, like those shown schematically in Fig. 1, the overall contribution of the radiators to the system mass is much larger because of the necessity of handling large amounts of thermal energy with massive energy conversion systems.

II.C. Relative Performance of Fission and Fusion Systems

Table II lists the specific masses of fusion power systems quoted in Ref. 7. Projections of this nature must be viewed with caution because the depth of the studies varies greatly, e.g., they range in their level of effort from a few person-weeks to several person-years. The specific masses in Table II can be grouped in three broad categories:

1. those from recent design studies done under U.S. Department of Energy (DOE) auspices (DOE 1 through 7)

2. those from recent non-DOE-supported design studies (non-DOE 1 through 7)

3. detailed NASA mission studies from 1958–1978 and a recent design of a laser fusion rocket (NASA 1, 2, and 3).

The design studies quoted as DOE 1, 2, and 3 were "mainline" D-T tokamak or D-T tandem mirror electric utility power plants. The thermal-specific mass, in kilograms per kilowatt of thermal power produced, quoted in DOE 1 and 2, is for the "fusion island" only and is already at the level of 6 to 7 kg/kW(thermal). If the mass of steam generators, turbines, generators, and all other balance of plant (BOP) equipment are neglected, the electrical specific mass of these mainline reactors would be a minimum of 13 to 21 kg/kW(electric). Realistically, specific masses at least double or triple these values can be expected if the BOP is accounted for. This is illustrated by DOE 3 in Table II for the D-T STARFIRE study, which arrived at an electrical specific mass of 53 kg/kW(electric) even without the massive radiators that would be required for space applications.

Entries DOE 4, 5, and 6 in Table II are DOE-sponsored design studies based on advanced fuels (DOE 4) or alternate confinement concepts (DOE 5 and 6), which are not currently a mainline objective of the DOE program. These indicate some improvement in specific mass, but even DOE 4, at 16 kg/kW(electric), is not competitive with the 4 to 9 kg/kW(electric)

TABLE II

Specific Masses of Fusion Power Systems

Item	System	Direct Rocket [kg/kW(thermal)]	Electrical Power [kg/kW(electric)]	Total Power Level	Reference
DOE 1	STARFIRE fusion island[a]	7.2	21[a]	3.51 GW(thermal)	9
DOE 2	Mirror Advanced Reactor Study fusion island[a]	5.7	13[a]	3.5 GW(thermal)	13
DOE 3	D-T STARFIRE power plant	---	53	1.2 GW(electric)	12[b]
DOE 4	D³He STARFIRE power plant	---	16	≈1.2 GW(electric)	12[b]
DOE 5	Reversed-field pinch reactor fusion island[a]	4.0	16[a]	~3 GW(electric)	7
DOE 6	Elmo Bumpy Torus Reactor fusion island[a]	11.0	36[a]	~4 GW(thermal)	7
DOE 7	Target recommended to DOE for fusion power plants	---	10	Unspecified	10
Non-DOE 1	Migma fusion electric	---	~2 to 3	1 MW(electric)	15,16
Non-DOE 2	Migma fusion electric	---	1.0	>8 MW(electric)	15,16
Non-DOE 3	D³He SAFFIRE field-reversed mirror reactor	5.0	5.5[c]	800 MW(thermal)	11
Non-DOE 4	Ohmically Heated Toroidal Experiment/ compact reversed-field pinch reactor fusion island[a,d]	0.33	---	1 GW(thermal)	14,18,19
Non-DOE 5	D³He tandem mirror reactor	0.5	1.0[c]	1 GW(thermal)	4[b]
Non-DOE 6	CANDOR fusion island[a]	8.2	---	61 MW(thermal)	7
Non-DOE 7	Solar-assisted reactor SDI burst power	---	0.50	1 GW(electric)	3
NASA 1	D³He direct rocket lower limit NASA studies	0.5	1.0[c]	200 MW(thermal)	1,2
NASA 2	D³He direct rocket upper limit NASA studies	3.0	3.5[c]	200 MW(thermal)	1,2
NASA 3	Laser fusion rocket	0.009	---	54 GW(thermal)	17

[a]Reactor only—no energy conversion equipment. Kilograms per kilowatt(electric) were found by dividing reactor mass by power plant net electrical power.
[b]See Ref. 20.
[c]Here, 0.5 kg/kW(electric) is added to D³He fusion systems for direct converter mass.
[d]This work was partially supported by Los Alamos National Laboratory.

expected of the fission electric space power systems listed in Table I.

Not only are these DOE mainline and alternate confinement concepts not competitive with fission electric systems for space applications by a large factor, but also there is concern within the fusion community that the fusion reactors represented by DOE 1 through 6 have such high specific masses that they may not be competitive for the ground-based electrical utility power plants for which they are intended. Accordingly, in 1984, the DOE charged panel 10 of its Magnetic Fusion Advisory Committee to survey fusion and fission primary energy sources and recommend a long-term target for future fusion reactors. Their recommendation, 10 kg/kW(electric), is listed as DOE 7.

The second group of design studies, non-DOE 1 through 7, produced specific masses ranging from 1.0 to 5.5 kg/kW(electric) for power levels ranging from 1 MW(e' .. i:c) to 1 GW(thermal). The third group of NASA design studies includes early (1958 to 1978) mission studies in which many person-years were invested (NASA 1 and 2). These produced specific masses in the range from 1 to 3.5 kg/kW(electric).

All of the NASA and non-DOE design studies, which use alternate confinement systems and/or advanced fuels, are consistent with specific masses of 2 to 3 kg/kW(electric) for multimegawatt systems as a reasonable expectation. Such values not only represent a factor of 2 to 3 improvement over projected fission electric systems but also are significantly less than the target suggested by DOE's panel 10 of the Magnetic Fusion Advisory Committee.

III. FACTORS AFFECTING FUSION FUEL SELECTION

III.A. Tritium in Space

Whatever the merits of the D-T reaction for electric utility power plant reactors, the constraints of the space environment, discussed below, make it desirable to consider other fusion reactions. Utilization of the D-T, deuterium-deuterium (D-D), or catalyzed D-D reactions would necessitate the use (f radiologically significant amounts of tritium in space, and one must ask whether the risks of doing so can be reduced to acceptable levels.

A benchmark for large-scale radiological accidents was established by the Chernobyl nuclear accident of April 1986 (Refs. 21 and 22). The approximate radioactive source terms and inventories associated with this accident are listed in the first column of Table III. As a consequence of this accident, ~50 MCi of biologically inert noble gases, mostly krypton and xenon, were released into the atmosphere. An additional 50 MCi of biologically active fission products were released and spread over a large portion of the Eurasian continent. It is instructive to compare these inventories

TABLE III

Fission and D-T Fusion Radiological
Hazard Comparison

Reactor Characteristic	Chernobyl Accident	STARFIRE D-T Tokamak
Biologically inert (noble) gas release (MCi)	~50	---
Biologically active radiation release (MCi)	~50	---
Tritium inventory (11.6 kg) (MCi)	---	~111
Core/blanket inventory (MCi)	~1500	6140

with the radioactive inventories associated with the STARFIRE D-T tokamak reactor,[9] a gigawatt level power plant fusion reactor. The STARFIRE reactor had a total tritium inventory of 11.6 kg, which is ~110 MCi of volatile radioactive material. This is more than twice as great as the biologically significant (non-noble gas) radioactivity released during the Chernobyl accident.

By comparing inventories and source terms in curies, it is intended to provide an indication of relative public acceptability, public perception of relative risk, and relative immediate consequences of an accident. Such immediate consequences include exposure of operating staff and emergency crews, the necessity of evacuating large areas, and other emergency measures taken for public safety. Long-term consequences such as genetic or somatic damage to individuals or populations would require, in addition, consideration of the relative biological effectiveness (RBE) of each species released, along with its environmental pathway and source term. While the RBE may be useful for assessing the long-term consequences of a particular accident, it probably has little impact on the social acceptance of a nuclear technology prior to its introduction.

If a D-T reactor were used in space, the penalties associated with a lithium-breeding blanket for the tritium would probably be so great that tritium fuel would be supplied from ground-based sources. In a direct fusion rocket, or in a fusion electric system based on a direct converter, it will be very difficult to recover the unburned tritium, and it is therefore prudent to assume that all unburned tritium is lost to space and unavailable for reinjection into the reactor. Since the burnup fraction of tritium will likely be in the 5 to 30% range for D-T reactors, much more tritium will be required to fuel a reactor than is actually burned to produce electrical power or propulsion. Depending on the power level, from 10 MW(thermal) to 1 GW(thermal), a space power or propulsion system might use from ~0.03 to 3 kg of tritium per day.

Safety considerations make it necessary to be concerned both about lifting this tritium fuel into orbit in the first place and then assuring that it does not reenter the atmosphere.

The particles trapped in the earth's magnetosphere are supplied by the solar wind and consist mostly of hydrogen with a small admixture of helium and other elements. If all of the hydrogen trapped in the magnetosphere was liquified, the liquid hydrogen would approximately fill an olympic-sized swimming pool. Thus, the total amount of matter in the magnetosphere is not very great, and one must be seriously concerned about the effects of adding charged particles or significant amounts of additional matter to that already present in the magnetosphere. The amount of matter in the magnetosphere is comparable to the propellant exhausted by many propulsion systems as they move through it. Since most particles trapped in the magnetosphere eventually find their way into the earth's atmosphere, one must be concerned about the possible effects of injecting tritium ions in the magnetosphere, which are later precipitated into the atmosphere by magnetohydrodynamic instabilities.

If tritium or any other radioactive nuclear fuel is used in space, the following accident scenarios must be addressed: (a) a Challenger-type accident in which the space shuttle ferrying the tritium into orbit blows up in the atmosphere and releases the tritium inventory, (b) reentry of the fuel inventory into the atmosphere as a result of atmospheric drag or an unintended change in the orbital elements of a spacecraft with a fusion reactor on board, or (c) leakage of unburned fusionable fuel into the atmosphere by such routes as trapping of its ions in the magnetosphere, followed by auroral precipitation in the earth's atmosphere.

III.B. Neutron Fluxes in Space

Probably the single most important factor in optimizing a space power or propulsion system is to minimize the initial mass that must be placed in earth's orbit, since transportation into orbit is very expensive. In consequence, there is a strong temptation to omit shielding to the maximum extent possible to conserve mass. The 14-MeV neutrons produced by the D-T reaction require at least 1 m of shielding to be slowed down. A spectrum of blanket designs is possible, ranging from full shielding to a bare reactor. In very unusual circumstances, a partially or fully shielded neutronic reactor might be lighter than a bare aneutronic reactor, but this appears unlikely in view of the mass penalty of radiators and energy-handling equipment required to deal with the thermal energy deposited in the shield. Here, we assess the environmental consequences of the limiting case, a bare reactor.

It has not always been realized that unshielded fluxes of neutrons, charged particles, and X rays can pose a serious environmental hazard over surprisingly large distances from an unshielded source. Let us consider a bare, unshielded fusion reactor, and focus on the consequences of an unshielded flux of neutrons from such a reactor. The flux of neutrons Φ_L from a point source of S neutrons per second at a distance of R_L is given by

$$\Phi_L = \frac{S}{4\pi R_L^2} \ \text{n/m}^2 \cdot \text{s} \ .. \tag{1}$$

The relationship among the power lost in the form of neutrons p_N, the total fusion power p_F, and the fraction of the power in neutrons f_N is given by

$$p_N = f_N p_F \ , \tag{2}$$

while the power in charged particles p_C is given in terms of the total fusion power produced by

$$p_C = (1 - f_N)p_F \ . \tag{3}$$

Combining Eqs. (2) and (3), the relation among the neutron power, the power in charged particles, and the fraction of the power in the form of neutrons is given by

$$p_N = \frac{f_N p_C}{1 - f_N} \ . \tag{4}$$

The source term from an unshielded fusion reactor generating neutrons is given in terms of the total neutron power P_N in megawatts, the electronic charge $e = 1.60 \times 10^{-19}$ C, and the energy E_N of the individual neutron in mega-electron-volts as follows:

$$S = \frac{P_N \ (\text{MW})}{eE_N \ (\text{MeV})} = \frac{f_N p_C \ (\text{MW})}{(1 - f_N)eE_N \ (\text{MeV})} \ \text{n/s} \ , \tag{5}$$

where Eq. (4) has been substituted for the neutron power in Eq. (5). By substituting Eq. (5) into Eq. (1) and solving for the standoff distance R_L, one obtains

$$R_L = \left[\frac{f_N p_C \ (\text{MW})}{4\pi e\Phi_L(1 - f_N)E_N \ (\text{MeV})} \right]^{1/2} \ \text{m} \ . \tag{6}$$

It is of interest to calculate the standoff distance based on radiological safety considerations for a typical fusion propulsion system. The design studies of Refs. 1 and 2 indicate that a propulsion system utilizing a direct fusion rocket might require ~200 MW of charged-particle power in the exhaust jet. For pure D-T fusion, the fraction of the energy released in the form of neutrons is $f_N = 0.80$, and the neutron energy $E_N = 14.1$ MeV. The occupationally acceptable safe dose for 40 h/week exposure to mega-electron-volt neutrons is ~10 n/cm^2·s^{-1} or 10^5 n/m^2·s^{-1} (Ref. 23). Since such a fusion propulsion system would start out orbiting the earth, the natural unit of length used to measure the standoff distance is the earth radius, $R = 6378$ km.

The neutron fraction, neutron energy, and safe standoff distance under the above assumptions are shown for an unshielded fusion reactor with isotropic neutron production in Table IV for five fusion reactions. The safe distances, beyond which the neutron

fluxes are below the occupational standard, are also given in earth radii. Clearly, an unshielded fusion reactor will generate such a large neutron flux that no unshielded person or thing can approach safely within a very large distance of it. If a more demanding standard was used, for example, 10% of the background radiation level, these standoff distances would be still larger. Note that the same consideration applies to

both unshielded magnetic and inertial fusion reactors, since the average of 200 MW for an unshielded propulsion system is based on the average power required for interplanetary missions.

Some of the environmental hazards posed by an *unshielded* fusion reactor in space are summarized in Fig. 6. These hazards could include the effects of neutrons, energetic reaction products, unburned fuel ions,

TABLE IV

Safe Distance from Unshielded Fusion Reactor with Isotropic Neutron Production*

Reaction	Neutron Fraction, f_N	Neutron Energy, E_n (MeV)	Safe Distance, R (km)	R/R_0
D-T	0.80	14.07	16 800	2.6
D-D	0.336	2.45	14 300	2.2
Catalyzed D-D	0.38	8.26	8 600	1.4
D^3He	0.02	2.45	2 900	0.45
p^6Li	0.05	1.75	5 500	0.86

*In this table we assume that (a) there is 200 MW of charged-particle power, (b) a radiologically safe dose for continuous exposure to mega-electron-volt neutrons is 10 $n/cm^2 \cdot s$, and (c) the earth radius $R_0 = 6378$ km.
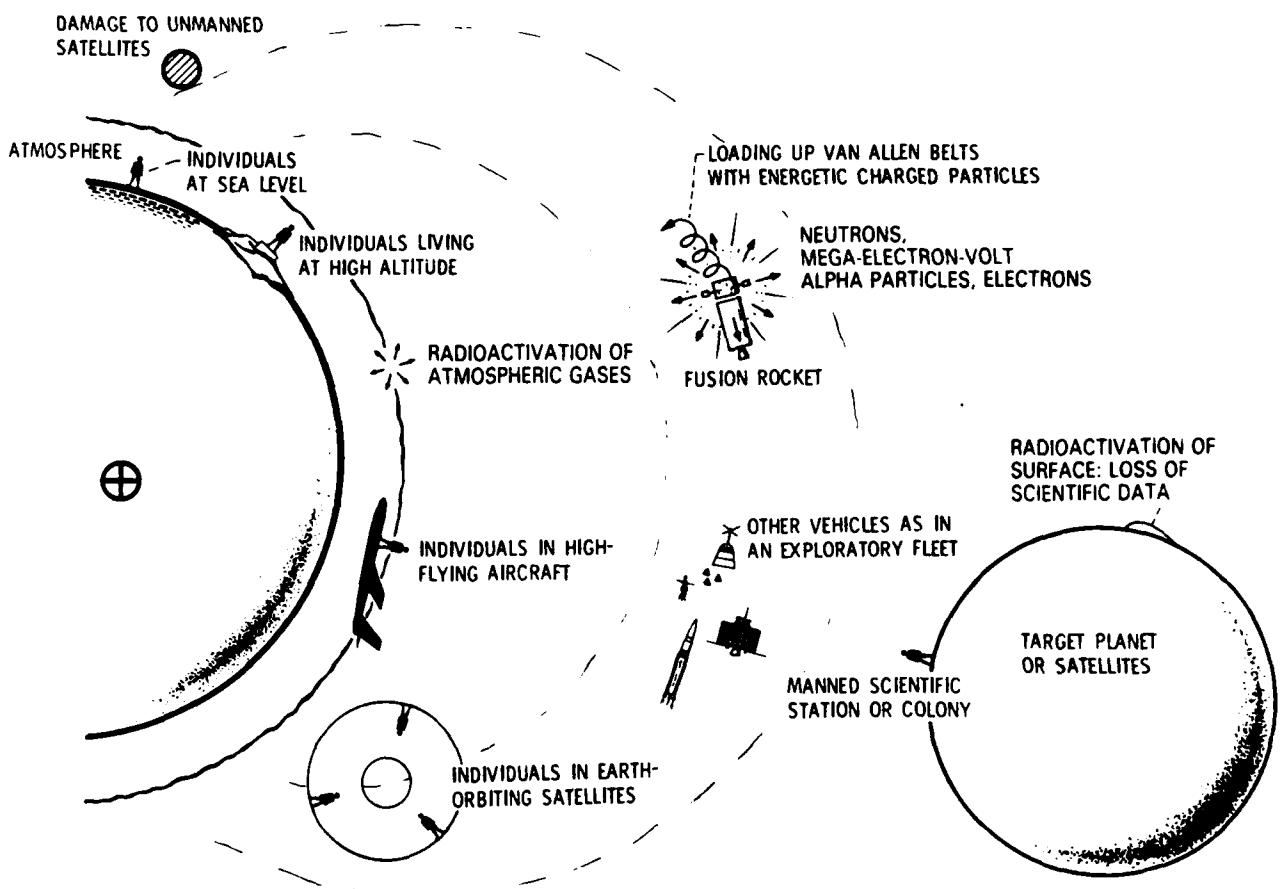

Fig. 6. Potential environmental hazards of fusion propulsion systems.

electrons, and X-ray radiation. At least some of these hazards would result from the use of a bare reactor, regardless of the fusion reaction used. These forms of radiation could load up the magnetosphere with energetic charged particles; cause damage to unmanned satellites in earth orbit; damage other spacecraft, as in an exploratory fleet or a space shuttle; affect individuals in earth-orbiting satellites or in high flying aircraft; activate atmospheric gases by direct interaction; and affect, at optical frequencies, the work of individuals such as astronomers at high altitudes or even at sea level.

The detrimental environmental effects of an unshielded fusion reactor are not limited to low earth orbit. If such an unshielded fusion reactor or propulsion system were to approach another planet or satellite, the unshielded radiation could lead to activation of the surface and loss of scientific data. It could affect a manned scientific station or colony. Unshielded radiation on a target planet or satellite surface could alter or erase the cumulative effect of aeons of integrated information from the solar wind, cosmic rays, or other long-term surface interaction processes.

The above considerations make it clear that neutrons should be shielded and not allowed to escape directly into space. Consequently, their thermal energy must be disposed of. In space, the only way in which an isolated spacecraft can dispose of waste heat is by radiation, and the necessary radiators then represent a significant mass penalty that must be paid to accommodate the presence of neutrons. These considerations suggest strongly that the best way of avoiding what must be either a safety hazard or a mass penalty is to use fusion reactions that generate the minimum possible amount of neutron, radiant, or thermal energy.

III.C. Neutronic Activation of Structure

Both fission and fusion reactors will activate their shielding and structure to some extent. In fission reactors, activation arises from fission products and the interaction of low energy (below 1-MeV) neutrons with the core and shielding materials; in fusion reactors, the activation arises from 14.1- or 2.45-MeV neutrons, which activate the material of the first wall and blanket. The magnitude of this activation is evident in the last line of Table III, where the nonvolatile core or blanket inventory is listed for the Chernobyl reactor at the time of the accident on April 26, 1986 (Refs. 21 and 22) and for the STARFIRE D-T tokamak after 1 yr of operation.[9] These inventories were the result of about a year of full-power operation at 1 GW of electrical power output in each case. These inventories are ~30 and 120 times, respectively, the radioactive release of the Chernobyl accident and are clearly much too large to dump into the atmosphere. Thus, any fission or D-T fusion reactor, once operated in space, is

likely to become a serious radiological safety hazard upon reentry into the atmosphere.

In low earth orbit, there is a narrow band of orbital altitudes within which manned operations are possible. Below ~300 km, atmospheric drag is so large that the orbit of a space station would decay in a relatively short period of time; above ~500 km, radiation fluxes from particles trapped in the magnetosphere are sufficiently high so that sustained manned operations are not possible. Parenthetically, it is not generally realized that the Apollo astronauts acquired a whole-body radiation dose of 50 rads during one round trip through the earth's magnetosphere. This is ~$\frac{1}{10}$ of the L-50 fatal dose.

Because of the hazard of the radioactive inventory of fission or fusion reactors, these reactors should be parked, after use, in a "nuclear safe orbit"; that is, an orbit that is sufficiently high above the earth's surface that atmospheric drag will not cause the reactor to reenter the atmosphere until the longest lived radionuclide of any significance decays. For fission reactors, the lowest nuclear-safe orbit is ~700 km, thus placing the parking orbit for nuclear fission reactors beyond the 500-mile limit where manned operations are possible. The radionuclides in activated D-T tokamak fusion reactors are, in most blanket designs, not as long lived as those of fission reactors and their nuclear-safe orbit may be somewhat lower than the 700 km appropriate for fission reactors.

The fact that the nuclear-safe orbit is likely to be above the altitude band where manned operations are possible leaves open the possibility that a fission or fusion reactor associated with a manned space station might reenter the atmosphere. If it did so, the last line of Table III implies that an amount, in curies, of radioactive material could be released into the atmosphere by the reentry process, which would be ~30 times the Chernobyl release for a gigawatt fission reactor, and ~120 times the Chernobyl release for a D-T fusion reactor comparable to the STARFIRE tokamak.

III.D. Performance of Fusion Fuels

The choice of a fusion reaction for space power and propulsion purposes depends on its performance in a burning plasma. Consider the idealized fusion power plant shown in Fig. 7 (Ref. 24, Chap. 8). In this power flow diagram, the plasma heating power needed to maintain the plasma in the steady state p_H and the fusion power p_F appears as thermal energy and is converted by an energy conversion system with efficiency η into a gross electrical power p_G. A fraction F of this gross electrical power is returned as recirculating electrical power p_R to keep the reactor operating. This recirculating electrical power is converted into plasma heating power with an efficiency η_i. Recirculating power required for purposes other than plasma heating

A-9
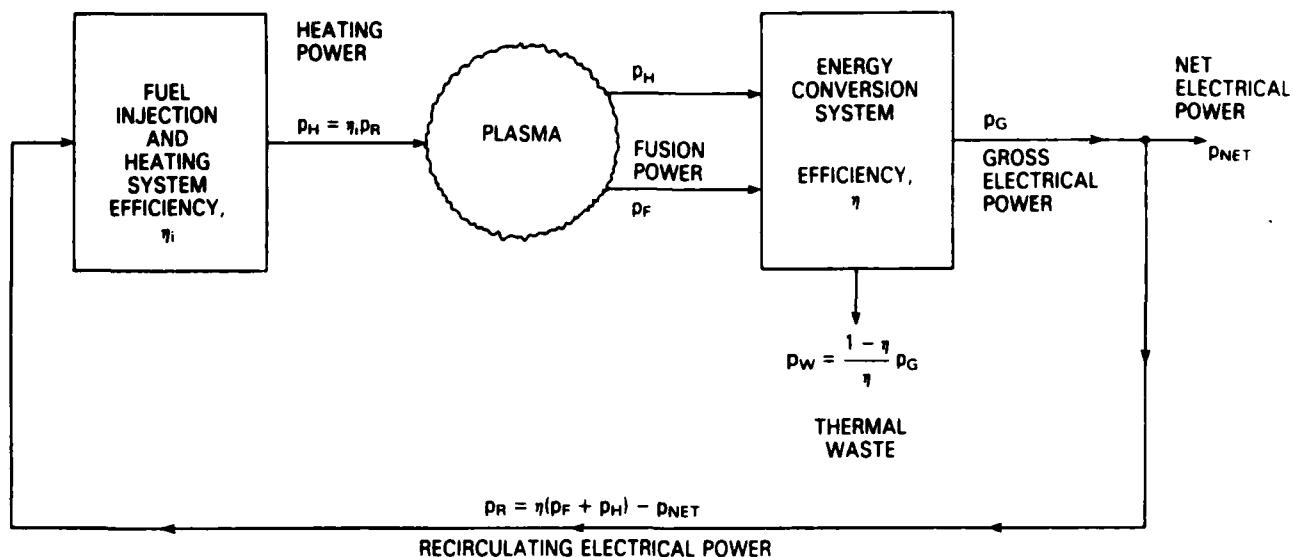
Fig. 7. Power flows in an idealized fusion power plant.

(such as cryogenic refrigerators or resistive coil losses) can be accounted for in this model by decreasing η_i below its true value to cover such requirements.

It can be shown (Ref. 24, p. 261) that the Lawson parameter $n_i \tau_c$, the product of number density and ion containment time, for the idealized fusion power plant shown in Fig. 7 is given by

$$n_i \tau_c = \frac{\frac{3}{2} e T' G(\gamma, Z)\left(\frac{1}{F \eta \eta_i} - 1\right)}{M E_{12} g_{12} \langle \sigma v \rangle_{12} - S(T')^{1/2} H(\gamma, Z)\left(\frac{1}{F \eta \eta_i} - 1\right)} ,$$

(7)

for a plasma with two fuels of mixture ratio γ and atomic numbers Z_1 and Z_2, where the ion and electron kinetic temperatures are assumed to be equal, e is the electronic charge, 1.602×10^{-19} C, the bremsstrahlung constant is $S = 1.625 \times 10^{-38}$, T' is expressed in electron volts, the parameter $G(\gamma, Z)$ is given by

$$G(\gamma, Z) = [1 + \gamma Z_1 + (1 - \gamma) Z_2] ,$$

(8)

the parameter $H(\gamma, Z)$ is given by

$$H(\gamma, Z) = [\gamma Z_1 + (1 - \gamma) Z_2]$$
$$\times [\gamma Z_1^2 + (1 - \gamma) Z_2^2] ,$$

(9)

the parameter g_{12} is given by

$$g_{12} = \gamma(1 - \gamma) \text{ unlike fuels} \qquad (10a)$$

and

$$g_{12} = \frac{1}{2} \text{ like fuels} , \qquad (10b)$$

and the heating power fraction $F \eta \eta_i$ is given by

$$F \eta \eta_i = \frac{\text{plasma heating power}}{\text{gross thermal output power}} . \qquad (11)$$

Equation (7) is a generalization of the Lawson criterion, which, in its original form, applied only to fusion power plants with 100% efficient plasma heating equipment ($\eta_i = 1.00$) and which also had no net power output ($p_{NET} = 0$). The parameter M in the denominator of Eq. (7) is the blanket multiplication factor, which accounts for additional energy generated in the blanket by, for example, neutron-induced reactions.

The power flow diagram in Fig. 7 demonstrates that the relationship among the heating power fraction, the power produced by fusion reactions p_F, and the required plasma heating power p_H is given by (Ref. 24, p. 259)

$$F \eta \eta_i = (p_H + p_F) = p_H . \qquad (12)$$

Because of the mass and reliability penalties associated with recirculating power flows in a magnetic fusion reactor, it is normally desirable that a fusion power plant for space application be self-sustaining (Ref. 24, p. 269), which means that the cold incoming fuel is heated to the reaction temperature by the charged reaction products. This condition for a self-sustaining fusion reaction can be stated as

$$f_c p_F = p_H . \qquad (13)$$

That is, the plasma heating power is supplied by the energy of the charged reaction products, where f_c is the fraction of the fusion energy released in the form of charged particles.

By substituting Eq. (13) into Eq. (12), one obtains

an expression for the heating power fraction in terms of the fraction of charged particles,

$$F\eta\eta_i = \frac{f_c}{1 + f_c} \ . \tag{14}$$

At the heating power fraction given by Eq. (14), the idealized fusion power plant described by Eq. (7) will operate in a self-sustaining mode. If Eq. (14) is substituted into Eq. (7), one obtains the Lawson parameter $n_i\tau_c$, given by

$$\eta_i = \frac{\frac{3}{2} kTG(\gamma, Z)}{f_c ME_{12}g_{12}\langle \sigma v \rangle_{12} - S(T')^{1/2}H(\gamma, Z)} \ . \tag{15}$$

This equation describes the position on the Lawson diagram that must be met for a magnetic fusion reactor to be self-sustaining.

In subsequent discussions, it will be assumed that fusion power plants considered for space application are self-sustaining in the sense of satisfying the modified Lawson criterion of Eq. (15). The Lawson diagram for self-sustaining fusion burns is shown in Fig. 8. Also shown are the Lawson parameter $n\tau$ and ion kinetic temperature T_i, which will allow a self-sustaining fusion reaction to take place for the D-T, D^{3}He, catalyzed D-D, and uncatalyzed D-D reactions.

Table V lists the characteristics of seven fusion reactions that have been considered for space and ground-based applications. Rows 1, 2, and 3 are fundamental physical properties of the reactions. The ranges shown for the energy of neutrons in the second line result from the different mixture ratios for the

fuels that might be used and also from uncertainties in the cross sections and branching ratios of the side reactions involved. The subsequent calculations were done with a common set of input assumptions, including: all fuel species are Maxwellian; equal ion and electron kinetic temperatures for all but the last two lines of the table; a 50:50 mixture ratio for unlike fuels; complete loss of the reaction product tritium and ^{3}He for the D-D reaction, and complete burning of these reaction products for the catalyzed D-D reaction; no synchrotron radiation; no reaction product buildup; no impurities in the plasma; a self-sustaining fusion reaction in the sense of satisfying Eq. (13), for lines 7 through 15; and a zero-dimensional "point" plasma model with no profile or boundary effects.

The ideal ignition temperature in row 4 is the temperature above which more fusion energy is deposited in charged particles in the plasma than is radiated away as bremsstrahlung. A steady-state, self-sustained burn is impossible below this kinetic temperature if the ion and electron kinetic temperatures are equal. Two reactions — the p^6Li and the p^{11}B — are not ignitable at any temperature, by a factor given in row 5. These reactions could be operated in the steady state only if the electron temperature could somehow be kept well below the ion kinetic temperature.

The reactivity is a parameter that is proportional to the fusion power density in a plasma that operates with a fixed plasma stability index β and a fixed magnetic field (Ref. 24, p. 279). The reactivity is

$$R_{12} = \frac{E_{12}\langle \sigma v \rangle_{12}g_{12}}{4[1 + \gamma Z_1 + (1 - \gamma)Z_2]^2(T_i')^2} \tag{16}$$

and has a maximum at the kinetic temperature listed in row 6. The ratio of this maximum reactivity temperature to that of the D-T reaction is shown in row 7. Note that four fusion reactions need operate only at temperatures from 1.23 to 6.15 times that of the D-T reaction to achieve their maximum power density.

The value of the Lawson parameter $n\tau$ at the maximum reactivity for a self-sustaining magnetic fusion reactor is shown in row 8, and its ratio to that of the D-T reaction is shown in row 9. Only relatively small factors of improvement in $n\tau$ over D-T are required. In the case of the D-D reaction, the reactivity maximum is below the ideal ignition temperature, the Lawson parameter cannot be calculated for a self-sustaining reactor if the reactor is not ignitable, and not enough cross-section data on the ^{3}He reaction is available above 1 MeV to allow the Lawson parameter to be calculated for this reaction.

The ion kinetic temperature at the minimum of the Lawson curve for a self-sustaining reactor is shown in row 10, and the ratio of this temperature to that of the D-T reaction is shown in row 11. The kinetic temperatures required to burn catalyzed D-D and D^{3}He are only a factor of ~4 above that of D-T. Rows 12 and 13 show that the Lawson parameters required to burn
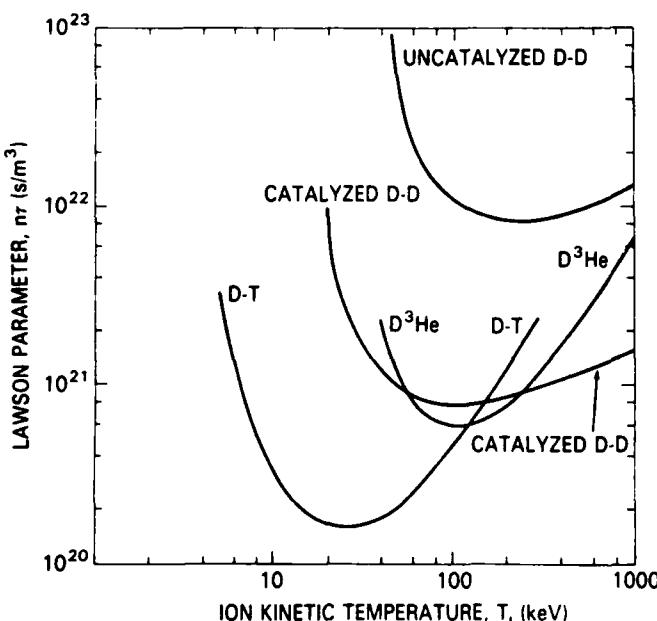

Fig. 8. Lawson diagram for self-sustaining fusion reactors utilizing the D-T, catalyzed D-D, D^{3}He, and uncatalyzed D-D reactions.

TABLE V

Fusion Fuel Characteristics*

Reaction Characteristics	Fusion Reaction						
	D-T	D-D	Catalyzed D-D	D³He	p^6Li	p^{11}B	³He³He
1. Fractional energy to neutrons, basic reaction (%)	80	33.6	38	0	0	0	0
2. Fractional energy to neutrons, basic + side react⁻ ...s (%)	80+	33.6	38	2 to 15	~5	~1	0
3. Energy released per reaction (MeV)	17.6	3.65	14.4	18.3	4.0	8.7	12.9
4. Ideal ignition kinetic temperature (keV)	4.2	42	18	32	a	a	820
5. Factor away from ideal ignition, p_B/p_F	---	---	---	---	4.6	3.0	---
6. Temperature of maximum reactivity (keV)	13	16	35	55	80	550	>1 MeV
7. Ratio of maximum reactivity temperature to that of D-T	1.0	1.23	2.69	4.23	6.15	42.3	>77
8. nτ at maximum reactivity (s/m³ × 10²⁰)	2.4	b	14	9.0	.	.	c
9. Ratio of nτ at maximum reactivity to that of D-T	1.00	---	5.83	3.75	---	---	---
10. Temperature of minimum Lawson parameter nτ (keV)	26	240	90	110	.	c	d
11. Ratio of temperature at nτ minimum to that of D-T	1.00	9.23	3.46	4.23	---	---	---
12. Minimum nτ for self-sustaining burn (s/m³ × 10²⁰)	1.60	84	7.4	6.0	.	.	d
13. Ratio of minimum nτ in (12) above to that of D-T	1.00	52.5	4.63	3.75	---	---	---
14. Cold electron nτ at maximum reactivity temperature (s/m³ × 10²⁰) for self-sustaining burn	2.12	120	11.2	6.06	384	51	>56
15. Ratio of cold nτ to that of D-T	1.0	56.6	5.28	2.86	18?	24	26.4

*In this table we assume that all fuel species are Maxwellian; $T_i = T_e$ for all but data in last two rows; 50:50 mixture ratio for unlike fuels; no synchrotron radiation; no reaction product buildup; no impurities in plasma; zero-dimensional, "point" plasma model; and lines 8 through 15 for a self-sustaining reactor.
aNot ignitable under assumptions above.
bIdeal ignition temperature is above temperature of maximum reactivity.
cUndefined for a nonignitable reaction.
dCross-section data not available above 1 MeV.

these reactions in a self-sustaining reactor are only a factor of ~4 above that of D-T. The Lawson curves for a self-sustaining fusion reactor are shown in Fig. 8 for the first four reactions listed in Table V.

Rows 14 and 15 show the Lawson parameter that could be achieved at the maximum reactivity temperature in row 6 if, somehow, the electrons could be kept cold enough for the bremsstrahlung radiation to be negligible. Here again, only modest increases above the Lawson parameter nτ required for the D-T reaction are needed for the catalyzed D-D and D³He reactions. The information in rows 6 through 15 indicates that, at least for magnetic fusion, the distance on the Lawson diagram from the D-T to the advanced fuel conditions is not as great as commonly supposed. The factors of 3 to 5 needed in kinetic temperature and the Lawson parameter to burn advanced fuels rather than

D-T are small compared to the many orders of magnitude in these quantities that have been achieved over the past two decades by the fusion community. These relatively small factors suggest that, at least for magnetic fusion, reactions other than D-T can be considered for space applications.

Figure 9 shows the D³He reaction for unequal electron and ion temperatures. The upper curve is the D³He self-sustaining Lawson curve also shown in Fig. 7. The curves below it show the effects of cooling the electron population to temperatures below that of the ion kinetic temperature. It is not clear what physical process could accomplish this result, but if the electron temperatures were made negligibly small, the minimum nτ of the D³He curve on the Lawson diagram would be comparable to that of the D-T reaction. Depressed electron kinetic temperatures could
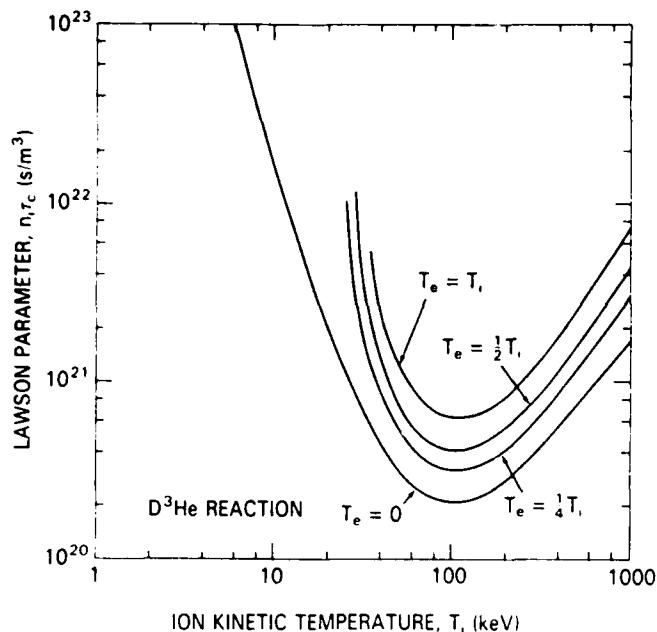
Fig. 9. Lawson diagram for the D³He reaction with unequal electron and ion kinetic temperatures.

also make such reactions as p^{11}B and p^6Li ignitable and greatly improve their attractiveness for reactor applications.

III.E. Availability of Fusionable Fuels

Most of the fusionable fuels listed in Table V are available for space applications in unlimited quantities. The only two fusionable fuels that may be in short supply are tritium and ³He. Tritium has a half-life for decay into ³He of 12.3 yr,

$$T \rightarrow^{12.3 \ yr} {}^3He + e \qquad (17)$$
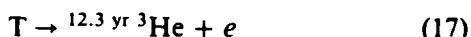
and is not found to any significant extent in nature. Helium-3 is a stable isotope of helium but is found with an isotopic abundance of only about one part in 10^6 on the surface of the earth.

Only a very limited number of fusion reactors will ever be required for space applications, and their fueling requirements will be far smaller than, for example, a ground-based fusion economy for electric utilities. Thus, for space applications, it becomes possible to consider sources of tritium and ³He that would not be feasible for ground-based electric utility applications.

In space, severe mass penalties will probably be associated with the recovery of unburned tritium fuel for reinjection into the plasma or with any attempt to breed tritium on a space vehicle by the neutron-lithium breeding reactions (Ref. 24, p. 202) that have been proposed for ground-based electric utility D-T power plant reactors. The relatively small amount of tritium required for space missions, compared to the much larger amounts that might be needed in ground-based

electric utility power plants, should make it possible to increase the tritium breeding ratio of ground-based power plants to an extent that will produce enough additional tritium for space missions.

Because of its extremely low isotopic abundance, very little ³He will be available from natural sources on the earth's surface. Another source of ³He is the decay of tritium, according to Eq. (17), which is used for weapons and other purposes. It is likely that the total amount of ³He that will be available early in the twenty-first century will be no more than a few hundred kilograms, an amount barely adequate for one or two space missions.

Other potential sources of ³He include the decay of tritium specially produced by fission reactors for space missions, and semicatalyzed D-D reactors, following the suggestion of Miley et al.,[25] which are part of a ground-based fusion economy using D-D reactions. The most promising source of large amounts of ³He appears to be heating regolith on the lunar surface, which has been implanted with ³He over geological ages by the solar wind.[7,26] It appears that essentially unlimited amounts of ³He would be available for space missions from sources on the lunar surface or the atmospheres of the outer planets or their satellites that have retained light elements in their atmospheres.

IV. FACTORS AFFECTING CONFINEMENT CONCEPT

In this section, some of the factors that affect the choice of confinement concept are examined. This includes the choice both between inertial and magnetic fusion energy and among magnetic containment concepts.

IV.A. Thermal Energy Radiation in Space

The disposal of unwanted thermal energy imposes a serious mass penalty on any power-generating system used for space missions. Radiators are a significant fraction of the total mass of fission or fusion power plants used for space applications, particularly if the power plant is used for generating electrical power rather than direct thrust. Direct fusion rockets can dispose of most of their thermal energy in the exhaust jet without having to process the energy through a Carnot cycle containing energy conversion equipment and radiators; when electrical power is required, large blocks of thermal power must be processed to generate the electrical requirements.

It is not generally appreciated by individuals who are accustomed to ground-based power plants that the mass penalty associated with radiators in space places a constraint on the ratio of the radiator temperature to the operating temperature in the core or blanket of the reactor. To see this, consider the Stefan-Boltzmann law, which gives the amount of power radiated p_{RAD}

by a radiator of temperature T_R with a total area A_R and emissivity ϵ, where σ is the Stefan-Boltzmann radiation constant:

$$p_W = p_{RAD} = \epsilon \sigma T_R^4 A_R \ . \tag{18}$$

Consideration of the power flow diagram of the idealized fusion power plant in Fig. 7 shows that the waste heat p_W is related to the gross electrical power p_G and the power plant efficiency η by the expression

$$P_W = \frac{1 - \eta}{\eta} p_G \ , \tag{19}$$

where the efficiency of the power plant can be written in terms of the Carnot efficiency η_c and the efficiency factor η_0, which represents the achievable fraction of the Carnot efficiency,

$$p_W = \left(1 - \frac{T_R}{T_H}\right)\eta_0 \ . \tag{20}$$

The cold temperature is the radiator temperature T_R, and the high temperature is the core or blanket coolant temperature T_H.

If Eqs. (19) and (20) are substituted into Eq. (18), one can obtain an expression for the area of the radiator A_R in terms of the temperature of the radiator and coolant T_H as follows:

$$A_R = \frac{p_G \left| \dfrac{T_H}{\eta_0} - T_H + T_R \right|}{(T_H - T_R)\epsilon \sigma T_R^4} \ . \tag{21}$$

Thermal radiators for space applications will be very large two-dimensional structures, the mass of which can be approximated by a mass density per unit area, ρ_R, kilograms per square metre. The mass of a radiator can then be written in terms of its area as follows:

$$M_R = \rho_R A_R = \frac{\rho_R p_G \left| \dfrac{T_H}{\eta_0} - T_H + T_R \right|}{(T_H - T_R)\epsilon \sigma T_R^4} \ . \tag{22}$$

In space-related systems, the designer has the option of varying the radiator temperature to minimize the radiator mass. If the minimum mass is calculated as a function of the coolant and radiator temperature for the limiting case of the Carnot efficiency, $\eta_0 = 1.0$, a derivative of Eq. (22) yields

$$\frac{\partial M_R}{\partial T_R} = 0 \Rightarrow T_R = \frac{3}{4} T_H \ . \tag{23}$$

Thus, for the Carnot efficiency, the radiator mass is minimized when the radiator temperature is three-fourths of the coolant temperature of the reactor. The ratio in Eq. (23) is a general result for the minimization of the radiator mass in space-related systems and is independent of whether it is a fission or fusion system. If the ratio of 0.75 for the radiator-to-coolant

temperature is substituted into Eq. (20) for the Carnot efficiency, one obtains a Carnot efficiency of

$$\eta_c = 0.25 \ . \tag{24}$$

IV.B. Engineering Constraints on Fusion Reactors

Space-related fusion systems will have to operate under constraints on reasonable size, magnetic induction, wall loading, and power density no less stringent than those of ground-based fusion power plants. It has been shown that magnetic fusion reactors, in order to be of reasonable size and total power output and to be within currently understood thermal or neutron wall-loading limits, will have fusion power densities in the range between 1 and 10 MW/m^3 (Ref. 24, Chap. 9). If the fusion power density is much below 1 MW/m^3, the power plants are too large to justify the required blanket and reactor structure that surround them; above 10 MW/m^3, thermal or neutron wall-loading limits come into play. If anything, the thermal or neutron wall-loading limits for space systems will be more severely constrained than for ground-based applications of fusion reactors because of the difficulty of replacing activated first-wall materials in space.

The fusion power density in a plasma with two species of fuel is given by

$$p_F E_{12} g_{12} n_i^2 \langle \sigma v \rangle_{12} \, W/m^3 \ . \tag{25}$$

Equation (25) makes it possible to relate a given fusion power density to the total ion number density n_i and the kinetic temperature of a particular fusion reaction between two fuel species. The plasma stability index beta is given by

$$\beta = \frac{2\mu_0 e T_i' n_i G(\gamma, Z)}{B^2} \ , \tag{26}$$

where the parameter $G(\gamma, Z)$ is given by Eq. (8), and B is the magnetic induction in the plasma, in tesla. For a given plasma stability index β, the ion kinetic temperature and the ion number density are constrained by the relationship

$$T_i' n_i = \frac{B^2 \beta}{2\mu_0 e G(\gamma, Z)} \ . \tag{27}$$

Figures 10 and 11 show the operating regimes for three fusion reactions of potential interest for space applications, plotted on the ion number density-kinetic temperature plane. Figure 10 shows the operating regime for hydrogenic reactions. The cross-hatched regions show the operating regimes for the D-T and catalyzed D-D reactions, subject to limits on power density between 1 and 10 MW/m^3. The lower bound on kinetic temperature is determined by the ideal ignition temperature, on the assumption that the electron and ion kinetic temperatures are equal. These regimes are determined, for the reactions indicated, by Eq. (25).
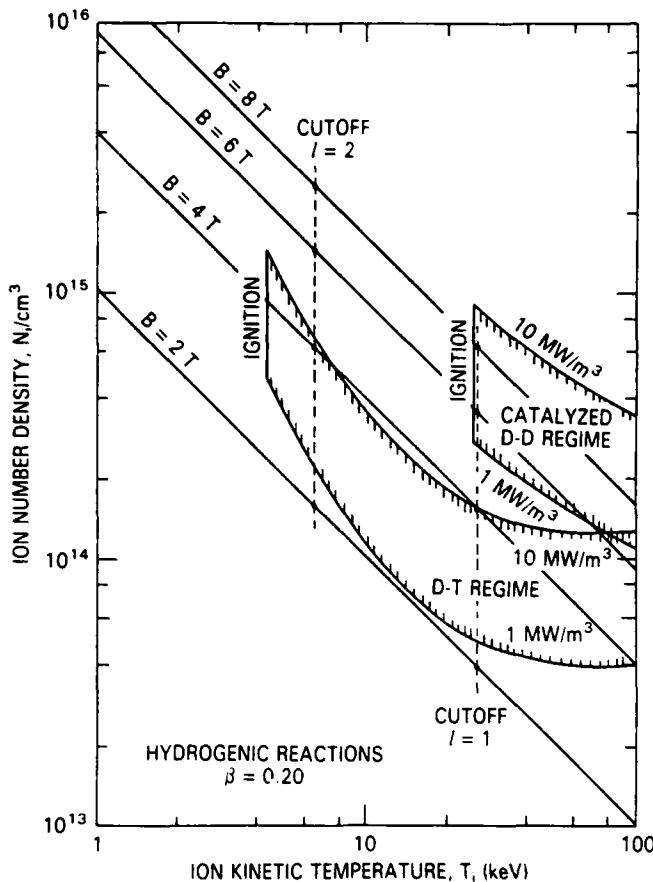
Fig. 10. Operating regime for the D-T and catalyzed D-D reactions in a $\beta = 0.20$ confinement system.
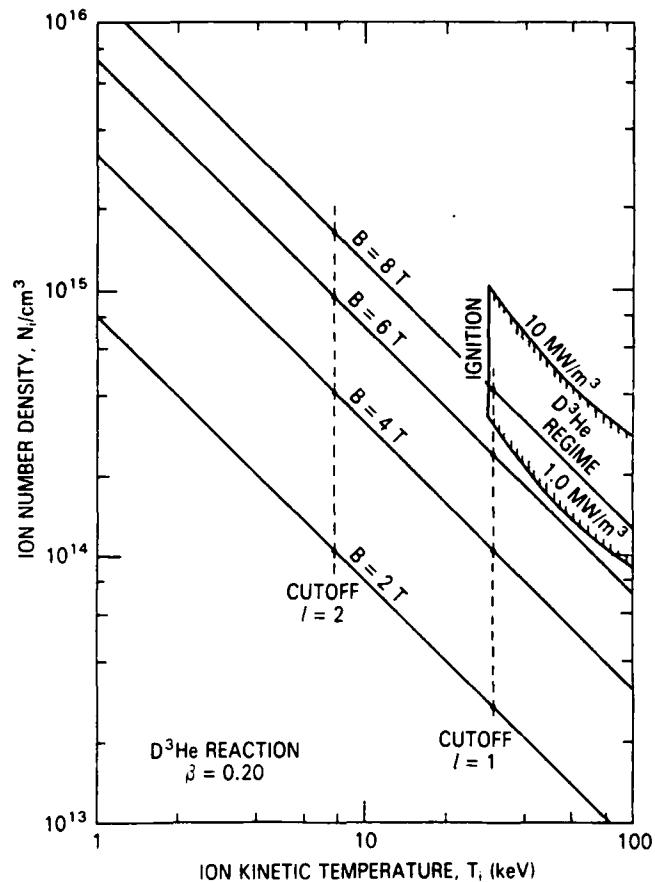
Fig. 11. Operating regime for the D^{3}He reaction in a $\beta = 0.20$ confinement system.

The straight lines running from the upper left to the lower right are defined by Eq. (27), for $2 \le B \le 8$ T, and for a plasma stability index beta of 20%.

For the D-T reaction, Fig. 10 indicates that magnetic inductions in the plasma between 2 and 4 T should be sufficient to maintain power densities between 1 and 10 MW/m^3. It also indicates, however, that the catalyzed D-D reaction requires magnetic inductions between 6 and 8 T to maintain fusion power densities between 1 and 5 MW/m^3. As has been shown elsewhere (Ref. 24, Chap. 9), for values of β lower than the 0.20 illustrated in Fig. 10, magnetic inductions stronger than those shown are required; for values of β above 0.20, the catalyzed D-D reaction can be burned in plasmas with weaker magnetic fields than those shown in Fig. 10.

Figure 11 shows the operating regime for the D^{3}He reaction in a magnetic confinement system with a plasma stability index of 0.20. At this beta, burning the D^{3}He reaction is marginal in terms of its demanding engineering requirements. Such a D^{3}He reactor could operate at a power density of only 2 or 3 MW/m^3 by using a magnetic induction in the plasma of ~8 T. At higher values of beta, above 0.4, the magnetic induc-

tion curves move to the upper right, and it becomes possible to burn the D^{3}He reaction at power densities up to 10 MW/m^3 in magnetic inductions well below 8 T, within reach of the current state of the art.

The results of a detailed study (Ref. 24, Chap. 9) indicate that the D^{3}He and catalyzed D-D reactions can achieve power densities up to 10 MW/m^3 under existing engineering constraints, second in this respect only to the D-T reaction. The D-T reaction can achieve power densities between 1 and 10 MW/m^3 at magnetic inductions below 8 T for values of the plasma stability index as low as a few percent. The catalyzed D-D and D^{3}He reactions require a beta of at least 0.20 to bring their operating regime down into the range of feasible magnetic inductions, here taken to be below 8 T in the plasma. This value of beta is approximately three times the best values achieved to date in tokamak experiments, such as the D III-D. It is therefore unlikely that these advanced fuels can be burned in the classical tokamak confinement configuration.

IV.C. Limits on Nonself-Sustaining Reactors

It is intuitively obvious that a fusion power plant that requires a large recirculating power fraction to

maintain the plasma will pay a severe penalty in mass and reliability, compared with a self-sustaining fusion reactor in which cold incoming fuel is heated to the operating temperature by charged reaction products and in which only small amounts of power are needed to operate the reactor. It is desirable to make this intuitive picture more quantitative, and this can be done by placing constraints on the heating power fraction, defined in Eq. (11), and then determining whether these constraints result in engineering parameters that might reasonably be achieved by proposed magnetic confinement systems requiring recirculating power flows.

A constraint on the heating power fraction $F\eta\eta_i$ can be obtained from the generalized Lawson criterion of Eq. (7) by noticing that Eq. (7) has a denominator consisting of the difference of two terms. When this denominator is zero, infinite values of the Lawson parameter $n\tau$ are implied. By setting the denominator of Eq. (7) equal to zero and solving for the heating power fraction, one can obtain the minimum possible heating power fraction that will lead to steady-state operation of a generalized fusion power plant,

$$(F\eta\eta_i)_{min} = \frac{S(T_i')^{1/2}H(\gamma, Z)}{Mg_{12}E_{12}\langle\sigma v\rangle_{12} + S(T_i')^{1/2}H(\gamma, Z)} \ .$$

(28)

Equation (28) places a limit on the power plant engineering parameters, which are on the left side of Eq. (28), and expresses this limit in terms of the kinetic temperature of the plasma and the characteristics of particular fusion reactions that appear in the terms on the right side of the equation.

The minimum heating power fraction given by Eq. (28) is plotted in Fig. 12 as a function of ion kinetic temperature for the fusion reactions listed in Table V. All magnetic fusion power plants with recirculating power flows and power flow diagrams given by Fig. 7 must operate above the curves shown in Fig. 12. Since steady-state magnetic fusion reactors will operate between ion kinetic temperatures of 10 and 100 keV, one must ask whether the heating power fraction required can be obtained in proposed power plant reactor concepts containing recirculating power flows. In this kinetic temperature range, there is quite a bit of margin for the D-T reaction to operate, but even the catalyzed D-D and D^3He reactions may not be able to simultaneously achieve the engineering parameters required to raise the heating power fraction above the values shown on this curve. These considerations require use of the D-T reaction in magnetic fusion power plants requiring large recirculating power flows.

It has been shown above that the Carnot efficiency, which minimizes the mass of the radiator in space-related fusion or fission systems, is 0.25; this is probably a reasonable guess for space-related power plant energy conversion systems in any case, since even ground-based technologies seldom reach values of $\eta = 0.40$. If we adopt a thermal efficiency of $\eta = 0.25$, then

$$(F\eta_i)_{min} = 4(F\eta\eta_i)_{min} \ .$$

(29)

The product of the recirculating power fraction F and the efficiency of the plasma heating equipment η_i is called the plasma heating power fraction and is

$$(F\eta_i)_{min} \equiv \frac{\text{plasma heating power}}{\text{gross electrical output power}} \ .$$

(30)

The plasma heating power fraction of Eq. (30) is plotted as a function of ion kinetic temperature in Fig. 13. Since magnetic fusion reactors will operate
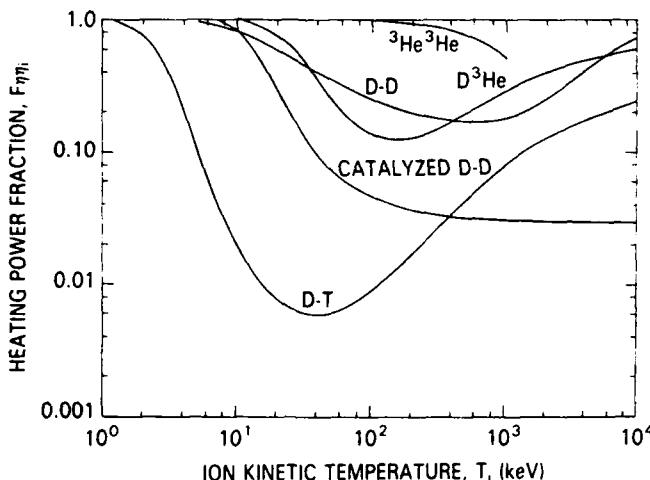

Fig. 12. The power plant heating power fraction $F\eta\eta_i$ as a function of ion kinetic temperature for several fusion reactions.
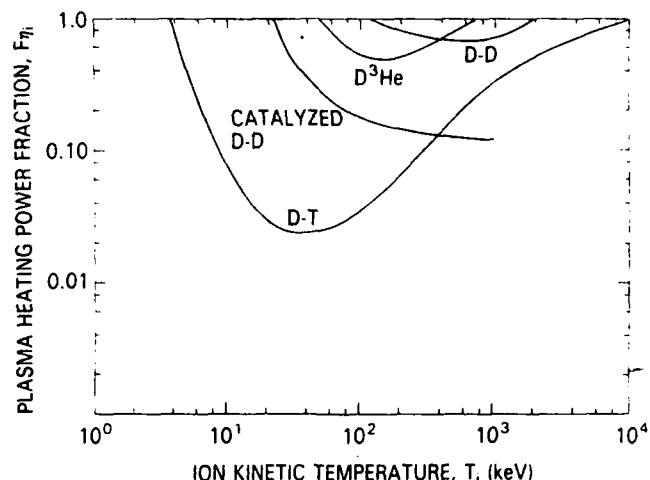
Fig. 13. The plasma heating power fraction $F\eta_i$ for several fusion reactions, based on optimization of minimum power plant mass.

between 10 and 100 keV, it is clear that the D-T reaction offers a substantial margin above the curve in which D-T fusion power plants with recirculating power can operate, even if the recirculating power fraction is relatively low and the plasma heating equipment rather inefficient. The plasma heating power fraction required for the catalyzed D-D and D^3He reactions, however, is so demanding that it is almost possible on these grounds alone to state that only the D-T reaction will be capable of operating a space-related fusion power plant requiring significant recirculating power flows to maintain the plasma.

Figures 12 and 13 were both drawn on the assumption that the plasma would have approximately equal ion and electron kinetic temperatures, consistent with current literature on D^3He and other advanced fuels. Figure 14 shows the limit on the plasma heating power fraction for the D^3He reaction, under conditions where the electron temperature is lower than the ion kinetic temperature. At the present state of development of fusion research, it is not clear what physical processes could bring about a severe depression of the electron kinetic temperature relative to the ion kinetic temperature. However, Fig. 14 indicates that if this became possible, then the plasma heating power fraction requirements might be sufficiently low, and that D^3He reactors employing significant recirculating energy flows to sustain the plasma might be possible. Except for this (perhaps rather unlikely) possibility of depressed electron kinetic temperatures, it appears that only the D-T reaction can be used in magnetic fusion power plants with large recirculating power flows, and that in all cases one should attempt to achieve fusion power plants for space applications that are self-sustaining and for which the energy flows are internalized within the plasma.

IV.D. Inertial Fusion in Space

Over the past 20 yr, numerous design studies have been done on space propulsion systems using inertial fusion. Most of these studies are of direct fusion rockets of the type indicated schematically in Fig. 4 in which the initiating energy pulse is provided by lasers or particle beams. There have been few, if any, studies of inertial fusion systems for the primary purpose of generating electrical power in space. The large recirculating power flows usually required for inertial fusion, and the resulting mass penalties, may have discouraged detailed studies of inertial fusion for such applications.

Another characteristic of most engineering design studies of inertial fusion propulsion systems is that, as indicated in Fig. 4, the neutrons and much of the radiant energy are unshielded and escape freely into the space environment. There appear to be few, if any, engineering design studies of inertial fusion space propulsion systems that fully shield the neutron, charged particle, and radiant energy fluxes produced by the explosion of the pellets.
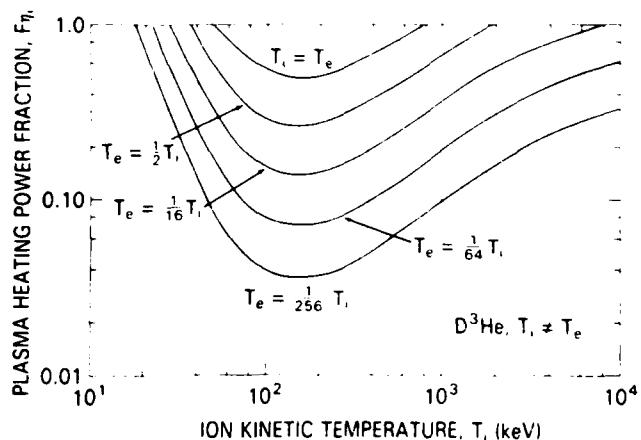

Fig. 14. The plasma heating power fraction for the D^3He reaction with ion kinetic temperatures greater than the electron kinetic temperature.

Another problem with inertial fusion space propulsion systems is that investigations of burn dynamics with classified computer codes indicate that the energy gains of advanced fuels are insufficient to marginal for a pellet burn.[7] Two unclassified papers[27,28] on advanced fuel inertial confinement show that a special pellet design (AFLINT) may be capable of burning the D-D reaction, although with very high recirculating power flows.[28] For reasons such as these, published design studies assume the D-T reaction, the very high reactivity of which assures an adequate pellet burn. If inertial fusion systems in space are limited to the D-T reaction, the implications of this are rather serious for the overall propulsion system. One must be concerned about the risk inherent in the tritium fuel, as described previously, and one must avoid contaminating either the atmosphere or the magnetosphere with radioactive tritium in the event of an accident or escape of the tritium as unburned propellant from the reactor.

V. CONCLUSIONS

V.A. Fission Versus Fusion Power in Space

If both are feasible, the choice between fission or fusion reactors for generating electrical power in space depends on the relative electrical-specific mass in kilograms per kilowatt(electric), which can be achieved by the two systems and also on their reliability, relative safety, and environmental impacts. The total mass of a fusion propulsion system generating only a few megawatts is likely to be small enough that a large relative mass penalty of one type of system over the other might be acceptable if that system offered significant advantages in safety, reliability, or environmental impact. Interplanetary propulsion systems using fission or fusion energy are likely to be so heavy, however,

that the specific mass will be a dominant factor in choosing between them. Figure 15 shows the result of some engineering design studies of fission and fusion systems, combined with a mission study for a manned round trip from Earth's orbit to Mars' orbit.[1,2] In the engineering design studies, the same data base was used for the mass of radiators, electrical generators, shielding, etc. for both the fission and fusion systems. The implied comparison in Fig. 15 is somewhat better founded than the comparison of Tables I and II, because it used this common data base for similar components of these propulsion systems.

These studies indicated that the nuclear fission electric propulsion system would have a specific mass of 7 to 9 kg/kW(electric), and that the direct fusion rockets would have a specific mass between 0.5 and 3 kg/kW(electric). The consequences of these different specific masses for a round trip to Mars are shown by the two curves, which indicate the round trip time for a one or two stage vehicle. These data show that a round trip to Mars might be made in as few as 90 to 240 days with a fusion propulsion system, but that the same trip might require from 290 days to more than 1 yr if the fission electric propulsion system, with its higher mass, were used.

V.B. Magnetic Versus Inertial Fusion in Space

For environmental and safety reasons discussed in Sec. V.A, it appears that inertial fusion is at a disadvantage with respect to magnetic fusion for application to space power and propulsion systems. Inertial fusion systems may be restricted to the D-T reaction, raising the possibility of contamination of the atmosphere and/or the magnetosphere with radioactive tritium; it appears difficult to shield the neutron, the charged particle, and the radiant energy fluxes that result from

the explosion of the pellets without paying a large mass penalty for D-T inertial fusion systems. It appears difficult to burn advanced fuels with reduced neutron production in inertial fusion systems because of the relatively low reactivity of advanced fuels relative to the D-T reaction. Unclassified studies of advanced fuel inertial confinement[27,28] have demonstrated the feasibility of a fusion burn, although with high recirculating powers.[28] Further research is needed to demonstrate really attractive inertial confinement fusion performance with advanced fuels. With the current evidence, it appears that safety and environmental considerations make inertial fusion systems a relatively more difficult prospect for space applications than magnetic fusion reactors, which, if they have low recirculating power flows, can burn advanced fuels.

V.C. Choice of Fusion Reaction for Space Applications

Figure 8 for the generalized Lawson criterion of various fusion reactions, and Figs. 10 and 11, which outline the physics and engineering constraints on hydrogenic and D^3He reactions, indicate that at kinetic temperatures below 100 keV, only the D-T, catalyzed D-D, and D^3He reactions are capable of producing power densities in the 1 to 10 MW/m^3 range at number densities, confinement times, and kinetic temperatures that are modest extensions of current D-T tokamak research.

If it is desired to minimize the transportation, handling, and leakage of tritium into the environment, only the catalyzed D-D and D^3He reactions are available. If it is further desired to minimize the radioactivation and shielding mass associated with high levels of neutron production, that leaves only the D^3He reaction. With the current evidence, it appears that the D^3He reaction is the all-around best choice for space applications of magnetic fusion energy.

V.D. Space-Related Constraints on Confinement Concepts

If magnetically confined advanced fuel fusion reactors are used in space, some general constraints can be placed on the confinement concepts that are required to burn advanced fusion fuels. Figures 10 and 11 imply that a plasma stability index $\beta > 0.20$ will be required to burn advanced fuels in magnetic fusion reactors with useful power densities in the 1 to 10 MW/m^3 range and with a magnetic induction in the plasma below 8 T. Figure 13 indicates that such advanced fuel magnetic fusion reactors should be self-sustaining, since the requirements on the plasma power fraction for the D^3He reaction would be very hard to satisfy in a propulsion system with significant recirculating power flows. Finally, reliability considerations will almost certainly bias the technology toward steady state rather than pulsed magnetic fusion concepts.
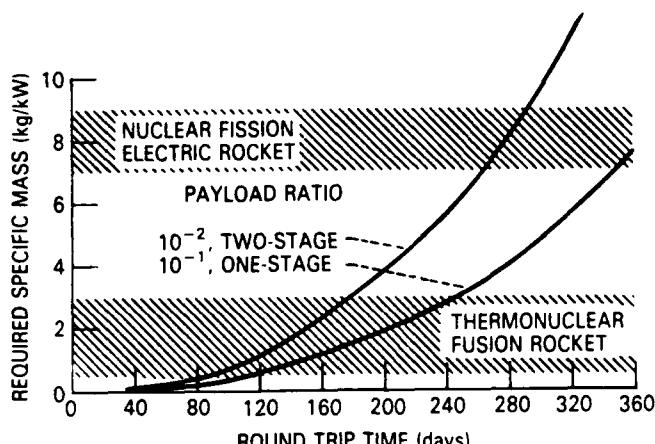
Fig. 15. Comparison of fission and fusion propulsion systems for a manned Mars expedition.[2] Type II propulsion — Earth orbit to Mars orbit and back.

REFERENCES

1. J. R. ROTH, W. D. RAYLE, and J. J. REINMANN, "Technological Problems Anticipated in the Application of Fusion Reactors to Space Propulsion and Power Generation," *Proc. Intersociety Energy Conversion Engineering Conf.*, Las Vegas, Nevada, September 21–25, 1970, Vol. I, p. 2 (1970).

2. J. R. ROTH, W. D. RAYLE, and J. J. REINMANN, "Fusion Power for Space Propulsion," *New Sci.*, 125 (Apr. 20, 1972).

3. G. L. KULCINSKI and J. F. SANTARIUS, "SOAR: Space Orbiting Advanced Fusion Power Reactor," presented at the Innovative Nuclear Space Power Institute Mtg., San Diego, California, June 9, 1987.

4. J. F. SANTARIUS, "D-³He Tandem Mirror Reactors on Earth and in Space," *APS Bull.*, 31, 9, 1499 (1986).

5. J. R. WETCH, A. DEGG, and K. KOESTER, "Megawatt-Class Nuclear Space Power System (MCNSPS)-Conceptual Design and Evaluation Report," NES-3-23867, National Aeronautics and Space Administration, Lewis Research Center (Mar. 1985).

6. J. SERCEL and S. KRAUTHAMER, "Multi-Megawatt Nuclear Electric Propulsion: First Order System Design and Performance Evaluation," presented at American Institute of Aeronautics and Astronautics Space Systems Technology Conf., San Diego, California, June 9–12, 1986, Paper 86-1202.

7. G. H. MILEY et al., *Advanced Fusion Power—A Preliminary Assessment*, Air Force Studies Board, National Academy of Science, NAS Press, Washington, D.C. (1987).

8. G. W. ENGLERT, "High-Energy Ion Beams Used to Accelerate Hydrogen Propellant Along Magnetic Tubes of Flux," NASA-TND-3656, National Aeronautics and Space Administration (1967).

9. C. C. BAKER et al., "STARFIRE—A Commercial Tokamak Fusion Power Plant Study," ANL/FPP-80-1, Vol. 1, p. 2-67, 2-68, Argonne National Laboratory (1980).

10. R. W. CONN and R. A. GROSS, "Report of Panel #10 on High Power Density Fusion Systems," presented to the U.S. Department of Energy Magnetic Fusion Advisory Committee (May 8, 1985).

11. G. H. MILEY, J. GILLIGAN, C. CHOI, and E. GREENSPAN, "Studies of High Efficiency, Advanced Fuel Fusion Reactors," EPRI-645-1, Elelctric Power Research Institute (Apr. 1981).

12. B. G. LOGAN, "³He Application in Tokamak Fusion," *APS Bull.*, 31, 9, 1499 (1986).

13. B. G. LOGAN et al., "Mirror Advanced Reactor Study (MARS) Interim Design Report," UCRL-53333, Lawrence Livermore National Laboratory (Apr. 1983).

14. R. G. HAGENSON, R. A. KRAKOWSKI, C. G. BATHKE, R. L. MILLER, M. J. EMBRECHTS, N. M. SCHNURR, M. E. BATTAT, R. J. LaBAUVE, and J. W. DAVIDSON, "Compact Reversed Field Pinch Reactors, Preliminary Engineering Considerations for RFP/OHTE Systems," 10200-MS, Los Alamos National Laboratory (Aug. 1984).

15. R. HO, "Advanced Fuel Fusion Application to Manned Space Propulsion," *J. Nucl. Instrum. Methods*, 144, 69 (1977).

16. R. HO, "Terrestrial and Space Applications of the Migma Controlled Fusion Concept," presented at the American Institute of Aeronautics and Astronautics/Strategic Air Command 11th Propulsion Conf., Anaheim, California, September 29–October 1, 1975, Paper 75-1263.

17. R. A. HYDE, "A Laser Fusion Rocket for Interplanetary Propulsion," UCRL-88857, Lawrence Livermore National Laboratory (Sep. 27, 1983).

18. R. L. HAGENSON and S. E. WALKER, "A Proposed 5-MA OHTE RFP Machine," presented at the Institute of Electrical and Electronics Engineers Int. Conf. Plasma Science, Saskatoon, Saskatchewan, Canada, May 19–21, 1986, Paper 2A6.

19. S. E. WALKER, "OHTE: An Alternate Pathway to Achieve Fusion," presented at the 20th Intersociety Energy Conversion Engineering Conf., Miami Beach, Florida, August 18–23, 1985, Paper 859408.

20. "Extraterrestrial Sources of ³He and the Potential for Fusion," presented at the 28th Annual Mtg. Plasma Physics Division of the American Physical Society, Baltimore, Maryland, November 3–7, 1986.

21. "Summary Report on the Post-Accident Review Meeting on the Chernobyl Accident," Safety Series No. 75-INSAG-1, pp. 5, 33, International Atomic Energy Agency, Vienna, Austria (1986).

22. J. F. AHEARNE, "Nuclear Power After Chernobyl," *Science*, 236, 673 (May 8, 1987).

23. "Basic Radiation Protection Criteria," Report No. 39, National Council on Radiation Protection and Measurements, Washington, D.C., p. 82 (1971).

24. J. R. ROTH, *Introduction to Fusion Energy*, Ibis Publishing, Charlottesville, Virginia (1986).

25. G. H. MILEY, F. H. SOUTHWORTH, C. K. CHOI, and G. A. GERDIN, "Catalyzed-D and D-^{3}He Fusion Reactor Systems," *Proc. 2nd Topl. Mtg. Technology of Controlled Nuclear Fusion*, Richland, Washington, September 21-23, 1976, Vol. 1, p. 119, U.S. Department of Commerce, National Technical Information Service.

26. L. J. WITTENBERG, J. F. SANTARIUS, and G. L. KULCINSKI, "Lunar Source of ^{3}He for Commercial Fusion Power," *Fusion Technol.*, **10**, 167 (1986).

27. G. H. MILEY, *Laser Interaction and Related Plasma Phenomena*, "The Potential Role of Advanced Fuels in Inertial Confinement Fusion," Vol. 5, p. 313, H. J. SCHWARZ et al., Eds., Plenum Press, New York (1981).

28. M. RAGHEB, G. H. MILEY, J. F. STUBBINS, and C. CHOI, "LOTRIT, An Alternate Approach to Inertial Confinement Fusion Reactors," *Proc. 6th Int. Conf. Alternative Energy Sources*, Miami Beach, Florida, December 12-14, 1983, Vol. 3, p. 285, T. N. VEZIROGLU, Ed., Springer-Verlag, New York (1985).

Theory of first-order plasma heating by collisional magnetic pumping

M. Laroussi[a] and J. Reece Roth
Department of Electrical and Computer Engineering, The University of Tennessee, Knoxville, Tennessee 37996-2100

Plasma heating by collisional magnetic pumping is investigated theoretically. This treatment yields solutions to the energy transfer equations in the form of an energy increase rate, which gives quantitatively the amount of energy increase per rf driving cycle. The energy increase rates (or heating rates) proportional to the first and second powers of the field modulation factor δ (defined as the ratio of the change in the magnitude of the magnetic field to its background dc value) are derived for an arbitrary rf waveform of the pumping magnetic field. Special cases are examined, including the sinusoidal and sawtooth pumping waveforms. The energy increase rate in the case of a sawtooth waveform was found to be proportional to the first power of δ (first-order heating). This heating rate is many orders of magnitude larger than heating for the sinusoidal case: The latter is proportional to the square of δ and is strongly dependent on the collisionality of the plasma. The use of a sawtooth pumping waveform improves the efficiency of collisional magnetic pumping and heating rates comparable to those possible with ion or electron cyclotron resonance heating methods may be achieved.

I. INTRODUCTION

Collisional magnetic pumping[1-6] is achieved by wrapping an exciter coil around a cylindrical plasma and perturbing the confining magnetic field $B = B_0[1 + \delta f(t)]$, where B_0 is the uniform steady-state background magnetic field, δ is the field modulation factor defined as $\delta = \Delta B / B_0$, and $f(t)$ is a periodic function of time. Figure 1 illustrates such a situation. The origins of collisional magnetic pumping date to the beginnings of fusion research in 1953,[1] when Spitzer and Witten proposed to heat a plasma with a sinusoidally perturbed magnetic field. The theory of collisional magnetic pumping with a sinusoidal magnetic perturbation was first published in the unclassified literature by Schluter in 1957.[2] Early theoretical research by Berger and others at the Princeton Plasma Physics Laboratory, following the work of Spitzer and Witten,[1] was summarized by Berger *et al.*[3] These authors, in agreement with Schluter,[2] quoted a heating rate proportional to the square of the magnetic field perturbation, which was also a strong function of the collision frequency of the plasma. The work of Berger *et al.*[3] appeared in subsequent texts[4-6] without embellishment. No further work on collisional magnetic pumping appears to have been done until recently,[7-9] possibly because the low heating rates resulting from a sinusoidal magnetic perturbation were of second order and orders of magnitude smaller than that of competitive heating methods such as ion or electron cyclotron resonance heating.

Contrary to ohmic heating, where the electric field is parallel to the confining axial magnetic field, the oscillating electric field in collisional magnetic pumping is produced by variation of the axial magnetic field and thus is perpendicular to the field. This type of heating is called "magnetic pumping" as a result of the existence of a compressional wave propagating perpendicular to the background magnetic field and causing the plasma to be cyclically compressed and relaxed by an alternating $E \times B$ force. This is illustrated in Fig. 2. The compressive wave is a magnetosonic wave (or magnetoacoustic wave). The magnetosonic wave is an extraordinary electromagnetic mode with a frequency well below the gyrofrequency. Contrary to Alfvén waves, which travel along B_0, magnetosonic waves travel across B_0 at the Alfvén speed $V_A = B_0(1/\mu n_0 m_i)^{1/2}$, where n_0 is the charged particle density, m_i is the ion mass, and μ is the permeability of the plasma.

To achieve collisional heating the following inequalities have to be satisfied[3]:

$$\tau_{cy} \ll \tau_c \sim \tau_f \ll \tau_{tr},$$

where τ_{cy}, τ_c, τ_f, and τ_{tr} are, respectively, the gyration period, the collision time, the period of the oscillating field, and the transit time of the particles through the heating region. The particles suffer many collisions while crossing the heating region, but since the period of the oscillating field is much larger than the gyration period, the magnetic moment of the particles is a constant of motion between collisions. The magnetic field assumes the form $B = B_0[1 + \delta f(t)]$, where $\delta \ll 1$, so that the external oscillator provides a small perturbation on the original static magnetic field. If the heating region is of length L and the parallel velocity of the particles is $v_\parallel$, the above inequalities can also be written as

$$v_\parallel / L \ll v_c \sim \omega \ll \omega_{cy},$$

where v_c, ω, and ω_{cy} are, respectively, the collision frequency, the driving frequency, and the gyrofrequency.

II. THEORETICAL ANALYSIS

In the absence of collisions, the constancy of the magnetic moment makes it possible to obtain a relationship

---

[a] Present address: Department of Electrical Engineering, Technical University, Sfax, Tunisia.
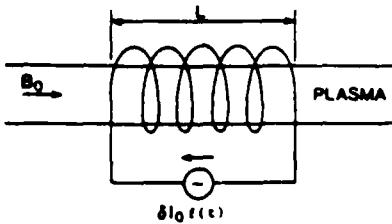
FIG. 1. Exciter coil around a cylindrical plasma.

between the time rate of change of the perpendicular component of the energy and the time rate of change of the magnetic field. Thus by taking the derivative of the magnetic moment $\mu = E_\perp/B$ with respect to time we obtain

$$\frac{d\mu}{dt} = 0 = \frac{1}{B}\frac{dE_\perp}{dt} - \frac{E_\perp}{B^2}\frac{dB}{dt}, \qquad (1)$$

from which we obtain

$$\frac{dE_\perp}{dt} = \frac{E_\perp}{B}\frac{dB}{dt}. \qquad (2)$$

The total energy E of the ions is given by

$$E = E_\| + E_\perp, \qquad (3)$$

where $E_\|$ is the ion energy along the magnetic field lines and $E_\perp$ is the ion energy perpendicular to the magnetic field lines, with two degrees of freedom.

If no collisions occur, the perpendicular component of the ion energy $E_\perp$ oscillates with the frequency ω and no net heating occurs. However, if collisions do occur, some of the energy in the perpendicular component is transferred to the parallel component $E_\|$. In kinetic equilibrium, the parallel component of the energy will be equal to one-half the perpendicular component as a result of equipartition. When the perpendicular component is driven by magnetic pumping, a periodic departure from equipartition occurs and energy can be transferred between the parallel and perpendicular components. This may be expressed mathematically by adding a collisional term to Eq. (2)[3]:

$$\frac{dE_\perp}{dt} = \frac{E_\perp}{B}\frac{dB}{dt} - \nu_c\left(\frac{E_\perp}{2} - E_\|\right), \qquad (4)$$

$$\frac{dE_\|}{dt} = \nu_c\left(\frac{E_\perp}{2} - E_\|\right). \qquad (5)$$

Now summing Eqs. (4) and (5) and using Eq. (3) one obtains

$$\frac{dE}{dt} = \frac{E_\perp}{B}\frac{dB}{dt} = \mu\frac{dB}{dt}. \qquad (6)$$

Thus the rate of change of the total ion energy is proportional to the magnetic moment and the time rate of change of the magnetic field.
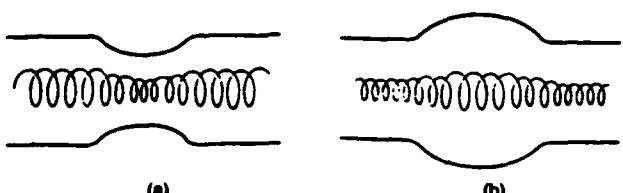
FIG. 2. Particle orbits in a sinusoidally perturbed magnetic field. (a) Plasma compressed during the positive half-cycle, (b) plasma relaxed during the negative half-cycle.

The net energy transfer can be obtained by taking the second derivative of Eqs. (6) and then using Eqs. (4) and (5) to eliminate the first derivative of the parallel and perpendicular components of the energy. Further, using Eq. (6) to eliminate the perpendicular component of energy one obtains

$$\frac{d^2E}{dt^2} - \left[-\frac{3}{2}\nu_c + \frac{d^2B}{dt^2}\left(\frac{dB}{dt}\right)^{-1}\right]\frac{dE}{dt} - \frac{\nu_c}{B}\frac{dB}{dt}E = 0. \qquad (7)$$

Substituting the expression $B = B_0[1 + \delta f(t)]$ for B into Eq. (7) yields

$$\frac{d^2E}{dt^2} + \left(\frac{3}{2}\nu_c - \frac{f''(t)}{f'(t)}\right)\frac{dE}{dt} - \nu_c\frac{\delta f'(t)}{1 + \delta f(t)}E = 0. \qquad (8)$$

Let

$$A(t) = \tfrac{3}{2}\nu_c - f''(t)/f'(t), \qquad (9)$$

$$g(t) = -\nu_c\{f'(t)/[1 + \delta f(t)]\}. \qquad (10)$$

Equation (8) can be written as

$$\frac{d^2E}{dt^2} + A(t)\frac{dE}{dt} + \delta g(t)E = 0. \qquad (11)$$

Equation (11) is a homogeneous linear differential equation of second order with periodic coefficients; it describes the change in the total energy of the particles due to collisional magnetic pumping. Examples of such equations are the Mathieu and Hill equations which appear in astronomical and other applications, where the stability and perturbation of periodic systems are at issue. The general solutions of these equations have been given by Floquet.[11] Floquet's theory predicts a solution of the following form:

$$E(t) = a_1 e^{\lambda_1 t}P_1(t) + a_2 e^{\lambda_2 t}P_2(t). \qquad (12)$$

The parameters λ_1 and λ_2 are called the characteristic exponents and can be calculated from the characteristic equation associated with the differential equation; $P_1(t)$ and $P_2(t)$ are periodic functions with a period equal to that of the coefficients of the differential equation. Since $\delta = \Delta B/B_0$ is a small quantity, Eq. (11) can be solved using a perturbation treatment around the parameter δ. The characteristic exponents λ_1 and λ_2 can be represented by the series[7,8]

$$\lambda_1 = -\tfrac{3}{2}\nu_c + \delta l_1 + \delta^2 l_2 + \cdots, \qquad (13)$$

$$\lambda_2 = \delta l_1 + \delta^2 l_2 + \dots. \qquad (14)$$

The solution associated with λ_1 is damped in time since the first term dominates the series and therefore does not represent steady-state heating. For this reason, only the solution associated with λ_2, with positive coefficients l_k, will be retained and used. The solution representing heating is then expressed as

$$E(t) = e^{\lambda_2 t}P_2(t). \qquad (15)$$

Now $P_2(t)$ can be expanded as a series of the powers of δ as

$$P_2(t) = P_{20} + \delta P_{21}(t) + \delta^2 P_{22}(t) + \cdots, \qquad (16)$$

where $P_{2i}(t)$ are periodic functions. The initial value is P_{20} and is set equal to 1 for the sake of simplicity. Now, by using the solution predicted by Floquet's theory[10] along with the above perturbation treatment, Eq. (11) can be solved for the different powers of the parameter δ.

A-22

M. Laroussi and J. R. Roth

Solving for the first power of δ, $g(t)$ can be expressed as

$$g(t) = -v_c f'(t),\tag{17}$$

$$E(t) = l_1 t + P_{21}(t).\tag{18}$$

Equation (11) is then reduced to

$$\frac{d^2 P_{21}(t)}{dt^2} + A(t)\frac{dP_{21}(t)}{dt} = K(t),\tag{19}$$

where

$$K(t) = -g(t) - l_1 A(t).\tag{20}$$

The homogeneous solution associated with Eq. (19) can be obtained by multiplying by the integrating factor[9]

$$\exp\left(\int_0^t A(u)du\right).$$

The homogeneous equation can then be written as

$$\frac{d}{dt}\left[\exp\left(\int_0^t A(u)du\right)\frac{dP_{21}}{dt}\right] = 0,\tag{21}$$

which leads to the solution

$$P_{21}(t) = C_1 + C_2\int_0^t e^{-a(s)}ds,\tag{22}$$

where

$$a(t) = \int_0^t A(u)du.\tag{23}$$

The general solution of Eq. (19) is calculated as follows. Multiplying Eq. (19) by the integrating factor $e^{a(t)}$ and integrating once, we find the expression

$$P'_{21}(t) = C_2 e^{-a(t)} + e^{-a(t)}\int_0^t K(s)e^{-a(s)}ds.\tag{24}$$

Integrating (24) gives

$$P_{21}(t) = C_1 + C_2\int_0^t e^{-a(s)}ds$$
$$+ \int_0^t e^{-a(s)}\left(\int_0^s K(u)e^{a(u)}\right)ds.\tag{25}$$

The second integral in Eq. (25) is integrated by parts and is

$$\int_0^t e^{-a(s)}\left(\int_0^s K(u)e^{a(u)}\right)ds$$
$$= \left(\int_0^t e^{-a(u)}du\right)\left(\int_0^t K(u)e^{a(u)}du\right)$$
$$- \int_0^t\left(\int_0^s e^{-a(u)}du\right)K(s)e^{a(s)}ds.\tag{26}$$

Equation (25) becomes

$$P_{21}(t) = C_1 + C_2\int_0^t e^{-a(s)}ds + \left(\int_0^t e^{-a(u)}du\right)$$
$$\times\left(\int_0^t e^{a(u)}K(u)du\right)$$
$$- \int_0^t e^{a(s)}\left(\int_0^s e^{-a(u)}du\right)K(s)ds.\tag{27}$$

The fact that $P_{21}(t)$ is a periodic function gives the conditions

$$P_{21}(T) - P_{21}(0) = 0,\quad P'_{21}(T) - P'_{21}(0) = 0.\tag{28}$$

Substituting (27) in conditions (28) leads to

$$C_2\int_0^T e^{-a(u)}du + \left(\int_0^T e^{-a(u)}du\right)\left(\int_0^T K(u)e^{a(u)}du\right)$$
$$- \int_0^T\left(e^{a(s)}\int_0^s e^{-a(u)}du\right)K(s)ds = 0,\tag{29}$$

$$C_2(e^{-a(T)} - e^{-a(0)}) + e^{-a(T)}\int_0^T K(s)e^{a(s)}ds = 0.\tag{30}$$

Note that $e^{-a(0)} = 1$. Equation (30) gives

$$C_2 = \frac{e^{-a(T)}}{1 - e^{-a(T)}}\int_0^T K(s)e^{a(s)}ds.\tag{31}$$

Substituting (31) into (29) and letting

$$Q(s) = e^{a(s)}\left(\frac{1}{1 - e^{-a(T)}}\int_0^T e^{-a(u)}du - \int_0^s e^{-a(u)}du\right)\tag{32}$$

leads to the condition

$$\int_0^T K(s)Q(s)ds = 0.\tag{33}$$

Substituting $K(t) = -g(t) - l_1 A(t)$ into Eq. (33) gives

$$l_1 = -\frac{\int_0^T g(s)Q(s)ds}{\int_0^T A(s)Q(s)ds}.\tag{34}$$

Substituting $A(t)$ from Eq. (9) and $Q(s)$ from Eq. (32) into the denominator and integrating by parts gives

$$\int_0^T A(s)Q(s)ds = T,$$

so that

$$l_1 = -\frac{1}{T}\int_0^T g(s)Q(s)ds.\tag{35}$$

Knowing that

$$g(t) = -v_c f'(t),$$
$$A(t) = \tfrac{3}{2}v_c - f''(t)/f'(t),$$

and

$$a(t) = \tfrac{3}{2}v_c t - \ln(f'(t)/f'(0)),$$

the final expression for l_1 is

$$l_1 = \frac{v_c}{T}\int_0^T \exp\left(\frac{3}{2}v_c s\right)\left[\frac{1}{1 - \exp(-\tfrac{3}{2}v_c T)}\right.$$
$$\times\int_0^T \exp\left(-\frac{3}{2}v_c u\right)f'(u)du$$
$$\left.- \int_0^s \exp\left(-\frac{3}{2}v_c u\right)f'(u)du\right]ds.\tag{36}$$

The term representing heating in Floquet's[10] solution, Eq. (15), is, after expanding $e^{\lambda_2 t}$,

$$E(t) = E_0 + \delta[l_1 t E_0 + P_{21}(t)] + \text{higher order terms.}\tag{37}$$

The energy increase in a period $T = 2\pi/\omega$ is

$$\Delta E = \delta l_1(2\pi/\omega)E_0,\tag{38}$$

where $P_{21}(T)$ and $P_{21}(0)$ cancel each other as a result of the periodicity of $P_{21}(t)$. Here E_0 is the initial value of the total particle energy. The energy increase rate is given by

$$\Delta E/T = \delta l_1 E_0.\tag{39}$$

III. SECOND-ORDER HEATING WITH A SINE WAVE PERTURBATION

Let us now assume, as previously,[1-3] that the background magnetic field has a sinusoidal perturbation superimposed on it according to the expression

$$B = B_0(1 + \delta \cos \omega t). \tag{40}$$

Substituting $f(t) = \cos \omega t$ in Eq. (36) for l_1, it is easily shown that $l_1 = 0$. In this case, the energy increase is proportional to a higher power of δ than the first. Another way of checking the result (40) and at the same time calculating the next coefficient l_2 in the expansion is to return to the initial differential equation (8) and substitute $\cos \omega t$ for $f(t)$. In doing this, Eq. (11) becomes

$$\frac{d^2E}{dt^2} - \left(-\frac{3}{2}\nu_c + \frac{\omega \cos \omega t}{\sin \omega t} \right)\frac{dE}{dt} + \frac{\delta\nu_c \sin \omega t}{1 + \delta \cos \omega t}E = 0. \tag{41}$$

Since $\delta \ll 1$, the term $(1 + \delta \cos \omega t)^{-1}$ can be expanded in a Taylor series:

$$(1 + \delta \cos \omega t)^{-1} \approx 1 - \delta \cos \omega t + \text{higher order terms.} \tag{42}$$

Substituting Eq. (42) into Eq. (41) one obtains

$$\frac{d^2E}{dt^2} - \left(-\frac{3}{2}\nu_c + \frac{\omega \cos \omega t}{\sin \omega t} \right)\frac{dE}{dt} + \delta\nu_c\omega \sin \omega t(1 - \delta \cos \omega t)E = 0. \tag{43}$$

Using Eq. (15) for the part of Floquet's solution[10] that represents heating and solving for the first power of δ, Eq. (43) becomes

$$\frac{d^2P_{21}}{dt^2} + \left(\frac{3\nu_c}{2} - \omega \cot \omega t \right)\frac{dP_{21}}{dt}$$
$$= -\frac{3}{2}l_1\nu_c + l_1\omega \cot \omega t - \nu_c\omega \sin \omega t, \tag{44}$$

where P_{20} is set equal to 1 for the sake of simplicity.
The homogeneous solution of Eq. (44) is

$$P_{21}(t) = C_1 e^{(3\nu_c/2)t}\{a \cos \omega t + b \sin \omega t\} + C_2, \tag{45}$$

where

$$a = -\omega/(\omega^2 + \tfrac{9}{4}\nu_c^2), \tag{46}$$

$$b = -\tfrac{3}{2}\nu_c/(\omega^2 + \tfrac{9}{4}\nu_c^2). \tag{47}$$

The particular solution of Eq. (44) is

$$P_{21}(t) = -l_1t + \nu_c a \sin \omega t - \nu_c b \cos \omega t + l_1 a \cot \omega t$$
$$+ (-l_1/\sin \omega t - \tfrac{3}{2}\omega)(a \cos \omega t + b \sin \omega t). \tag{48}$$

Now setting the secular term equal to zero [since $P_{21}(t)$ is periodic] one obtains the result $l_1 = 0$. This is in agreement with what was previously predicted. Solving for the second power of δ, Eq. (43) becomes

$$\frac{d^2P_{22}}{dt^2} + \left(\frac{3}{2}\nu_c - \omega \cot \omega t \right)\frac{dP_{22}}{dt}$$
$$= -\tfrac{3}{2}l_2\nu_c + l_2\omega \cot \omega t + \nu_c\omega \sin \omega t \cos \omega t$$
$$- \nu_c\omega \sin \omega t P_{21}(t). \tag{49}$$

As previously, the interesting part of the solution is the particular solution and the important part of the particular solution is the part containing the secular term P_{sec}. The latter is found to be

$$P_{sec} = (\tfrac{3}{2}l_2\nu_c b + al_2\omega - \tfrac{1}{6}\nu_c\omega a)t. \tag{50}$$

Setting term (50) equal to zero and solving for l_2, we obtain

$$l_2 = \nu_c\omega^2/6(\omega^2 + \tfrac{9}{4}\nu_c^2). \tag{51}$$

To calculate the energy increase per cycle, the expression for the energy has to be expanded as

$$E(t) = e^{\lambda_s t}P_2(t)$$
$$= (1 + \delta^2l_2t + \cdots)[P_{20} + \delta P_{21}(t) + \delta^2P_{22}(t) + \cdots]. \tag{52}$$

Retaining only up to the second-order terms in δ, $E(t)$ can be expressed as

$$E(t) = P_{20} + \delta P_{21}(t) + \delta^2[P_{22}(t) + l_2tP_{20}] + \text{higher order terms in } \delta. \tag{53}$$

At $t = 2\pi/\omega$, the energy has increased by

$$\Delta E = \delta^2 l_2(2\pi/\omega)E_0. \tag{54}$$

Inserting the expression for l_2 in Eq. (54) gives

$$\Delta E = \delta^2 E_0(\pi/3)[\nu_c\omega/(\tfrac{9}{4}\nu_c^2 + \omega^2)] \text{ joules/cycle.} \tag{55}$$

The energy increase rate is found by dividing ΔE by $\Delta t = 2\pi/\omega$ sec/cycle and taking the differential limit

$$\frac{dE}{dt} = \frac{\delta^2}{6}\frac{\omega^2\nu_c}{\tfrac{9}{4}\nu_c^2 + \omega^2}E_0 \text{ Joules/sec.} \tag{56}$$

The result (56) agrees with the one found by Schluter[2] and Berger et al.[3] Equation (56) can be written as

$$\frac{dE}{dt} = \frac{E_0}{\tau_H} = \alpha E_0, \tag{57}$$

where τ_H is the heating time defined as

$$\tau_H \equiv 6[(\tfrac{9}{4}\nu_c^2 + \omega^2)/\delta^2\omega^2\nu_c] \tag{58}$$

and $\alpha \equiv 1/\tau_H$ is the heating rate coefficient. The optimum frequency at which the heating rate coefficient is maximum is

$$\omega_{opt} = \tfrac{3}{2}\nu_c \tag{59}$$

and the value of α at this frequency is

$$\alpha_{max} = \delta^2\nu_c/12. \tag{60}$$

For a highly collisional plasma, $\nu_c \gg \omega$ and the heating rate can be approximated by

$$\frac{dE}{dt} \approx \frac{2}{27}\frac{\delta^2\omega^2}{\nu_c}E_0. \tag{61}$$

On the other hand, for a relatively collisionless plasma, $\nu_c \ll \omega$ and the heating rate can be expressed as

$$\frac{dE}{dt} \approx \frac{\delta^2\nu_c}{6}E_0. \tag{62}$$

As seen in the above analysis, the heating rate is proportional to ν_c in the low collisionality case and to ν_c^{-1} in the

A-24

M. Laroussi and J. R. Roth

ghly collisional case. Figure 3 is a schematic plot of the ating rate coefficient α, the inverse of Eq. (58), versus the llision frequency. The fact that the collision magnetic imping heating rate for a sinusoidal excitation has a maximum at $v_c = 2\omega/3$ can be used as a diagnostic for the effec- e collision frequency; the maximum energy coupling to e plasma occurs here and can be measured with standard rf chniques.

To get a feeling for how different the rates of energy crease are in the above two cases, let us consider a plasma fusion interest operating at the following parameters: $= 2$ keV, $A = 2$, $n = 10^{19}/\text{m}^3$, $L = 0.5$ m, and $B_0 = 2.0$ The binary particle collision frequency in this case is $= v_{ii} = 1/\tau_{ii} \approx 313$ Hz, leading to a heating rate coefficient

$$\alpha = \delta^2 v_c/6 = 52\ \delta^2/\text{sec}. \tag{63}$$

ow if anomalous resistivity is present in the plasma, the llision frequency due to turbulence, etc. can be on the or- er of 5 MHz,[11] leading to a maximum heating rate coefficient of

$$\alpha_{max} = \delta^2 v_c/12 = 4.2\ 10^5\ \delta^2/\text{sec}. \tag{64}$$

rom the examples (63) and (64) it can be seen that the llisionality of the plasma can make a big difference to the ficiency of this heating method. If the plasma is turbulent, articles not only collide among themselves (binary or Cou- mb collisions), but also scatter off the fluctuating electric ld associated with the turbulence: As a result of this latter rocess, an anomalous momentum loss occurs, which en- ances the collision frequency. These enhanced total colli- on frequencies have been observed in our laboratory using method based on broadening of the electron cyclotron ab- rption resonance.[11] These anomalous momentum losses om the electron population should be equivalent in every ay to those arising from binary coulomb (or electron neu- al) collisions. This enhanced collision frequency, called e "effective collision frequency," is found to be 10–20 mes higher than the binary collision frequency.[11]

I. FIRST-ORDER HEATING WITH A SAWTOOTH ERTURBATION

The dependence of the heating rate coefficient on the quare of the field modulation factor δ constitutes a major
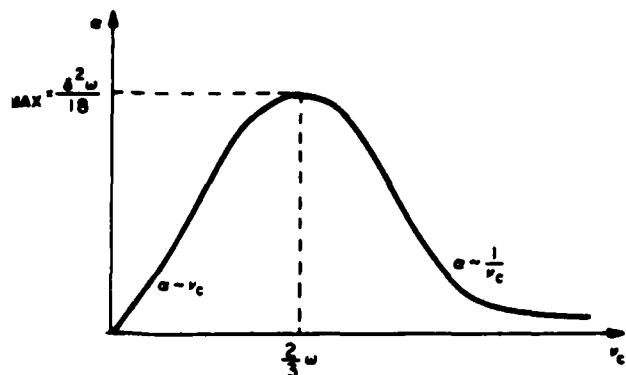
IG. 3. Heating rate coefficient versus collision frequency.
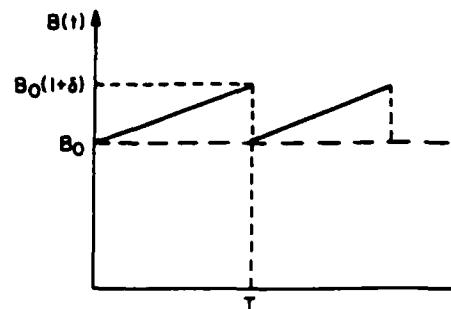
FIG. 4. Magnetic field waveform for a sawtooth perturbation.

disadvantage for the application of a sine wave perturbation: This is because δ is a small number, which makes δ^2 even smaller; therefore, a relatively small energy increase is achieved. In Ref. 9 it was shown that a triangular waveform, with a ramp down that is adiabatic in the sense of preserving the magnetic moment of the particles, also leads to second- order heating by collisional magnetic pumping. A heating rate coefficient proportional to the first power of the field modulation factor would be an improvement. To accom- plish this, a perturbation function satisfying Eq. (33) has to be found. Various modulation waveforms for $B(t)$ have been tried: The choice of these had the physical basis that a undi- rectional flow of energy had to be maintained, in contrast with the sinusoidal case, where the magnetic field in the heating region is cyclically above and below the background value. This leads to a gain of perpendicular energy in the positive half-cycle and a loss of energy in the negative-half cycle. Any heating is therefore a second-order effect result- ing from small differences of large numbers. Also important in the choice of the perturbation function is the ability to pump the plasma adiabatically and repeatedly for periods of time separated by very short durations during which the plasma is not allowed to relax. A sawtooth perturbation has been found to be an answer to the above requirements.

If a sawtooth perturbation is applied, the total magnetic field expression takes the form

$$B = B_0(1 + \delta t/T), \quad \text{for } nT \leqslant t < (n+1)T. \tag{65}$$

For the remainder of this section, the time $t = T^-$ is defined as the time just before the magnetic field sharply decreases $[B(T^-) = B_0(1 + \delta)]$ and the time $t = T^+$ is defined as the time at which the magnetic field is equal to its background value B_0. Figure 4 shows the waveform assumed for the mag- netic field. The perturbation function is a repetitive ramp with a period equal to $T = T^+$. Since an instantaneous drop of the current generating this perturbation of the magnetic field is not feasible, an appropriate assumption would be that the fall time of the current is shorter than the collision time and is nonadiabatic in the sense that the magnetic moment is not conserved during the drop of the magnetic field.

The differential equation describing the change of ener- gy during the time interval $[0,T]$ is given by

$$\frac{d^2E}{dt^2} + \frac{3}{2}\ v_c\ \frac{dE}{dt} - v_c\ \frac{\delta/T}{1 + \delta t/T}\ E = 0. \tag{66}$$

M. Laroussi and J. R. Roth

The term $(1 + \delta t/T)^{-1}$ can be expanded as

$$(1 + \delta t/T)^{-1} = 1 - \delta t/T + \cdots . \tag{67}$$

Substituting Eq. (67) into Eq. (66) one obtains

$$\frac{d^2E}{dt^2} + \frac{3}{2} \nu_c \frac{dE}{dt} - \nu_c \frac{\delta}{T}\left(1 + \frac{\delta t}{T} + \cdots\right)E = 0. \tag{68}$$

Retaining only the terms to first order in δ in order to solve for first-order heating, Eq. (68) becomes

$$\frac{d^2E}{dt^2} + \frac{3}{2} \nu_c \frac{dE}{dt} - \nu_c \frac{\delta}{T} E = 0. \tag{69}$$

The solution of Eq. (69) is

$$E(t) + C_1 e^{r_1 t} + C_2 e^{r_2 t}, \tag{70}$$

where r_1 and r_2 are given by

$$r_1 = \tfrac{3}{4} \nu_c \{ -1 + [1 + \tfrac{8}{9}(\delta/\nu_c T)]^{1/2}\}, \tag{71}$$

$$r_2 = \tfrac{3}{4} \nu_c \{ -1 - [1 + \tfrac{8}{9}(\delta/\nu_c T)]^{1/2}\}. \tag{72}$$

The term $(1 + \tfrac{8}{9} \delta/\nu_c T)^{1/2}$ can be expanded as

$$[1 + \tfrac{8}{9}(\delta/\nu_c T)]^{1/2} = 1 + \tfrac{4}{9}(\delta/\nu_c T)$$
$$+ \text{ higher order terms.} \tag{73}$$

Substituting Eq. (73) into the expressions for r_1 and r_2 and retaining only the first-order terms in δ, we obtain

$$r_1 = \tfrac{1}{3}(\delta/T), \tag{74}$$

$$r_2 = -\tfrac{3}{2} \nu_c [2 + \tfrac{1}{3}(\delta/\nu_c T)]. \tag{75}$$

The initial conditions are given by

$$E(0) = E_0, \tag{76}$$

$$\left.\frac{dE}{dt}\right|_{t=0} = \frac{\delta}{T} \frac{2}{3} E_0. \tag{77}$$

Applying the initial conditions (77) to the expression of $E(t)$ and solving for C_1 and C_2 yields

$$C_1 = E_0, \tag{78a}$$

$$C_2 = 0. \tag{78b}$$

The solution of Eq. (69) subject to the initial conditions (78a) and (78b) is

$$E(t) = E_0 e^{(2/3)\delta(t/T)}. \tag{79}$$

This solution is only good in the time interval $0 < t < T$ and for $\delta/\nu_c T \ll 1$. At $t = T^-$, the energy is

$$E \sim E_0 e^{(2/3)\delta} \sim E_0(1 + \tfrac{2}{3}\delta), \tag{80}$$

which yields

$$\Delta E = E(T^-) - E(0) = \tfrac{2}{3} \delta E_0. \tag{81}$$

Now let us examine what happens to the energy during the sharp fall of the magnetic field between T^- and T^+. During this time, the assumption of the constancy of the adiabatic invariant may be violated; thus we have

$$\frac{d\mu}{dt} = \frac{1}{B} \frac{dE_1}{dt} - \frac{E_1}{B^2} \frac{dB}{dt} . \tag{82}$$

Equation (82) can be written as

$$\frac{d\dot{E}}{dt} = \mu \frac{dB}{dt} + B \frac{d\mu}{dt} . \tag{83}$$

Since no collisions occur between T^- and T^+, we have

$$\frac{dE_\parallel}{dt} = 0. \tag{84}$$

Summing Eqs. (83) and (84), we obtain

$$\frac{dE}{dt} = \mu \frac{dB}{dt} + B \frac{d\mu}{dt} . \tag{85}$$

Equation (85) can also be written as

$$\frac{\Delta E}{\Delta t} + \mu \frac{\Delta B}{\Delta t} + B \frac{\Delta \mu}{\Delta t} \tag{86}$$

or

$$\Delta E = \mu \Delta B + B \Delta \mu. \tag{87}$$

The change in magnetic moment $\Delta \mu$ is given by

$$\Delta \mu = \mu(T^+) - \mu(T^-), \tag{88}$$

with

$$\mu(T^-) = E_1(T^-)/B_0(1 + \delta), \tag{89}$$

$$\mu(T^+) = E_1(T^+)/B_0. \tag{90}$$

Since no collisions occur between T^- and T^+, we assume that no appreciable change in the perpendicular energy occurs. Thus we have

$$E_1(T^+) \approx E_1(T^-) = (1 + \delta)E_1(0). \tag{91}$$

As a result of equipartition we have

$$E_1(0) = \tfrac{2}{3} E_0,$$

which yields

$$\Delta \mu = \tfrac{2}{3} \delta(E_0/B_0). \tag{92}$$

Inserting Eq. (92) into Eq. (87) and substituting ΔB by $(-\delta B_0)$ we obtain

$$\Delta E = -\mu(T^-)\delta B_0 + B(T^-)\tfrac{2}{3} \delta(E_0/B_0). \tag{93}$$

Using the facts that

$$\mu(T^-) = \tfrac{2}{3}(E_0/B_0), \tag{94}$$

$$B(T^-) = (1 + \delta)B_0, \tag{95}$$

Eq. (93) becomes

$$\Delta E = \tfrac{2}{3} \delta^2 E_0. \tag{96}$$

Summing Eqs. (96) and (81) the energy increase per cycle is found to be

$$\Delta E = \tfrac{2}{3} \delta(1 + \delta)E_0. \tag{97}$$

Since $\delta \ll 1$, Eq. (97) can be approximated as

$$\Delta E = \tfrac{2}{3} \delta E_0. \tag{98}$$

The heating rate dE/dt is given by

$$\frac{dE}{dt} = \frac{\delta \omega}{3\pi} E_0, \tag{99}$$

where the period of the sawtooth is taken as $T = 2\pi/\omega$.

Equation (99) suggests that first-order heating is achievable with a sawtooth perturbation and that the heating rate is independent of the collision frequency.[9] This is an interesting result and of key importance for fusion machines, where the mean free path is larger than the plasma length.

To check this result, the generalized theory for first-order heating already presented is applied.[9] Substituting

M. Laroussi and J. R. Roth

$f'(t)$ by its value for a sawtooth perturbation in Eq. (36) yields the value of the coefficient l_1:

$$l_1 = \omega/3\pi. \tag{100}$$

Using Eq. (39), the heating rate is found to be

$$\frac{dE}{dt} = \delta l_1 E_0 = \frac{\delta\omega}{3\pi} E_0 = \beta E_0, \tag{101}$$

where β is the heating rate coefficient given by

$$\beta = \delta\omega/3\pi. \tag{102}$$

Equation (102) is in agreement with the result of Eq. (99).[9] The independence of Eq. (102) of the collision frequency is a consequence of the collisionless "resetting" of the magnetic induction during the sudden drop on the trailing edge of the sawtooth in Fig. 4. This effect allows the perpendicular energy to increase linearly in time without a decrease associated with the decreasing magnetic field. This perpendicular energy will be carried to the parallel components as long as there are any collisions at all. Thus the drop at the trailing edge of the sawtooth need not be so fast as to be nonadiabatic in the sense of violating the constancy of μ; the drop-off time can be any duration shorter than the collision time.

V. COMPARISON BETWEEN FIRST-ORDER COLLISIONAL MAGNETIC PUMPING AND OTHER PLASMA HEATING METHODS

In order to have a quantitative idea of how beneficial it is to achieve first-order heating by collisional magnetic pumping, we have to answer the following question: How does this heating rate compare to other plasma heating methods?

First, let us compare the two heating rate coefficients obtained when sinusoidal and sawtooth perturbations are applied to collisional magnetic pumping. For this, the ratio of the two coefficients given by Eq. (102) and the inverse of (58) is taken to be

$$\beta/\alpha = (\delta\omega/3\pi)\left[6(\tfrac{9}{4} v_c^2 + \omega^2)/\delta^2\omega^2 v_c\right], \tag{103}$$

where β and α are, respectively, the heating rate coefficients for a sawtooth and a sinusoidal perturbation. Assuming that the rf driving frequency and the field modulation factor δ are the same for both cases the ratio (103) becomes

$$\beta/\alpha = (\tfrac{9}{2} v_c^2 + 2\omega^2)/\pi\delta\omega v_c. \tag{104}$$

If the plasma is highly collisional, we have $v_c \gg \omega$ and Eq. (104) becomes

$$\beta/\alpha = (9/2\pi)(v_c/\delta\omega). \tag{105}$$

The ratio (105) is much larger than unity. For a small δ and a large collision frequency to driving frequency ratio, β can be as much as three orders of magnitude larger than α.

If the plasma is "collisionless," we have $\omega \gg v_c$ and Eq. (104) becomes

$$\beta/\alpha = (2/\pi)(\omega/\delta v_c). \tag{106}$$

As in case (105) the ratio (106) is much larger than unity; for a small value of δ and a large ω/v_c, β can be two or three orders of magnitude larger than α.

The ratio β/α is minimum when $\omega = (3/2) v_c$, and it is given by

$$\beta/\alpha = 6/\pi\delta. \tag{107}$$

Equation (107) is still a number greater than 1. For a field modulation factor of 1%, we have

$$\beta = 191 \alpha. \tag{108}$$

It therefore appears that in all cases first-order heating is an improvement on second-order heating. First-order heating provides a heating rate coefficient at least one order of magnitude larger than otherwise possible with second-order heating.

Ion or electron cyclotron resonant heating is one of the most efficient and widely used heating methods in fusion experiments: The maximum energy increase per cyclotron period obtained by this method is given by[6]

$$\Delta E_\perp = \pi E(2mE_\perp)^{1/2}/B_0, \tag{109}$$

where E is the electric field amplitude of the wave, B_0 is the background magnetic field, and $E_\perp$ is the perpendicular component of the energy whose equipartitioned value is equal to 2/3 of the total energy. The energy increase rate is given by

$$\gamma = \Delta E_\perp/\tau_c = qE(E_\perp/2m)^{1/2}, \tag{110}$$

where τ_c is the cyclotron period given by

$$\tau_c = 2\pi m/qB. \tag{111}$$

To compare the energy increase rate (110) to the one obtained by first-order heating with collisional magnetic pumping, their ratio is taken to be

$$\beta E_0/\gamma = [\delta\omega(2m)^{1/2}/3\pi qE](E_0/E_\perp^{1/2}). \tag{112}$$

To acquire a quantitative idea of the ratio (112), consider the following characteristic values of the plasma parameters: Let $\omega = 2\pi 10^7$ rad/sec, $\delta = 10^{-2}$, $E = 100$ V/cm, $E_0 = 1$ keV, and the plasma consists of helium ions. The value of $\beta E_0/\gamma$ is

$$\beta E_0/\gamma = 7.45\%.$$

Keeping in mind that the ratio (112) is taken for the maximum value that the ICRH (ion cyclotron resonance heating) rate γ can reach, it can be concluded that first-order collisional magnetic pumping is a heating method that may be competitive with other widely used methods such as ICRH.

VI. CONCLUSION

The equations describing the rate of change of the energy of the particles in a plasma adiabatically pumped with collisional magnetic pumping are presented. A general solution for first-order heating along with particular solutions to the energy increase rate for two specific magnetic field perturbations are derived.

When a sinusoidal perturbation is superimposed on the background magnetic field, a heating rate proportional to the second power of the field modulation factor δ is obtained. This is in agreement with the results of Schluter[2] and Berger et al.[3] This heating rate is also strongly dependent on the collisionality of the plasma. A maximum heating rate is

Phys. Fluids B, Vol. 1, No. 5, May 1989

A-27

M. Laroussi and J. R. Roth

achieved when the driving rf frequency is 1.5 times larger than the collision frequency.

The application of a sinusoidal perturbation has two major drawbacks. The first drawback is the dependence of the heating rate on the second power of the field modulation factor δ, this number is less than unity and its square is even smaller. The second drawback is the strong dependence of the heating rate on the collision frequency. This is especially disadvantageous for a fusion-grade plasma, where the mean free path is larger than the plasma length. These two drawbacks result in a small energy increase rate. In the past, these factors apparently led researchers to neglect this heating method.

In the search for more satisfactory results, a heating rate proportional to the first power of the field modulation factor and weakly dependent on the collision frequency was needed. A sawtooth perturbation proved to be an appropriate choice. The heating rate for this case is two to three orders of magnitude larger than that for second-order heating and is comparable to other widely used plasma heating methods. An experimental demonstration of this first-order heating has been presented elsewhere.[9]

[1]L. Spitzer, Jr. and L. Witten, *AEC Research and Development Report* (Princeton Plasma Physics Laboratory, Princeton, 1953).
[2]A. Schluter, Z. Naturforsch. A 12, 822 (1957).
[3]J. M. Berger, W. A. Newcomb, J. M. Dawson, E. A. Friedman, R. M. Kulsrud, and A. Lenard, Phys. Fluids 1, 301 (1958).
[4]T. Kammash, *Fusion Reactor Physics* (Ann Arbor Science, Ann Arbor, MI, 1975).
[5]K. Miyamoto, *Plasma Physics for Nuclear Fusion* (MIT, Cambridge, MA, 1979).
[6]J. R. Roth, *Introduction to Fusion Energy* (InPrint, Charlottesville, VA, 1986).
[7]M. Laroussi, in *Proceedings of the Southeastern Symposium on System Theory* (IEEE Computer Society, Washington, DC, 1986), pp. 475–479.
[8]M. Laroussi and J. R. Roth, in *Proceedings of the Seventh Topical Conference on Applications of Radio Frequency Power to Plasmas*, Kissimmee, FL, AIP Conf. Proc. No. 159 (AIP, New York, 1987), pp. 438–441.
[9]M. Laroussi, Ph.D. thesis, The University of Tennessee at Knoxville, 1988.
[10]M. G. Floquet, Annales ENS 12, 47 (1883).
[11]J. R. Roth and P. D. Spence, in *Proceedings of the 18th International Conference on Phenomena in Ionized Gases*, Swansea, Wales (The Institute of Physics, Bristol, UK, 1987), Vol. 4, pp. 614–615.

Phys. Fluids B. Vol. 1. No. 5, May 1989

A-28

M. Laroussi and J. R. Roth

Computational treatment of collisional magnetic pumping

M. Laroussi[a] and J. Reece Roth

The University of Tennessee, Knoxville, Department of Electrical and Computer Engineering, Knoxville, Tennessee 37996-2100

When collisional magnetic pumping is applied to a plasma, the heating rate depends strongly on the nature of the waveform of the magnetic perturbation, whether sinusoidal, triangular, or sawtoothed in time. Numerical solutions to the energy transfer problem are obtained when these waveforms are applied to heat a plasma, and compared with previously obtained analytical results using small perturbation theory where these results are available. A specially written FORTRAN program computes the numerical values of the parallel, perpendicular, and total energy at each time increment. The plasma heating rates and optimum heating conditions derived from this study are in good agreement with analytical limiting cases and available experimental data, except when the perturbation amplitude becomes large er analytical results no longer hold.

I. INTRODUCTION

Magnetic pumping is achieved by wrapping an exciter coil around a cylindrical plasma and perturbing the confining magnetic field $B = B_0[1 + \delta f(t)]$, where B_0 is the uniform steady-state background magnetic field, δ is the field modulation factor defined as $\delta = \Delta B / B_0$, and $f(t)$ is a periodic function of time. Contrary to Ohmic heating, where the electric field is parallel to the confining axial magnetic field, in magnetic pumping the oscillating electric field is produced by variation of the axial magnetic field and thus is perpendicular to it. This type of heating was called "magnetic pumping" due to the existence of a compressional wave perpendicular to the background magnetic field, causing the plasma to be cyclically compressed and relaxed by an alternating $E \times B$ force. Under favorable conditions, the mechanical energy exerted by the compressing force would ultimately be absorbed by the plasma and lead to heating of the charged particles.

Depending on how plasma parameters and the driving force relate to each other, different heating regimes are obtained. In the case of collisional magnetic pumping, which is the main interest of this paper, the collisions are the mediator between the rf field and the charged particles. To achieve heating by collisional magnetic pumping, the charged particles should collide before leaving the heating region. Mathematically, the following inequalities have to be satisfied:

$$\omega_{tr} \ll v_c \sim \omega \ll \omega_{cy},$$

where ω_{tr}, v_c, ω, and ω_{cy} are, respectively, the transit frequency through the heating region, the collision frequency, the rf field frequency, and the particle gyrofrequency.

Magnetic pumping was first suggested as a heating method (for the Stellarator) by Spitzer and Witten in 1953.[1] A theoretical analysis was published by Schluter,[2] and also by Berger et al.[3] a few years later. These papers constitute most of the very limited early literature on this subject. This was so because heating by magnetic pumping was first part of a classified project, and later was neglected due to the attention given to other more promising heating methods, such as ion-cyclotron resonance heating. After a fallow period of nearly 30 years, there has been a revival of interest in this heating method.[4-9] This interest is a result of the demonstration that heating proportional to the field modulation factor δ rather than its square is possible. This enhanced heating rate can be comparable with other rf-based methods, such as ion- or electron-cyclotron resonance heating.[4-9]

II. AVAILABLE ANALYTICAL RESULTS

The process of energy transfer between the rf field and the charged particles has been studied analytically, starting from the assumption that for a magnetic field slowly varying in time and space, the magnetic moment (defined as the ratio of the perpendicular component of the kinetic energy to the magnetic field) is a constant of the motion. It can be shown[2-7] that a general equation relating the change in the total energy of a particle to the change of the magnetic field can be derived. This equation is

$$\frac{d^2E}{dt^2} - \left[-\frac{3}{2}v_c + \frac{d^2B}{dt^2}\left(\frac{dB}{dt}\right)^{-1} \right]\frac{dE}{dt} - \frac{v_c}{B}\frac{dB}{dt}E = 0. \quad (1)$$

This homogeneous, linear, second-order differential equation has periodic coefficients that can go to infinity periodically. Such equations usually appear in astronomical studies, and their general solution was given by the French mathematician Floquet.[10] Using Floquet's theory and a perturbation treatment, Schluter[2] and Berger et al.[3] derived the energy increase rate when a sinusoidal perturbation is applied. The energy can be written in terms of the collisionality parameter $v_c T$, where $T = 2\pi/\omega$ is the period of the periodic perturbation, and $v_c T$ itself is the number of collisions per field period. The energy increase rate for a sinusoidal perturbation is

$$\Delta E = \delta^2 E_0 \left[2\pi^2 v_c T / 3 \left(\tfrac{3}{4}v_c^2 T^2 + 4\pi^2 \right) \right] \text{ eV/cycle}, \quad (2)$$

where δ is the field modulation factor and E_0 is the initial energy in electron-volts. The analytical heating rates are all a

---
[a] Present address: Department of Electrical Engineering, Technical University, Sfax, Tunisia.

function of the initial energy E_0, because Eq. (1) is a statement about the thermally adiabatic heating rate, and not about a complete energy balance of the plasma. In a steady-state complete energy balance, the plasma particles would lose the "memory" of their initial energy, in favor of the prevailing kinetic temperature.

The optimum collisionality parameter, at which the energy increase rate is a maximum, is

$$v_c T = 4\pi/3 \text{ collisions/cycle}, \tag{3}$$

and the value of this maximum energy increase rate is

$$(\Delta E)_{\max} = \delta^2 E_0 (\pi/9) \text{ eV/cycle}. \tag{4}$$

For a highly collisional plasma, $v_c T \gg 1$, and the energy increase rate can be approximated,

$$\Delta E \approx \delta^2 E_0 (8\pi^2/27) \times (1/v_c T) \text{ eV/cycle}, \tag{5}$$

while for a relatively collisionless plasma, $v_c T \ll 1$, and the energy increase rate becomes

$$\Delta E \approx \delta^2 E_0 (v_c T/6) \text{ eV/cycle}. \tag{6}$$

These energy increase rates are valid for small magnetic field perturbations $\delta \ll 1$. The upper limit of the validity of these expressions can best be determined by computational investigation of Eq. (1) with a sinusoidal magnetic perturbation.

Equation (1) has recently been solved for the general case in which an arbitrary periodic perturbation function $f(t)$ is assumed.[4,5,7] A condition for the achievement of a heating rate proportional to the *first* power of the field modulation factor δ has been derived.[5,7] It is found that a sawtooth perturbation satisfies the condition for first-order heating, and the energy increase rate for this case is

$$\Delta E = \tfrac{2}{3}\delta E_0 \text{ eV/cycle}. \tag{7}$$

For this case, the energy increase rate for $\delta \ll 1$ is independent of the collisionality parameter, and is two or three orders of magnitude larger than the energy increase rate of the sinusoidal perturbation giving rise to Eq. (2). Over what range of δ this improved heating might prove valid is, again, best determined with a computational investigation of a sawtooth waveform in Eq. (1).

III. COMPUTATIONAL ANALYSIS

The theoretical treatment of collisional magnetic pumping[1-5] provides us with small perturbation solutions to the energy increase rate and how it relates to the collisionality of the plasma. However, this approach fails to give a quantitative picture of the evolution of the energy with time from the instant that collisional magnetic pumping is turned on, and also fails to give insight into the conditions for which this small perturbation solution is no longer valid. For this purpose, a numerical solution to the energy transfer equation is sought. This solution provides us with numerical values of the energy for each time increment. This series of numbers can be plotted on an energy–time diagram. The energy increase rate can be easily extracted from such a diagram and compared with the analytical prediction discussed above.

The equations describing the variations of the parallel and perpendicular components of the energy are given by[5,7]

$$\frac{dE_\parallel}{dt} = v_c \left(\frac{E_\perp}{2} - E_\parallel \right) \tag{8}$$

and

$$\frac{dE_\perp}{dt} = \frac{E_\perp}{B} \frac{dB}{dt} - v_c \left(\frac{E_\perp}{2} - E_\parallel \right). \tag{9}$$

Since the total energy is the sum of $E_\parallel$ and $E_\perp$, we also have

$$\frac{dE}{dt} = \frac{dE_\parallel}{dt} + \frac{dE_\perp}{dt}. \tag{10}$$

The magnetic field is given by

$$B = B_0 [1 + \delta f(t)], \tag{11}$$

which gives

$$\frac{1}{B} \frac{dB}{dt} = \frac{\delta f'(t)}{1 + \delta f(t)}. \tag{12}$$

Let

$$E_\parallel = x,$$
$$E_\perp = y,$$

and

$$F(t) = \delta f'(t)/[1 + \delta f(t)].$$

Equations (8) and (9) can be written as

$$\frac{dx}{dt} = -v_c x + 0.5 v_c y, \tag{13}$$

and

$$\frac{dy}{dt} = -v_c x - 0.5 v_c y + y F(t). \tag{14}$$

For a given value of the collision frequency v_c, a perturbation function $f(t)$, and initial values x_0 and y_0, numerical values of x and y are computed and tabulated for each time step. A plotting routine furnishes the plots of x vs t and y vs t. The total energy is also plotted as $z = x + y$. The FORTRAN program used has the flexibility of entering the values of the collision frequency v_c, the period of the rf waveform T, the field modulation factor δ, the initial values of the energy components, the total energy of the particles in electron-volts, and the time step size. The y axis of the plots represents energy in electron-volts and the x axis represents time in units of the period of the rf waveform T. The number of periods plotted can be changed, allowing one to follow the evolution of the energy far enough in time to observe any transient period, along with any steady state reached. This program is available as an appendix to Ref. 7, or from the authors.

Three waveforms have been studied, the sinusoidal, triangular, and sawtooth waveform. These waveforms can be, or have been, implemented experimentally.[7,9] This not only allows a comparison between theory and experiment, but also gives a sense of practicality to this work. Since the collision frequency and how it relates to the rf frequency is an important parameter that affects the heating rate, we define a *collisionality parameter*, $v_c T$, given by the product of the collision frequency and the period of the rf wave. The collisionality parameter is a dimensionless number that indicates how many collisions occur during one rf period. By varying $v_c T$, different regimes are obtained and the resulting

Phys. Fluids B, Vol. 1, No. 6, June 1989

A-30

M. Laroussi and J. R. Roth
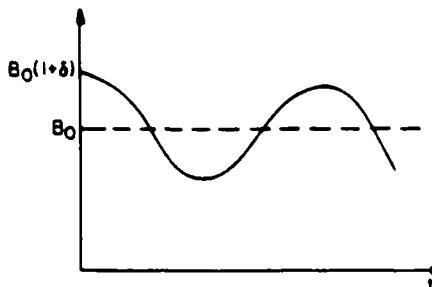
FIG. 1. Magnetic field waveform for a sinusoidal perturbation.


FIG. 3. Total energy versus time for $\delta = 0.1$, $v_c T = 0.2$, $E_0 = 300$ eV, and a sinusoidal perturbation.

heating rates are computed from the plots of the energy versus time.

IV. APPLICATION TO A SINE WAVE

When a sine wave perturbation is applied, results similar to those first considered by Schluter[2] and Berger et al.[3] should be obtained. Figure 1 shows the waveform of the magnetic field assumed. For a "collisionless" plasma ($v_c T = 0.2$), shown in Figs. 2 and 3, the total energy of a particle oscillates with the field with only a very small increase in its average value. This is consistent with the lack of energy transfer between the parallel and perpendicular components of the energy. For this case, the values of the field modulation factor δ, and of the initial energy E_0, are chosen to be, respectively, 0.1 and 300 eV. Figure 2 shows that after a transient period of about $12T$, where T is the period of the driving rf waveform, the parallel component of the energy reaches a plateau at a level less than its initial value. This is a phase-dependent effect, and averages out to the initial value over all initial phase angles for $f(t)$. For a collisional plasma ($v_c T = 6$), Figs. 4 and 5 show that the average value of the energy increases with time at a rate of about 0.85 eV/cycle, if $E_0 = 300$ eV and $\delta = 0.10$.

FIG. 4. Parallel component of the energy versus time for $\delta = 0.1$, $v_c T = 6$, $E_0 = 300$ eV, and a sinusoidal perturbation.
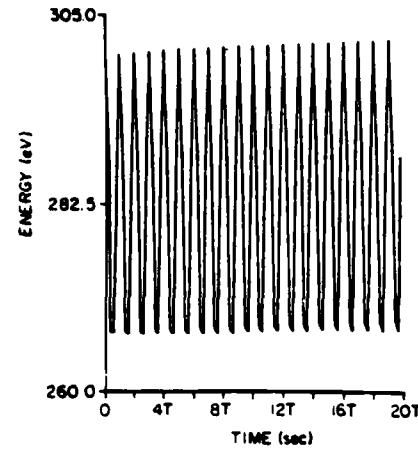

FIG. 2. Parallel component of the energy versus time for $\delta = 0.1$, $v_c T = 0.2$, $E_0 = 300$ eV, and a sinusoidal perturbation.

FIG. 5. Total energy versus time for $\delta = 0.1$, $v_c T = 6$, $E_0 = 300$ eV, and a sinusoidal perturbation.

A-31

M. Laroussi and J. R. Roth
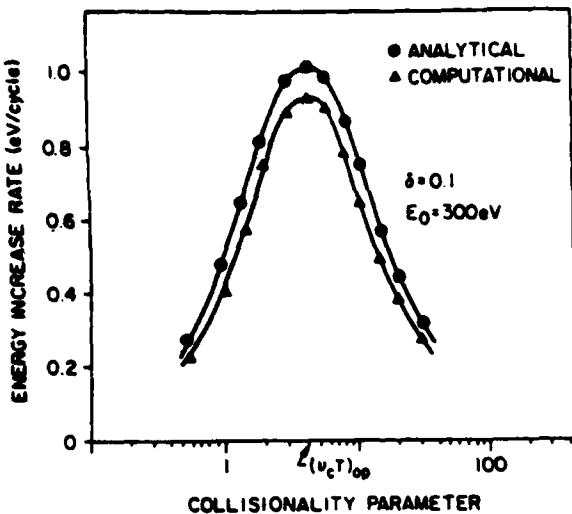
FIG. 6. Energy increase rate versus collisionality parameter for $\delta = 0.1$, $E_0 = 300$ eV, and a sinusoidal perturbation.

In Fig. 6, the energy increase rate is plotted against the collisionality parameter $v_c T$ at a field modulation factor of $\delta = 0.1$ and an initial value of energy of 300 eV. The solid dots represent analytical results from Eq. (2), while the triangles represent the computational results obtained from energy plots similar to Figs. 2–5. The results show good agreement with the analytical prediction. The energy increase rate is peaked, with a maximum at an optimum value of the collisionality parameter of about 4.2, in agreement with Eq. (3).

Figure 7 is a plot on a log–log scale of the energy increase rate as a function of the field modulation factor for several values of the collisionality parameter, and an initial

FIG. 7. Energy increase rate versus field modulation factor for $E_0 = 300$ eV, several collisionality parameters, and a sinusoidal perturbation.

FIG. 8. Magnetic field waveform for a triangular perturbation.

value of the energy of 300 eV. A slope of 2 indicates that the energy increase rate is proportional to the second power of the field modulation factor δ^2, which is also in agreement with Eq. (2). The small perturbation approximation represented by Eq. (2) is good out to at least a field modulation factor of $\delta = 0.40$.

V. APPLICATION TO A TRIANGULAR WAVEFORM

A triangular waveform of adjustable shape was selected to study collisional magnetic pumping computationally because it is a general case, one limit of which is a sawtooth waveform. Figure 8 shows the magnetic field when a triangular perturbation is applied. If the ramping down time, $(T - L)$, is gradually reduced until it becomes zero, a transition to a sawtooth waveform is achieved. This allows one to write a simple algorithm capable of showing the change in the energy waveform when the transition between triangular and sawtooth waveforms occurs.

First, a symmetrical triangular waveform with $L = T/2$ and a collisional case is applied by setting the collisionality parameter $v_c T$ equal to 10. This implies ten collisions per field period. A field modulation factor of $\delta = 0.1$ is chosen. As seen in Figs. 9–11, the parallel, perpendicular, and total


FIG. 9. Parallel component of the energy versus for $\delta = 0.1$, $v_c T = 10$, $E_0 = 300$ eV, and a triangular perturbation

A-32

M. Laroussi and J. R. Roth
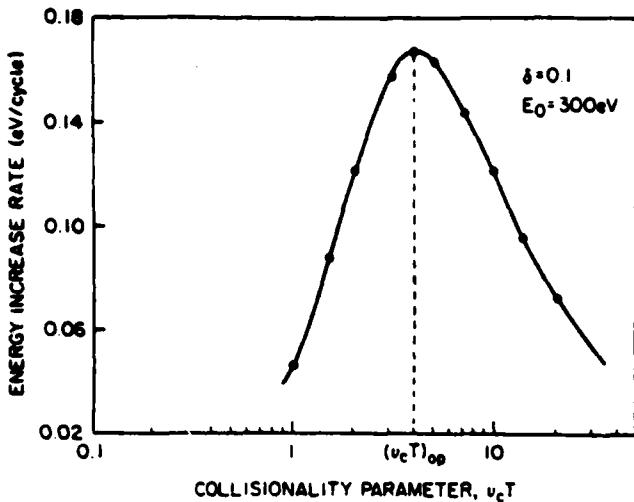
FIG. 15. Energy increase rate versus collisionality parameter for $\delta = 0.1$, $E_0 = 300$ eV, and a triangular perturbation.

which results in zero energy gain. For the sinusoidal perturbation, Eq. (2) predicts a small heating rate of 0.05 eV/cycle, which may be too small to be apparent in Fig. 14.

Setting the collisionality parameter equal to 20, an energy increase is also obtained, but of smaller magnitude than the $v_c T = 10$ case. This, with the data in Figs. 9–14, indicates that the energy increase rate has a maximum at some
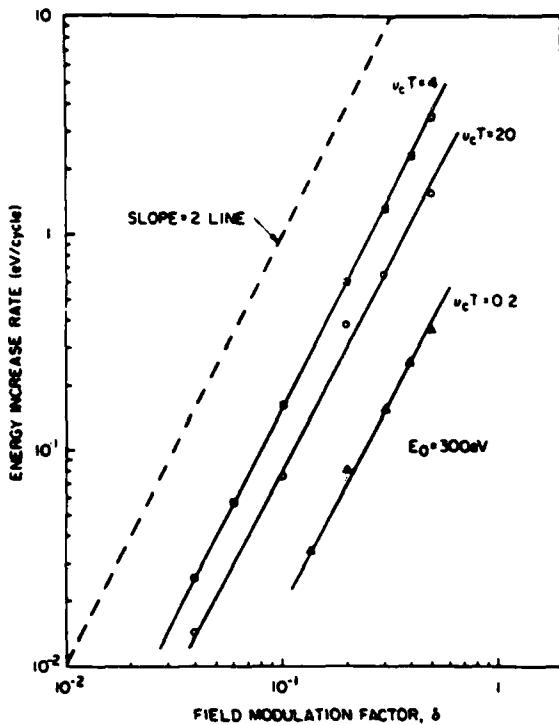
FIG. 16. Energy increase rate versus field modulation factor for $E_0 = 300$ eV, several collisionality parameters, and a triangular perturbation.
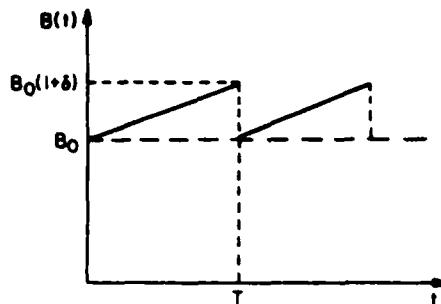
FIG. 17. Magnetic field waveform for a sawtooth perturbation.

optimum value of the collisionality parameter. Figure 15 shows a plot of the energy increase rate versus collisionality parameter at a field modulation factor of $\delta = 0.1$, and an initial value of the energy of $E_0 = 300$ eV. The maximum energy increase rate is very close to the collisionality parameter of $v_c T = 4\pi/3$ predicted by Eq. (3) for the sinusoidal perturbation case; the maximum value of the energy increase rate in Fig. 15, $\Delta E \approx 0.17$ eV/cycle, is well below the maximum value of $\Delta E = 1.05$ eV/cycle predicted by Eq. (4) for the sinusoidal driving waveform.

The energy increase rate has been plotted in Fig. 16 against the field modulation factor on a log–log scale for several values of the collisionality parameter. For all values of the collisionality parameter, it has been found from solutions similar to Figs. 9–14, that the energy increase rate is proportional to the second power of the field modulation factor. This dependence holds at least up to $\delta = 0.50$. The above analysis has been done for several nonzero ramping down times but no quantitative effects on the energy increase rate have been observed.

VI. APPLICATION TO A SAWTOOTH WAVEFORM

When a sawtooth perturbation is applied to collisional magnetic pumping, the magnetic field assumes the waveform shown in Fig. 17. Many collisionality regimes have
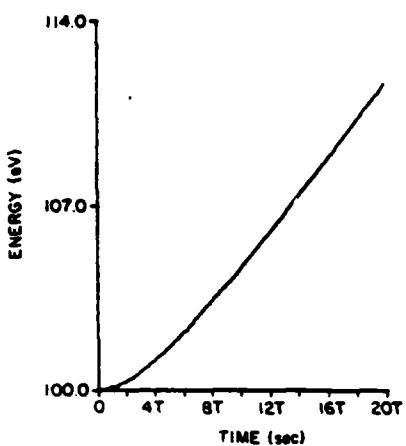
FIG. 18. Parallel component of the energy versus time for $\delta = 0.01$, $v_c T = 0.2$, $E_0 = 300$ eV, and a sawtooth perturbation.

A-33
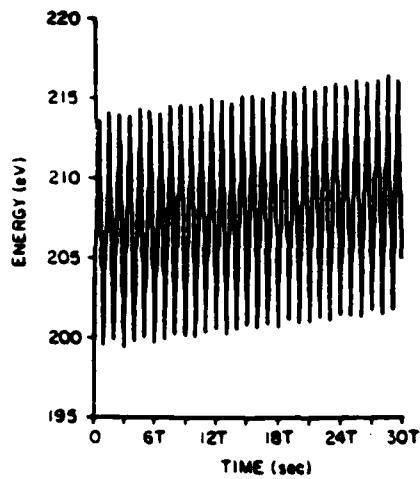
FIG. 10. Perpendicular component of the energy versus time for $\delta = 0.1$, $v, T = 10$, $E_{\shortparallel} = 300$ eV, and a triangular perturbation.
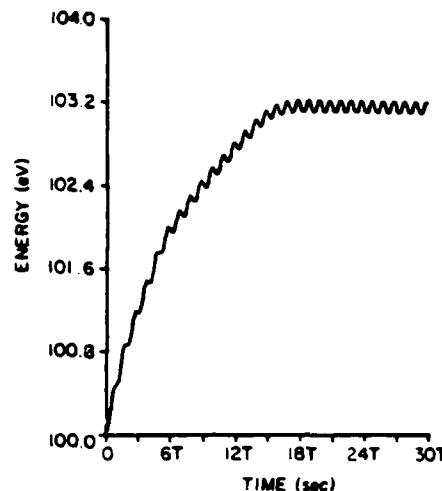
FIG. 12. Parallel component of the energy versus time for $\delta = 0.1$, $v, T = 0.1$, $E_{\shortparallel} = 300$ eV, and a triangular perturbation.

energy oscillate with the field but their average values increase with time. The total energy increase per cycle for a particle with an initial energy of 300 eV is about 0.12 eV. This compares with about 0.75 eV/cycle, predicted by Eq. (2) for the sinusoidal case.

Now if the collisionality parameter is equal to 0.1, a low-collisionality case is obtained for which one collision occurs each ten field periods (see Figs. 12–14). As shown in Fig. 14, the total energy oscillates with the field, but its average value does not increase significantly with time. The explanation of this can be seen in Fig. 12, which shows the parallel component of the energy as a function of time. For a transient period lasting approximately $15T$, where T is the period of the driving rf waveform, the parallel energy increases, but soon reaches a saturation plateau. As the field pumps the plasma further, no energy transfer between the perpendicular component of the energy and its parallel component occurs,
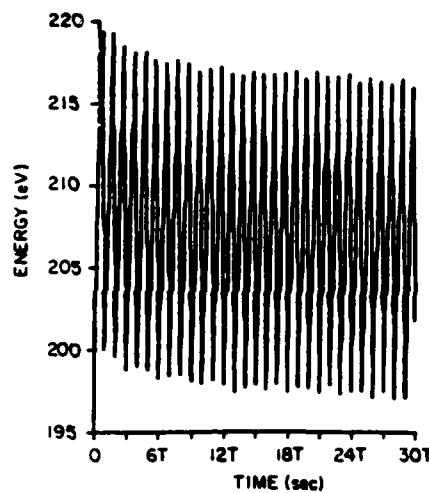
FIG. 13. Perpendicular component of the energy versus time for $\delta = 0.1$, $v, T = 0.1$, $E_{\shortparallel} = 300$ eV, and a triangular perturbation.
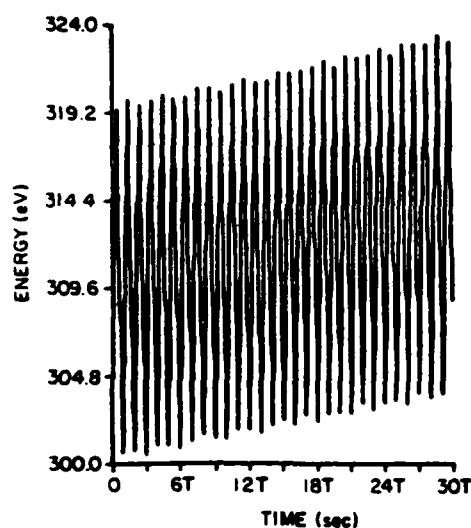
FIG. 11. Total energy versus time for $\delta = 0.1$, $v, T = 10$, $E_{\shortparallel} = 300$ eV, and a triangular perturbation.
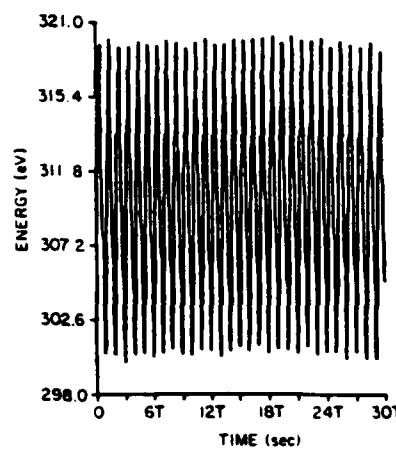
FIG. 14. Total energy versus time for $\delta = 0.1$, $v, T = 0.1$, $E_{\shortparallel} = 300$ eV, and a triangular perturbation.
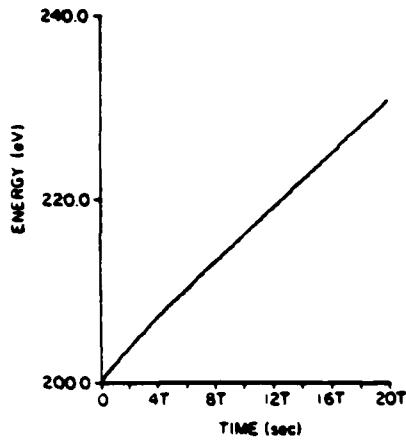
A-34

FIG. 19. Perpendicular component of the energy versus time for $\delta = 0.01$, $v_c T = 0.2$, $E_0 = 300$ eV, and a sawtooth perturbation.

FIG. 21. Total energy versus time for $\delta = 0.01$, $v_c T = 6$, $E_0 = 300$ eV, and a sawtooth perturbation.

been tried but the energy increase rate was independent of the collisionality parameter, as predicted by Eq. (7). Contrary to the triangular and sinusoidal waveform cases, the energy does not oscillate, but keeps increasing with time, at a rate of 20 eV/cycle when a particle of 300 eV initial energy and a field modulation factor of $\delta = 0.10$ are assumed. This linear increase is a consequence of a lack of thermal equilibrium during the sharp drop-off at the trailing edge of the waveform.[5,7] Figures 18–20 show the behavior with time of the parallel, perpendicular, and total energy for a collisionless plasma ($v_c T = 0.2$). Figure 21 shows the total energy versus time for a collisionless plasma ($v_c T = 6$).

The energy increase rate versus the collisionality parameter is plotted in Fig. 22, for a field modulation factor of 0.01 and an initial energy of 300 eV. The solid dots represent the analytical results predicted by Eq. (7), and the triangles represent computational results obtained from the energy plots. These results are in excellent agreement, and confirm the fact that the energy increase rate is independent of the plasma collisionality for the sawtooth driving waveform.

FIG. 22. Energy increase rate versus collisionality parameter for $\delta = 0.01$, $E_0 = 300$ eV, and a sawtooth perturbation.

FIG. 20. Total energy versus time for $\delta = 0.01$, $v_c T = 0.2$, $E_0 = 300$ eV, and a sawtooth perturbation.
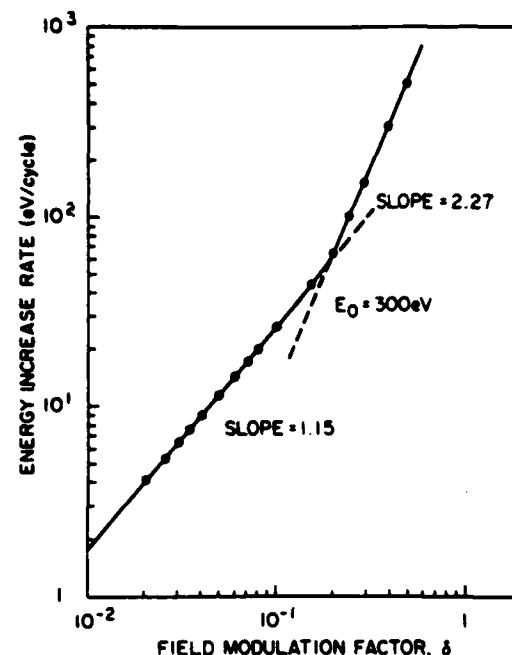
FIG. 23. Energy increase rate versus field modulation factor for $E_0 = 300$ eV and a sawtooth perturbation.

A-35

M. Laroussi and J. R. Roth

A log–log plot of the energy increase rate versus the field modulation factor δ is shown in Fig. 23. It shows that for $\delta < 0.20$, the relationship is linear with a slope near 1, but for $\delta > 0.20$ the slope is no longer unity (it is about 2.27). This is consistent with the analytical result of Eq. (7), which predicts first-order heating only for small field modulation factors. Figure 23 indicates that the small perturbation assumption on which Eq. (7) is based breaks down above $\delta = 0.20$. Figure 23 also indicates that for large field modulation factors, $\delta > 0.20$, the heating rate reverts to the second-order (δ^2) dependence characteristic of a sinusoidal perturbation, but with an amplitude about 15 times that predicted by Eq. (4), the highest possible heating rate for small sinusoidal perturbations.

VII. CONCLUSIONS

The above analysis shows that the plasma collisionality plays an important role in the viability of collisional magnetic pumping as a plasma heating method if sine wave or triangular perturbing waveforms are used. It also confirms that the heating rate is proportional to the square of the field modulation factor δ for these waveforms, when this modulation factor is much less than unity. This was predicted analytically for the sinusoidal waveform.[1-5] To achieve the best heating performance in these cases, operation at an optimum collisionality is required. The optimum collisionality parameter, $v_c T$, is $4\pi/3$ for both the sinusoidal and triangular waveforms. Away from this maximum, the energy increase rate falls off rapidly, leading to lower heating performance. The triangular waveform appears not to heat as well as the sinusoidal waveform by a factor of 5 or more, as indicated by a comparison of Figs. 6 and 15.

The computational analysis shows that the energy increase rate is indeed independent of the collisionality parameter when a sawtooth perturbation is applied. It also confirms that first-order heating is achievable for small values of the field modulation factor, less than 0.20. The energy increase rate in this case is many orders of magnitude larger than the one obtained when a sinusoidal perturbation is used. Experimental implementation of heating with the sawtoothed waveform is described elsewhere.[7-9]

ACKNOWLEDGMENT

[1] L. Spitzer, Jr. and L. Witten, *AEC Research and Development Report*, Princeton, 1953.
[2] A. Schluter, Z. Naturforsch. **12a**, 822 (1957).
[3] J. M. Berger, W. A. Newcomb, J. M. Dawson, E. A. Friedman, R. M. Kulsrud, and A. Lenard, Phys. Fluids **1**, 301 (1958).
[4] M. Laroussi, in *Proceedings of the Southeastern Symposium on System Theory* (IEEE Computer Society, Washington, DC, 1986), pp. 475–479.
[5] M. Laroussi and J. R. Roth, Physics of Fluids B (in press).
[6] J. R. Roth, *Introduction to Fusion Energy* (Inprint, Inc., Charlottesville, VA, 1986).
[7] M. Laroussi, Ph.D. dissertation, The University of Tennessee at Knoxville, 1988.
[8] M. Laroussi and J. R. Roth, in *Proceedings of the Seventh Topical Conference on Applications of Radio Frequency Power to Plasmas*, Kissimmee, FL, AIP Conf. Proc., No. 159 (AIP, New York, 1987), pp. 438–441.
[9] J. R. Roth and M. Laroussi, in *Proceedings of the 8th International Symposium on Plasma Chemistry* (International Union of Pure and Applied Chemistry, Tokyo, Japan, 1987), Vol. 4, pp. 2405–2410.
[10] M. G. Floquet, Annales E.N.S. **12**, 47 (1883).

Investigation of the nonlinear behavior of a partially ionized, turbulent plasma in a magnetic field

Scott A. Stafford,   Mark Kot,   and J. Reece Roth

'estigation of the nonlinear behavior of a partially ionized, turbulent plasma a magnetic field

Scott A. Stafford,[a] Mark Kot,[b] and J. Reece Roth

UTK Plasma Science Laboratory, Department of Electrical and Computer Engineering, University of Tennessee, Knoxville, Tennessee 37996-2100

In this paper, a number of the methods of nonlinear dynamics are applied to the study of electrostatic turbulence in a magnetized, steady-state, partially ionized plasma. Electrostatic potential fluctuations were obtained by using a capacitative probe. These signals were captured, digitized, and recorded with a LeCroy transient recorder system interfaced to an IBM-AT personal computer. A commercially available software program was used to calculate power spectra, to reconstruct and plot phase portraits, take Poincaré sections, compute correlation dimensions and Lyapunov exponents, and to perform other manipulations of the time series of electrostatic potential fluctuations obtained from the plasma. Evidence of low-dimensional chaos was sought, and trends were investigated which related the state of the turbulence to such plasma parameters as the anode voltage (rms electrostatic potential), background gas pressure (collisionality), and magnetic induction. These variables were found to have a significant effect on the nonlinear dynamics of the plasma.

TRODUCTION

In the past 25 years, research in nonlinear dynamics has rished, and new concepts have been developed to quantiıaotic behavior. Many of these concepts had their origin ıe work of Edward Lorenz, a meteorologist interested in behavior of a simplified set of equations which model 'ection in the atmosphere.[1] Since then these concepts : been applied to fluid flow,[2] chemical reactions,[3] the ading of diseases,[4] and biological rhythms.[5]

The purpose of this research is to apply the various tools ınlinear dynamics to electrostatic potential fluctuations sured in a steady-state, magnetized plasma in order to for evidence of low-dimensional chaos, and to look for ds in the parameters which describe the state of the turnce. Chaos-related concepts which were used in this y were reconstructed phase portraits, Poincaré sections, elation dimensions, and Lyapunov exponents.

There are several reasons why these concepts are useful ıe study plasma turbulence. In plasmas, turbulence imquasirandom fluctuations of the electric field and partiumber densities. The issue of turbulence is important in usion community. It is generally suspected that turbu: is the cause of anomalous particle and energy losses are an important obstacle to the success of the tokamak ınement concept. These transport losses across the cong magnetic-field lines are much higher than that pre:d by neoclassical transport theory. It is the usual asption that turbulence consists of infinitely many degrees :edom, each corresponding to an independent oscillator. ın determining the effects of turbulence on particle or gy transport in plasma, it is important to know whether a few frequency components dominate or if there is

actually an infinite number of them. This is a principal motivation to look for chaotic behavior in a plasma.

The remainder of this paper is organized as follows: Section II reviews some concepts of nonlinear dynamics which we have found useful in describing our data. Section III describes prior literature on the application of nonlinear dynamics to plasma experiments, Sec. IV the experimental apparatus, and Sec. V the application of the concepts of Sec. II to a characteristic plasma signal. Section VI describes the effects of varying the plasma parameters on the nonlinear dynamical characteristics of the plasma. Finally, we draw some conclusions from our studies, and make recommendations for further work.

II. CONCEPTS OF NONLINEAR DYNAMICS

In characterizing our experimental data, we have found the following concepts from nonlinear dynamics to be useful.

A. Phase space

The dynamics of a system may be represented most conveniently in a phase space or state space of its dependent variables. The state of the system at any particular instant may be represented as a point in this multidimensional space, and the time evolution of the system appears as an orbit or trajectory in the space. For simple mechanical systems, the dependent variables are often the position and velocity for each degree of freedom. If the simple mechanical system is dissipative, orbits typically tend toward some sort of simple attractor (e.g., equilibria, limit cycles, etc.) or strange attractor.

The use of a phase space presupposes that one can actually measure all of the dependent variables simultaneously. This is, in fact, seldom the case for real experimental systems. Indeed, an experimentalist working with a complex

sent Affiliation: General Dynamics, Inc., Fort Worth, Texas.
sent Affiliation: Department of Applied Mathematics, University of shington, Seattle, Washington.

system may not even know the nature of all the dependent variables. Fortunately, Packard et al.[6] suggested and Takens[7] has shown that one can reconstruct certain important dynamical properties of the true attractor from the time series of a *single* dependent variable. The method of reconstruction is straightforward; given the time series for a single dependent variable $X(t)$, an embedding dimension m, and a time delay τ, one constructs a time series of vectors $[X(t), X(t + \tau), X(t + 2\tau),...,X(t + (m - 1)\tau]$. If the true attractor is contained in a d-dimensional manifold, the choice of an embedding dimension $m \geqslant 2d + 1$ will, for almost every choice of coordinate and time delay, yield an embedding of the original manifold. The resulting reconstructed attractor may not look exactly like the original, but it will, nevertheless, share the same fractal dimension and Lyapunov exponents.

B. Poincaré sections

The idea of reducing a continuous time system (or flow in phase space) to a discrete time system (or map) of lower dimension first appeared in Poincaré's[8] study of the three-body problem of celestial mechanics. Any such discrete time system of reduced dimension is, as a result, almost invariably referred to as a Poincaré map. The usual strategy in constructing a Poincaré map is to take a cross section or Poincaré section of an orbit in a phase space. In three dimensions, one takes a plane of suitable orientation (transverse to the flow) and looks at only those points where the orbit hits the plane. The Poincaré section is the plane and the points of intersection; the Poincaré map is the rule that takes one from one point of intersection to the next.

C. Correlation dimension

Physicists have recently become interested in fractal dimensions as a means of characterizing dynamical systems, (see Farmer, Ott, and Yorke[9]). An early attempt to estimate one such fractal dimension, capacity, by box counting was confounded by slowly converging sequences obtained at high computational cost, prompting investigators such as Greenside et al.[10] to characterize box counting as impractical. Correlation dimension was subsequently introduced by Grassberger and Procaccia[11] as a lower bound on capacity, and has since gained wide acceptance.

The correlation dimension is, in effect, a scaling exponent that describes how the number of points in an m-dimensional sphere changes with the radius of the sphere. One gets a handle on this scaling exponent via a correlation integral. Consider, for example, the set of points on an attractor. If the system is chaotic, sensitive dependence on initial conditions will guarantee that points far apart in time will be spatially uncorrelated. Points close together in time will, in turn, show spatial correlation. The correlation integral is defined as[11]

$$C(r) = \lim_{N \to \infty} \frac{1}{N(N - 1)} \sum_{i=1}^{N} \sum_{j=1}^{N} H(r - |x_i - x_j|), \quad (1)$$

where $C(r)$ is a measure of this spatial correlation. The parameter N is the total number of points, and H is the Heaviside function, which is defined as $H(x) = 1$ for positive x

and $H(x) = 0$ for x less than or equal to zero.

Obviously, $C(r)$ increases from zero, for very small values of r, to one, for very large r. The main argument by Grassberger and Procaccia[11] is that for small r

$$C(r) \sim r^{\nu}. \quad (2)$$

If this is true, the correlation dimension is defined as

$$\nu = \lim_{r \to 0} (\log C(r)/\log r). \quad (3)$$

D. Lyapunov exponents

Chaotic systems exhibit a sensitive dependence on initial conditions; trajectories that are initially close together separate exponentially fast. For this reason, Lyapunov exponents play an important role in the study of chaotic systems. Roughly speaking, Lyapunov exponents characterize the mean rate of convergence or divergence of trajectories that neighbor a given trajectory or attractor. The plural is used because there is a spectrum of Lyapunov exponents, each exponent characterizing orbital divergence in a particular direction. For example, let x_0 be the distance between two starting points. A short period of time later the distance will be

$$x(t) = x_0 e^{\lambda t}, \quad (4)$$

where λ is the Lyapunov exponent. One can imagine beginning with an infinitesimal m sphere centered on some point of an attractor. Under the flow of the dynamical system, the sphere is transformed into an m ellipsoid. Each Lyapunov exponent defines the rate of growth or decay of an axis of the ellipsoid.[12] An attractor with a positive Lyapunov exponent is chaotic. There is a close relationship between the Lyapunov exponents of an attractor and its dimension.[13]

III. PREVIOUS APPLICATIONS OF NONLINEAR DYNAMICS TO PLASMA EXPERIMENTS

Since the development of nonlinear dynamics, most applications have been in the field of fluid dynamics, particularly fluid turbulence. Since fluid and plasma turbulence are strongly related, it was just a matter of time before the concepts of nonlinear dynamics were utilized by plasma researchers. Around 1980 publications on this subject began to appear. The first articles reported on the study of sets of differential equations.[14-22]

By the mid 1980s researchers began looking for experimental evidence of deterministic chaos in plasmas. Held and Jeffries[23] produced interesting results from their experiment on electron-hole plasmas generated in steady-state electric and magnetic fields in germanium crystals. A second experiment performed on a solid-state plasma was conducted by Martin, Leber, and Martienssen.[24] They studied the electrical conduction characteristics of barium sodium niobate ($Ba_2NaNb_5O_{15}$) crystals.

The nonlinear behavior of electron beam oscillations has been studied by Boswell.[25] Braun et al. conducted experiments on a variety of electrical discharge tubes.[26] I and Wu have attempted to compute the correlation dimension for density fluctuations of an rf-generated plasma.[27] Chaotic behavior has been observed in a pulsed plasma discharge by

J. Appl. Phys., Vol. 68, No. 2, 15 July 1990

A-39

Stafford, Kot, and Roth

g and Wong.[28] This experiment was performed on a unmagnetized plasma device. Cheung, Donovan, and also reported observing chaos in a steady-state plasma rge.[29]

the past several years researchers have applied the t of correlation dimension to some of the major toka-periments. A few of these appear to exhibit low-di-nal chaos, while others do not. Arter and Edwards ned a study on the Divertor and Injection Tokamak ment's (DITE) Mirnov oscillations.[30] In this experi-magnetic-field fluctuations were observed with eight coils. These were equally spaced in poloidal angle he tokamak. Their data resulted in a correlation di-n of approximately 2.1. Low-frequency magnetic-ictuations were measured on the TOSCA device by t al.[31] This study yielded a correlation dimension of imately 2.4. Cote et al. also examined the Joint Euro-orus' (JET) MHD activity. These data were acquired ickup coils located inside the vacuum vessel. For co-modes, the correlation dimension fell between 2.4 and wley, Simm, and Pochelon studied the broadband tic and density fluctuations in the Tokamak Chauf-lven (TCA) plasma.[32] Data were obtained with mag-robes and a CO_2 laser phase contrast diagnostic. discharges were analyzed, but no saturation in slope served. Zweben et al. examined edge turbulence in the iak Fusion Test Reactor (TFTR).[33] They attempted pute the correlation dimension from floating poten-ctuations. Their results were unclear because of an iently large scaling region. A CO_2 laser scattering

technique was employed by Barkley et al. to measure density fluctuations on Tokamak Fontenay-aux-Roses (TFR) plasmas.[34] This experiment produced interesting results. The correlation dimension was obtained, and was shown to depend upon the wave number of the measured signal. The dimension was 2.6 and 3.2 for wave numbers of 6 and 18 cm^{-1}, respectively.

The characteristic experiment described above consisted of exhaustively analyzing data from a single or a very few experimental runs. Almost no information is available on the functional dependence of the nonlinear dynamical characteristics of plasma on such parameters as collisionality, electric field strength, magnetic induction, number densities, etc. This investigation therefore is devoted to investigating the functional dependence of these characteristics on the plasma parameters.

IV. EXPERIMENTAL APPARATUS AND DATA HANDLING SYSTEM

The experimental data for this study were obtained on a Penning discharge plasma. The conventional Penning discharge was developed by F. M. Penning in the late 1930's.[35] The original design was modified by Roth in such a way that a Penning discharge could be used to generate a large volume, steady-state plasma in a magnetic mirror field.[36] This configuration is called a "modified Penning discharge," and has been used in plasma physics research to produce highly turbulent, hot ion plasmas.

The vacuum vessel of the Penning discharge used in this

Experimental apparatus.

J. Appl. Phys., Vol. 68, No. 2, 15 July 1990

Stafford, Kot, and Roth

A-40
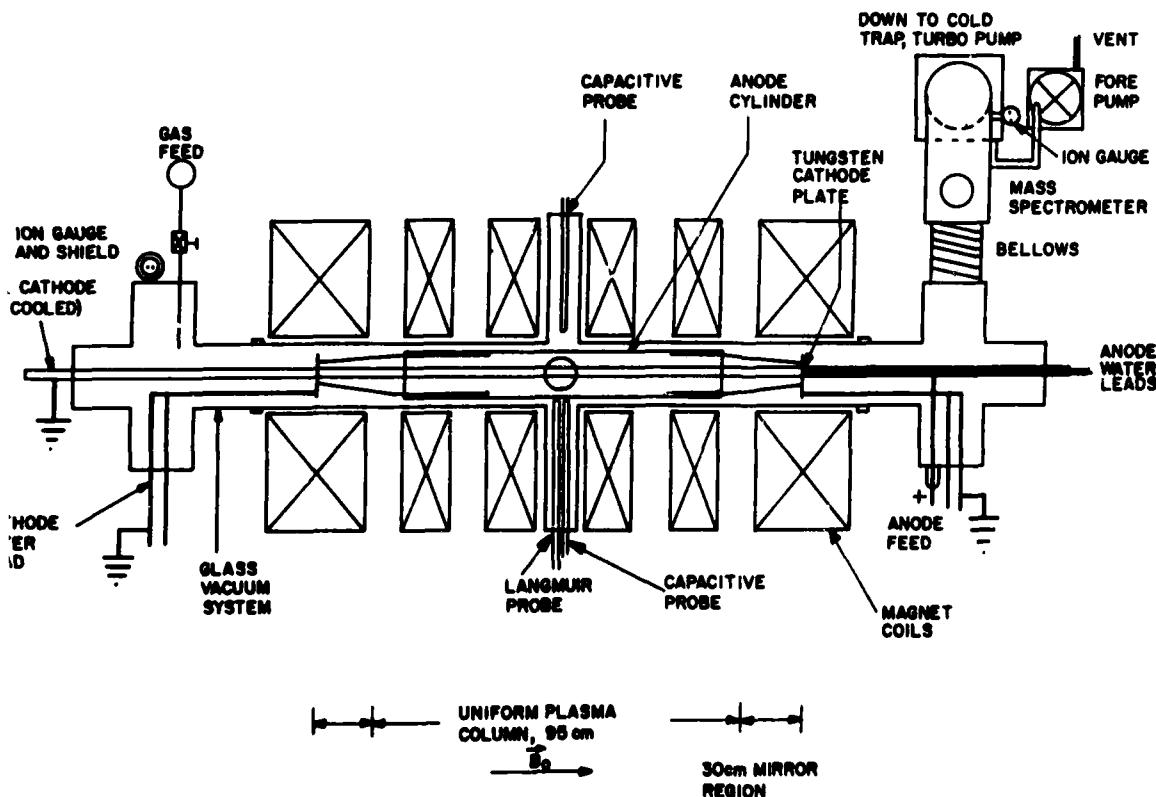
Axial Magnetic Field Profile
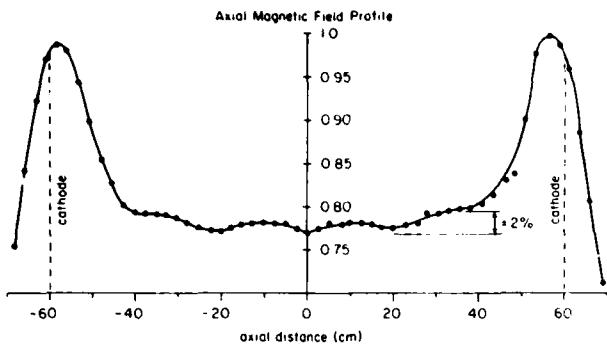
FIG. 2. Normalized axial magnetic field.

experiment is a cylindrical section of 15-cm Pyrex pipe. As shown in Fig. 1, the vessel is surrounded by confining magnetic-field coils. The sixteen water-cooled coils are arranged to produce a magnetic mirror. The normalized axial magnetic field is shown in Fig. 2. The region of constant field strength is approximately 95 cm in axial length. The mirror ratio, B_{min}/B_{max}, is about 0.77. The maximum field at the midplane is approximately 0.2 T.

The gas to be ionized is fed into the system through a leak valve located at one end of the vacuum vessel. Helium was used for all data runs in this experiment. The vacuum pump is at the other end of the vessel. This consists of a mechanical pump in series with a turbomolecular pump. Pressure is monitored by two ion gauges, one at each end of the experimental volume. The base pressure of the system is approximately 5 μT. Also installed in the system is a mass spectrometer, which is used to monitor the composition of the gas inside the vacuum vessel.

A Penning discharge employs an anode ring and two cathodes. The anode is situated at the midplane with the cathodes placed at each end. The anode consists of a ring of copper tubing which is water cooled. The cathodes are grounded, water-cooled circular tungsten disks. The background gas is ionized by applying a dc voltage to the anode, thus trapping electrons bound to magnetic field lines in an axial electrostatic potential well. The electrons remain trapped in this potential well until they ionize the neutral background gas. This process cascades until the electron production and loss processes are in balance. The applied voltage is generally a few kilovolts, with the current being several tens to several hundreds of milliamperes. The anode supply can provide up to 40 kV and 1 A.

The arrangement of the Penning discharge allows easy access to the plasma for diagnostics. Diagnostics that have been applied previously to characterize this plasma include capacitive probes, Langmuir probes, a retarding potential energy analyzer, a microwave scattering system, a microwave interferometer, and microwave equipment used to study electron cyclotron resonance absorption. Instruments used in this investigation include a radial capacitive probe and a radial Langmuir probe. This Penning discharge produces a steady-state, weakly ionized plasma. The electron

number density measured with a Langmuir probe is characteristically 2.5×10^9 cm^{-3}. The electron kinetic temperature tends to range between 40 and 100 eV, while the ion kinetic temperature is an order of magnitude or more higher.

A Penning discharge plasma tends to be quite turbulent. This is because a variety of instabilities are active. These instabilities can be excited by density gradients, temperature gradients, and $E \times B$ drift waves.[37] For this experiment, it was desired to drive a coherent $E \times B$ drift mode in the plasma. This was accomplished with two major modifications to the classical Penning discharge arrangement. As illustrated in Fig. 1, a long cylindrical anode is used in place of an anode ring. A coaxial cathode is used along with two cathode plates. This arrangement produces a radial electric field which is independent of distance along the axis of the anode region. This radial electric field creates an $E \times B$ drift wave at the outer edge of the plasma. By observing a radial profile of the potential fluctuations, it was determined that the $E \times B$ mode was of significant amplitude only at the plasma edge. Also, the frequency of this mode was seen to depend inversely upon the magnetic-field strength and to be directly proportional to the anode voltage.[38]

A block diagram of the data acquisition and handling system is shown in Figure 3. The first element of the system is a capacitive probe. The probe is constructed of semirigid coaxial cable. The outer conductor and insulation has been removed and a small sphere soldered to the tip to allow the center conductor to pick up the potential fluctuations. The signal detected by the capacitive probe is fed into a Tektronix 1121 amplifier. The signal is then band-pass filtered through the use of two Krohn-Hite 3200 filters. The high pass filter is set at 1.0 kHz in order to remove any 60-Hz line noise. The low pass filter is set at 1 MHz to avoid aliasing effects.

The filtered signal is digitized by a LeCroy 8210 waveform analyzer. This analog-to-digital converter can process up to four signals simultaneously. The maximum sampling rate is 1 MHz for each channel and the data have ten bits of resolution. The transient recorder is housed in a LeCroy 8013A CAMAC benchtop mainframe, which is controlled with an IBM-AT personal computer. Once the fluctuations were digitized and stored on the hard disk drive, they were then processed using a commercial software package. This package is entitled "Dynamical Software" and is available from Dynamical Systems, Inc.[39]

V. CHARACTERISTIC PLASMA SIGNAL

The time history of a relatively coherent plasma signal is shown in Fig. 4. One can easily see that the signal contains a dominant frequency, and there also appears to be evidence of a beat frequency. Though the lower frequency contains very little power, both can be observed in the signal's auto power spectrum, which is shown in Fig. 5. The reconstructed phase portrait is shown in Fig. 6. Upon first observation, the attractor appears possibly to be chaotic; but after taking a Poincaré section, shown in Fig. 7, this does not appear to be the case.

The next step is to estimate the correlation dimension of the signal. Fig. 8 shows the correlation integral plots. Certain features of these plots should be discussed. First, there

A-41
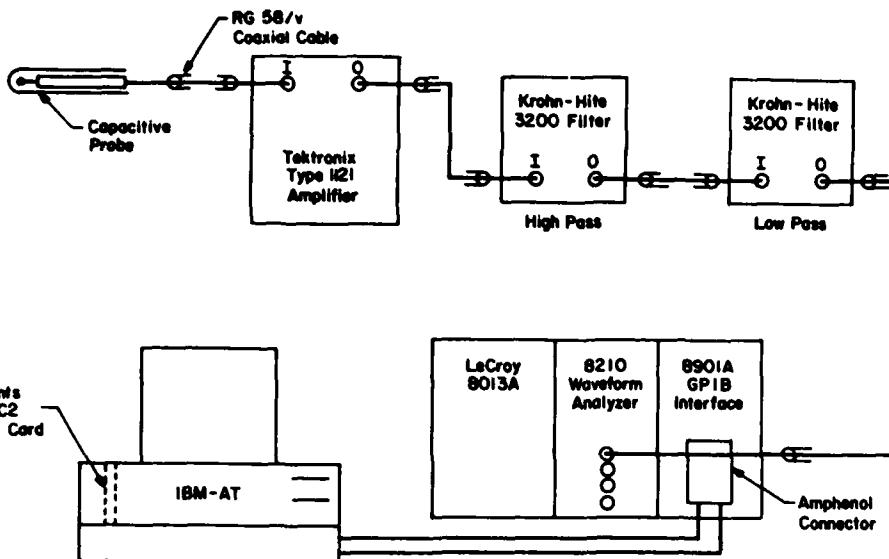
FIG. 3. Block diagram of data acquisition system.

are the "stair steps" that appear at small scale sizes. These are due to the discrete intervals in the data which result from the digitizing process. This effect also appears in the derivative plots. At the small-scale sizes the derivative values bounce up and down. This is a result of the "stair steps" in conjunction with the differencing method used to calculate the derivatives.

Another feature of the correlation integral plots is the distinct knee that appears in midrange for higher embedding dimensions. This effect has been observed in other data, and is said to be due to spurious correlations.[40] These spurious correlations greatly restrict the extent of the scaling region. This problem can be avoided by using many more than our 2000 data points. Unfortunately, this is impractical because of the required computation time; especially when using a personal computer such as ours for processing. For this rea-

son, only 2000 data points were used throughout this study. According to Smith, 2000 points should be sufficient to accurately estimate correlation dimensions less than three.[41]

One other characteristic of these curves that should be mentioned is related to the dynamical noise of the system. Noisy data create two separate regions in the correlation integral plots.[42] At scale sizes below the noise level, the noise dominates and the slope increases with embedding dimension. Above the noise level, low-dimensional behavior will emerge, if it exists. This effect can be seen in Fig. 8, especially in the derivative plot. At most scale sizes the noise dominates, but there is a narrow region where the slope appears to saturate. Between the noise and the outer bounds of the attractor itself, the scaling region is very limited. The only
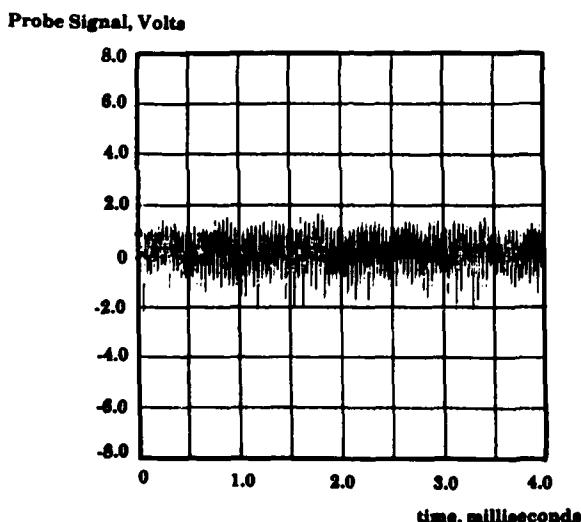
FIG. 4. Time history of plasma fluctuation signal
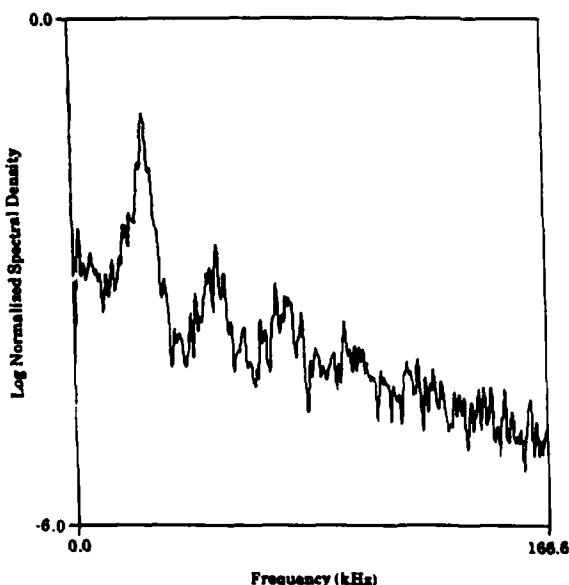
FIG. 5. Fourier power spectrum associated with the signal in Fig. 4.

Stafford, Kot, and Roth
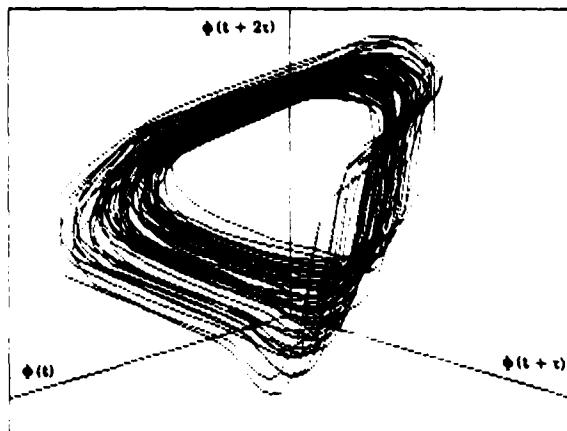
FIG. 6. Reconstructed phase portrait of the plasma signal in Fig. 4.

FIG. 8. Correlation integral plots for the plasma signal in Fig. 4

available scaling region in this case yields a correlation dimension of approximately 1.9.

Attempts were also made to estimate the largest Lyapunov exponent of this signal. Unfortunately, the standard method of measuring the Lyapunov exponents from a single time series is not suitable for noisy data.

VI. EFFECTS OF VARYING PLASMA PARAMETERS

This section consists of data for which plasma parameters were changed in order to study their effects on the state of the plasma turbulence. Three sets of data ere examined, each describing the functional dependence of a different variable. The three plasma parameters were the gas pressure, anode voltage, and magnetic-field strength.

A. Variation of gas pressure

For this set of data, the helium gas pressure was varied from 260 to $1670\,\mu T$ in five increments. The variation of the electron number density, electron kinetic temperature, and plasma floating potential measured with a Langmuir probe

for the different runs is shown in Fig. 9. The effects of the pressure on the power spectra of the fluctuations can be seen in Fig. 10. For the first four runs, the signal is quite coherent and the peak frequency is 25 to 30 dBm above the noise floor. Once the pressure reaches $1200\,\mu T$, the signal strength drops considerably.

The reconstructed phase portraits, all with the same axis
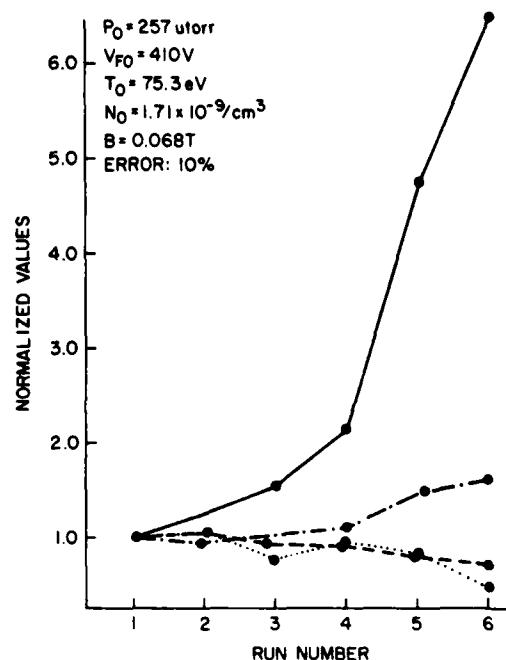
FIG. 9. Variation of plasma parameters with helium gas pressure. The parameters are as follows: —, pressure; ·····, electron kinetic temperature; ----; floating potential; and -·-·-·, electron number density.

FIG. 7. Poincaré section taken from the attractor in Fig. 6.

J. Appl. Phys., Vol. 68, No. 2, 15 July 1990

Stafford, Kot, and Roth

A-43
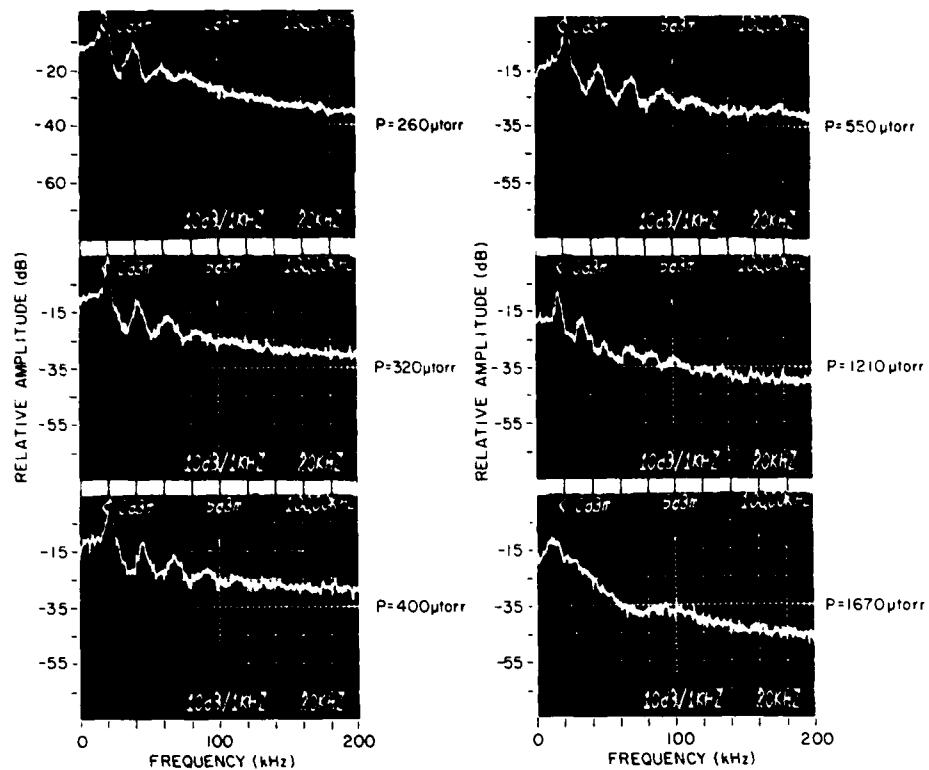
FIG. 10. Potential fluctuations for varying helium gas pressure.
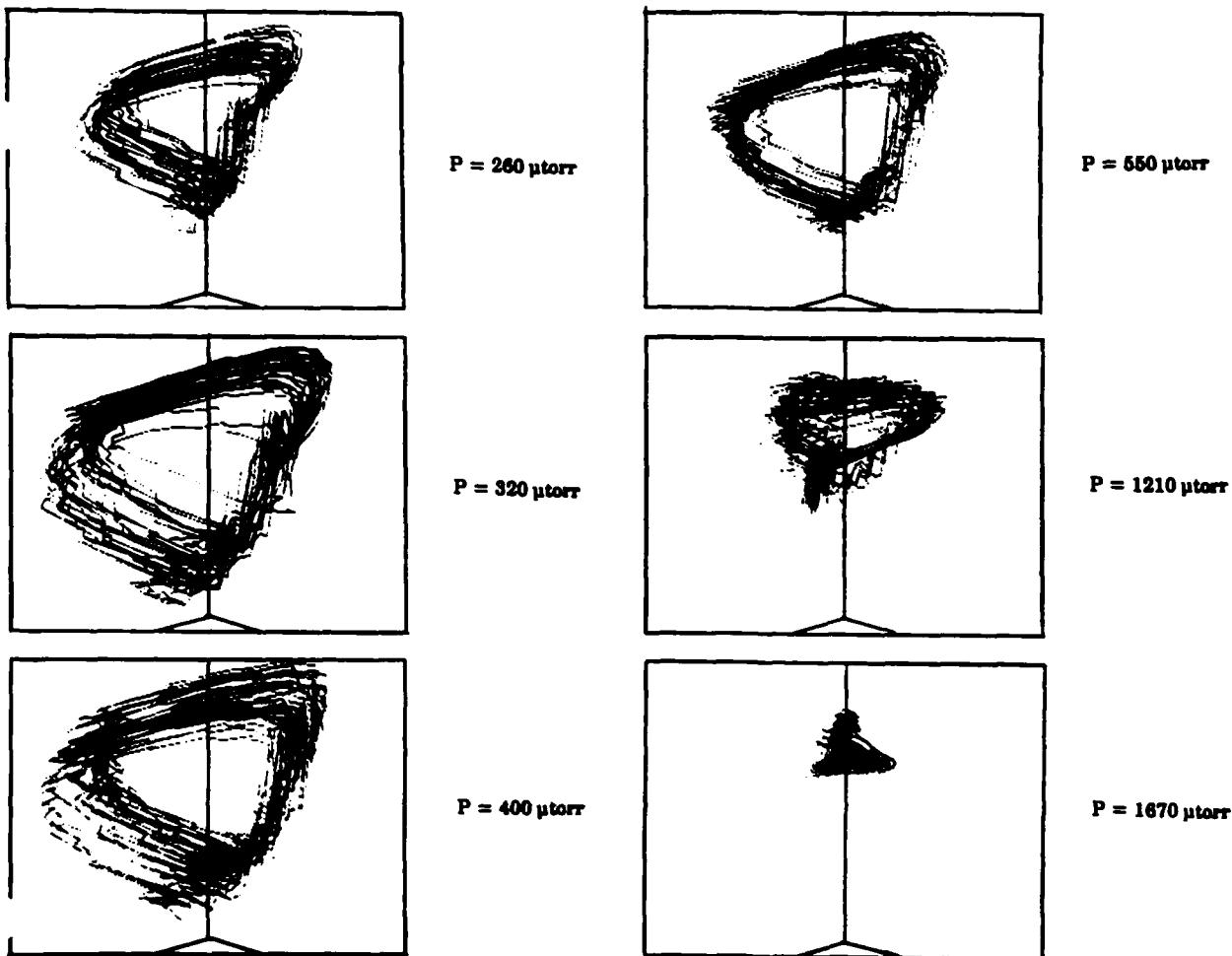
FIG. 11. Reconstructed phase portraits for varying helium gas pressure.

J. Appl. Phys., Vol. 68, No. 2, 15 July 1990   Stafford, Kot, and Roth

A-44

TABLE I. Correlation dimension for varying gas pressure.

Run number	Pressure (μTorr)	Dimension
1	257	2.5
2	321	2.2
3	395	2.0
4	548	1.95
5	1214	N.C.
6	1667	N.C.

FIG. 13. Variation of plasma parameters with anode voltage. The parameters are as follows: —, anode voltage; ····, electron kinetic temperature; - - - -, floating potential; and ·-··-··-, electron number density.

scales, are shown in Fig. 11. Their features corroborate the power spectra. The signal starts out fairly coherent and remains so until the fifth run. The drop in amplitude of the power spectrum corresponds to the decrease in size of the attractor. By the time the pressure reaches its highest value, the motion has become considerably less coherent. The correlation dimension was estimated for each run. The first four runs showed evidence of a narrow scaling region where a dimension could be inferred, as well as a region where the noise dominated. By Run 5, the scaling region began to disappear, and by Run 6, the slope was steadily increasing with embedding dimension, which implies that the fluctuations had become totally random. Table I lists the correlation dimensions that were obtained for each run. These values are plotted as a function of pressure in Fig. 12.

B. Variation of anode voltage

For the second set of data, the voltage applied to the anode was varied. This voltage controls the dc radial electric field acting on the plasma. The variation of plasma parameters measured with a Langmuir probe is plotted for the different run conditions in Fig. 13. Figure 14 shows the effect of the anode voltage on the Fourier power spectra. The peak frequency is originally about 15 dBm above the noise floor.

After increasing the applied voltage by a factor of 2, the peak frequency is approximately 25 dBm above the noise. The power spectra show a steady increase in frequency and amplitude as the anode voltage is increased.

Figure 15 shows the reconstructed phase portrait for each run, with all of them drawn to the same axis scale. The principal difference is that the size of the attractor increases with anode voltage. This is explained by the increasing amplitude of the fluctuations with voltage. Also, the phase portraits become slightly more coherent as the voltage is increased.

Again, the correlation dimension was computed for each run. By closely observing the correlation integral and derivative graphs, it is evident that the plots for each run exhibit two distinct regions. Similar to the previous cases, there exists a very small scaling region in which the dimension could be determined. Table II lists the values for each run. They are also plotted as a function of the anode voltage in Fig. 16.

C. Variation of magnetic field

The control parameter for the third set of data was the magnetic field strength, which was varied over a range of 0.034–0.182 T. The plasma parameters measured with a Langmuir probe are plotted in Fig. 17. Figure 18 shows the effect of the magnetic-field strength on the fluctuations' power spectra. For $B = 0.034$ T, there is a small peak in the spectrum. This peak becomes much more prominent for the next two runs, but is then damped somewhat when the magnetic field is increased to 0.084 T. As the field is increased

FIG. 12. Plot of correlation dimension as a function of helium gas pressure.

A-45
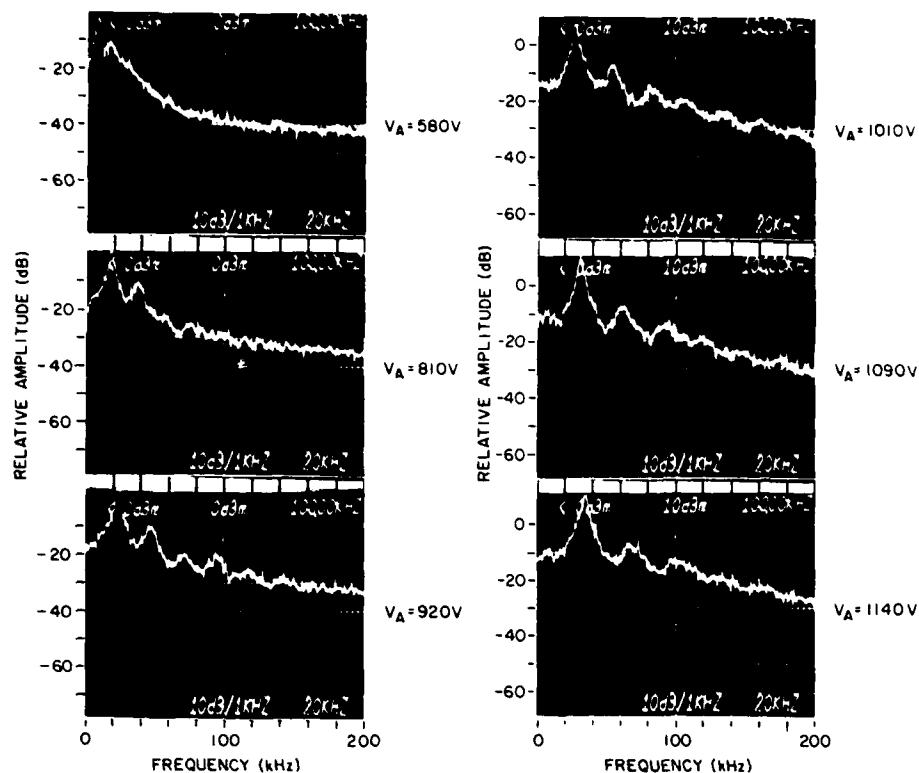
FIG. 14. Potential fluctuations for varying anode voltage.
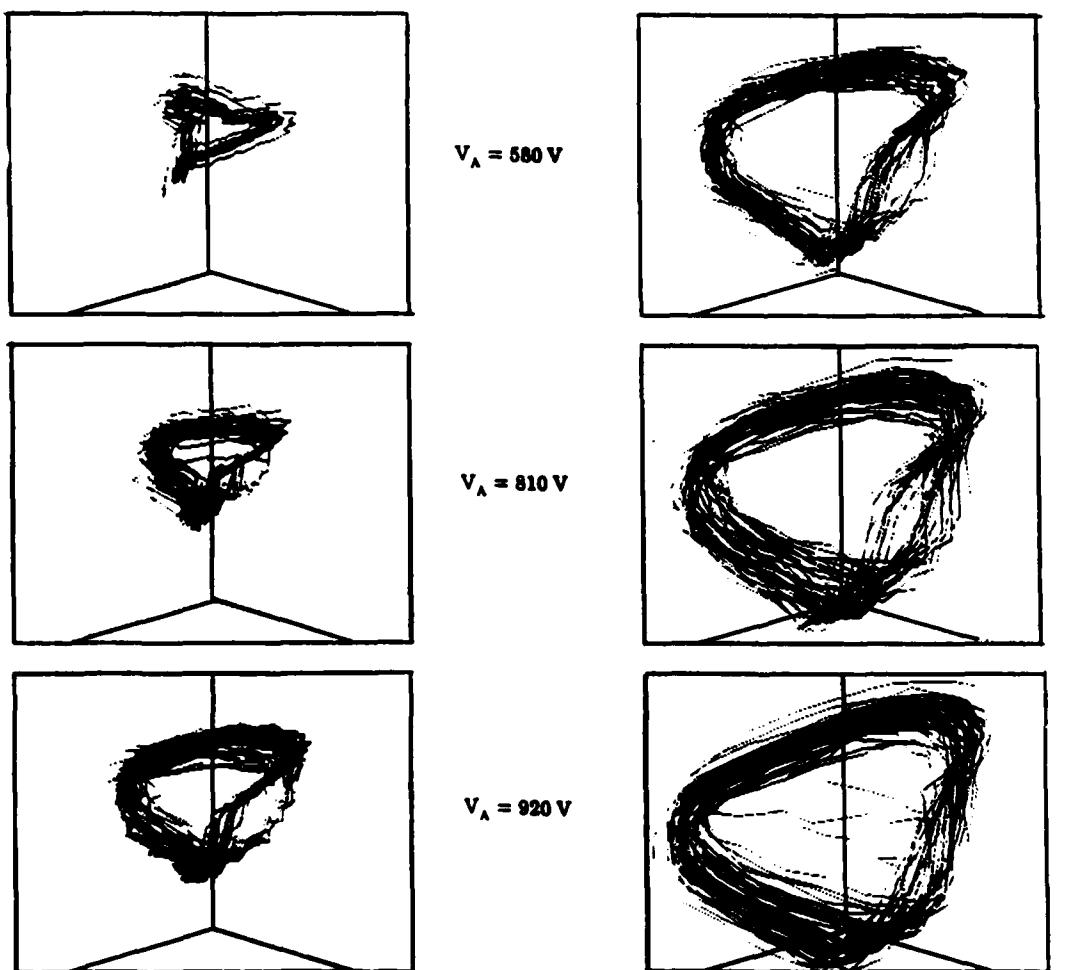
FIG. 15. Reconstructed phase portraits for varying anode voltage.

Stafford, Kot, and Roth

A-46

TABLE Correlation dimension for varying anode voltage.

Run number	Anode voltage (V)	Dimension
1	580	2.14
2	810	2.05
3	920	1.96
4	1010	1.68
5	1090	1.86
6	1140	2.20

further, the relative signal strength of the peak continues to decrease.

The reconstructed phase portraits are shown in Fig. 19. The first run exhibits a slight hint of periodicity. The trajectory becomes much more coherent over the next two runs, but this is lost as the magnetic field is increased further. By Run 6, the trajectory is filling up a volume in phase space, which is characteristic of random signals. All of these observations are consistent with what was learned from the power spectra.

When correlation dimensions were computed, convergence was seen only for Run 3. For this case, the correlation integral and derivative curves exhibited two distinct regions, and once again the correlation dimension was found to be approximately 2.0. In all of the other runs of this set, the slope continued to increase with embedding dimension, implying that the fluctuations were random.

VII. CONCLUSIONS

In this research, it was possible to observe two states of plasma turbulence, one quasiperiodic and one random. The transition between the two states is not well defined or sudden. It was also found that the neutral gas pressure, closely related to electron collisionality in this plasma, and the magnetic induction have a strong effect on the nature of the turbulence, while the anode voltage appears to affect only the amplitude of the turbulence. For lower pressures, the fluctuations were relatively coherent, but for pressures above a

FIG. 17. Variation of plasma parameters with magnetic-field strength. The parameters are as follows: —, magnetic field strength; ····, electron kinetic temperature; - - - -, floating potential; and -·-·-·-, electron number density.

millitorr they become random. The magnetic-field strength yielded coherent oscillations only for small and midrange values; perhaps surprisingly, the fluctuation amplitudes became smaller and more random as the magnetic induction was increased above 0.1 T.

In those cases in which the correlation dimension could be obtained, it was found to be approximately 2.0. This implies that another oscillation besides the E/B drift is present. The dynamical noise was sufficiently large in our experiments that accurately measuring the correlation dimension was difficult, and it was practically impossible to measure the largest Lyapunov exponent.

For future research along these lines, it became apparent that more than 2000 data samples (possibly 8000 or more) are needed to accurately determine the correlation dimension of our plasma data, and this will require the much higher speed of a mainframe computer.

It also would be interesting to induce another oscillation into the system. This could be accomplished by periodically varying either the applied electric or magnetic fields. The electric field would be the most likely candidate, since it can be varied rather easily. This has been done previously in our laboratory by applying a high-voltage rf signal to an effector probe.[43]

ACKNOWLEDGMENTS

FIG. 16. Plot of correlation dimension as a function of anode voltage.

J Appl. Phys., Vol. 68, No. 2, 15 July 1990   Stafford, Kot, and Roth

A-47
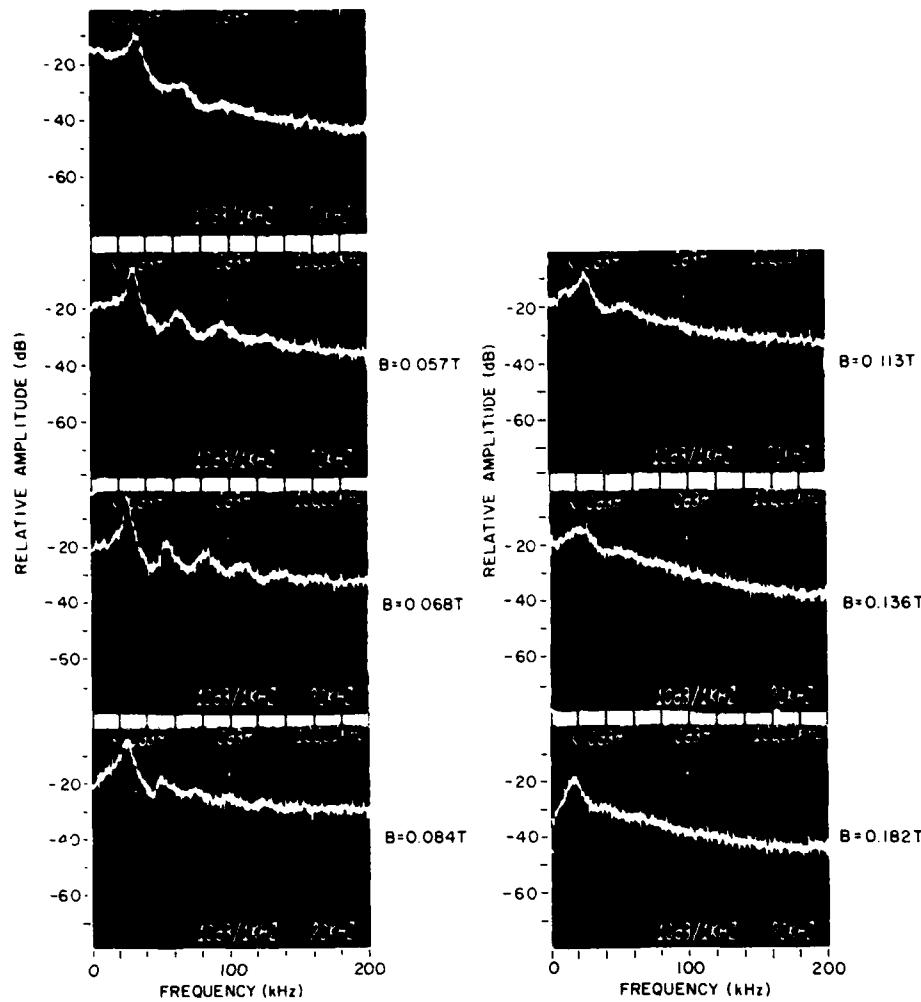
FIG. 18. Potential fluctuations for varying magnetic-field strength.
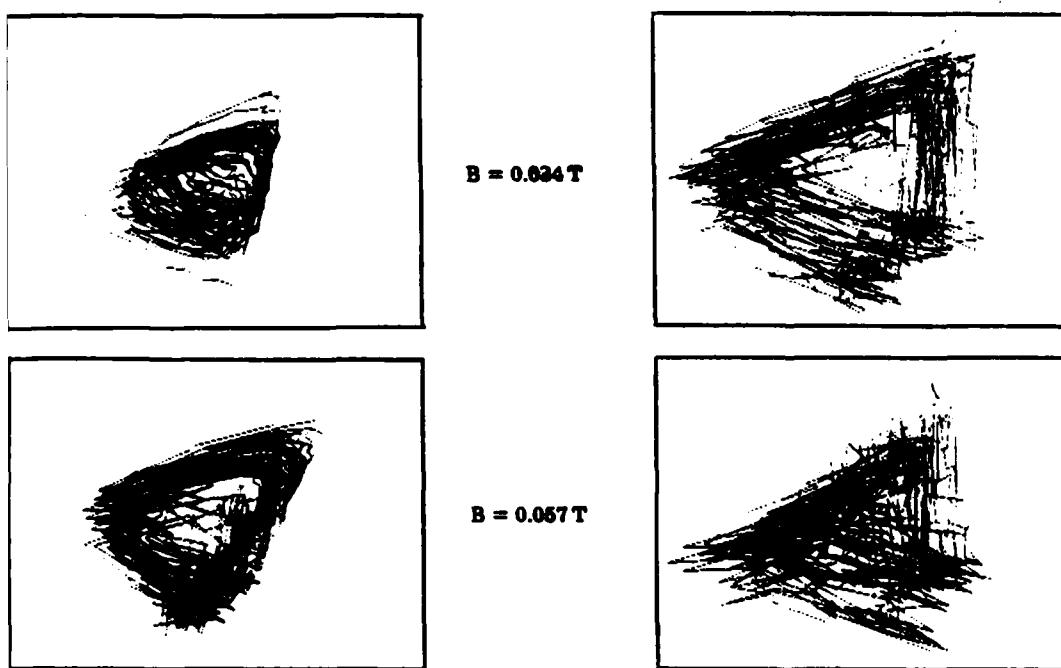
FIG. 19. Reconstructed phase portraits for varying magnetic-field strength.

Stafford, Kot, and Roth

B = 0.068 T

B = 0.136 T

B = 0.182 T
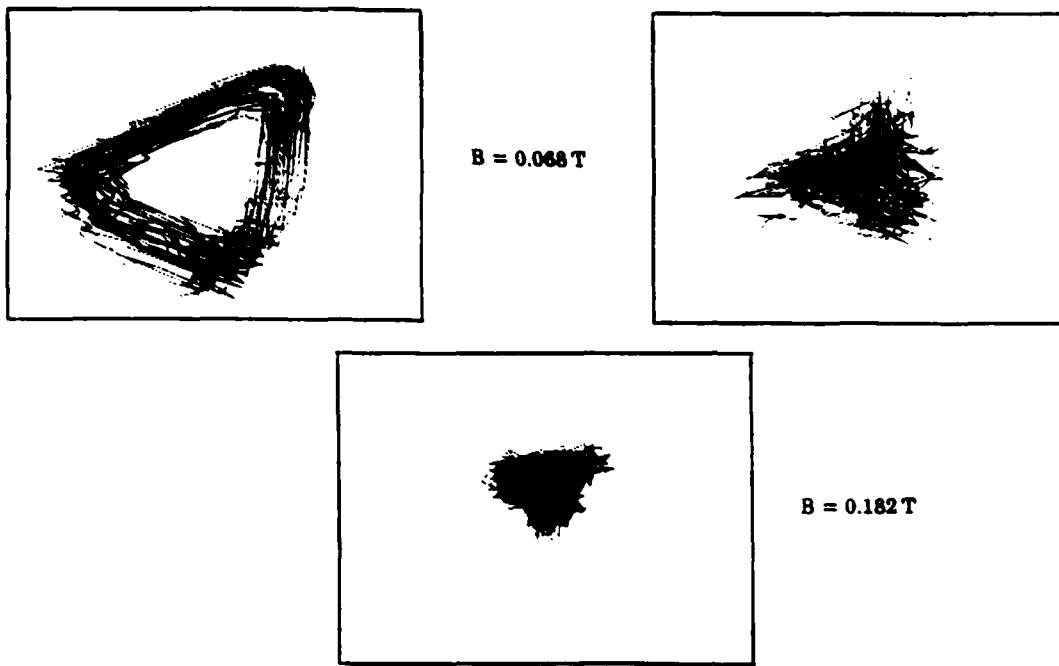
FIG. 19. *Continued.*

[1] E. N. Lorenz, J. Atmos. Sci. **20**, 130 (1963).

[2] A. Brandstater, J. Swift, H. L. Swinney, A. Wolf, J. D. Farmer, E. Jen, and P. J. Crutchfield, Phys. Rev. **51**, 1442 (1983).

[3] R. H. Simoyi, A. Wolf, and H. L. Swinney, Phys. Rev. Lett. **49**, 245 (1982).

[4] W. M. Schaffer and M. Kot, J. Theor. Biol. **112**, 403 (1985).

[5] L. Glass, X. Guevau, and A. Shrier, Physica D **7**, 89 (1983).

[6] N. H. Packard, J. P. Crutchfield, J. D. Farmer, and R. S. Shaw, Phys. Rev. Lett. **45**, 712 (1980).

[7] F. Takens, in *Dynamical Systems and Turbulence*, edited by D. A. Rand and L. S. Young (Springer, New York, 1981).

[8] H. Poincaré, *Les Methodes Nouvelles de al Mecahnique Celeste* (Gauthier-Villars, Paris, 1899).

[9] J. D. Farmer, E. Ott, and J. A. Yorke, Physica D **7**, 153 (1983).

[10] H. S. Greenside, A. Wolf, J. Swift, and T. Pignaturo, Phys. Rev. A **25**, 3453 (1982).

[11] P. Grassberger and I. Procaccia, Phys. Rev. Lett. **50**, 346 (1983).

[12] A. Wolf, in *Chaos*, edited by A. V. Holden (Princeton University Press, Princeton, 1986), pp. 273–290.

[13] J. L. Kaplan, and J. A. Yorke, in *Lectures Notes in Mathematics*, edited by H. O. Peitgen and H. O. Walther (Springer, Berlin, 1979), p. 730.

[14] A. Wolf, J. B. Swift, H. L. Swinney, and J. A. Vastano, Physica D **16**, 285 (1985).

[15] J. C. Adam, M. N. Bussac, and G. Laval, in *Intrinsic Stochasticity in Plasmas*, edited by G. Laval and D. Gresillon (Les Editions de Physique, Courtaboeuf, France, 1980), p. 415.

[16] Y. M. Treve and O. P. Manley, in *Intrinsic Stochasticity in Plasmas*, edited by G. Laval and D. Gresillon (Les Editions de Physique, Courtaboeuf, France, 1980) p. 393.

[17] H. Lashinsky, in *Intrinsic Stochasticity in Plasmas*, edited by G. Laval and D. Gresillon (Les Editions de Physique, Courtaboeuf, France, 1980), p. 425.

[18] P. K. C. Wang, J. Math Phys. **21**, 398 (1980).

[19] J. -M. Wersinger, J. M. Finn, and E. Ott, Phys. Fluids, **23**, 1142 (1980).

[20] J. Weiland and J. P. Mondt, Phys. Fluids, **28**, 1735 (1985).

[21] F. Jingquing and Z. Liulai, Chin. Phys. (USA) **8**, 461 (1988).

[22] M. Pettini, A. Vulpiani, J. H. Misguich, M. D. Leener, J. Orban, and R. Balescu, Phys. Rev. A. **38**, 344 (1988).

[23] G. A. Held and C. D. Jeffries, in *Dimensions and Entropics in Chaotic Systems*, edited by G. Mayer-Kress (Springer, New York, 1986), p. 158.

[24] S. Martin, H. Leber, and W. Martienssen, Phys. Rev. Lett., **53**, 303 (1984).

[25] R. W. Boswell, Plasma Phys. Contr. Fusion, **27**, 405 (1985).

[26] T. Braun, J. A. Lisboa, R. E. Francke, and J. A. C. Gallas, Phys. Rev. Lett. **59**, 613 (1987).

[27] L. I. and M. -S. Wu, Phys. Lett. A **124**, 271 (1987).

[28] P. Y. Chung and A. Y. Wong, Phys. Rev. Lett. **59**, 551 (1987).

[29] P. Y. Cheung, S. Donovan, and A. Y. Wong, Phys. Rev. Lett. **61**, 1360 (1988).

[30] W. Arter and D. N. Edwards, Phys. Lett. A **114**, 84 (1986).

[31] A. Cote, P. Haynes, A. Howling, A. W. Morris, and D. C. Robinson, in *12th European Conference on Controlled Fusion and Plasma Physics*, edited by L. Pocs and A. Montvai (European Physical Society, Geneva, 1985), Vol. 2, p. 450.

[32] M. L. Sawley, W. Simm, and A. Pochelon, Phys. Fluids **30**, 129 (1987).

[33] S. J. Zweben, D. Mands, R. V. Budny, P. Efthimion, E. Fredrickson, H. Greenside, K. W. Hill, S. Hiroe, S. Kilpatrick, K. McGuire, S. S. Medley, H. K. Park, A. T. Ramsey, and J. Wilgen, J. Nucl. Mater. **145–147**, 250 (1987).

[34] H. J. Barkley, J. Andreoletti, F. Gervais, J. Olivain, A. Quemenevur, and A. Truc, Plasma Phys. Contr. Fusion **30**, 217 (1988).

[35] F. M. Penning and K. Nienhuis, Phillips Tech. Rev. **11**, 116 (1949).

[36] J. R. Roth, Rev. Sci. Instrum. **37**, 1100 (1966).

[37] M. Laroussi, Ph.D. dissertation, University of Tennessee at Knoxville, 1988.

[38] S. Stafford, Master's thesis, University of Tennessee at Knoxville, 1989.

[39] W. M. Schaffer, G. L. Truty, and S. L. Fulmer, Dynamical Software Users Manual, 1988 (unpublished).

[40] J. Theiler, Phys. Rev. A **34**, 2427 (1986).

[41] L. A. Smith, Phys. Lett. A, **133**, 283 (1988).

[42] A. Ben-Mizrachi, I. Procaccia, and P. Grassberger, Phys. Rev. A **29**, 975 (1984).

[43] P. D. Spence and J. R. Roth, in *Proceedings of the 18 International Conference on P' nomena in Ionized Gases* (The Institute of Physics, Bristol, England, 1987), Vol. 2, p. 358.

ABSORPTION AND REFLECTION OF MICROWAVES BY A NON-UNIFORM PLASMA NEAR THE ELECTRON CYCLOTRON FREQUENCY*

M. Laroussi, C. Liu, and J. R. Roth
Plasma Science Laboratory
University of Tennessee, Knoxville, TN 37996-2100

ABSTRACT

In this paper, we report experimental measurements and numerical computations on the absorption and reflection of microwave radiation near the electron cyclotron frequency. In our model the wave is launched in the extraordinary mode into a cold, steady state, weakly ionized, nonuniform two-dimensional plasma slab with a uniform background magnetic field parallel to the surface. We compare computational and experimentally measured values of the absorption and reflection for selected values of the plasma number density, and collision frequency. These parametric dependences are investigated for normal incidence by computer simulations using cold plasma theory[1,2] and compared with recent experimental measurements[2] made at normal incidence on a plasma generated by a classical Penning discharge.

INTRODUCTION

We have recently taken experimental measurements on the attenuation of microwaves by a magnetized cylindrical plasma column. The wave is launched at normal incidence in the extraordinary mode. The plasma through which the wave travels is a cylindrical column with a uniform axial magnetic field, generated by a classical Penning discharge[3]. The attenuation of the wave is measured by an S-parameter test set of an HP 8510 network analyzer. A computer simulation program is used to computationally calculate the attenuation, absorption, and reflection for the same experimental plasma conditions under which the attenuation measurements are taken. A detailed description of this program is published elsewhere. This program is based on cold plasma theory[1]. The plasma is modeled as a series of uniform plasma slabs. The wave is partly absorbed and partly reflected at each slab boundary. The simulation results are then compared to the experimental measurements. The plasma conditions are changed from one run to the other so as to cover a wide variations of number density and collision frequency.

DISCUSSION

The Classical Penning discharge on which the experimental measurements are taken is shown in Fig. 1.
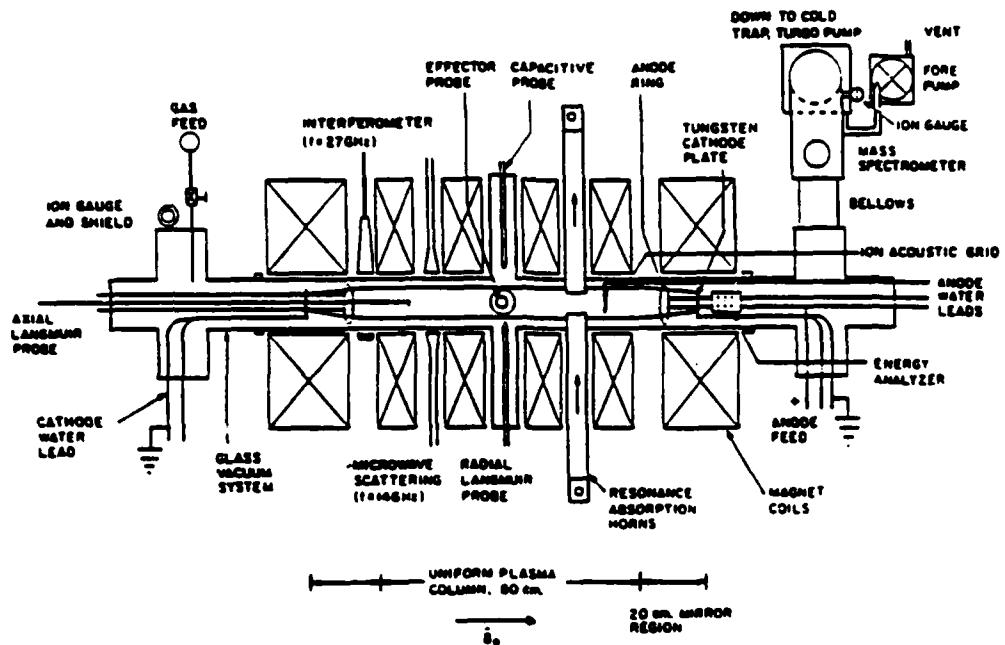
Fig. 1 Classical Penning discharge.

The launching and receiving horns are placed across the plasma diameter. Fig. 2 shows
such a configuration, with the network analyzer measuring the transmission coefficient
S_{21} for a particular range of frequency.
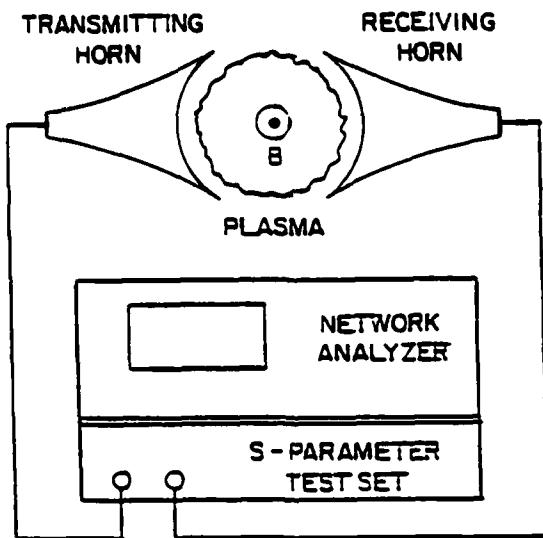
Fig. 2 Experimental setup for attention measurement.

The wave attenuation occurs near the electron cyclotron frequency[1,2], ω_{cy}. For this
reason, the swept frequency range is chosen to be few hundreds of MHz below and
above ω_{cy}. Table I shows the three different plasma conditions under which the
experimental attenuation measurements are taken.

Table I Experimental plasma conditions

	Units	PCL-11	PCL-12	PCL-14
He Gas Pressure	μTorr	75	85	110
Anode Voltage	KV	1.45	1.5	1.05
Anode Current	mA	26.1	47.0	14.7
Magnetic Field	Tesla	0.129	0.128	0.13
Electron Gyrofr.	GHz	3.63	3.6	3.655
Collision Freq.	MHz	20	30	15

The plasma conditions are chosen so as to have different number density and collision frequency from one experimental run to the other. The experimental runs are labeled PCL-#.

Fig.3 shows the radial profiles of the number density, electron kinetic temperature and plasma potential for experimental run PCL 11. These profiles are measured by a radially inserted Langmuir probe. The zero on the x-axis represents the center of the plasma and the six is the edge of the plasma located at 6 cm from the center. We assume that these profiles are symmetric with respect to the plasma axis.

RUN PCL 11

T_e, x10eV, ————

n_e, x10^{15} x m^{-3}, —————

V , VOLTS, —————
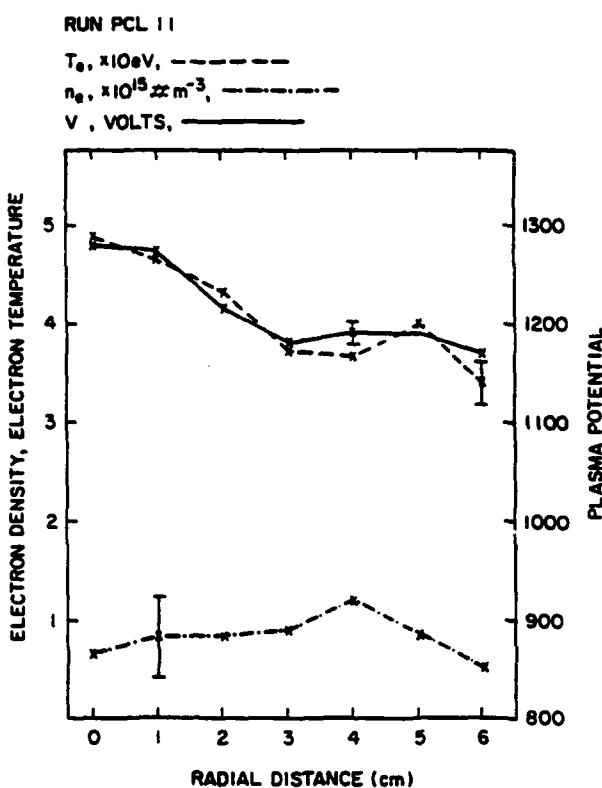

Fig. 3 Radial profiles of the number density, electron temperature,and plasma potential for run PCL 11.

The measured density profile is then inserted in the computer simulation and the corresponding attenuation is computed and compared to the experimentally measured one. Fig. 4 shows the number density radial profile used in the simulation. Fig. 5 shows the measured and computed attenuation versus frequency curves. A relatively good agreement between the two curves is noted.
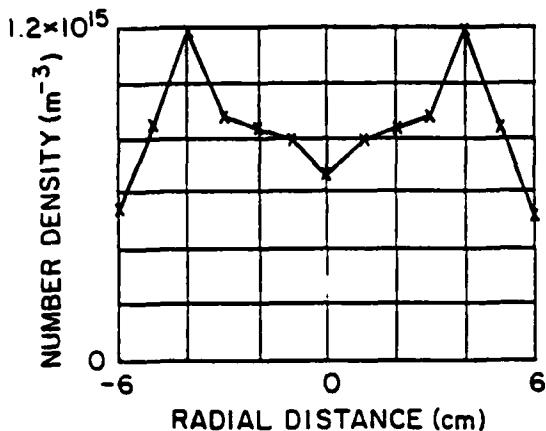

Fig. 4 Radial number density profile used in computation.
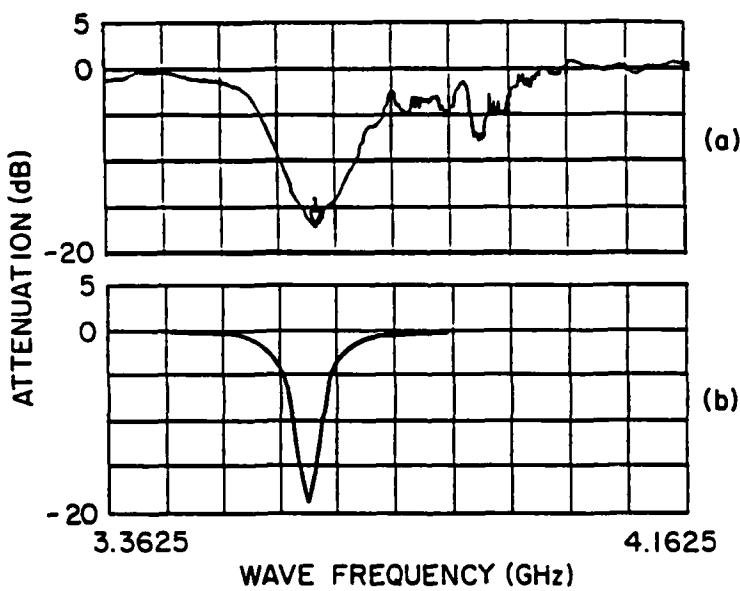
Fig. 5 Attenuation vs. frequency for run PCL 11
(a) experimental, (b) computational

Fig. 6 shows the absorption, $A_b(\omega)$, and reflection, $R(\omega)$, versus frequency curves. $A_b(\omega)$ and $R(\omega)$ are the ratios of the total absorbed power and the total reflected power by the incident power. These curves are computational results. It can be noted that the peak absorbed power is about 80% of the incident power. The peak reflected power is a little over 10% of the incident power.
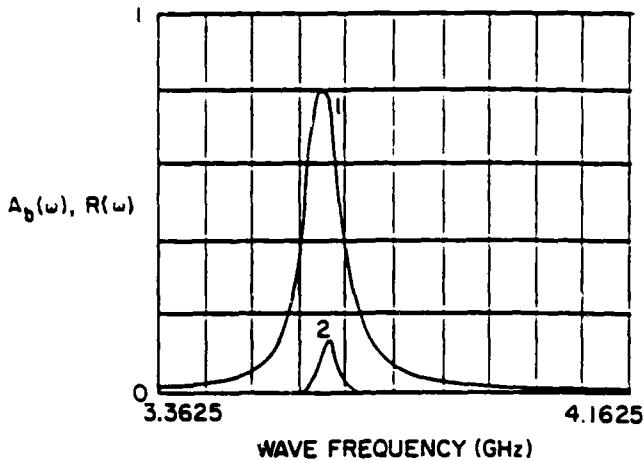
Fig. 6 Absorption (1) and reflection (2) vs. frequency for run PCL 11.

Fig. 7 through Fig. 10, and Fig. 11 through Fig. 14 show respectively the results for runs PCL 12 and PCL 14. One can clearly notice that for the case of run PCL 12, where the number density and the collision frequency are high, we get more attenuation and a higher peak of the absorption curve than for the other two runs. On the other hand, run PCL 14 which has the lowest number density and collision frequency, displays a smaller attenuation and a lower peak of the absorption curve than for the other runs. This leads to the conclusion that the attenuation and absorption of microwaves by a plasma are directly dependent on the plasma number density and the plasma collisionality. The higher the number density the more the attenuation, and the higher the collision frequency the more the absorption. The reflection is also dependent on these plasma parameters. One can note that the $R(\omega)$ curve is broader for higher collision frequencies.
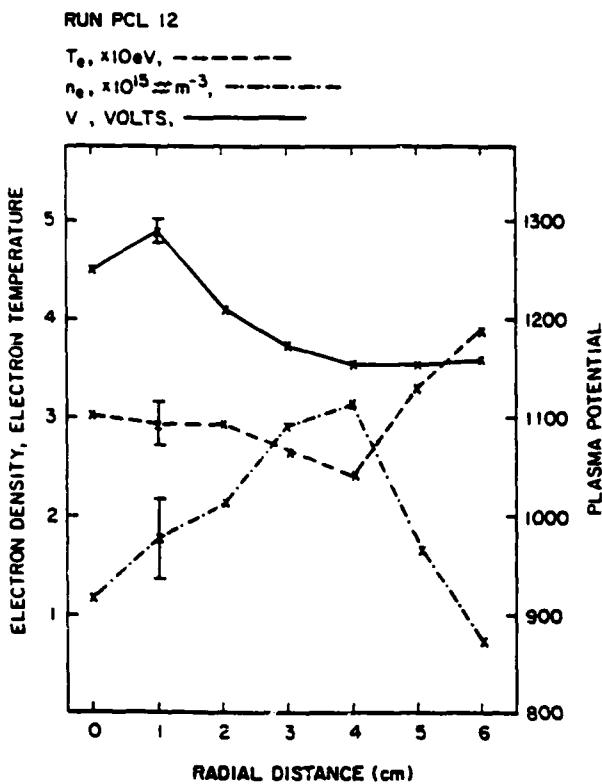
Fig. 7 Radial profile of the number density, electron temperature, and plasma potential for run PCL 12.

A-54
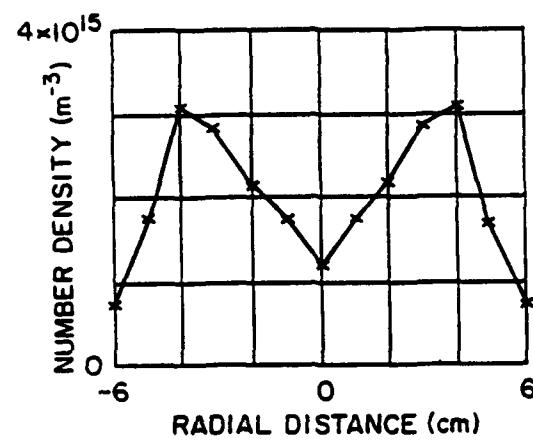
Fig. 8 Radial number density profile used in computation.
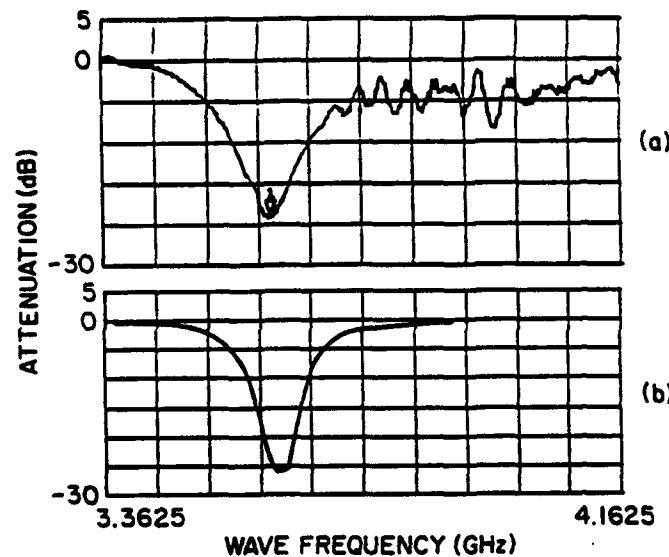
Fig. 9 Attenuation vs. frequency for run PCL 12
(a) experimental, (b) computational.
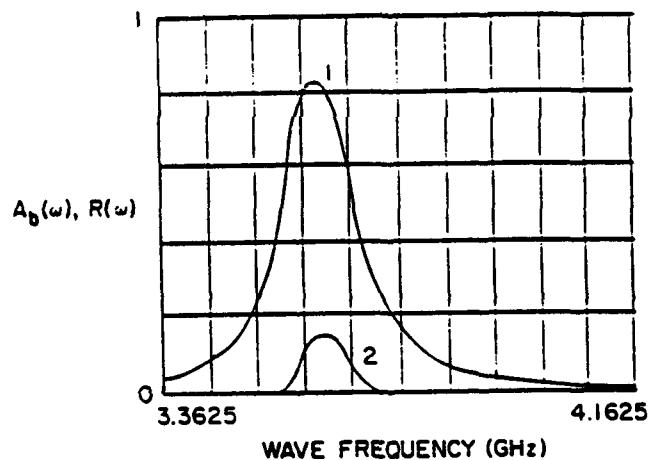
Fig. 10 Absorption (1) and reflection (2) vs. frequency for run PCL 12.
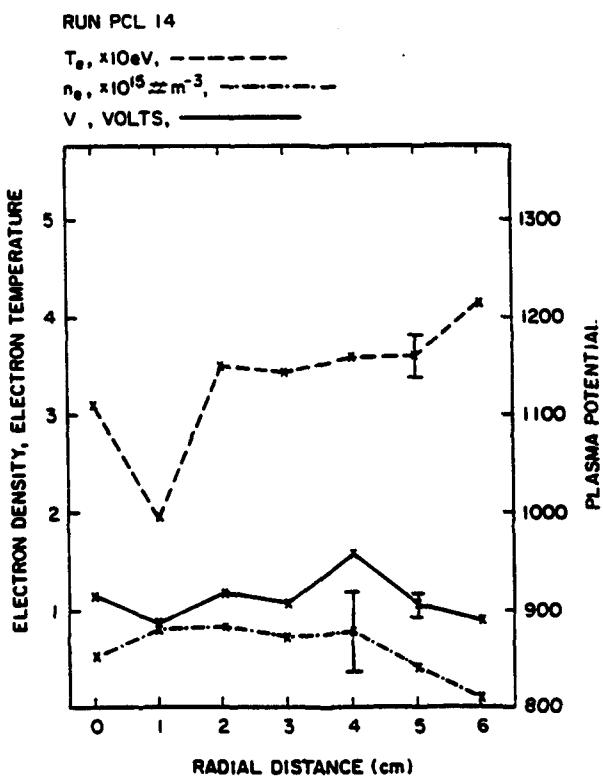
Fig. 11 Radial profile of the number density, electron temperature, and plasma potential for run PCL 14.
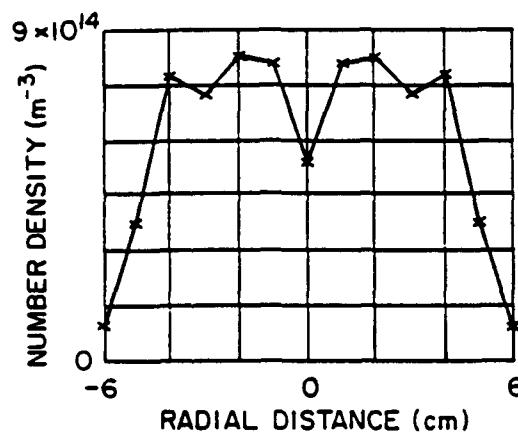
Fig. 12 Radial number density profile used in computation.
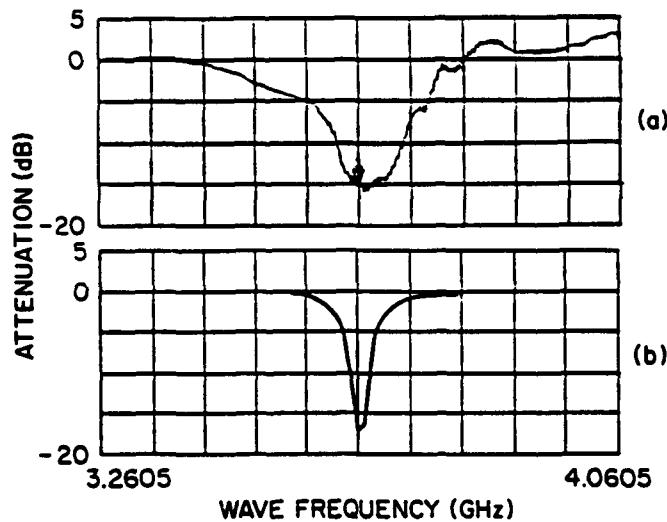
Fig. 13 Attenuation vs. frequency for run PCL 14
(a) experimental, (b) computational.
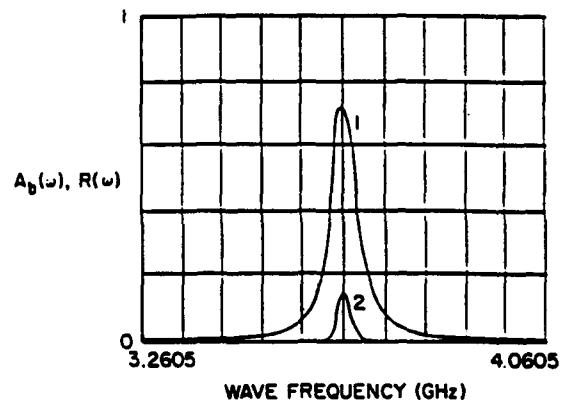
Fig. 14 Absorption (1) and reflection (2) vs. frequency for run PCL 14.

CONCLUSION

A study of the attenuation, absorption, and reflection of microwaves by a plasma has been presented. The attenuation is both measured experimentally and calculated computationally. A good agreement is obtained. The absorption and reflection are calculated computationally. It is found that the plasma number density and the collision frequency have a direct effect on the amount of absorbed and reflected power, and thus on the total power attenuation. Although the above study is a preliminary one it gives a good insight on the effects of the plasma properties on the propagation of microwaves through a magnetized plasma.

REFERENCES

1. M. A. Heald and C. B. Wharton, Plasma Diagnostics with Microwaves, Krieger Pub., Huntington, N. Y., (1978).
2. M. Laroussi and J. Reece Roth, Proc. IEEE International Conf. on Plasma Science, Cat. # 91CH3037-9, (1991), P. 146.
3. F. M. Penning and K. Nienhuis, Philips Tech. Rev., Vol. 11, No. 116, (1949), pp. 116-122.

BACK-SCATTERING CROSS-SECTION OF A CYLINDRICAL UNIFORM PLASMA COLUMN

Mounir Laroussi and J. Reece Roth

Plasma Science Laboratory
Electrical and Computer Engineering Department
University of Tennessee
Knoxville, Tennessee
37996-2100

Abstract

In monostatic radar applications it is the signal back to the source that is responsible for target detection. The back-scattering cross-section allows one to calculate the amount of power reflected back in the direction of incidence. In this paper, we develop theoretically and calculate computationally the back-scattering cross-section of a cylindrical column of magnetized plasma with a uniform number density. The effect of the plasma number density and of the collision frequency are investigated.

I. Introduction

In this paper, we calculate theoretically and computationally the back-scattering cross-section of a uniform cylindrical plasma column with a background uniform axial magnetic field. An electromagnetic wave in the microwave range is assumed to be incident on the plasma column with an arbitrary angle of incidence. The wavelength of the wave is assumed to be comparable to the plasma diameter. The plasma is modeled as a lossy dielectric [1]. The wave is partly refracted inside the plasma and partly scattered at different angles of reflection (See Fig. 1).

INCIDENT WAVE

BACK-SCATTERED WAVE

SCATTERED WAVE

B_0

a

z

y

PLASMA

θ

x

REFRACTED WAVE
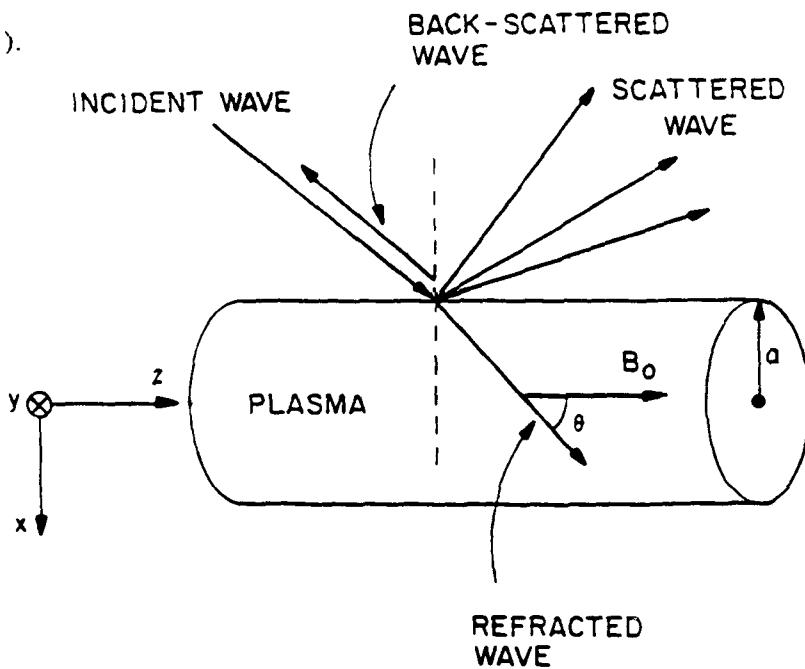
Fig. 1. Incident wave scattered by a lossy cylindrical plasma column.

It is the wave reflected back in the direction of incidence that is of interest. The back-scattering cross-section is a measure of how much power is reflected back to the source [2]-[5]. An investigation on the effects of plasma parameters on the back-scattering cross-section is presented. This discussion is based on a computer simulation in which the dielectric constant of the plasma is calculated from cold plasma theory [6]-[7], and parametric variations can be entered independently. The simulation results are presented in the form of plots of the back-scattering cross-section versus the wave frequency.

II.   Back-Scattering Cross-Section

In monostatic radar detection applications, it is the signal back to the source that determines the detectability of a target. For this reason, the back-scattering cross-section, $O(\omega)$, is of practical interest. The back-scattering cross-section is defined as the ratio of the scattered power per unit length, P_s, at an angle $\phi = \pi$ with respect to the incident direction of propagation, divided by the scalar magnitude of the incident poynting vector, S_i, at the location of the scatterer [2]-[4].

$$O(\omega) \; = \; \frac{P_s(\phi \; = \; \pi)}{S_i} \qquad (1)$$

This section presents the calculation of the back-scattering cross-section of a cylindrical plasma which has a uniform number density and a uniform axial magnetic field. The dielectric constant, $\tilde{\varepsilon}_r$, for a wave of

frequency ω propagating through a magnetized plasma at an angle θ with respect to the background magnetic field is given by [6]

$$\tilde{\varepsilon}_r = 1 - \frac{\dfrac{\omega_p^2}{\omega^2}}{\left[1 - j\dfrac{v}{\omega} - \dfrac{\dfrac{\Omega^2}{\omega^2}\sin^2\theta}{2\left(1 - \dfrac{\omega_p^2}{\omega^2} - j\dfrac{v}{\omega}\right)}\right] \pm \left[\dfrac{\dfrac{\Omega^4}{\omega^4}\sin^4\theta}{4\left(1 - \dfrac{\omega_p^2}{\omega^2} - j\dfrac{v}{\omega}\right)^2} + \dfrac{\Omega^2}{\omega^2}\bullet\cos^2\theta\right]^{1/2}},$$

(2)

where ω_p, Ω, and v are respectively the plasma frequency, the gyrofrequency, and the collision frequency. The - sign is for right handed polarization and the + sign is for a left handed polarization. $\tilde{\varepsilon}_r$ is also expressed as

$$\tilde{\varepsilon}_r = \varepsilon_r - j\frac{\sigma}{\omega\varepsilon_0},$$

(3)

where σ is the plasma conductivity, given by

$$\sigma = \frac{n e^2}{m v}.$$

(4)

The parameters n, e and m are respectively the number density, the electron charge, and the electron mass. For a collisional plasma with number densities ranging from 10^{14} m^{-3} to 10^{17} m^{-3} the conductivity

ranges from few mho/m to few tens of mho/m. The plasma in this case can be considered as a lossy medium.

The electric field of a sinusoidal plane wave incident on a cylindrical plasma column and traveling in the x-direction (see Fig. 1), is expressed as

$$E_i = E_0 \exp(j(k_1 x - \omega t)), \tag{5}$$

where k_1 is the wave number in free space. In cylindrical coordinates $e^{jk_1 x}$ can be expanded as

$$e^{jk_1 x} = \sum_0^\infty \varepsilon_n \ (j)^n \ J_n(k_1 r)\cos(n\phi). \tag{6}$$

where

$$\varepsilon_n \begin{cases} 1 & n = 0 \\ 2 & n \geq 1 \end{cases}$$

and $J_n(k_1 r)$ is the Bessel function of the first kind and of order n. In cylindrical coordinates the electric field of the incident wave is expressed as

$$E_i = E_0 \ e^{-j\omega t} \sum_0^\infty \varepsilon_n \ (j)^n \ J_n(k_1 r)\cos(n\phi). \tag{7}$$

Similarily, the electric field of the scattered wave is given by

$$E_s = E_0\, e^{-j\omega t} \sum_0^{\infty} A_n \varepsilon_n\, (j)^n\, H_n^{(1)}(k_1 r) \cos(n\phi), \qquad (8)$$

where $H_n^{(1)}(k_1)$ is the Hankel function of the first kind, representing a wave propagating outward from the plasma column.

At the surface of the plasma the wave has to satisfy the appropriate boundary conditions. The electric field on the outside of the surface is the sum of the incident and the scattered fields. This is expressed as

$$E = E_i + E_s \quad,$$

or

$$E = E_0\, e^{-j\omega t} \left(\sum_0^{\infty} \varepsilon_n (j)^n J_n(k_1 r)\cos(n\phi) + \sum_0^{\infty} A_n \varepsilon_n (j)^n H_n^{(1)}(k_1 r)\cos(n\phi) \right).$$

$$(9)$$

The electric field inside the plasma surface is the transmitted field, expressed as

$$E_t = E_0\, e^{j\omega t} \sum_0^{\infty} B_n\, \varepsilon_n\, (j)^n\, J_n(k_2 r)\cos(n\phi), \qquad (10)$$

where k_2 is the wave number in the plasma. At the plasma radius, r=a, we have the following boundary conditions

$$E_i + E_s = E_t \quad ,$$

and

$$\frac{\partial (E_i + E_s)}{\partial r} = \frac{\partial E_t}{\partial r} \quad ,$$

which leads to the following equations

$$J_n(k_1a) + A_n H_n^{(1)}(k_1a) = B_n J_n(k_2a), \qquad (11)$$

and

$$k_1 J_n'(k_1a) + A_n k_1 H_n^{(1)'}(k_1a) = k_2 B_n J_n'(k_2a). \qquad (12)$$

Solving for the expression A_n yields

$$A_n = \frac{k_2 J_n(k_1a) J_n'(k_1a) - k_1 J_n(k_2a) J_n'(k_1a)}{k_1 J_n(k_2a) H_n^{(1)'}(k_1a) - k_2 J_n'(k_2a) H_n^{(1)}(k_1a)}. \qquad (13)$$

Thus the scattered wave field is given by

$$E_s = E_0 e^{-j\omega t} \sum_0^\infty \varepsilon_n (j)^n A_n H_n^{(1)}(k_1r) \cos(n\phi).$$

The ratio of the scattered power by the incident power is given by

$$S(\phi) = \frac{|E_s|^2}{|E_i|^2} = \left| \sum_0^\infty \varepsilon_n \, (j)^n \, A_n \, H_n^{(1)}(k_1 r) \cos(n\phi) \right|^2 . \quad (14)$$

For back-scattering we have $\phi = \pi$, which yields

$$S(\pi) = \left| \sum_0^\infty \varepsilon_n \, (j)^n \, A_n \, H_n^{(1)}(k_1 r) \, (-1)^n \right|^2 . \quad (15)$$

When r becomes large, as it is the case in radar applications, $H_n^{(1)}(k_1 r)$

can be approximated as

$$H_n^{(1)}(k_1 r) \approx \left(\frac{2}{\pi \, k_1 r} \right)^{1/2} \exp\left(j\left(k_1 r - n\frac{\pi}{2} - \frac{\pi}{4} \right) \right) \quad k_1 r \to \infty$$

Inserting into Equation (15) yields

$$S(\pi) = \frac{2}{\pi \, k_1 r} \left| \sum_0^\infty (-1)^n \, \varepsilon_n \, A_n \right|^2 . \quad (16)$$

The total back-scattered power is obtained by integrating over the entire

plasma outer surface. Thus, the back-scattering cross-section is given

by

Back-Scattering Cross-Section

$$O(\omega) = \int_0^{2\pi} s(\pi) \, r \, d\phi \quad,$$

which yields

$$O(\omega) = \frac{4}{k_1} \left| \sum_0^\infty (-1)^n \, \varepsilon_n \, A_n \right|^2 , \qquad (17)$$

where the coefficients A_n are given by Equation (13). The wave numbers k_1 and k_2 are given by

$$k_1 = \frac{\omega}{c} \quad,$$

and

$$k_2 = \frac{\omega}{c} \, \text{Re} \, (\sqrt{\tilde{\varepsilon}_r}) \quad.$$

Re represents the real part and $\tilde{\varepsilon}_r$ is the complex dielectric constant

III. Numerical Results

In the following calculations, the plasma is modeled as a cylindrical lossy dielectric. These calculations are based on the results presented in section II. The computer simulation program is structured as shown in Fig. 2. First the plasma number density, the magnetic field strength, the plasma radius, the effective collision frequency, the angle
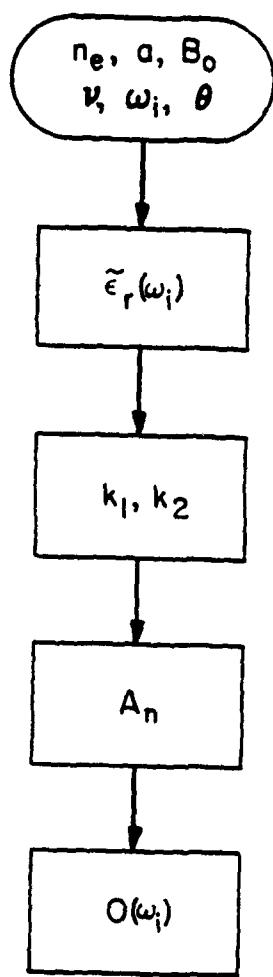
Fig. 2. Block diagram showing the main steps in the calculation of the back-scattering cross-section.

of propagation with respect to the magnetic field, and the wave frequency range are entered. Next, the program calculates the dielectric constant of the plasma column for each frequency step. Once this is done, the free space and the plasma wave numbers are computed and the coefficients A_n are deduced. Finally the backscattering cross-section is calculated using Equation (17). Only the first ten terms in the summation are used. This has been shown to be a good approximation[3] for $k_1 a \leq 10$.

The simulation results are presented as plots of the back-scattering cross-section, $O(\omega)$, versus frequency. Various plasma conditions are achieved by changing the number density and the collision frequency. The backscattering cross-section dependence on each parameter is investigated by varying the value of that parameter while keeping the others constant. $O(\omega)$ has the dimension of length since it is the ratio of outward flowing power per unit length divided by the incident power per unit area. This is also shown in Equation (17) where k_1 has the dimension of inverse length. To find the back-scattered power per unit length of the cylindrical plasma, one has to multiply $O(\omega)$ by the incident power per unit area. Figure 3 and Figure 4 show respectively $O(\omega)$ Vs. frequency for a center density of $N_O = 10^{15}$ m^{-3} and $5 \ 10^{15}$ m^{-3}, and for three values of the collision frequency $\nu = 20$ MHz, 10 MHz, and 5 MHz. One can note that the higher the number denstiy the broader $O(\omega)$ is, and the lower the collision frequency the more numerous are the sharp peaks. This is further illustrated in figure 5
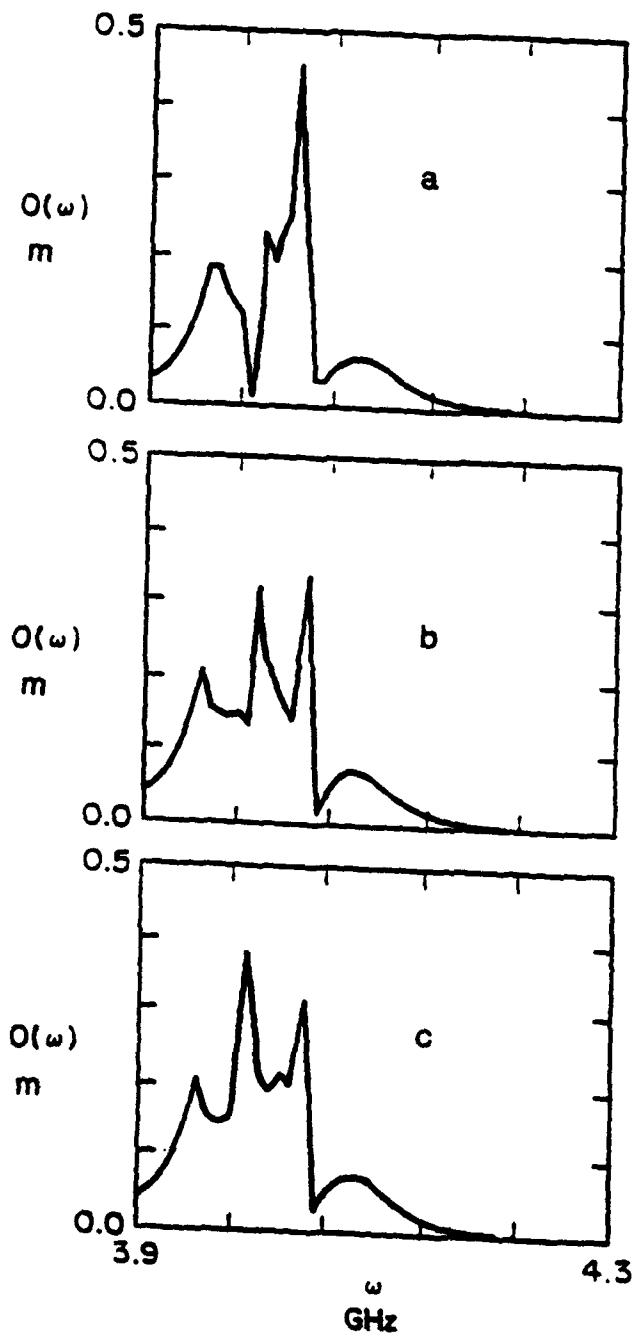
Fig. 3.   Back-scattering cross-section versus wave frequency, $\theta = 60^\circ$, $\Omega = 4$ GHz, $N_0 = 10^{15}$ m^{-3}: (a) $\nu = 20$ MHz, (b) $\nu = 10$ MHz, (c) $\nu = 5$ MHz.
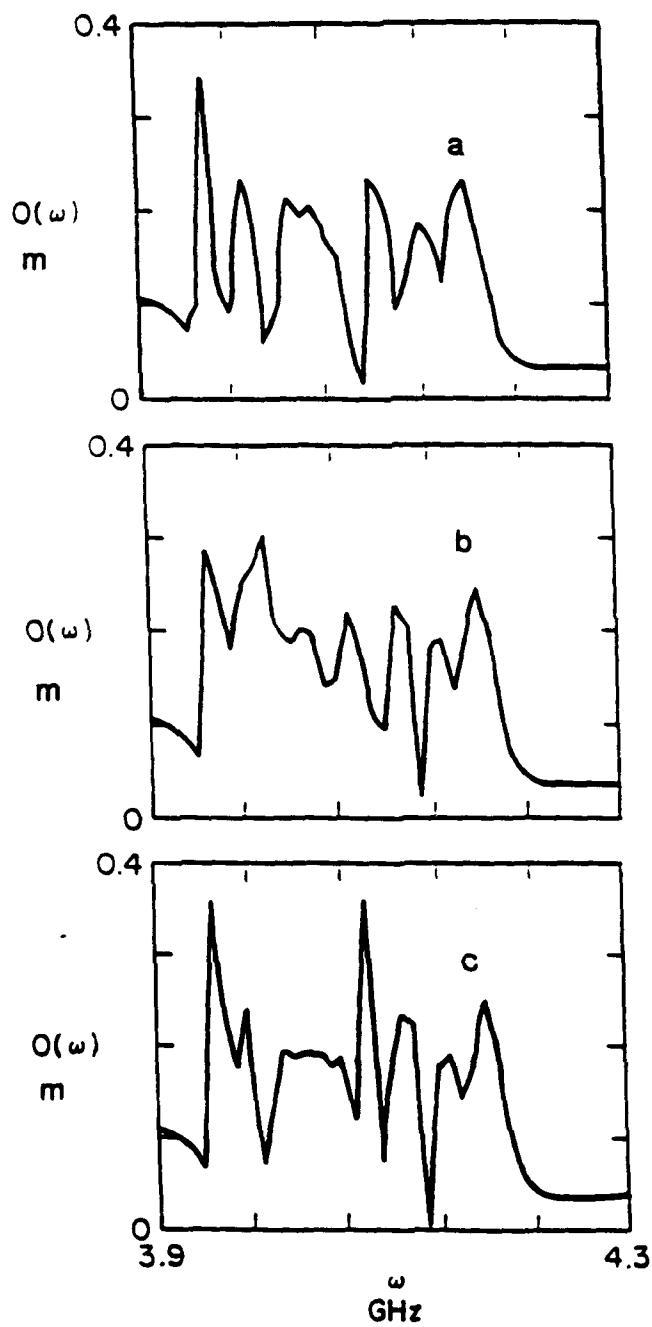
Fig. 4.   Back-scattering cross-section versus wave frequency, $\theta = 60^\circ$, $\Omega = 4$ GHz, $N_o = 510^{15}$ m^{-3}: (a) $\nu = 20$ MHz, (b) $\nu = 10$ MHz, (c) $\nu = 5$ MHz.
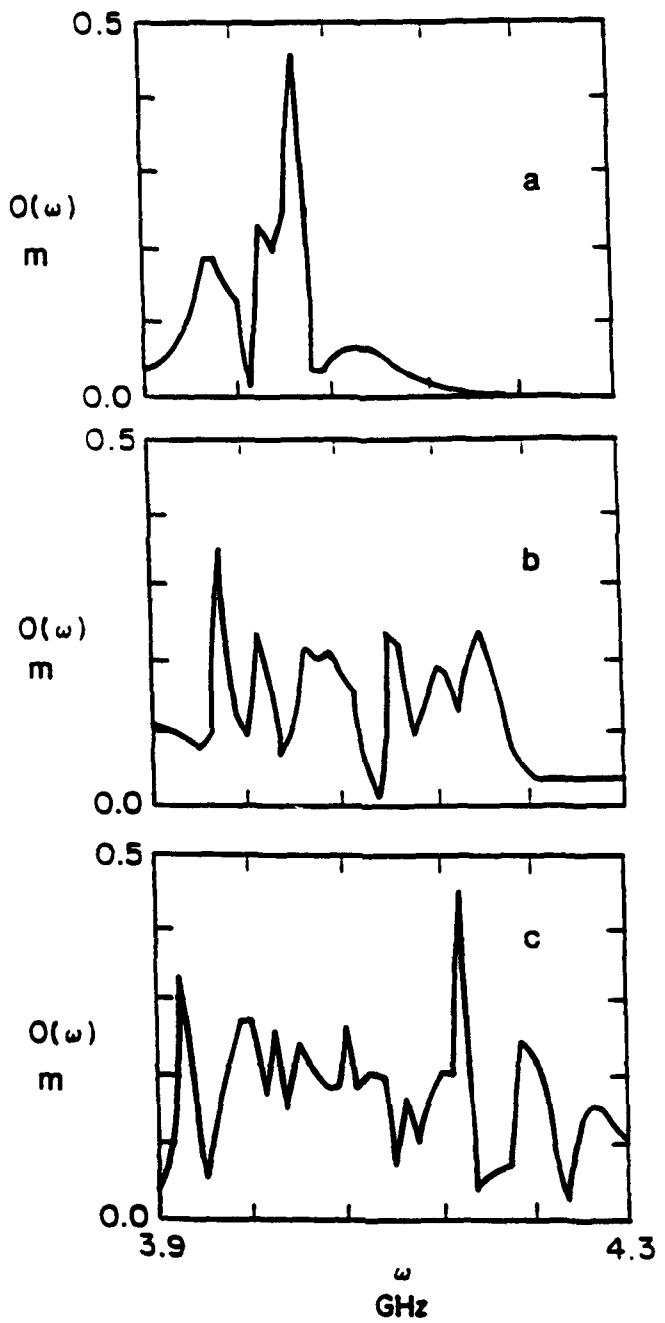
Fig. 5. Back-scattering cross-section versus wave frequency, $\theta = 60^{\circ}$, $\Omega = 4$ GHz, $v = 20$ MHz: (a) $N_0 = 10^{15}$ m^{-3}, (b) $N_0 = 5 \cdot 10^{15}$ m^{-3}, (c) $N_0 = 10^{16}$ m^{-3}.

which shows $O(\omega)$ Vs. frequency for a collision frequency of $v = 20$ MHz and for three values of the center density $N_0 = 10^{15}$ m^{-3}, 5×10^{15} m^{-3} and 10^{16} m^{-3}. This figure shows clearly that for increasing number densities the back-scattering cross-section curve has more structure and displays a broader range with an increasing number of peaks. This result leads to the following conclusion: To keep the signal reflected back to the source small, a low density but collisional plasma is needed.

IV. Conclusion

The back-scattering cross-section is an important parameter in monostatic radar applications. it gives a measure of how much power is reflected back to the source. In this paper, we developed theoretically the expression of the back-scattering cross-section of a magnetized cylindrical plasma column, modeled as a lossy dielectric. The effects of the plasma number density and the effective collision frequency have been studied computationally. It is found that low density but highly collisional plasma are low back-scatterers. The weakly ionized but highly turbulent plasma generated by Penning discharges satisfy such requirements [8]. Experimental results taken on such a plasma will be published elsewhere.

Acknowledgement

References

[1]   J. R. Wait, and L. C. Walters, "Reflection of Electromagnetic Waves from a Lossy Magnetoplasma" *Radio Sci. J. Res.*, Vol. 68D, No. 1, pp. 95-101, 1964.

[2]   J. R. Mentzer, *Scattering and Diffraction of Radio Waves*, Pergamon Press, New York, 1955.

[3]   R. W. King, and T. T. Wu, *The Scattering and Diffraction of Waves*, Harvard University Press, 1959.

[4]   C. C. H. Tang, "Backscattering from Dielectric-Coated Infinite Cylindrical Obstacles" *J. Appl. Physics*, Vol. 28, No. 5, pp. 628-633, 1957.

[5]   P. M. Morse, and H. Feshbach, *Methods of Theoretical Physics*, Part II, McGraw-Hill, New York, 1953.

[6]   M. A. Heald and C. B. Wharton, *Plasma Diagnostics with Microwaves*, Krieger Pub., New York, 1978.

[7]   M. Laroussi and J. Reece Roth, "Reflection of Electromagnetic Radiation from a Non-Uniform Plasma Slab at an Arbitrary Angle of Incidence", *Proceedings of the 1991 International Conference*

on Plasma Science, Williamsburg, VA, CAT# 91CH3037-9, p. 146, 1991.

[8] M. Laroussi, *Ph.D. Dissertation*, University of Tennessee, Knoxville, 1988.

A TUNABLE MICROWAVE
NOTCH ABSORBER FILTER

Mounir Laroussi

UTK Plasma Science Laboratory
Department of Electrical & Computer Engineering
University of Tennessee
Knoxville, TN 37996-2100

Abstract

A magnetized plasma column is found to be a notch absorber of microwave radiation propagating in the extraordinary mode. Based on this fact, a compact tunable microwave filter is designed and tested successfully. The center frequency of the absorbed band can be varied by adjusting the background magnetic field stength. The 3dB bandwidth and amount of attenuation are functions of the plasma current. These characteristics offer a great tunability, often sought after in microwave devices. This filter can find applications in microwave measurement systems where filtering of unwanted harmonics and spurious signals can directly affect the accuracy and resolution of the measurements.

Introduction

In many microwave measurement systems filtering of unwanted harmonics and spurious signals affect the quality of the measurements. A tunable filter would be an attractive and versatile device, which could be used in combination with cheaper signal sources. In this paper, we propose a cheap, easy to design and construct, tunable microwave notch absorber filter. This filter is based on the fact that for the x-mode of propagation, the dielectric constant of a magnetized plasma shows a resonant behavior near the electron cyclotron frequency. Thus, the wave attenuation factor due to the presence of the plasma is maximum at that frequency. Since the cyclotron frequency depends on the magnetic field strength, it follows that the frequency of maximum attenuation can be tuned by adjusting the background magnetic field. It is also found that for a plasma generated by a DC glow discharge, the 3dB bandwidth and amount of attenuation are functions of the discharge current. Hence, the filter presented here, is tunable both in frequency range and magnitude. A prototype of this device was designed and tested successfully.

Theoretical Background

Based on cold plasma theory, it has been shown both theoretically and experimentally [1] - [5] that an electromagnetic wave polarized in the extraordinary mode and propagating through a magnetized plasma undergoes a power attenuation of several tens of dBs. This power attenuation occurs only in a small frequency band the center of which is near the electron cyclotron frequency given by

$$\Omega = \frac{eB}{m_e} \tag{1}$$

where e, m_e, and B are respectively the electronic charge, mass, and the background magnetic field. This attenuation is due to a resonant behavior of the complex dielectric constant, near the electron cyclotron frequency. The complex dielectric constant for the x-mode of propagation is given by Appleton [5]

$$\tilde{\varepsilon}_{ex} = 1 - \frac{\omega_{pe}^2 / \omega^2}{1 - j\frac{\nu}{\omega} - \frac{\Omega^2 / \omega^2}{1 - \omega_{pe}^2 / \omega^2 - j\nu/\omega}} \tag{2}$$

where ω, ω_{pe} and ν are respectively the wave frequency, the electron plasma frequency, and the collision frequency.

The propagation coefficient of a wave having $\exp(j\omega t - \tilde{\gamma}z)$ as a phase factor is given by

$$\tilde{\gamma} = j\sqrt{\tilde{\varepsilon}}\,\frac{\omega}{c} \qquad (3)$$

where ω is the wave frequency and c is the speed of light. $\tilde{\gamma}$ is also expressed as

$$\tilde{\gamma} = \alpha + j\beta \qquad (4)$$

where α is the attenuation coefficient and β is the phase coefficient . Using equations (3) and (4), the attenuation coefficient can be expressed as

$$\alpha = -\frac{\omega}{c}\mathrm{Im}\left(\sqrt{\tilde{\varepsilon}}\right) \qquad (5)$$

where Im stands for imaginary part. Near the electron cyclotron frequency, α is maximum for a wave polarized in the x-mode. Since $\tilde{\varepsilon}_{ex}$ is function of both the collision frequency, ν, and the plasma frequency, ω_{pe}, the width and amount of attenuation are functions of both the collision frequency and the number density. This leads to a very interesting development: A magnetized plasma column, through which an electromagnetic wave is propagating in the x-mode, is in fact a microwave notch absorber filter. The absorbed band can be preselected by adjusting the background magnetic field strength, and the bandwidth and attenuation can be adjusted by changing the plasma collision frequency and number density. Therefore, a filter with unique features could be designed, based on the above principle. This filter would be tunable since its center frequency, bandwidth and amount of attenuation can be selected by respectively adjusting the background magnetic dield, the collision frequency, and the plasma number density.

Experimental Setup

In this section, the design of the filter is presented. The plasma is generated inside a pyrex glass vacuum vessel by means of a glow discharge established between two disc-shaped electrodes. The dimensions of the vessel and electrodes are shown in Figure 1.
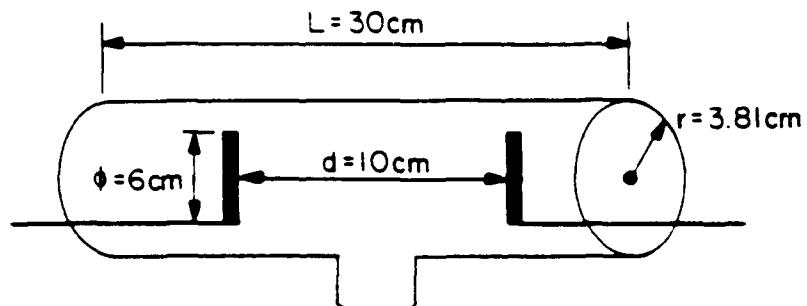
Fig. 1 Vacuum vessel with disc-shaped electrodes

Two permanent magnets are placed on the outside of the vacuum vessel. The magnets are placed such that one has its south pole and the other its north pole facing the glass. This way, magnetic field lines are established between the two electrodes. Figure 2 shows such an arrangement.
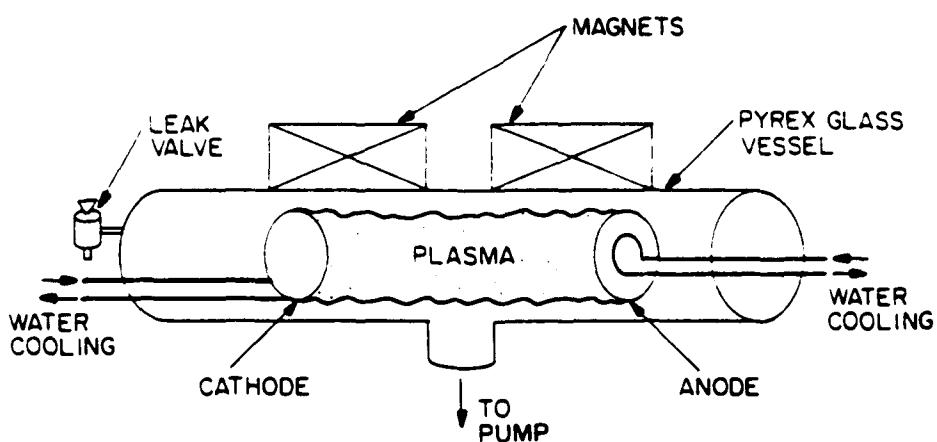

Fig. 2 Experimental arrangement with magnets

Magnetic field strength up to 1100 Gauss was established between the two electrodes. The system is pumped down by a mechanical pump. Working pressures in the 30-80 m Torr range were used. Air was used as the background gas, but a leak valve could be used to introduce a different working gas.

Two S-band microwave horns are placed across the vessel, facing each cther. One horn is the transmitter, and the other is the receiver. The wave is launched such that the E-field is perpendicular to the magnetic field lines. An HP 8510 network analyzer, equipped with an S-parameters test set, is used to measure the power attenuation. This network ar. yzer is capable of swept measurements between 40 MHz and 18 GHz with a dynamic range of 80dB. Figure 3 shows the experimental setup.

TRANSMITTING HORN

NOTCH ABSORBER FILTER

NETWORK ANALYZER

S-PARAMETER TEST SET

RECEIVING HORN

HIGH VOLTAGE POWER SUPPLY
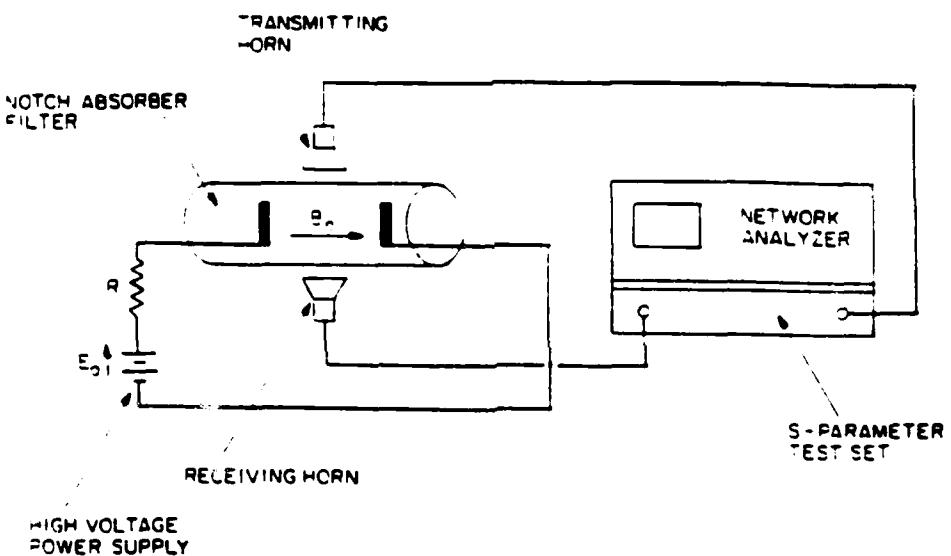
Fig. 3 Experimental setup for attenuation measurements

Experimental Results

In this section, experimental measurements of the power attenuation and its dependence on the magnetic field strength and the discharge current, are presented. The discharge is operated at a regime where the current can be changed over a wide range without a substantial change in the voltage between the two electrodes. The attenuation data are all normalized with respect to the plasma-off case. Figure 4 shows the normalized attenuation when the plasma is off. A 0 dB flat curve is seen between 2.2 GHz and 3 GHz.
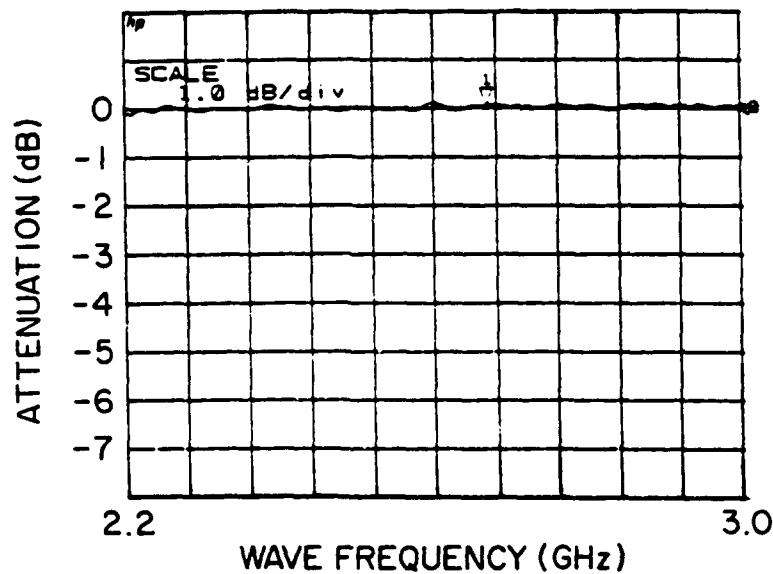
Fig. 4 Normalized attenuation with plasma off

Figures 5 through 7 show the attenuation versus frequency for increasing discharge current, a constant magnetic held strength of 950 Gauss, a pressure of 70 m Torr, and a voltage of 700 V. It is seen that with increasing discharge current the peak of the attenuated band increases, and its width gets narrower. Figures 8 and 9 show respectively the peak attenuation and the 3dB bandwidth versus discharge current. The peak of the attenuation is an increasing function of the current with an increase rate of about 1.17 dB per 10 mA. The 3dB bandwidth is a decreasing function with two different rates, one at low current discharge, 41.53 MHz per 10 mA current increase, another at high current, 1.33 MHz per 10 mA current increase.

Figure 10 shows the attenuation versus wave frequency for almost similar plasma conditions but for two different magnetic field strengths, 950 Gauss and 970 Gauss. It is clearly seen that for this small variation in the magnetic field strength, a change of the band center frequency occurs. The two respective center frequencies, actually corresponds to the two different values of the electron cyclotron frequency. This proves the tunability of the filter with respect to the applied magnetic field.

Conclusions

A tunable notch absorber microwave filter operating in the S-band has been designed, constructed, and tested successfully. The magnetic field strength and discharge current are the control parameters. The magnetic field controls the center frequency of the attenuated band, and the
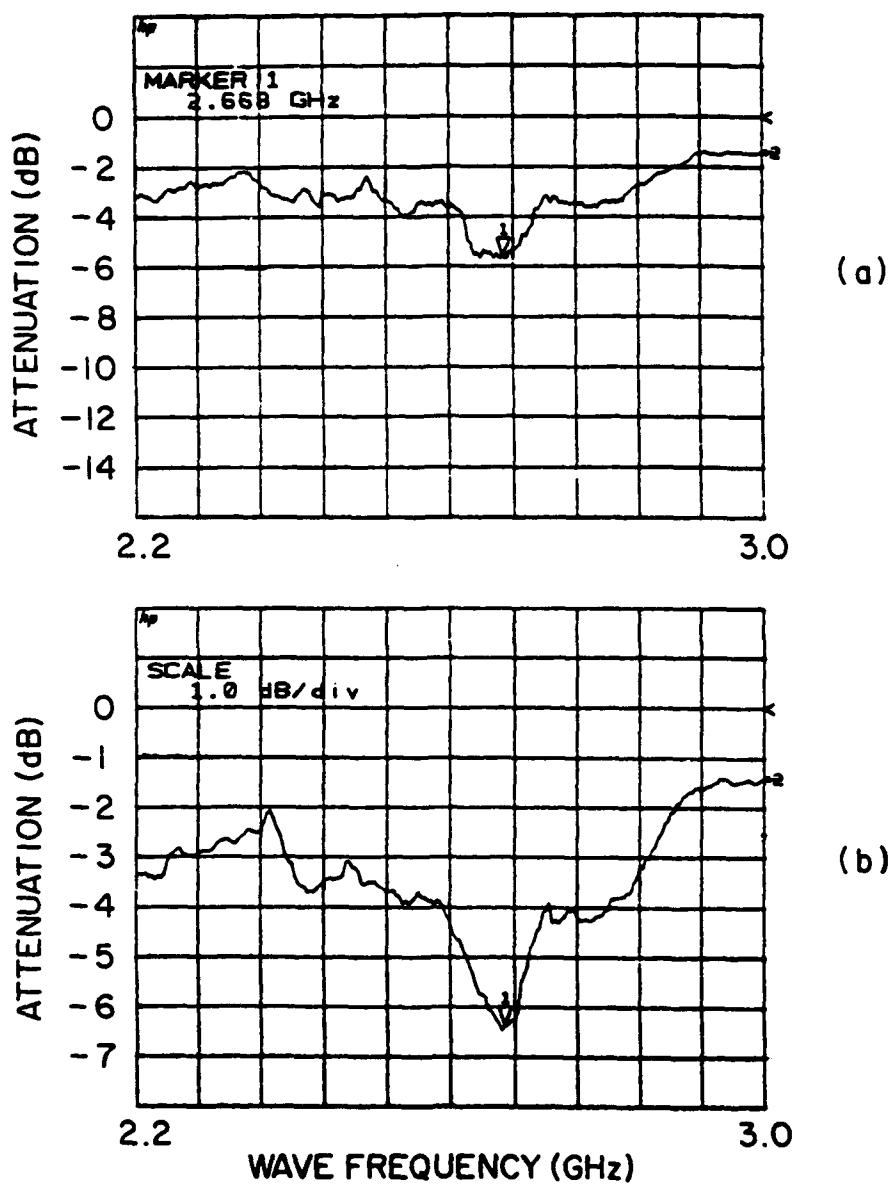
Fig.5   Attenuation   Vs.   frequency   for
V=700V;P=70mTorr;B=950Gauss;and (a)I=98mA,
(b)I=110mA.
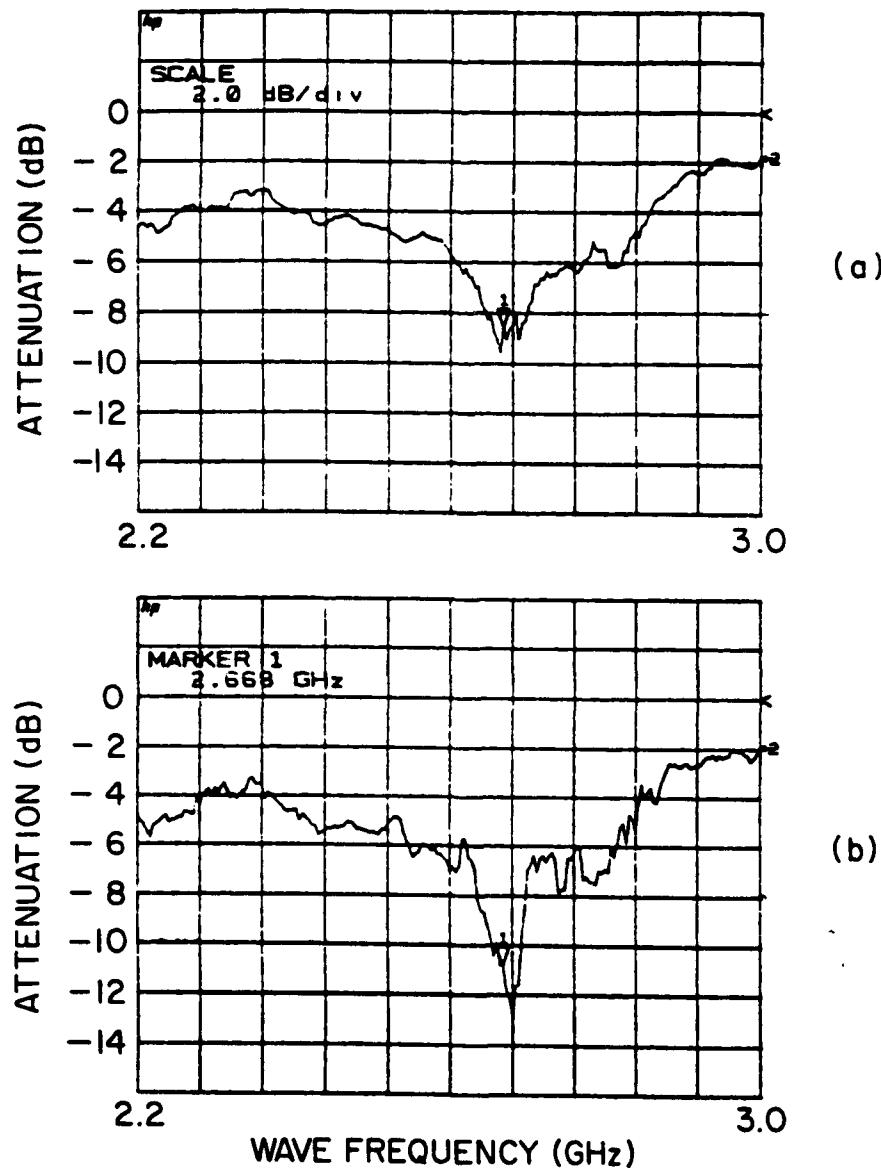
Fig.6   Attenuation vs. frequency for V=700V;P=70mTorr;B=950Gauss;and (a)I=150mA, (b)I=200mA.
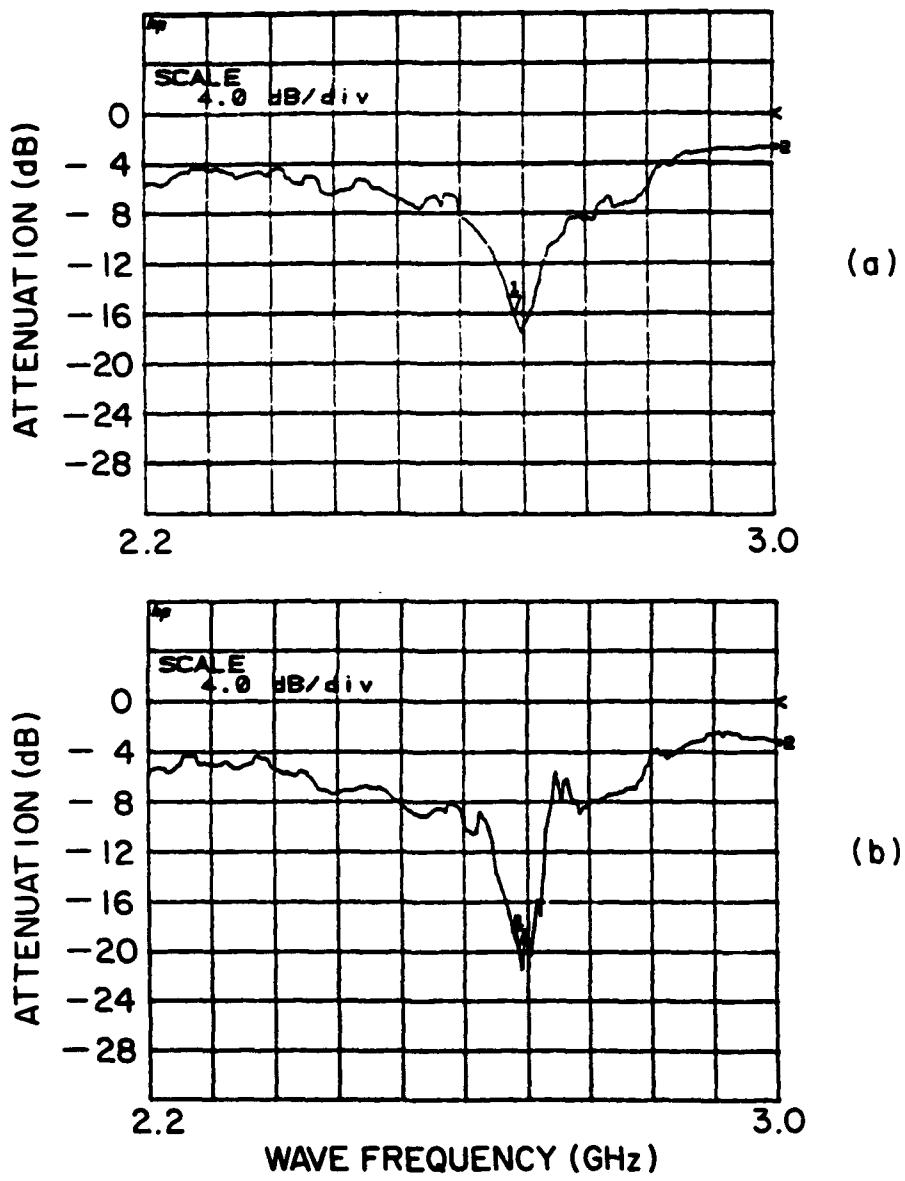
Fig.7   Attenuation   Vs.   frequency   for
V=700V;P=70mTorr;B=950Gauss;and (a)I=250mA,
(b)I=300mA.
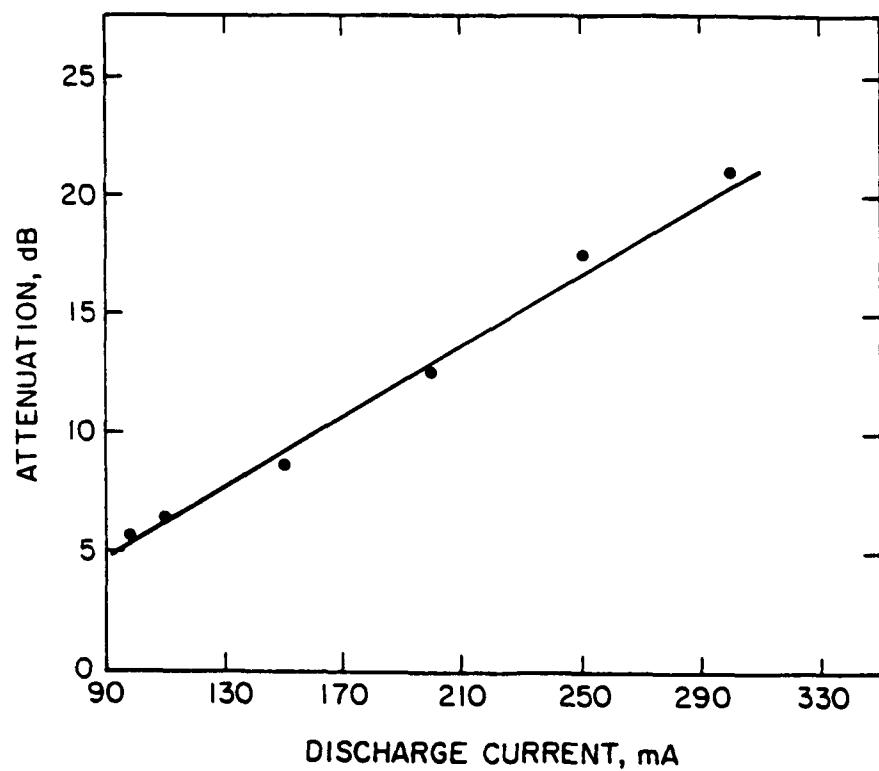
Fig.8 Attenuation Vs. discharge current at =2.668GHz;V=700V;and P=70mTorr.
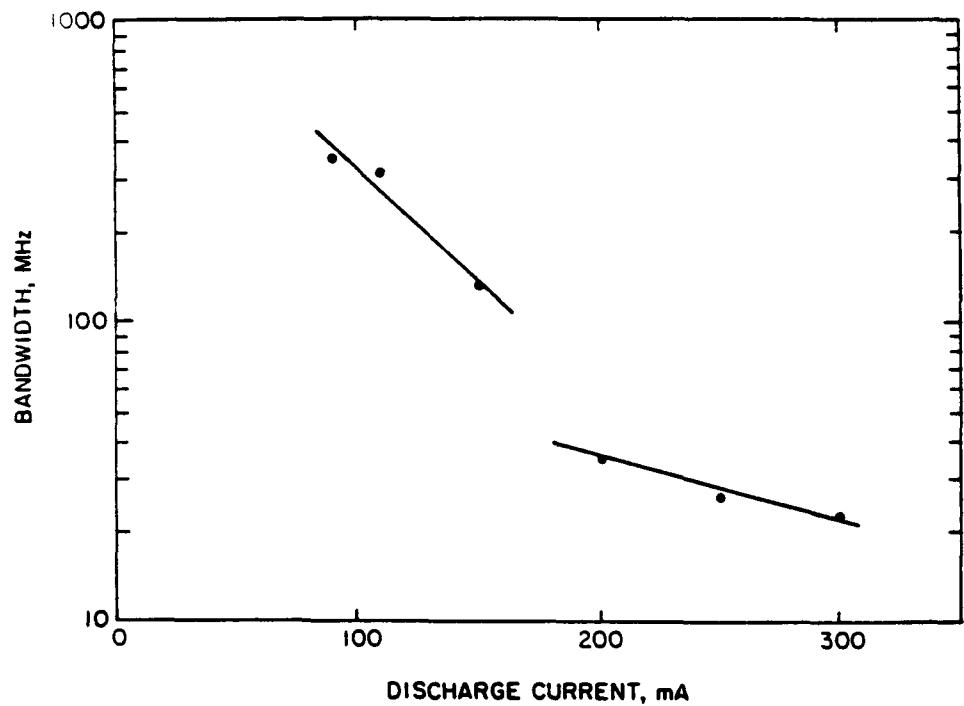
Fig.9 3dB bandwidth Vs. discharge current for V=700V;P=70mTorr;and B=950Gauss.
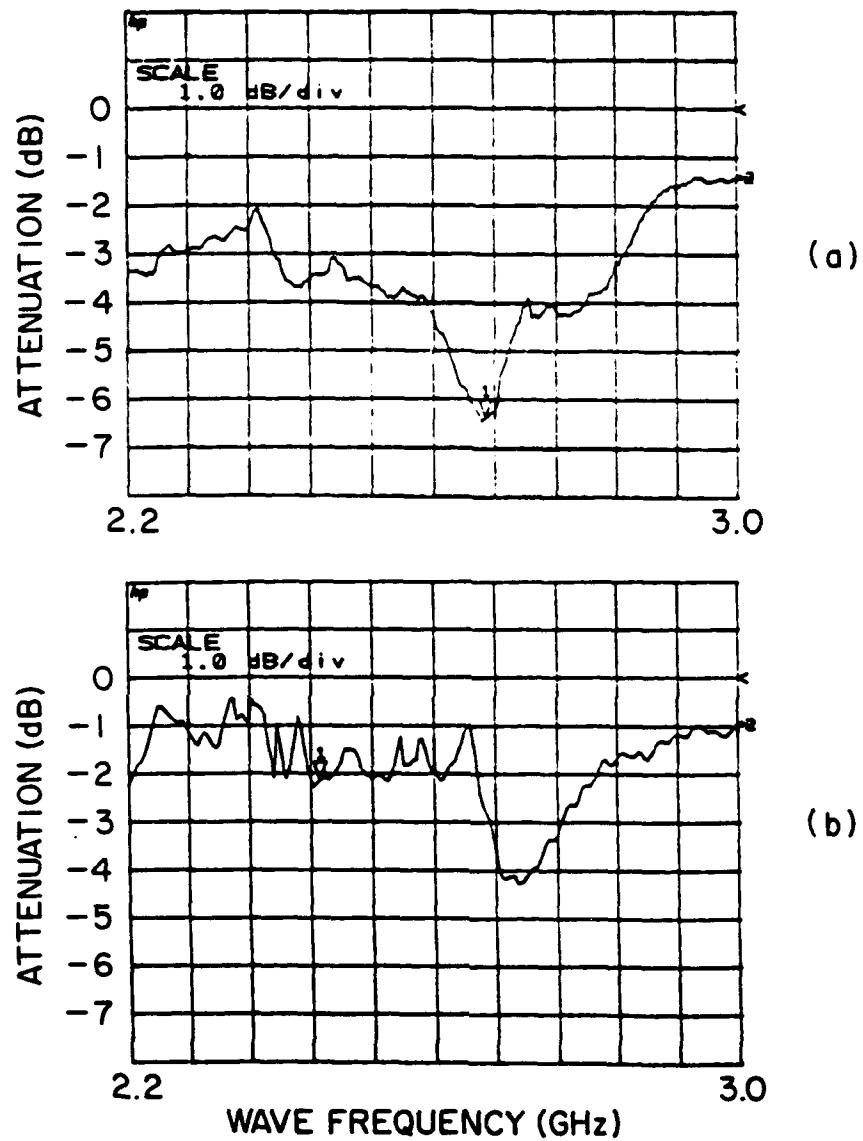
Fig.10 Attenuation vs. frequency for V=700V; P=70mTorr; (a) B=950Gauss, (b) B=970Gauss.

discharge current controls the amount of attenuation and the bandwidth of the frequency band. These two parameters are adjusted externally, which gives the operator easy controllability. This filter is easy to to design and to construct at minimal costs. Its applications are numerous in microwave measurements systems where unwanted harmonics and spurious signals affect the accuracy and resolution of the measurements. It also could be used in Radar Cross Section measurement systems to remove images and spurs from the I. F. Depending on its switching speed, it could also be used in microwave systems with cheap signal sources.

Acknowledgement

References

[1]   J. Reece Roth, "Microwave Absorption System", United States Patent Number 4,989,006, Jan. 29, 1991.

[2]   L. Henry Combs, Chaoyu Liu, and J. Reece Roth, "Studies of Microwave Absorption by a Plasma Near the Electron Cyclotron Frequency", Bulletin of the American Physical Society, Vol. 35, No. 9, p. 2068, Oct. 1990.

[3]   M. Laroussi and J. R. Roth, "Reflection of Electromagnetic Radiation from a Non-Uniform Plasma Slab at an Arbitrary Angle of Incidence", Proceedings of the 1991 IEEE International Conference on Plasma Science, Williamsburg, VA, CAT# 91CH3037-9, p. 146, June 1991.

[4]   M. Laroussi, C. Liu, and J. R. Roth, "Absorption and Reflection of Microwaves by a Non-Uniform Plasma Near the Electron Cyclotron Frequency", Proceedings of the 9th APS Topical Conference on Radio Frequency Power in Plasma, Charleston, SC, p. 37-45, 1991.

[5]   M. A. Heald and C. B. Wharton, Plasma Diagnostics with Microwaves, Krieger Pub. Huntington, N.Y., 1978.

Numerical Calculation of the Reflection, Absorption, and Transmission of Microwaves by a Nonuniform Plasma Slab

Mounir Laroussi, *Member, IEEE*, and J. Reece Roth, *Fellow, IEEE*

Abstract—In this paper we study the reflection, absorption, and transmission of microwaves by a magnetized, steady-state, two-dimensional, nonuniform plasma slab. A discussion on the effect of various plasma parameters on the reflected power, absorbed power, and transmitted power is presented. The nonuniform plasma slab is modeled by a series of subslabs. Even though we assume that the number density is constant in each subslab, the overall number density profile across the whole slab follows a parabolic function. The partial reflection coefficient at each subslab boundary is computed along with the absorption at each subslab. The total reflected, absorbed, and transmitted powers are then deduced and their functional dependence on the number density, collision frequency, and angle of propagation is studied.

Fig. 1. Experimental setup for attenuation measurement.

I. INTRODUCTION

IN this paper, we investigate computationally the reflection, absorption, and transmission of microwaves by a magnetized steady-state plasma slab. This paper is motivated by a recent interest in using plasmas as absorbers or reflectors of microwave energy, depending on the particular application [1]–[8]. In our paper we are mainly concerned with finding the appropriate parameter regimes of a plasma which either minimizes reflection and/or maximizes absorption. The incident wave is assumed to be a plane wave launched at an arbitrary angle of incidence to the slab, with a vertical polarization. The plasma is cold, weakly ionized, steady-state, nonuniform, and collisional. A parabolic plasma density profile is assumed across the slab thickness. The background magnetic field is uniform and parallel to the surface. This geometry approximates a cylindrical plasma column used in an ongoing experimental investigation. In this experiment the plasma column is generated by a classical Penning discharge [5]. The density profile in this configuration could be parabolic or hollow, depending on the design of the electrodes. Fig. 1 shows a cross section of the plasma with the experimental setup used to measure the power attenuation. The plasma is modeled as a series of two-dimensional partial slabs with the wave being absorbed in each slab and reflected at each slab boundary [9]–[15]. This model is acceptable as a first approximation under the assumption that the plasma properties
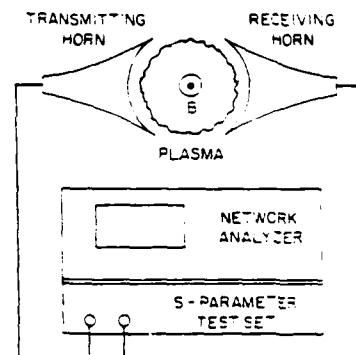
vary slowly along the wave propagation path [16]. The partial reflection coefficients at each slab boundary are computed along with the total power reflected out of the plasma. The total absorbed and transmitted powers are also computed. The dependence of the reflected, absorbed, and transmitted power on the plasma number density, the collision frequency, and the angle of propagation is investigated.

II. POWER CALCULATION

A plane wave with oscillatory field having a time dependence $e^{j\omega t}$, propagating in a lossy medium, such as a plasma, obeys the following Maxwell's equations

$$\nabla \times E = -j\omega\mu_r\mu_o H, \tag{1}$$

$$\nabla \times H = (\sigma + j\omega\epsilon_r\epsilon_o)E \tag{2}$$

where $J = \sigma E$ is used. Defining the complex dielectric constant as

$$\tilde{\epsilon}_r = \epsilon_r - j\frac{\sigma}{\omega\epsilon_o}. \tag{3}$$

Equation (2) can be written as

$$\nabla \times H = j\omega\tilde{\epsilon}_r\epsilon_o E. \tag{4}$$

The resulting wave equation is

$$\nabla^2 E = \frac{\mu_r\tilde{\epsilon}_r}{c^2}\frac{\partial^2 E}{\partial_t^2} \tag{5}$$

where c is the speed of light. A plane wave propagating in the x-direction with a phase dependence $\exp(j\omega t - \tilde{\gamma}x)$ is a

solution to (5). $\tilde{\gamma}$ is the complex propagation constant given by

$$\tilde{\gamma}^2 = -\mu_r \tilde{\epsilon}_r \frac{\omega^2}{c^2} \qquad (6)$$

or

$$\tilde{\gamma} = j\frac{\omega}{c}(\mu_r \tilde{\epsilon}_r)^{1/2}. \qquad (7)$$

$\tilde{\gamma}$ is generally expressed as [16]

$$\tilde{\gamma} = \alpha + j\beta \qquad (8)$$

where α is the attenuation coefficient and β is the phase coefficient. The complex refractive index is expressed in terms of $\tilde{\gamma}$ or in terms of $\tilde{\epsilon}_r$ as follows /belowdisplayskip16pt

$$\tilde{\mu} = -j\tilde{\gamma}\frac{c}{\omega} \qquad (9)$$

$$\tilde{\mu} = (\mu_r \tilde{\epsilon}_r)^{1/2}. \qquad (10)$$

The complex dielectric constant $\tilde{\epsilon}_r$ for a plane wave propagating through a cold plasma at an arbitrary angle of incidence was derived by Appleton [16]. $\tilde{\epsilon}_r$ is given by (11) below where $\omega_p, \Omega, \nu, \theta$ are, respectively, the plasma frequency, the gyrofrequency, the effective collision frequency, and the angle of propagation with respect to the static background magnetic field. The $-$ sign is for a right-hand polarization, and the $+$ sign is for a left-hand polarization. The expression of $\tilde{\epsilon}_r$ has a resonant behavior around the electron cyclotron frequency. Consequently, the attenuation of a wave propagating through a cold plasma is maximum around the cyclotron frequency [5], [7], [8], and [16].

In this section Appleton's result is used in the calculation of the amount of reflection, absorption, and transmission of a plane wave by a stratified plasma slab, the total thickness of which is equal to the diameter of a cylindrical plasma column used for experimental comparison. This plasma column is considered to have 12 cm in width, with a parabolic density profile and a maximum at the center (see Fig. 2). The incident wave travels at an angle of incidence θ_i and crosses the plasma at an angle θ with respect to the axial magnetic field.

The plasma column is modeled as 12 adjacent, homogeneous, and two-dimensional plasma slabs, 1 cm wide. The first 6 layers are of increasing density, and the 6 remaining layers are of decreasing density, and they approximate a parabolic distribution. The wave travels from one slab to the other with a reflection at each interface (see Figs. 3 and 4). Only 3 of the 12 layers are shown in Fig. 3. The
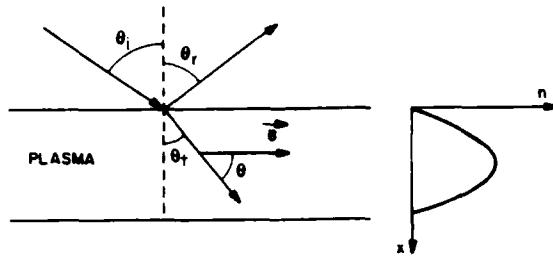

Fig. 2. Microwaves incident on a nonuniform plasma.
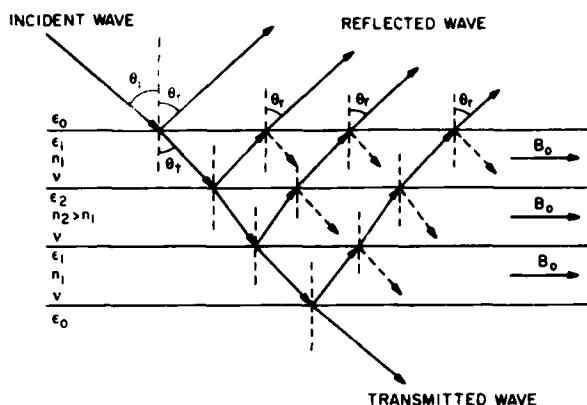
Fig. 3. Reflection and refraction from successive plasma slabs, $n_2 > n_1$.

choice of 12 slabs is motivated by experimental considerations: Experimentally, the number density profile is measured by introducing a Langmuir probe at 12 radial positions. The measured number density is then used as input in our model and a direct comparison between experiment and computation is performed [8]. The complex dielectric function is calculated for each slab and the reflection coefficient at each interface is deduced. The total transmitted, reflected, and absorbed powers are then computed. The total reflected power is computed neglecting multiple reflections between slab interfaces.

The reflection coefficient of a wave traveling from a slab located at X_i with a complex dielectric constant $\tilde{\epsilon}_r(\omega, X_i)$ to a slab located at X_{i+1} with a complex dielectric constant $\tilde{\epsilon}_r(\omega, X_{i+1})$ is calculated from the condition of continuity of the wave impedance at the boundary [17]–[19]. For a vertical

$$\tilde{\epsilon}_r = \tilde{\mu}^2 = 1 - \frac{\dfrac{\omega_p^2}{\omega^2}}{\left[1 - j\dfrac{\nu}{\omega} - \dfrac{\dfrac{\Omega^2}{\omega^2}\sin^2\theta}{2\left(1 - \dfrac{\omega_p^2}{\omega^2} - j\dfrac{\nu}{\omega}\right)}\right] \pm \left[\dfrac{\dfrac{\Omega^4}{\omega^4}\sin^4\theta}{4\left(1 - \dfrac{\omega_p^2}{\omega^2} - j\dfrac{\nu}{\omega}\right)^2} + \dfrac{\Omega^2}{\omega^2}\cdot\cos^2\theta\right]^{1/2}} \qquad (11)$$

$$\frac{\sin \theta_i}{\sin \theta_T} = \left(\frac{\epsilon(\omega, x_{i+1})}{\epsilon(\omega, x_i)} \right)^{1/2}$$
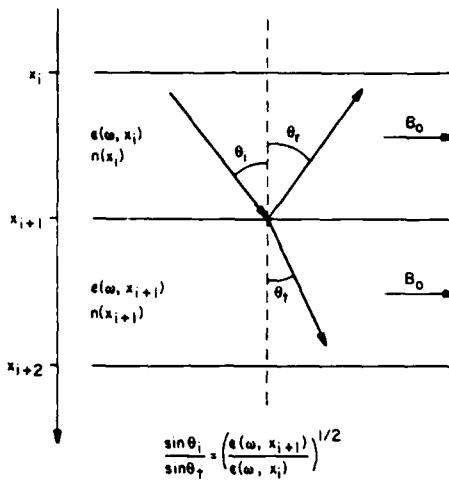
Fig. 4. Reflection and refraction of a wave by two adjacent slabs.

extraordinary mode polarization, the reflection coefficient is found to be

$$\Gamma(\omega, X_{i+1}) =$$

$$\frac{\dfrac{\tilde{\epsilon}_r(\omega, X_{i+1})}{\tilde{\epsilon}_r(\omega, X_i)} \cos \theta_i - \left(\dfrac{\tilde{\epsilon}_r(\omega, X_{i+1})}{\tilde{\epsilon}_r(\omega, X_i)} - \sin^2 \theta_i \right)^{1/2}}{\dfrac{\tilde{\epsilon}_r(\omega, X_{i+1})}{\tilde{\epsilon}_r(\omega, X_i)} \cos \theta_i + \left(\dfrac{\tilde{\epsilon}_r(\omega, X_{i+1})}{\tilde{\epsilon}_r(\omega, X_i)} - \sin^2 \theta_i \right)^{1/2}}. \quad (12)$$

Equation (12) represents Fresnel's formula in the plane of incidence. The total reflection coefficient, $\Gamma_T(\omega)$, is given by the sum of the partial reflection coefficients at each boundary, weighed by their respective attenuation factors. This attenuation is due to the damping of the wave as it travels through the plasma slabs. The wave damping represents a power absorption in the plasma. Thus $\Gamma_T(\omega)$ is given %

$$\Gamma_T(\omega) = \sum_{i=1}^{12} \Gamma(\omega, Xi)(q(\omega, X_i))^2 \quad (13)$$

where $q(\omega, X_i)$ is

$$q(\omega, X_i) = 1 - \exp \left(-\alpha(\omega, X_i) \cdot \frac{X_i}{\sin \theta} \right). \quad (14)$$

$\alpha(\omega, X_i)$ is the attenuation coefficient at the location X_i. The square of $q(\omega, X_i)$ is used because the wave has to travel twice the distance between the plasma surface and the slabs' interfaces before it is reflected back out of the plasma. The total reflected power is given by

$$P_R = P_{inc} |\Gamma_T(\omega)|^2 \quad (15)$$

or

$$\frac{P_R}{P_{inc}} = |\Gamma_T(\omega)|^2. \quad (16)$$

The total transmitted power is calculated by first computing the attenuation coefficient α_i of each slab, and then by
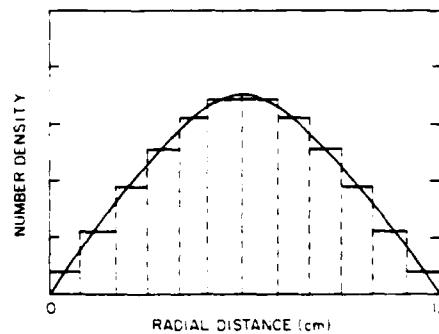

Fig. 5. Approximate parabolic density profile.

multiplying together the attenuation factors due to each slab. The attenuation factor contributed by slab i is given by

$$F_i = e^{-\alpha_i \cdot d / \sin \theta} \quad (17)$$

where α_i and d are, respectively, the attenuation coefficient of slab i and the slab width. The total attenuation factor is thus

$$F_T = \prod_i F_i. \quad (18)$$

The transmitted power P_{tr} is equal to the incident power P_{inc} multiplied by the total attenuation factor. The total absorbed power P_{abs} can then be deduced by subtracting the sum of the total reflected power P_r and the total transmitted power from the incident power

$$P_{abs} = P_{inc} - P_r - P_{tr}. \quad (19)$$

III. NUMERICAL RESULTS

In this section, the computer simulation results are presented and discussed. The reflected, absorbed, and transmitted power calculations for the plasma model described in Section II are presented, and their dependence on plasma parameters is investigated.

To calculate the total reflected power, the plasma is divided into 12 slabs with sharp boundaries separating them. The number density is constant in each slab, but the overall density profile follows a parabolic curve. This is illustrated in Fig. 5. Fig. 6 shows the steps taken in the calculation of the reflected power. First, the distance step size, the frequency range and step size, the magnetic field, the collision frequency, the angle of propagation, and the density profile function, $f(x_i)$, are entered. Once this is done, the program calculates the number density and the dielectric constant of each slab. Then, the partial reflection coefficients at each slab interface, $\Gamma(\omega, x_i)$, are determined. Finally, the total power reflected by the plasma is deduced. The results are presented as plots of the ratio of the reflected power by the incident power, against wave frequency in the vicinity of the upper hybrid frequency. The Y-axis is a semilogarithmic scale with a maximum of 1 (all incident power is reflected).

The transmitted power and the absorbed power are computed as explained in Section II. The absorption results are presented as plots of the ratio of the absorbed power by the incident power against wave frequency. The transmission results
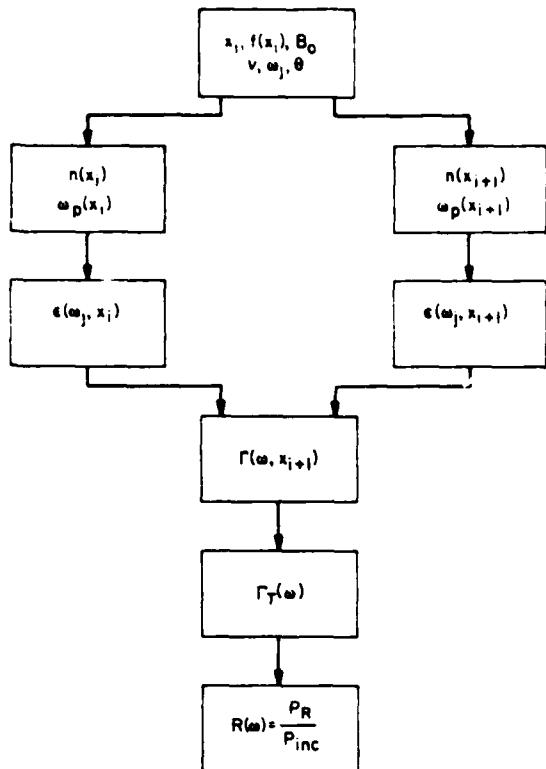
Fig. 6. Block diagram showing the main steps in the calculation of the reflected power.

Fig. 7. Reflected power per unit incident power versus wave frequency, $\theta = 60°$; $\Omega = 4$ GHz; $N_o = 10^{15} \, m^{-3}$: (1) $\nu = 20$ MHz, (2) $\nu = 10$ MHz, (3) $\nu = 5$ MHz.

Fig. 8. Reflected power per unit incident power versus wave frequency, $\theta = 60°$; $\Omega = 4$ GHz; $\nu = 20$ MHz: (1) $N_o = 10^{15} \, m^{-3}$, (2) $N_o = 5 \cdot 10^{15} \, m^{-3}$, (3) $N_o = 10^{16} \, m^{-3}$.

are presented as plots of the transmitted power, normalized with respect to the incident power, against wave frequency.

In the following discussion the choice of the values of the plasma parameters is based on the availability of numerous measurements taken on our experimental setup. A direct comparison between experiment and simulation allowed us to test the validity of our model [8]. The magnetic field is assumed constant throughout the plasma with a value of $B = 0.143$ T. This corresponds to a resonance near 4 GHz. The angle of propagation is arbitrarily chosen equal to 60°. The plasma number density is chosen in the $10^{15} \, m^{-3}$ range which is typical of our experimental plasma. Fig. 7 shows the reflected power fraction versus frequency for a center density of $N_o = 10^{15} \, m^{-3}$ and for three values of the collision frequency, $\nu = 20$ MHz, 10 MHz, and 5 MHz. Experimentally, these collision frequencies are achieved by a careful adjustment of the background pressure and the anode voltage of the penning discharge. Various pressure and voltage ranges are possible. In [5] a pressure range from 600 to 800 μtorr was used. The corresponding anode voltage range was from 900 to 1300 V.

From Fig. 7 it is seen that the peak reflected power decreases for increasing collision frequency. Fig. 8 shows the reflected power fraction versus frequency for a collision frequency of 20 MHz and three values of the center number density, $N_o = 10^{15} \, m^{-3}, 5 \times 10^{15} \, m^{-3}$, and $10^{16} \, m^{-3}$. It is clear that the reflected power greatly increases with increasing number density. It can be concluded that a low density but highly collisional plasma greatly reduces the amount of reflection. The two requirements, namely, low density and high
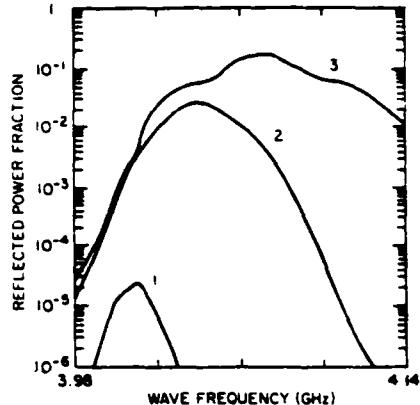
collision frequency, seem hard to achieve simultaneously. The weakly ionized but turbulent plasma generated by Penning discharges achieve such conditions [20]. Binary collisions are not dominant in the plasmas, but rather effective collisions which transfer momentum between the turbulent waves and the particles [16],[20],[21]. Experimental results taken on such a plasma will be published elsewhere.

Fig. 9 shows the absorbed power fraction versus frequency for a center number density $N_o = 10^{15} \, m^{-3}$ and for three values of the collision frequency, $\nu = 20$ MHz, 10 MHz, and 5 MHz. It is seen that the peak absorbed power decreases with increasing collision frequency. This is a counter intuitive result. Physically, this can be explained on the basis that for infrequent collisions, the particles spiral out to large gyroradii where they fall through a large potential difference, and therefore absorb more energy from the wave [5]. This can also be seen by the approximate solution of (11) for $\omega \Omega$, and for the simple case where $\theta = 90°$. For $\omega \sim \Omega$ and $\theta = 90°$ (11) becomes

$$\bar{\epsilon}_r = 1 - \frac{\omega_p^2}{\Omega^2 - j\nu\Omega - \dfrac{\Omega^2}{1 - \dfrac{\omega_p^2}{\Omega^2} - j\dfrac{\nu}{\Omega}}}. \qquad (20)$$

For $\omega_p/\Omega \ll 1$ and $\nu/\Omega \ll 1$, (20) can be expressed as

$$\tilde{\epsilon}_r = 1 - j\frac{\omega_p^2}{\nu\Omega}. \tag{21}$$

The propagation constant $\tilde{\gamma}$ is given by (7) and (8) as

$$\tilde{\gamma} = j\frac{\omega}{c}\sqrt{\tilde{\epsilon}_r} \tag{7}$$

and

$$\tilde{\gamma} = \alpha + j\beta \tag{8}$$

where α is the attenuation coefficient. For $\omega \cdot \Omega$ and by using (7) and (8), α is given by

$$\alpha = -\frac{\Omega}{c}\mathrm{Im}\left(\sqrt{\tilde{\epsilon}_r}\right) \tag{22}$$

where Im stands for imaginary part. $\tilde{\epsilon}_r$ can be expressed as

$$\tilde{\epsilon}_r = |\tilde{\epsilon}_r|e^{j\phi} \tag{23}$$

where $|\tilde{\epsilon}_r|$ represents the module of $\tilde{\epsilon}_r$, and ϕ represents its argument, given by

$$|\tilde{\epsilon}_r| = \left(1 + \frac{\omega_p^4}{\nu^2\Omega^2}\right)^{1/2} \tag{24}$$

and

$$\phi = \mathrm{Arc}\tan\left(\frac{-\omega_p^2}{\Omega\nu}\right). \tag{25}$$

The square root of $\tilde{\epsilon}_r$ is given by %

$$\sqrt{\tilde{\epsilon}_r} = |\tilde{\epsilon}_r|^{1/2}e^{j\phi/2}. \tag{26}$$

The imaginary part of $\sqrt{\tilde{\epsilon}_r}$ is given by %

$$\mathrm{Im}\left(\sqrt{\tilde{\epsilon}_r}\right) = \left(1 + \frac{\omega_p^4}{\nu^2\Omega^2}\right)^{1/4}\sin\left(\frac{\phi}{2}\right). \tag{27}$$

Thus, the attenuation coefficient α is given by

$$\alpha = -\frac{\Omega}{c}\left(1 + \frac{\omega_p^4}{\nu^2\Omega^2}\right)^{1/4}\sin\left(\frac{\phi}{2}\right). \tag{28}$$

Equation (28) shows that α is a decreasing function of the collision frequency and an increasing function of the number density. Fig. 10 shows the absorbed power fraction versus frequency for a collision frequency $\nu = 20$ MHz, and for three values of center number density $N_o = 10^{15}\,\mathrm{m}^{-3}, 5 \times 10^{15}\,\mathrm{m}^{-3}$, and $10^{16}\,\mathrm{m}^{-3}$. It is clearly seen that the amount of absorbed power increases with number density. This increase eventually reaches a saturation value since for high number
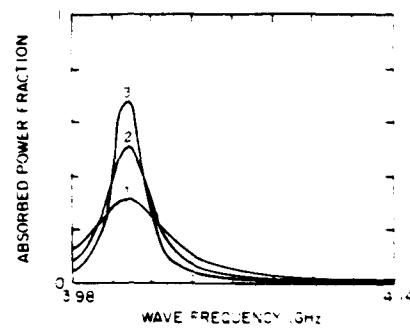

Fig. 9. Absorbed power per unit incident power versus wave frequency. $\theta = 60°; \Omega = 4$ GHz; $N_o = 10^{15}\,\mathrm{m}^{-3}$; (1) $\nu = 20$ MHz, (2) $\nu = 10$ MHz. (3) $\nu = 5$ MHz.
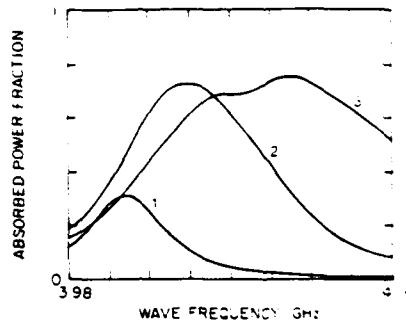

Fig. 10. Absorbed power per unit incident power versus wave frequency. $\theta = 60°; \Omega = 4$ GHz; $\nu = 20$ MHz; (1)$N_o = 10^{15}\,\mathrm{m}^{-3}$. (2) $N_o = 5 \cdot 10^{15}\,\mathrm{m}^{-3}$. (3) $N_o = 10^{16}\,\mathrm{m}^{-3}$.
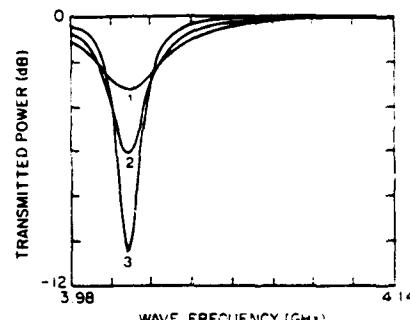

Fig. 11. Transmitted power versus wave frequency, $\theta = 60°; \Omega = 4$ GHz; $N_o = 10^{15}\,\mathrm{m}^{-3}$; (1)$\nu = 20$ MHz, (2) $\nu = 10$ MHz, (3) $\nu = 5$ MHz.

densities more collisions occur, which tends to decrease the amount of absorbed power.

The previously reached results can be seen on the transmitted power versus frequency graphs. Fig. 11 shows the transmitted power normalized with respect to the incident power versus frequency for a center number density $N_o = 10^{15}\,\mathrm{m}^{-3}$, and for three values of the collision frequency $\nu = 20$ MHz, 10 MHz, and 5 MHz. The peak transmitted power greatly increases with increasing collision frequency. Fig. 12 which represents the transmitted power versus frequency for a collision frequency $\nu = 20$ MHz, and three values of the center number density $N_o = 10^{15}\,\mathrm{m}^{-3}, 5 \times 10^{15}\,\mathrm{m}^{-3}$, and $10^{16}\,\mathrm{m}^{-3}$, shows that the transmitted power greatly decreases with increasing number density.
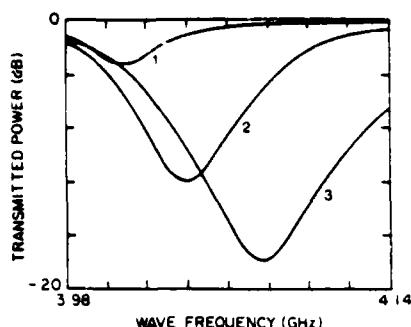
Fig. 12. Transmitted power versus wave frequency, $\theta = 60°; \Omega = 4$ GHz; $\nu = 20$ MHz: (1) $N_o = 10^{15} \, m^{-3}$, (2) $N_o = 5 10^{15} \, m^{-3}$, (3) $N_o = 10^{16} \, m^{-3}$.
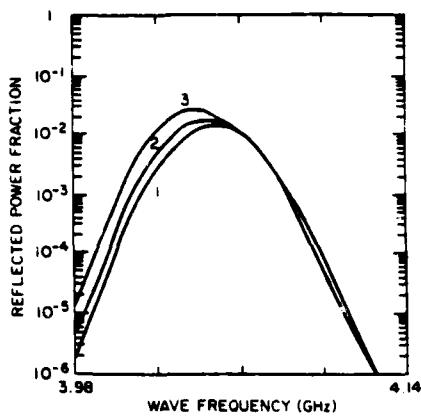

Fig. 13. Reflected power per unit incident power versus wave frequency, $\Omega = 4$ GHz; $N_o = 5 \cdot 10^{15} \, m^{-3}; \nu = 20$ MHz: (1) $\{\theta = 90°, (2)\theta = 72°, (3)\theta = 60°$.
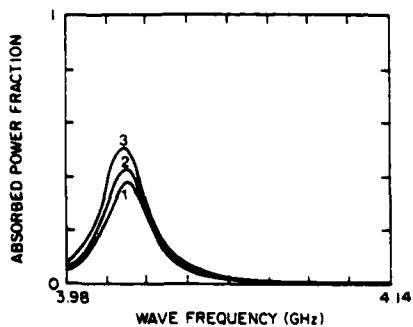

Fig. 14. Absorbed power per unit incident power versus wave frequency, $\Omega = 4$ GHz; $N_o = 10^{15} \, m^{-3}; \nu = 10$ MHz: (1) $\theta = 90°, (2)\theta = 72°, (3)\theta = 60°$.

Figs. 13, 14, and 15 show, respectively, the reflected power fraction, absorbed power fraction, and normalized transmitted power versus frequency for three values of the propagation angle with respect to the background static magnetic field, θ. It is seen that for smaller θ we get more reflection, more absorption and consequently less transmission.

IV. CONCLUSION

This study of the reflection, absorption, and transmission of microwaves by a nonuniform magnetized plasma has led to several important results. We showed the effects of two key plasma parameters, namely the number density and the collision frequency. It is found that a low density but collisional plasma is less reflective of microwaves. On the other
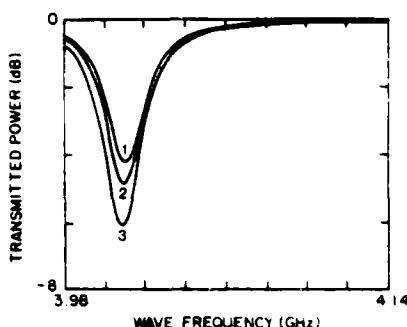

Fig. 15. Transmitted power versus wave frequency, $\Omega = 4$ GHz; $N_o = 10^{15}$ $m^{-3}; \nu = 10$ MHz; (1) $\theta = 90°, (2)\theta = 72°, (3)\theta = 60°$.=S

hand, a high density but less collisional plasma greatly reflects and absorbs microwaves. These results show that in practice a magnetized plasma could be tailored to act either as a reflector or absorber of microwave radiation. Enhanced reflection and absorption has direct applications in communications [22].

REFERENCES

[1] R. J. Vidmar, "On the use of atmospheric plasmas as electromagnetic reflectors and absorbers," *IEEE Trans. Plasma Sci.*, vol. 18, pp. 733–741, 1990.
[2] J. Santoru, D. J. Gregoire, and R. W. Schumacher, "Electromagnetic wave absorption in unmagnetized plasmas," *Bulletin of the Amer. Physical Soc.*, vol. 35, no. 9, p. 2067, 1990.
[3] A. Y. Ho and S. P. Kuo, "Scattering and broadband absorption of microwaves by an arc plasma column," *Bulletin of the Amer. Physical Soc.*, vol. 35, no. 9, p. 2067, 1990.
[4] O. C. Eldridge, J. E. Scharer, M. H. Bettenhausen, N. T. Lam, and S. F. Chang, "Experiments and Analysis of Wave Absorption, Reflection and Scattering in Plasmas," *Bulletin of the Amer. Physical Soc.*, vol. 35, no. 9, p. 2067, 1990.
[5] L. H. Combs, C. Liu, and J. R. Roth, "Studies of microwave absorption by a plasma near the electron cyclotron frequency," *Bulletin of the Amer. Physical Soc.*, vol. 35, no. 9, p. 2068, 1990.
[6] W. W. Destler, J. E. Degrange, H. H. Fleischmann, J. Rodgers, and Z. Segalov, "Experimental studies of high power microwave reflection, transmission, and absorption from a plasma-covered plane boundary," *J. Appl. Phys.*, vol. 69, no. 9, pp. 6313–6318, 1991.
[7] M. Laroussi and J. Reece Roth, "Reflection of electromagnetic radiation from a nonuniform plasma slab at an arbitrary angle of incidence," in*Proc. of the 1991 IEEE Int. Conf. on Plasma Sci.*, Williamsburg, VA, CAT#91 CH3037-9, p. 146, 1991.
[8] M. Laroussi, C. Liu, and J. Reece Roth, "Absorption and reflection of microwaves by a nonuniform plasma near the electron cyclotron frequency," *Proc. 9th APS Topic. Conf. Radio Freq. Power in Plasma*, Charleston, SC, 1991, pp. 37–45.
[9] J. R. Wait, *Electromagnet. and Plasmas.* New York: Holt, Rinehart, and Winston, 1968.
[10] F. A. Albini and R. G. Jahn, "Reflection and transmission of electromagnetic waves at electron density gradients," *J. Appl. Phys.*, vol. 32, no. 1, pp. 75–82, 1961.
[11] W. P. Allis, S. J. Buchsbaun, and A. Bers, *Waves in Anisotropic Plasmas.* Cambridge, MA: MIT Press, 1963.
[12] V. L. Ginzburg, *Propagat. Electromagnet. Waves in Plasma* New York: Gordon Breach, 1961.
[13] J. R. Wait and L. C. Walters, "Reflection of electromagnetic waves from a lossy magnetoplasma," *Radio Sci. J. Res.*, vol. 68D, no. 1, pp. 95–101, 1964.
[14] G. H. Price, "Propagation of electromagnetic waves through a continuously varying stratified anisotropic medium," *Radio Sci. J. Res.*, vol. 68D, no. 4, pp. 407–418, 1964.
[15] J. R. Wait, *Electromagnetic Waves in Stratified Media.* New York: Pergamon, 1962.

[16] M. A. Heald and C. B. Wharton, *Plasma Diagnostics with Microwaves.* New York: Krieger, 1978, pp. 71–94.
[17] S. Y. Liao, *Microwave Devices and Circuits.* Englewood Cliffs, NJ: Prentice-Hall, 1980.
[18] R. E. Collin, *Foundations for Microwave Engineering.* New York: McGraw-Hill, 1966.
[19] E. C. Jordan, *Electromagnetic Waves and Radiating Systems.* Englewood Cliffs, NJ: Prentice-Hall, 1950.
[20] M. Laroussi, Ph.D. dissertation, University of Tennessee, Knoxville, 1988, pp. 163–171.
[21] A. A. Galeev and R. Z. Sagadeev, *Basic Plasma Physics II,* M. N. Rosenbluth and R. Z. Sagadeev, Eds. Amsterdam: North Holland, 1984, pp. 271–274 and pp. 284–286.
[22] J. Reece Roth, *Microwave Absorption System,* U. S. Patent Number 4 989 006, Jan. 29, 1991.

Mounir Laroussi (S'84–M'86) was born in Sfax, Tunisia, on August 9, 1955. He received the B.S. degree from the Faculty of Technical Sciences of Sfax, Tunisia, the M.S. degree from the School of Electricity and Radio of Bordeaux, France, and the Ph.D. degree from the University of Tennessee, Knoxville, in June 1988, all in electrical engineering.

He worked as an Assistant and Associate Professor at the School of Engineering of Sfax, from 1988 to 1990. He then joined the Plasma Science Laboratory of the University of Tennessee. He is currently working in the field of plasma cloaking, plasma ion implantation, and on microwaves interaction with plasmas.

Dr. Laroussi is a member of Sigma Xi.

J. Reece Roth (SM'81–F'91) received the B.S. degree in physics from M.I.T., Cambridge, in 1959 and the Ph.D. degree in engineering physics from Cornell University, Ithica, NY, in 1963.

He joined the NASA Lewis Research Center in Cleveland, OH, in 1963, where he was principal Investigator of the Lewis Electric Field Bumpy Torus Project until 1978. He is presently Professor of Electrical Engineering at the University of Tennessee, Knoxville. His current work at the UTK Plasma Science Laboratory is devoted to magnetized plasma cloaking and industrial plasma engineering, including corrosion inhibition by plasma ion implantation. In the past 25 years, he has authored or co-authored more than 120 archival publicat... ns.

Dr. Roth is an Associate Fellow of the American Institute of Aeronautics and Astronautics, a Life Member of the AAAS and Sigma Xi, and a member of the IEEE Nuclear and Plasma Sciences Society, the American Physical Society, and the American Nuclear Society. In the IEEE, he was a member of the original organizing committee which set up the Nuclear and Plasma Sciences Society, and was chairman of the committees which wrote the constitution and bylaws for both the NPSS and the Plasma Science and Applications Committee of the NPSS. He served on the Excom of the PSAC from its founding until 1977, and for additional terms from 1980 to 1982, 1985 to 1987, and 1990 to 1992. He also served previously as an Elected Member-at-Large of the NPSS AdCom from 1974 to 1977. He served as Secretary of AdCom in 1975. In addition, he was an Associate Editor of the TRANSACTIONS ON PLASMA SCIENCE from its initiation in 1973 to December 1984, and served as Chairman (1984–1985), and in other offices of the East Tennessee Section of the IEEE, and as General Chairman of the IEEE Southeastcon'88.

BALL LIGHTNING: WHAT NATURE IS TRYING TO TELL THE PLASMA RESEARCH COMMUNITY

J. Reece Roth, Fellow, IEEE
UTK Plasma Science Laboratory
Department of Electrical and Computer Engineering
University of Tennessee
Knoxville, Tennessee 37996-2100

ABSTRACT

Ball lightning has been extensively observed in atmospheric air, usually in association with thunderstorms, by untrained observers who were not in a position to make careful observations. These chance sightings have been documented by polling observers, who constitute perhaps five percent of the adult U.S. population. Unfortunately ball lightning is not accessible to scientific analysis, because it cannot be reproduced in the laboratory under controlled conditions. Natural ball lightning has been observed to last longer than 90 seconds, and to have diameters from one centimeter to several meters. The energy density of a few lightning balls has been observed to be as high as 20,000 joules per cubic centimeter, well above the limit of chemical energy storage of, for example, TNT at 2000 joules per cubic centimeter. Such observations suggest a plasma-related phenomenon with significant magnetic energy storage. If this is the case, ball lightning should have very interesting implications for fusion research, industrial plasma engineering, and military applications, as well as being of great theoretical and practical interest to the plasma research community.

INTRODUCTION

In the closing years of the 20th Century, there remain very few natural phenomena on the human scale which remain inaccessible to scientific analysis. Ball lightning is such a

phenomenon. Although the existence of ball lightning has been generally acknowledged by the scientific community since the death of Richmann, who was killed by ball lightning in the summer of 1753 in St. Petersberg, Russia during an attempt to extend Benjamin Franklin's kite experiment, no one has yet been able to reproducibily create ball lightning in the laboratory. As a result, the scientific study of ball lightning under controlled, reproducible conditions has not been possible.

Ball lightning is defined as a glowing, self-luminous sphere moving slowly or floating in the atmosphere, and is usually associated with lightning strokes or thunderstorm activity. Ball lightning is much more rare than a lightning stroke, and its occurrence at random times and places has made its scientific study very difficult. In the United States, ball lightning has been observed by approximately 5% of the adult U.S. population at some time in their lives. What is now known about the characteristics of ball lightning is the product of a large body of random observations by untrained observers, many of whom were participants in a frightening experience. This data base is useful, however, because it provides important constraints on theoretical models of ball lightning.

Perhaps because the phenomenon of ball lightning is a scientific mystery, the literature of ball lightning is voluminous. Ball lightning has been placed in the context of ordinary atmospheric electrical and lightning discharges by Uman (ref. 1) and by Golde (ref. 2). Two additional books, entirely on the subject of ball lightning, have been written by Singer (ref. 3) and by Barry (ref. 4). These latter two books contain some of the better documented sightings of ball lightning, summarize information on its characteristics, discuss inconclusively various theoretical models for ball lightning, and report attempts to reproduce ball lightning artifically under controlled conditions.

The characteristic observation of ball lightning occurs approximately 80% of the time after a lightning stroke or during a thunderstorm. The lightning ball can be from a centimeter to 1.5 meters in diameter; almost all colors of the visible spectrum have been

reported; their durations have been from a few seconds to longer than 150 seconds; they appear to have neutral buoyancy, and either sink very slowly to the ground, or float above the ground at a constant height; they rarely make noise until they suddenly disappear, with a noise that ranges from a barely audible popping sound, to a major explosion. An ozone-like or sulfurous odor is sometimes associated with ball lightning, and when they terminate, their behavior ranges from simply winking out of existence, to a major explosion which can do more damage than a hand grenade. In those cases in which lightning balls have come in contact with human observers, the results range from a barely perceptible tingling sensation, through stunning, to death.

Attempts have been made to obtain quantitative information about ball lightning by detailed polling of adult members of the public who have seen ball lightning at some time in their lives. Typically, such a poll will consist of a first round in which the staff of a major national laboratory or other institution will be asked whether they have ever seen ball lightning. Those who reply affirmatively are asked to fill out a more detailed questionnaire, designed to elicit every type of qualitative or quantitative information which might be available from an untrained observer without scientific instruments. The results of several of these polls are cited in refs. 3 and 4. During the 1960's, surveys of the staff at two national laboratories in the United States provided a large database of ball lightning observations. At the Oak Ridge National Laboratory, in Oak Ridge, Tennessee, J. R. McNally, Jr. circulated questionnaires to 15,923 staff members, which elicited 498 reports of ball lightning observations (ref. 5). Also in the 1960's, W. D. Rayle surveyed 4,400 staff members at the NASA Lewis Research Center in Cleveland, Ohio, and obtained 180 reports of ball lightning observations (ref. 6).

Attempts have been made for at least a century to create ball lightning in the laboratory. Barry (ref. 4) describes an experiment conducted Cira 1910 in Norway which involved shorting the terminals of a 10 MW DC generator, which produced long-lived,

free-floating electrical discharges which were photographed and had characteristics similar to those of ball lightning. In references 3 and 4 it is reported that many observations of a ball lightning phenomenon were made in World War II submarines. In these submarines, switching an inductive load (an electric motor which drove the propellers) connected to a large battery bank, which typically involved 200 VDC and currents of 15,000 amperes, produced electrical arcs in the switchgear that occasionally generated small luminous spheres a few centimeters in diameter. The properties of these spheres were indistinguishable from those of ball lightning. Such ball lightning also was generated in experiments at the Philadelphia Naval Shipyard. More recently, Alexeff and Rader (ref. 7) have reported looped electrical sparks in the Holifield National Accelerator at the Oak Ridge National Laboratory, which may be a predecessor to the formation of a ball lightning-like electrical discharge. In none of these experiments on ball lightning-like phenomena were quantitative observations made, beyond attempts at photography.

In relatively recent experiments involving RF excitation, Powell and Finkelstein (see ref. 3 and 4) were able to generate a glowing, steady-state ball of plasma at, or slightly below atmospheric pressure in laboratory experiments, but only with steady-state RF energy input. More recently, Ohtsuki and Ofuruton (ref. 8) have reported the generation of plasma fireballs formed by microwave interference in air. The frequency was 2.45 GHz, at power levels from 1 to 5 kw. These microwave-generated fireballs at 1 atmosphere lasted several minutes, and were reported to have lasted from one to two seconds after the microwave power was turned off. These microwave generated atmospheric plasmas are hard to understand in terms of known dissociation processes in air, but the requirement for steady state RF energy input makes the relevence of these experiments to ball lightning unclear.

CHARACTERISTICS OF BALL LIGHTNING

In this section we review the properties of ball lightning as revealed by a large data base of observations documented in references 1 to 6, and in reference 9. In this section we also summarize material that has been used elsewhere in a different context (ref. 10).

Appearance of Ball Lightning - In approximately 80% of cases, ball lightning is observed after a lightning stroke or in association with thunderstorm activity. There apparently are no observations of the formation of lightning balls, which is unfortunate because such observations might provide important clues to the physical mechanisms of their formation and structure. Usually, ball lightning is observed singly, but there are isolated reports of three or more lightning balls being observed simultaneously. Ball lightning is sometimes seen to sink relatively slowly through the atmosphere before striking the ground, but most frequently it appears to float, descending very slowly toward the ground, or even suspended at a constant distance above the ground. Ball lightning is usually observed to be spherical, hence its name, but isolated instances of oval or spindle shapes have also been reported.

There appear to be very few if any reports of structure within ball lightning, most observers reporting simply a luminous, featureless, spherical ball. Ball lightning has been observed to have a wide range of luminosity, ranging from barely visible above ambient light levels, to being intensely and dazzlingly luminous. The colors reported have ranged across the entire visible spectrum, with some bright blue, and others yellow, orange, or red in color. Observers are usually unaware of any sound being emitted by ball lightning, although most observations are made at a significant distance from it. Several observers have reported the sudden termination of ball lightning. Sometimes this occurs with no visible effects, and silently, or with a barely audible popping sound. On other occasions, the disappearance of ball lightning is accompanied by a loud explosion.

Ball lightning has been observed to move against the prevailing wind, to follow electrical wires or electrical conductors, and sometimes to hover in one place for many seconds. A significant observation has been repeated independently by a number of observers, and is very difficult to reconcile with many ball lightning models. Ball lightning has moved toward a glass window, disappeared on one side, reappeared on the other side, and has continued on its way by moving away from the other side of the window. A related observation are the several occasions on which ball lightning has been observed moving down the aisle of a passenger airplane in flight, after the plane had been struck by lightning.

Diameter of Ball Lightning - A distribution function of ball lightning diameter, in centir..eters, is shown on Figure 1, taken from Singer (ref. 3). These data were provided by four surveys of large populations, each containing the number of cases indicated in the upper portion of the figure. These distributions start out with a very low frequency of occurrence at small diameters, rise through a maximum, and then decrease for large diameters. The fall-off of observations at small diameters is probably due to observer bias, since small objects are less likely to be noticed than large ones, particularly as the distance between the observer and ball lightning increases. These data indicate that the most probable diameters are somewhere between 15 and 50 centimeters, and diameters of a meter or more have been observed. Indeed, individual reports exist of ball lightning more than two meters in diameter.

When the cumulative distribution function of these data is plotted as a function of the ball lightning diameter, an interesting log-normal relationship emerges. Figure 2, taken from Rayle (ref. 6), shows that the cumulative distribution of ball lightning diameters observed in his and in the McNally surveys both have a log-normal distribution, with a median diameter of about 30 centimeters. The cumulative distribution of charge transferred by lightning strokes is also plotted on Figure 2. This also obeys a log-normal distribution,

but with a different slope, suggesting a different standard deviation and a different underlying physical mechanism. Here, the defects of observer bias apparently do not come into play until one gets below a diameter of 5 centimeters or so; at the high end, the data remain log-normal until ball lightning diameters of approximately 1.5 meters.

Ball Lightning Lifetime - The questionnaire distributed in connection with the major ball lightning surveys discussed in refs. 3 and 4 attempted to establish a lifetime for the ball lightning. These lifetime data were very likely to have been subject to observer bias, since ball lightning which existed for a few seconds or less hardly allowed time to identify the phenomenon as ball lightning, and was probably less likely to come to the attention of an observer in any case. In addition, most observers were frightned by the ball lightning, and this disturbed their normal ability to estimate elasped time accurately, and in many cases caused them to leave the scene before the ball lightning disappeared. On the ordinate of Figure 3, taken from Rayle (ref. 6), is plotted the cumulative distribution function of reports of ball lightning durations less than a given duration T, and on the abscissa is plotted the duration of the ball lightning in seconds. Data from both the McNally (ref. 5) and Rayle (ref. 6) database are plotted. The median duration, 0.5 on the ordinate, is about 3 to 5 seconds; in both surveys a few durations in excess of 36 seconds were observed. Some ball lightning has been observed to last for several minutes. These rel tively long lifetimes (by fusion confinement standards) are one of the most intriguing features of ball lightning, and motivated several of the surveys including those in references 5 and 6.

Ball Lightning Energy Content - The database of ball lightning observations has been carefully worked over in an attempt to determine the energy content of ball lightning. In some cases observers reported information on effects or damage resulting from the final disappearance or explosion of ball lightning. In a few cases, trained observers, including military munitions experts, were able to observe this damage at first

hand after the event, and to make more refined estimates of the amount of energy required to produce the observed damage. Such investigations are described by Singer and Barry (refs. 3 and 4). These investigations have shown that ball lightning may have a total energy content ranging from 0.01 joule, to values greater than 10 megajoules. The energy content of a hand grenade is approximately 1 megajoule, for comparison. A characteristic value for the energy content of ball lightning is approximately 10 to 100 joules. This energy content is dangerous, since it takes only about 1 joule of electrical energy to kill a human being. Indeed, there are several reports in the literature of individuals being injured or killed by ball lightning, including the classic case of Richmann.

Ball Lightning Energy Density - In about 13 cases, discussed by Barry (ref. 4), enough information was available to estimate not only the energy content of the ball lightning, but also its energy density. A log-normal cumulative probability distribution for these data are plotted in Figure 4, from Barry (ref. 4). These data fall along a straight line, indicating a log-normal distribution, with a median energy density of approximately 5 joules per cubic centimeter, and extreme values ranging from less than 10^{-3} joules per cubic centimeter, to values higher than 10^5 joules per cubic centimeter.

The very high value of the energy density at the upper end of the distribution is significant, both in its implications for fusion and military applications, and as a constraint on possible models for ball lightning. For example, fully ionized and dissociated atmospheric air would have an energy content of about 170 joules per cubic centimeter, far below the upper range of the data shown. The more energetic forms of ball lightning are therefore inconsistent with a model based on a ball of ionized plasma which recombines during the lifetime of the ball lightning. Energy densities in excess of 10^4 joules per cubic centimeter also appear to rule out a chemical origin for the more energetic forms of ball lightning. For example, the energy density of TNT, which has one of the highest energy contents of any solid explosive, is about 2000 joules per cubic centimeter, far below the

maximum observed for ball lightning. Almost the only energy storage mechanism for energy densities above 1000 joules per cubic centimeter is stored magnetic energy, probably an important clue to the physics of ball lightning.

Ball Lightning Mass Density - The mass density of ball lightning can be estimated from the fact that it usually appears to float above the surface of the earth at a constant height as though it were a bubble of hot gas, with neutral buoyancy. This characteristic suggests that the mass density of ball lightning is close to that of atmospheric air, about 1.3×10^{-3} grams per cubic centimeter.

Ball Lightning Kinetic Pressure - Ball lightning is observed to maintain an approximately constant diameter during its entire lifetime, thus suggesting a balance between the external atmospheric pressure, and the net kinetic pressure of the plasma/magnetic field configuration inside the ball lightning. Since the external pressure on ball lightning is 1 atmosphere, this places an upper bound on the net kinetic pressure inside the ball lightning of no more than 10^5 newtons per square meter.

The characteristics of ball lightning discussed above are summarized in Table 1. The low and high values reported in this Table are near the extreme wings of the observed distribution of properties; the characteristic values are the most probable or median values reported in the literature, such as references 2 to 6.

BALL LIGHTNING MODELS

The intriguing characteristics of ball lightning have elicited a wide variety of proposed models to explain the phenomenon. Here we divide ball lightning models into three principal groups: The older models of ball lightning formation, which are discussed in the books by Singer (ref. 3) and Barry (ref. 4); Fusion-related models, in which ball lightning has been identified with 1 or more successful magnetic containment configurations used in fusion research; and finally, the Koloc model, put forward by Paul

M. Koloc, which seems best to incorporate extensive ball lightning observations with physical processes familiar as part of the world-wide magnetic fusion program.

Older Ball Lightning Models

In this section we discuss some ball lightning models from the older literature on the subject.

Psychogenic Models - It is sometimes suggested, even in recent times, that ball lightning has no physical existence, and is psychogenic in origin, being the result of after-images of lightning strokes, reflections, optical illusions, hallucinations, or mass hysteria. This school of thought puts ball lightning in a class with aliens from outer space descending from unidentified flying objects, and the appearance of religious icons in the sky. The present consensus of ball lightning investigators is that these psychogenic explanations are inconsistent with a large body of observations, including many cases in which several observers saw the same phenomenon. Another factor inspiring confidence in the observations is the log-normal distribution functions which have emerged from large numbers of reported observations, such as those in Figures 2 and 4 above. It may be particularly significant that the log-normal distribution for ball lightning diameter in Figure 2 was observed at two different sites, at different times, in different parts of the United States, and that the same type of log-normal distribution function is also known to describe the physics of the total charge contained in lightning strokes.

Chemical Models - Chemical models for ball lightning are still taken very seriously, particularly in Japan (ref. 9). In these models, ball lightning is explained as the result of chemical reactions in the atmosphere, the origin of which might be chemically active species generated by a lightning stroke, or the ignition of gaseous fuels such as swamp gas or methane by atmospheric electricity. The chemical model is consistent with the significant minority of ball lightning observations that have been made in the absence of

thunderstorms or lightning strokes, and the relatively low energy density of many examples of ball lightning which can be explained by the energy provided by chemical reactions. However, the chemical model is inconsistent with a significant number of observations of extreme damage done by ball lightning, and the high energy densities at the upper end of the range shown in Figure 4. The chemical model of ball lightning has enough currency that some ball lightning investigators suggest that ball lightning may consist of two different types, one having a chemical origin, and the other not.

RF Energy Models - A third model for ball lightning formation originated in Russia, and is sometimes called the Kapitza model after its originator, the physicist Peter Kapitza. This model sees ball lightning as an atmospheric plasma generated by intense radio frequency power created by lightning strokes or atmospheric electricity. Indeed, the RF experiments of Powell and Finkelstein (see ref. 4) and the similar experiments of Ohtsuki and Ofuruton (ref. 8) have generated self-luminous plasma balls which resemble ball lightning in many respects. This RF-generated "ball lightning", however, requires a large continuous input of radio frequency power, and such steady state sources of RF energy are known to be inconsistent with the natural phenomenon, where radio frequency interference, for example, is rarely observed in association with ball lightning.

The Vortex Plasmoid - Finally, a model based on a self-contained magnetically confined plasma, the "vortex plasmoid", has been discussed by Singer (ref. 3) and is illustrated in Figure 5, taken from Reference 3. This model sees ball lightning as a luminous, self-contained toroidal plasma configuration having a large toroidal current ring, the magnetic field of which interacts with the earth's magnetic field. One difficulty with this model is that the observed motion of ball lightning appears to be independent of the local direction of the earth's magnetic field at the point of observation. This model has inspired more recent attempts to understand the physics of ball lightning, such as that Witalis (ref. 11), for example.

Fusion-Related Ball Lightning Models

Ball lightning differs from the plasmas used in magnetic fusion research in several significant ways. First, there is no analog in fusion research to the existence of a confined plasma at one atmosphere. Fusion experiments start out at a moderately good vacuum, and operate at pressures well below one torr. In fusion experiments, variation of the surrounding neutral background gas pressure has little effect on the equilibrium or stability of the plasma, beyond the possible introduction of impurities. Also in fusion research, there is no analog to the free-floating plasma bubble which is the characteristic feature of ball lightning. All magnetic fusion experiments at present are tied down to external confining magnetic field coils, even though in some fusion confinement configurations, such magnetic fields play relatively a minor role in confining the plasma.

Several dozen alternate magnetic containment configurations have been discussed in reference 12, and a few of these have characteristics which tempt one to draw an analogy to ball lightning, even though the most similar of the known magnetic containment configurations differ from ball lightning in the ways described in the previous paragraph. First is the Astron or Field Reversed Mirror, illustrated in Figure 6, in which a torus of plasma containing a large axisymmetric circulating current is confined in the midplane of a magnetic mirror geometry. The plasma current flows in a sense opposite to that in the coils which generate the mirror magnetic field, thereby generating a diamagnetic field, reducing the magnetic field on the axis. If one eliminated the external field coils, and allowed the torus of plasma to form an insulating blanket against the surrounding neutral gas, the result would look very similar to ball lightning. A field reversed, highly diamagnetic ring of plasma which can be moved from place to place and manipulated by guiding magnetic fields has been described recently by Sudan (ref. 13).

A similar fusion-related magnetic confinement geometry which resembles ball lightning is generated by the Field-Reversed Theta Pinch (ref. 12), which is illustrated in Figure 7. In this configuration, an elongated torus of plasma with large diamagnetic currents is confined by a magnetic mirror field generated by a theta pinch. The plasma configuration and magnetic field geometry look very similar to that of the Field Reversed Mirror, although they are arrived at by very different means. The Field Reversed Theta Pinch relies on transient means of plasma production, and is transient itself (see Ref. 14).

Finally, the Spheromak configuration (ref. 12) illustrated in Figure 8 probably resembles ball lightning more closely than any other fusion-related magnetic containment configuration, partly because of its efficient confinement by the self-generated magnetic field produced by currents inside the toroidal plasma, and partly because of the relatively weak external magnetic field necessary to stably restrain the Spheromak plasma. The Spheromaks also have a "separatrix", which separates the externally produced magnetic field from those generated by the current flowing in the toroidal plasma. The site of this separatrix would be a natural place to expect a gas blanket or mantle to form, if it were surrounded by dense neutral gas. Some interesting experimental observations on the current profiles and other characteristics of a Spheromak plasma have been reported by al-Karkhy, et al (ref. 15), and these provide a database against which eventual measurements on ball lightning might be compared. Some theoretical aspects of self-confined plasmas from an MHD point of view have been reported by Witalis (ref. 16).

All three of the fusion-related magnetic containment geometries discussed above are similar, consisting of a toroidal plasma with a large current, strong enough to generate a poloidal magnetic field which keeps the plasma contained. They all possess a separatrix, and require external magnetic field coils, the strength of which differs from one configuration to the next, to provide plasma equilibrium. In ball lightning, the pressure of the surrounding atmosphere may take the place of the magnetic pressure provided by the

external magnetic field required to stabilize these geometries. The theory of these three magnetic containment configurations will probably form a useful basis for understanding the physical processes in ball lightning, especially the fundamental work of Witalis (ref. 11, 16).

THE KOLOC MODEL FOR BALL LIGHTNING FORMATION

A recent model for ball lightning formation is due to P. M. Koloc (refs. 17, 18). Koloc's model is considerably more detailed than the older models, is better grounded in advances recently made in fusion research, and describes in detail the formation process as well as the ultimate ball lightning product. This model has resulted in a United States patent (ref. 19).

According to the Koloc model, the physical processes which produce ball lightning begin with a lightning stroke, and end with ball lightning after proceeding through a series of sequential steps listed in Table 2. In this model, the first step in the formation of ball lightning is the creation of a linear Z-pinch by the ionized channel associated with an ordinary lightning stroke, illustrated in Figure 9. The large currents in the plasma channel squeeze the plasma, due to the azimuthal field generated by the high axial current flowing in the lightning stroke. The plasma forms a Bennett-pinch like equilibrium (ref. 12), between the outward kinetic pressure of the plasma, and the inward force of the poloidal field. This balance is unstable, and will lead to the growth of kink and sausage instabilities. In the kink instability, illustrated in Figure 10, the initially axisymmetric cylindrical channel will tend to bend into a helical spiral, which looks much like a single strand of a multi-strand rope. It is this stage of the Koloc model that may have been observed in the high voltage sparks reported in reference 7. This unstable equilibrium worsens as a result of the poloidal magnetic field being stronger on the inside of the curved plasma than it is on the outside.

The Koloc model develops as the kink instability grows in a nonlinear manner, resulting in an extreme distortion of the cylindrical channel into a series of helical turns, looking like a helical spring, illustrated on Figure 11. The current in adjacent turns of the coil illustrated in Figure 11 flows in the same direction, and tend to attract each other, leading to collapse and the formation of a single torus, in the manner indicated in Figure 12. The result is a torus of plasma with a circulating current greater than that in the original lightning channel by a factor equal to the number of turns in the helix that formed it. After the torus forms, the main lightning channel can be pinched off by the "sausage" or pinch instability (ref. 12), illustrated in Figure 13. In the sausage instability, a small perturbation in the diameter of the plasma leads to a change in the current density, and a corresponding change in the azimuthal magnetic field. A small constriction tends to grow as the current density and azimuthal magnetic field increase, and this instability can lead to pinching off the plasma channel above and below the torus shown in Figure 12.

Thus far, the Koloc model depends on well understood plasma phenomena which have been repeatedly observed in the laboratory. However, if a bare torus of highly ionized plasma were to exist in the atmosphere without some form of shielding from neutral atmospheric gases, the electron-neutral scattering and energy dissipation would quench the plasma on a time scale measured in milliseconds. To deal with this objection, the Koloc model assumes that the torus of Figure 12 forms a thin shell of very hot electrons, as indicated schematically in Figures 12 and 14, which insulates the plasma torus from the surrounding neutral gas. This thin layer is called the "mantle" in the Koloc model. These hot electrons are maintained by currents flowing along lines of longitude from one pole of the dipole to the other, which heat the electrons in the thin shell to relativistic energies, high enough to have scattering cross sections consistent with the long lifetimes observed in ball lightning. The energy required to maintain this thin shell of relativistic electrons is supplied

by the slow collapse of the dipolar magnetic field and by the stored magnetic energy in the circulating current of the torus.

The outcome of the processes described above is a torus of plasma, containing a large circulating current, which generates a dipolar magnetic field confined within a shell of hot electrons. Immediately outside the hot electron boundary is a partially ionized gas which fades off into the surrounding neutral atmosphere. In the Koloc model, illustrated in Figure 14, ball lightning is thought of as a plasma bubble, with number densities lower than that of the atmosphere surrounding it, but with kinetic temperatures and magnetic pressures which provide an expansionary force to keep the plasma bubble inflated against the pressure of the surrounding atmosphere. Detailed models have been developed by Koloc for the hot electron boundary, and for the physical processes in the mantle which allow ball lightning to maintain itself in the atmosphere for long periods of time (refs. 17, 18).

The magnetic containment configuration described by the Koloc model is very similar to that of the Spheromak, the Field Reversed Mirror, or the Astron, except that it does not require an external magnetic field for confinement. The ultimate confinement mechanism in the case of ball lightning would be the surrounding neutral atmosphere. If the Koloc model is correct, the ball lightning plasma could be compressed or rarefied by increasing or decreasing the pressure of the surrounding neutral gas. A similar magnetic mechanism for high current diamagnetic ion rings has been suggested by Sudan (ref. 13).

The requirement for a relativistic shell of electrons surrounding the plasma torus is probably the least satisfactory aspect of the Koloc model, and the one that thus far has no precedent in laboratory plasma physics. The presence of significant numbers of relativistic electrons as an essential feature of a ball lightning model would seem to be inconsistent with the very low energy content implied by some ball lightning observations. This aspect

A-111

of the Koloc model was formulated to deal with the very long lifetime which ball lightning is observed to have in atmospheric air.

Another mechanism than relativistic energies by which the electrons could have a very long confinement time and low scattering cross section is if they were scattering in a Ramsauer gas. The Ramsauer gases are those gases which, due to quantum mechanical effects, have very low electron neutral scattering cross sections at low electron energies. Figure 15 shows electron-neutral scattering cross sections for several gases taken from reference 20. Of the gases shown, argon is a Ramsauer gas, with an electron-neutral scattering cross section far lower than that of other common gases. Until recently, there was no reason to think that ball lightning could reasonably contain a Ramsauer gas, and thus have a long electron-neutral scattering time. It has become known however (ref. 11) that some nitrogen oxides are Ramsauer gases. It is possible that during the intense plasma chemistry associated with a lightning stroke, the oxygen and nitrogen of the atmosphere may combine to form nitrogen oxides, which may be Ramsauer gases. These Ramsauer gases may then permit the electron population to remain energetic for far longer than would be the case if the electrons were to scatter against ordinary oxygen or nitrogen molecules.

IMPLICATIONS OF BALL LIGHTNING OBSERVATIONS

The large body of ball lightning observations indicate very strongly that it is a real phenomenon, the physics of which should be explainable in terms of known physical processes. If we are willing to grant the reality of ball lightning, then what are the implications of interest to the plasma research community? One feature of ball lightning which motivated several of the surveys cited previously (refs. 5 and 6) is the long duration of ball lightning, ranging from less than a second, up to more than 130 seconds. These times are much longer than the containment time required for a net power producing fusion plasma, and so the existence of ball lightning suggests a plasma confinement method which

A-112

may be of fusion relevance, if only because of its ability to confine plasma for periods of time far longer than those required for fusion applications. The physical processes responsible for the long lifetime of ball lightning may be of interest in fusion research, for the additional reason that it might tell us with what gases we might surround the fusion plasma in order to minimize charge exchange and electron-neutral scattering losses.

Another feature of ball lightning observations is the large energy density and energy content associated with some ball lightning observations. Energy densities of greater than 10^4 joules per cubic centimeter indicate a magnetic energy storage mechanism in ball lightning, and total energies up to 10 megajoules indicate plas as energetic enough to be of fusion relevance. The magnetic containment method responsible for ball lightning would be of interest to fusion research because of the MHD stability of ball lightning over many of tens of seconds.

In addition to suggesting that there are new and previously unknown physical mechanisms for magnetic containment of plasmas and the long duration, stable confinement of plasma in atmospheric air, ball lightning has potential applications in at least three areas in which the plasma research community has been active. These potential areas of application include ball lightning as a military weapon, potential fusion applications of ball lightning, and the implications of ball lightning for industrial plasma processing at one atmosphere.

BALL LIGHTNING AS A MILITARY WEAPON

Suppose it were possible to generate ball lightning with an apparatus which was small and light enough to be mobile, but not small enough to be portable, like small arms. In order to do much damage, a lightning ball would have to store at least 1 megajoule of energy, and a capacitor bank large enough to store this energy would be too large to be easily portable.

Effects on Troops

Perhaps the most significant effect of ball lightning on troops might be psychological. If no simple countermeasures to ball lightning could be developed, the sight of a lightning ball approaching an individual would probably inspire fear and panic, and cause very significant distraction. The ball lightning literature contains many reports of individuals who were stunned by ball lightning and a few, like Richmann, who died from contact with ball lightning. It is not clear whether this spectrum of effects on humans is the result of a range of stored energy, or some other factor associated with ball lightning, but it is moderately clear that if ball lightning could be formed at will, it should be possible to achieve an effect on humans that ranges from stunning to death.

Ball lightning would have a number of advantages over kinetic weapons based on ordinary firearms, in that the operator of a ball lightning projector should be able to adjust the ball lightning to acheive a spectrum of effects ranging from brief stunning to death. A ball lightning weapon could therefore be used in police work at a setting which was known not to be fatal, or adjusted for lethal effect when used in warfare. Another potential advantage of ball lightning over kinetic weapons is that there appear to be no reports of ball lightning stunning people and then leaving them maimed. Thus, ball lightning would probably disable troops without permanently injuring or maiming them, one of the ancient disadvantages of kinetic weapons.

Effects on Equipment

For reasons outlined above, including the observation of very high energy densities, ball lightning appears to be energized by stored magnetic energy, which in natural ball lightning can reach levels of at least 10 megajoules. The lightning balls can be thought of as a form of portable electromagnetic pulse. If a lightning ball were to come into contact with antennas or any solid state electronic system, the high voltages and high

A-114

currents associated with sudden decay of the stored magnetic energy would probably damage or destroy any electromagnetic receiver. A ball lightning projector could probably irreversibly damage most sophisticated weapons used on the modern battlefield which contain solid state electronic components.

It is also likely that, if ball lightning can be accurately aimed, it should be possible to trigger munitions with the sudden and rapid decay of its stored magnetic energy, and to effect other forms of physical destruction. The literature of ball lightning contains numerous descriptions of severe damage done by the explosion of a lightning ball. In a few cases, explosives experts have identified the energy content of the source as being greater than 10 megajoules. Many cases have been reported of large trees or substantial masonry structures being demolished. These observations indicate that ball lightning should have a substantial capacity for physical destruction, but the potential drawback of this is that the capacitor banks which would be needed to supply such a ball lightning projector are relatively heavy and cumbersome at the level of multi-megajoules of stored energy.

APPLICATION OF BALL LIGHTNING TO FUSION REACTORS

Suppose that it became possible to generate ball lightning in the laboratory and that the plasma parameters of ball lightning could be made to include the densities, kinetic temperatures, and containment times required to meet the Lawson criterion. As a stimulus to ball lightning research for fusion applications, it is useful to consider the fusion-relevant characteristics of ball lightning, and the potential advantages of ball lightning fusion reactors.

Fusion-Relevant Characteristics of Ball Lightning

Some of the fusion-relevant characteristics of ball lightning are listed in Table 3. In column 1 are listed characteristics which are relevant to fusion applications, and on which information is available from the existing ball lightning data base. In the second column is the range of parameters from the available ball lightning observations for the characteristics in the first column, and in the third column are shown the approximate requirements for a net power producing, self-sustaining DT fusion reactor. It is evident that the duration of ball lightning is longer than the particle containment time needed for a net power producing fusion reactor.

The second row of Table 3 indicates that the energy density of ball lightning can be far higher than the one joule per cubic centimeter characteristic of a self-sustaining DT fusion reaction. The third line of Table 3 indicates that ball lightning can be of a size large enough to provide significant amounts of fusion power, if fusion energy densities of 1 to 10 megawatts per cubic meter could be maintained in a ball lightning fusion reactor. The fourth row indicates that the kinetic pressure of ball lightning, approximately 1 atmosphere, is comparable to the kinetic pressure, $p = nkT$, of a magnetic fusion reactor, which would range from 1.6 to 10 atmospheres for DT and advanced fuels, respectively.

The ion and electron number density in ball lightning is very poorly known and would have to be somewhere below 2.7×10^{19} particles per cubic centimeter, the particle number density of the neutral atmosphere. In a net power producing DT fusion reactor, an ion number density of about 10^{14} per cubic centimeter would be required, and advanced fuel reactors would require densities of perhaps two or three times this value (ref. 12). Finally, in the last line of Table 3 the kinetic temperature of ball lightning is very poorly known but must be more than the temperature of atmospheric air. For a self sustaining DT fusion reactor, the kinetic temperature of the ions must be about 10 keV, with values of 3 to 5 times this value required to burn advanced fuels.

Potential Advantages of Ball Lightning Reactors

The first potential advantage of ball lightning reactors might be small size and power output. Existing studies of DT Tokamak fusion power plants (ref. 12) suggest that such reactors must produce several gigawatts of thermal power and be so costly and large in size that they cannot be used for anything other than central station electric utility powerplants. The observed size of ball lightning is an encouraging indication that a fusion reactor based on ball lightning might be small enough to be used in mobile applications and of small enough power output that applications of considerably smaller scale than electric utility powerplants could be considered.

The ability of ball lightning to exist in stable equilibrium at one atmosphere suggests that, if desired, a ball lightning fusion reactor could be operated at one atmosphere, like ordinary fossil fuel boilers, or at least without the necessity of an expensive vacuum system. This also implies that a knowledge of the physical processes which allow ball lightning to exist at one atmosphere might have implications for the selection of the gas which should surround a fusion plasma in order to minimize charge exchange or scattering losses. On a more speculative note, the capability of ball lightning to operate at one atmosphere also suggests that more exotic applications of ball lightning fusion powerplants, such as rocket engines for earth takeoff, or fusion powered turbojets, may be possible.

The fact that nature produces ball lightning without costly or complicated equipment is an encouraging indication that, once we understand how ball lightning is formed, the equipment needed to produce a ball lightning fusion plasma will itself be simple and require only relatively simple containment equipment, by current standards of magnetic fusion research.

Another potential advantage of ball lightning fusion reactors is that the balance between the external atmospheric pressure, and the kinetic pressure of the plasma should

allow the plasma number density, temperature, and fusion power output to be controlled by compression or expansion of the neutral gas surrounding the ball lightning plasma. If one compresses the surrounding neutral gas, it is reasonable to expect that an adiabatic compression of the confining magnetic field and its associated plasma will occur, leading to a hotter, denser plasma and greater power output. Thus, while the ball of plasma is undergoing fusion reactions, the power output should be capable of being adjusted on demand. This type of reaction control was contemplated by Koloc, in his U.S. patent (ref. 19).

Finally, the ball lightning literature contains reports of ball lightning which lasted for durations of well over 100 seconds. There apparently is a slight tendency for small ball lightning to last for somewhat shorter times than large diameter ball lightning, but on the basis of existing observations, it seems reasonable to expect that ball lightning reactor plasmas, once formed, should last at least 10 to 100 Lawson containment times, and allow a virtually complete fusion burn without refueling. It is not possible to say at this time whether a refueling mechanism could be found which would allow the magnetic field in a ball lightning reactor to regenerate itself and maintain the plasma in the steady state; most likely, a ball lightning fusion reactor will be a repetitively pulsed device, similar to that suggested by Koloc (ref. 19).

Ball Lightning Fusion Reactor Concepts

The potential small size and ability of a ball lightning fusion reactor to operate in the atmosphere open up a large variety of potential applications which are not possible to most other magnetic fusion containment concepts, because of their unavoidably large size (ref. 12). Such potential applications include space power and propulsion systems, where power outputs ranging from 100 kilowatts to 200 megawatts are required, a range not easily supplied by the DT Tokamak or other mainline magnetic fusion concepts. The

possibility of a ball lightning fusion reactor operating in the atmosphere may open up, for the first time, a realistic possibility of a fusion rocket capable of operating from the surface of the earth to low earth orbit. Prior to the emergence of this concept, fusion power and propulsion systems for space applications were restricted to the vacuum of outer space.

The potential small size and simplicity of ball lightning generation and confinement equipment would open up a wide range of mobile applications of fusion reactors for land, sea, and air transportation. It is intriguing that ball lightning as small as 1 or 2 centimeters in diameter has been observed. If something this small were capable of fusion reactions, fusion engines for automobiles, trains and trucks would not be out of the question. Even if a ball lightning fusion powerplant required plasmas with dimensions of several meters, applications to submarines and surface ships might be possible. The capability of ball lightning to operate in the atmosphere raises the possibility of a fusion energy source for aircraft, with a turbojet engine or fanjet engine using fusion rather than chemical fuel in the combustor. Another application which will follow from the potential small size and simplicity of a ball lightning fusion reactor is that distributed, household primary energy sources might be possible, in which every individual household and apartment building could have its own fusion reactor to provide heating, air conditioning, water purification, and electrical power.

IMPLICATIONS OF BALL LIGHTNING FOR INDUSTRIAL PLASMA PROCESSING

In the field of industrial plasma engineering, nearly all industrial plasma processing except that done with thermal plasmas is accomplished at low pressures inside elaborate and expensive vacuum systems. The cost of vacuum systems and the energy cost of vacuum pumping tend to dominate the cost of nearly all products made below atmospheric pressure by industrial plasma processing methods. From the above discussion, it is

reasonably clear that one implication of the existence of ball lightning is that steady state, low power glow discharges in atmospheric air should be possible. These glow discharges probably will involve a Ramsauer-effect gas, such as argon or a nitrogen oxide. The production of such atmospheric glow discharges should be possible with a minimal investment in capital equipment, and without the requirement of a vacuum system.

Potential Features of Ball Lightning Industrial Plasmas

Since ball lightning is observed to occur at one atmosphere and in atmospheric air, it seems a reasonable implication that steady state glow discharges which are to be used for industrial plasma processing should also be possible at one atmosphere and without the requirement of expensive vacuum systems. The relatively long lifetime and relatively low levels of energy dissipation associated with ball lightning observations imply that a one atmosphere glow discharge based on ball lightning physics not only can be of a relatively small size, but also of a relatively small power consumption. This is especially important by comparison with the vacuum systems required for low pressure plasma processing. Not only are the vacuum systems a very expensive capital investment, but a great deal of power is needed to drive the required vacuum pumps to run such systems.

Potential Industrial Applications of Ball Lightning Plasmas

The production of a steady state glow discharge at one atmosphere of pressure would make possible under ambient conditions a number of industrial plasma processing operations which now must be done in vacuum sysems. These processes include the antistatic surface treatment of plastic films; plasma chemical surface reactions, in which active chemical species produced by the plasma will react with the surface to produce a desired effect; and plasma surface treatment to improve the wettability, dyeability or printability of textiles and other fabrics. In addition a one atmosphere glow discharge plasma could provide synthetic or destructive plasma chemistry at one atmosphere, without

the necessity to operate in a vacuum system. By using the proper heterogeneous surface chemical reactions, the deposition of thin films or their etching at 1 atmosphere may also be possible.

Perhaps one of the most extensive and significant potential applications of atmospheric glow discharge plasmas might be the deposition and etching of microelectronic circuits at one atmosphere, rather than at low pressures in a vacuum system. Naturally, the approach would have to be substantially different than the deposition and etching techniques currently used at low pressures. For example, one would probably have to rely on heterogeneous surface chemical reactions to lay down thin films, and one would have to rely on the plasma-chemical equivalent of placer mining to etch patterns on surfaces under a mask. These atmospheric placer mining techniques would consist of blowing air or background gas laden with active species from the plasma downward on the mask, and etching away the substrate by heterogeneous chemical reactions with the film.

SUMMARY

If the potential of ball lightning plasmas for military applications, fusion reactors, and industrial plasma processing is to be realized, a beginning needs to be made on the basic research and developmental work needed to provide the necessary information about ball lightning physics. One of the principal reasons that ball lightning is not better understood is that, as a random natural event which cannot yet be duplicated in the laboratory, it is not accessible to scientific investigation, and it has not been possible, except in rare chance encounters, to apply scientific instruments to make measurements of its characteristics. Clearly, a major task is to reliably and reproducibly generate ball lightning in the laboratory. When this is done, ball lightning should be accessible to scientific investigation, and to the application of modern plasma diagnostic methods. These

methods should provide information which will either confirm, modify, or replace the Koloc and other models discussed above.

Once information becomes available from experimental investigation of laboratory created ball lightning, then theoretical modeling of ball lightning can proceed. This modeling will probably proceed rapidly, in view of the large body of knowledge already available in the fusion community relating to the Spheromak and other similar plasma containment configurations. This theoretical understanding should also allow one to generate ball lightning in the steady state, and to determine scaling laws that relate ball lightning number densities, kinetic temperatures, and containment times so that some indication will become available concerning the region of plasma parameter space that ball lightning is capable of covering.

ACKNOWLEDGEMENT

References

1. Martin A. Uman: <u>Lightning</u>, McGraw Hill Book Co. New York, N.Y. (1969), pp. 243-248.

2. R. H. Golde, Editor: <u>Lightning: Vol. I. Physics of Lightning</u>, Chapter 12, S. Singer, "Ball Lightning" Academic Press, New York, N.Y. (1977), pp 409-436.

3. Stanley Singer: <u>The Nature of Ball Lightning</u>, Plenum, N.Y. (1971), ISBN 306-30494-5.

4. James D. Barry: <u>Ball Lightning and Bead Lightning</u>, Plenum Press, N.Y. (1980), ISBN 0-306-40272-6.

5. J. Rand McNally, Jr.: <u>Preliminary Report on Ball Lightning</u>, ORNL Report #3938, May, 1966, STAR Accession #N66-32479.

6. Warren D. Rayle, <u>Ball Lightning Characteristics</u>, NASA Technical Note TND-3188, January, 1966, STAR Accession #N66-15316.

7. I. Alexeff and M. Rader: "Observation of Closed Loops in High Voltage Discharges: A Possible Precursor of Magnetic Flux Trapping", <u>IEEE Trans. Plas. Sci.</u> Vol. 20, No. 6 (1992), pp 669-671.

8. Y. H. Ohtsuki and H. Ofuruton: "Plasma Fireballs Formed by Microwave Interference in Air", <u>Nature</u> Vol. 350, 14 March 1991, 139-141.

9. Y. H. Ohtsuki and H. Ofuruon: "Nature of Ball Lightning in Japan" <u>IL Nuovo Cimento</u>, Vol. IOC, No. 5, (1987), pp. 577-580.

10. J. Reece Roth: "<u>Ball Lightning as a Route to Fusion Energy</u>", Proc. 13th Symp. on Fusion Energy, Vol. II, IEEE Cat. No 89CH2820-9 (1989), pp. 1407-11.

11. E. Witalis: "Ball Lightning as a Magnetized Air Plasma Whirl Structure" <u>J. Meteorology</u>, Vol. 15 (1990) pp. 121-128.

12. J. Reece Roth: Introduction to Fusion Energy, Ibis Publishing, Charlottesville, VA (1986), ISBN 0-935005-07-2.

13. R. N. Sudan: "High-Current Ion-Ring Accelerator", Phys. Rev. Lett., Vol. 70, No. 11, (1993), pp. 1623-1626.

14. J. T. Slough, et al.: "Confinement and Stability of Plasmas in a Field-Reversed Configuration", Phys. Rev. Lett., Vol. 69, No. 15 (1992), pp. 2212-2215.

15. A. Al-Karkhy, P. K. Browning, G. Cunningham, S. J. Gee, and M. G. Rusbridge: "Observations of the Magnetohydrodynamic Dynamo Effect in a Spheromak Plasma", Phys. Rev. Lett., Vol. 70, No. 12, (1993), pp. 1814-1817.

16. E. A. Witalis: "Hall Magnetohydrodynamics and its Applications to Laboratory and Cosmic Plasma" IEEE Trans. on Plas. Sci., Vol. PS-14, No. 6 (1986), pp 842-848.

17. Paul M. Koloc: "The Plasmak Configuration and Ball Lightning" Proc. International Symposium on Ball Lightning, Tokyo, Japan, July, 1988

18. Paul M. Koloc: "Plasmak Star Power for Energy Intensive Space Applications" Fusion Technology Vol. 15, March 1989, pp. 1136-41.

19. Paul M. Koloc: Method and Apparatus for Generating and Utilizing a Compound Plasma Configuration, United States Patent 4,023,065, May 10, 1977.

20. R. Geller and J. Hosea: "Electron-Neutral Scattering Cross Sections", Report EUR-CEA-FC-459, March, 1968.

Figure Captions

Figure 1 - Distribution function of ball lightning diameters from four surveys, incorporating the number of repor... observations shown at the top of the Figure. From Singer (ref. 3).

Figure 2 - Cumulative distribution of ball lightning diameters from two surveys (squares and diamonds), and the charge transferred by lightning strokes (circles), from Rayle (ref. 6).

Figure 3 - Cumulative distribution function of reported ball lightning durations from the McNally (ref. 5) and the Rayle (ref. 6) surveys, from reference 6.

Figure 4 - Log-normal cumulative distribution of the energy density of ball lightning, in joules per cubic centimeter (Barry (ref. 4)).

Figure 5 - The vortex plasmoid model for ball lightning, from Singer (ref. 3).

Figure 6 - A compact torus generated in an axisymmetric magnetic mirror. A high beta, diamagnetic plasma is formed in the midplane which reverses the magnetic field, on the axis and forms a region of minimum magnetic field, from Roth (ref. 12).

Figure 7 - The field reversed theta pinch, from Roth (ref. 12).

Figure 8 - The spheromak configuration. A weak vertical magnetic field stabilizes a toroidal current carrying plasma, from Roth (ref. 12).

Figure 9 - A cylindrical current carrying plasma corresponding to a lightning channel in Bennett pinch equilibrium. From Roth (ref. 12).

Figure 10 - Development of the kink instability in the lightning channel of Figure 9. The helically twisted plasma looks like a single strand of multistrand rope, and the instability is driven by the stronger magnetic field on the inside radius of curvature, from Roth (ref. 12).

Figure 11 - Nonlinear evolution of the kink instability prior to torus formation. Illustration from Koloc (ref. 19).

Figure 12 - Torus formation in the Koloc model, from Koloc (ref. 19).

Figure 13 - Development of the sausage or pinch instability due to axial perturbations in the plasma column diameter. Such perturbations can cut the plasma torus off from the main lightning stroke after the torus formation shown on Figure 11, from Roth (ref. 12).

Figure 14 - The end point of the Koloc model, showing a toroidal, plasma insulated from the surrounding neutral gas by a high energy electron shell. The "kernel" forms a plasma-like bubble, which is maintained by a combination of magnetic and plasma pressure against the pressure of the surrounding atmosphere.

Figure 15 - Total electron-neutral collision frequencies for four gases, from reference 20, showing the Ramsauer minimum for argon gas.

Table I

Properties of Ball Lightning

Property	Low Value	Characteristic Value	High Value
Diameter, cm	1 cm.	10-15 cm.	150 cm
Duration, sec.	1 sec.	3-6 sec.	100 sec.
Energy content, J	0.01J	10-100	10^7
Energy density, J/cm^3	10^{-3}	$5J/cm^3$	10^5
Mass density, $grams/cm^3$	1.0×10^{-3}	1.3×10^{-3}	1.5×10^{-3}
Kinetic pressure, n/m^2	1×10^5	1.016×10^5	1.1×10^5

Table II

**THE KOLOC MODEL FOR
BALL LIGHTNING FORMATION**

1.   The Z-Pinch

2.   Bennett Pinch Equilibrium

3.   The Kink Instability

4.   Nonlinear Growth of the Kink Instability

5.   Torus Formation

o.   The Sausage Instability

7.   Mantle Formation

Table III

Fusion-Relevant Characteristics of Ball Lightning

Characteristics	Ball Lightning Observations	Self-Sustaining DT Fusion Requirements
Duration	1 sec to > 100 sec	1 to 10 sec.
Energy Density	10^{-3} to 10^5 J/cm^3	1 J/cm^3
Diameter	~ 1 cm to 2 meters	> 1 meter
Kinetic Pressure	~ 1 atm.	1.6 to 10 atm.
Number Density	Poorly known	~ 10^{14}/cm^3
Kinetic Temperature	Poorly known, > 0.025 eV	10^4 eV

Table Captions

Table 1 - Properties of ball lightning.

Table 2 - The Koloc model for ball lightning formation.

Table 3 - Fusion-relevant characteristics of ball lightning, compared with self-sustaining DT fusion requirements.
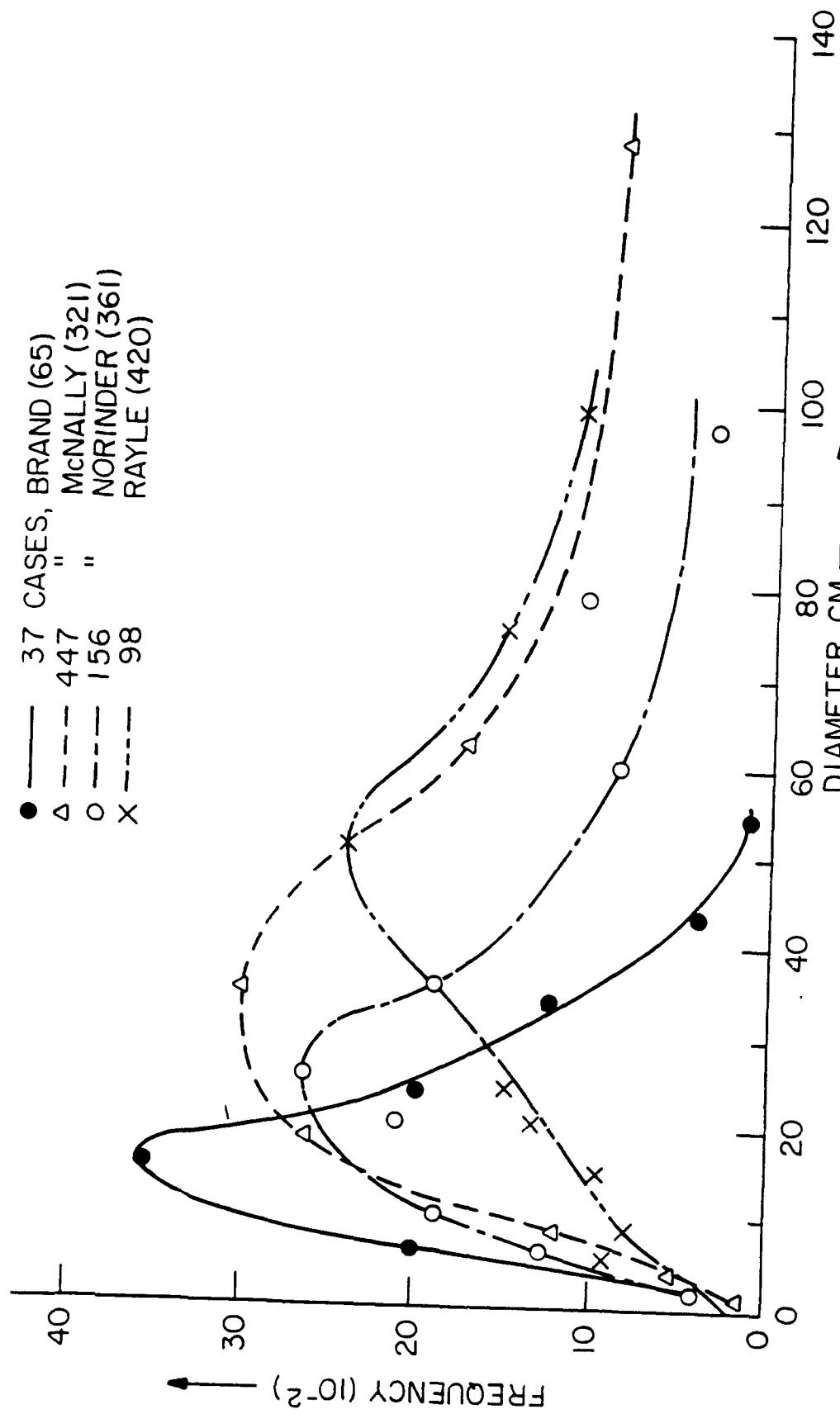
DISTRIBUTION FUNCTION OF BALL LIGHTING DIAMETERS. SINGER (REF. 3)

FIGURE I

A-131

PROBABILITY PLOT: DIAMETER (RAYLE, REF. 6)

DIAMETER OF BALL LIGHTNING, IN.; OR CHARGE TRANSFERRED BY LIGHTNING STROKES, COULOMBS (y-axis)

PERCENT OF OCCURRENCES WITH LESS THAN INDICATED VALUE OF ORDINATE PARAMETER (x-axis)

□ PRESENT SURVEY
◇ McNALLY (REF. I)
○ LIGHTNING-STROKE CHARGE (REF. I6)

FIGURE 2

INTEGRATED DISTRIBUTION: DURATION

McNALLY (REF. 5)

RAYLE (REF. 6)

FRACTION OF REPORTS OF DURATION LESS THAN D

DURATION, sec.

FIGURE 3

A-133
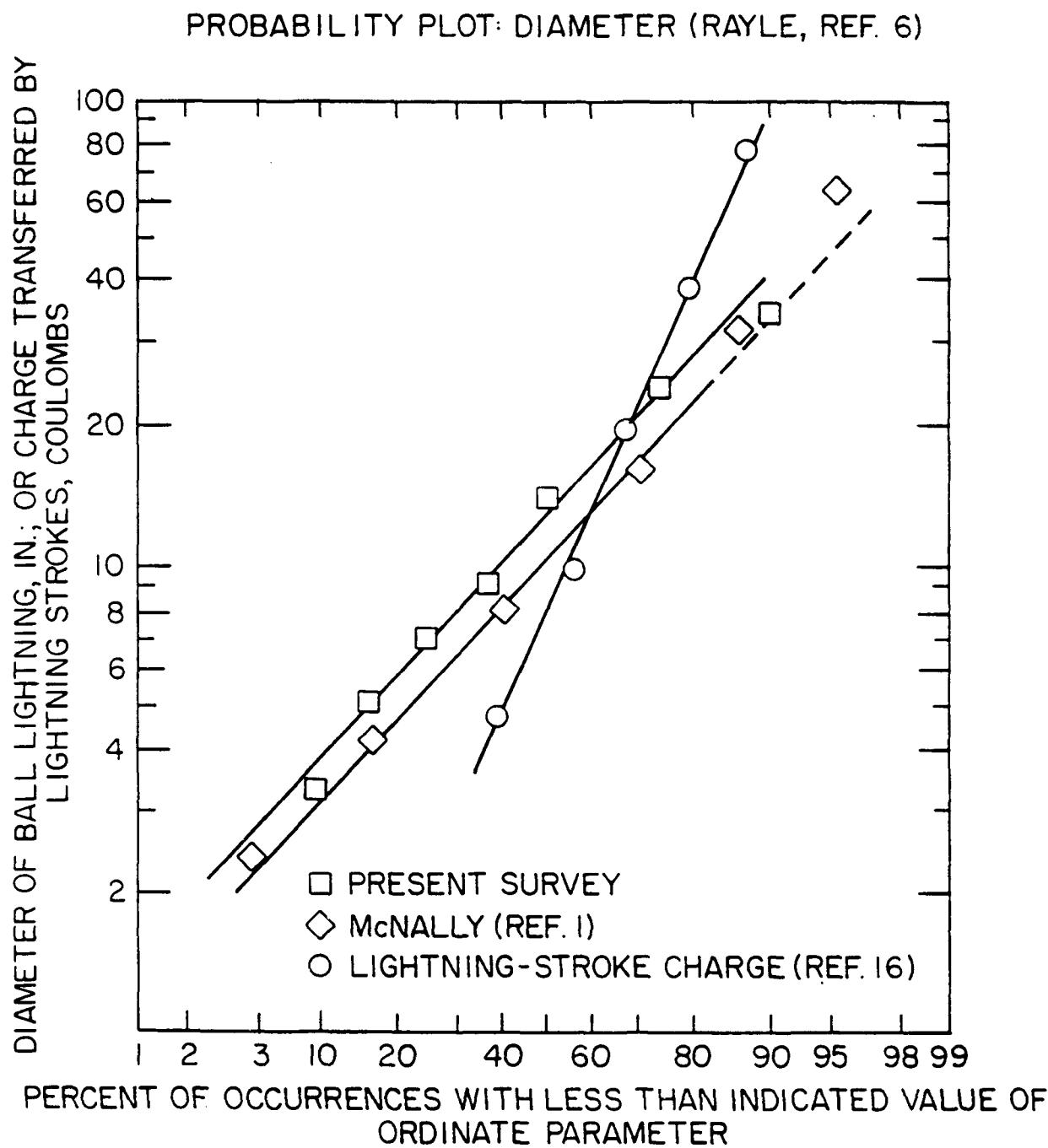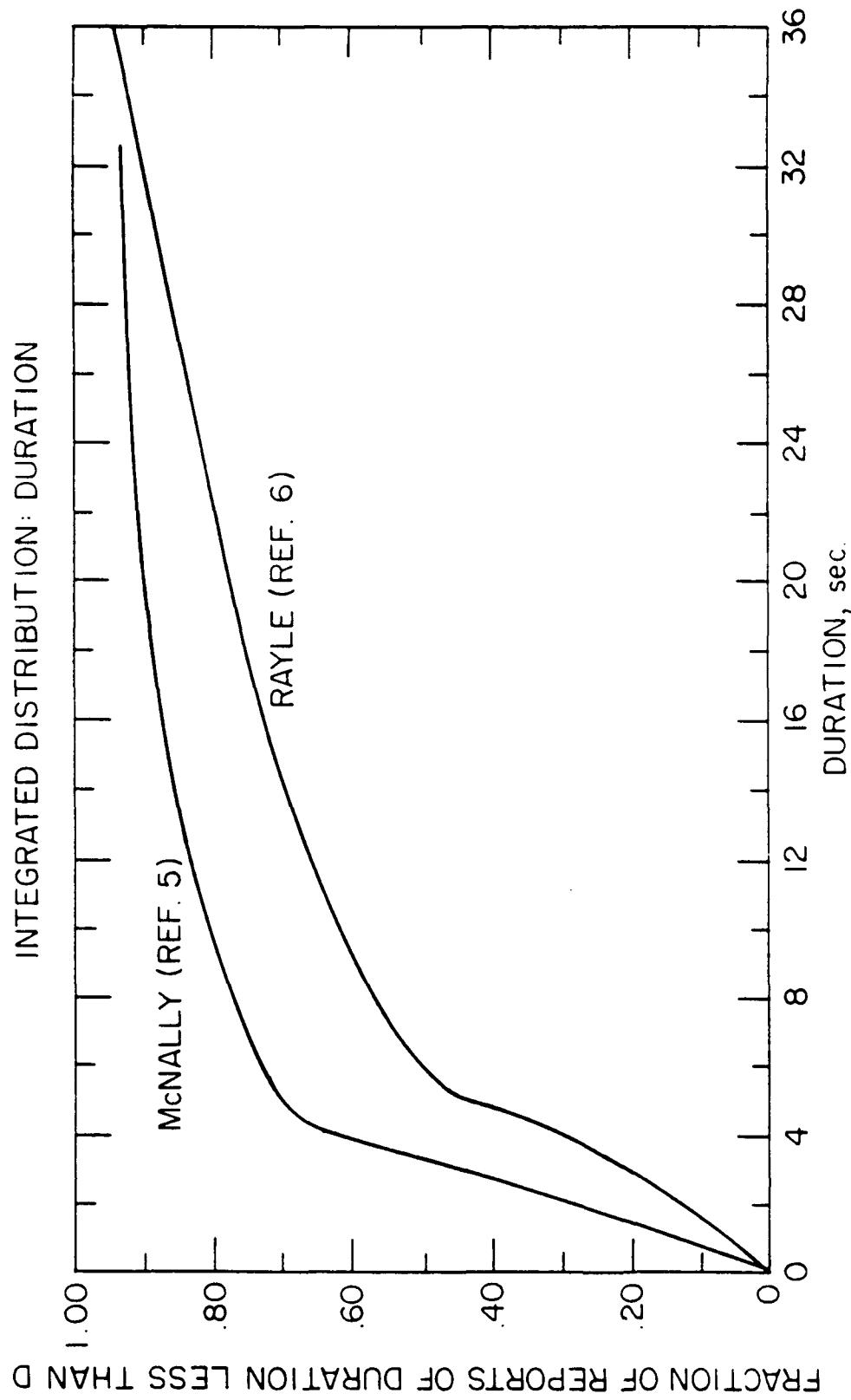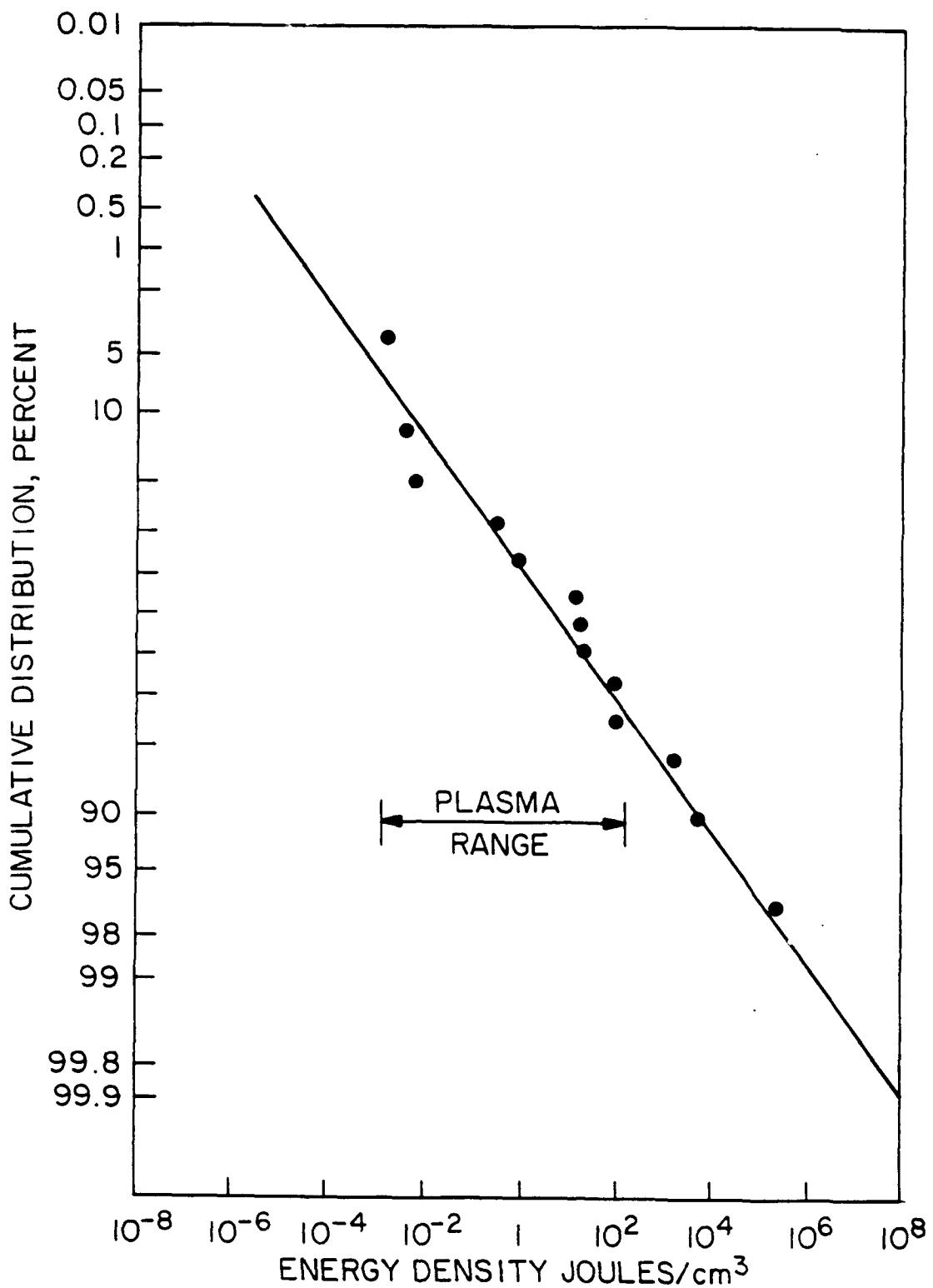
CUMULATIVE DISTRIBUTION FUNCTION OF
BALL LIGHTNING ENERGY DENSITY. BARRY (REF. 4)

FIGURE 4

A-134

MAGNETIC
FIELD
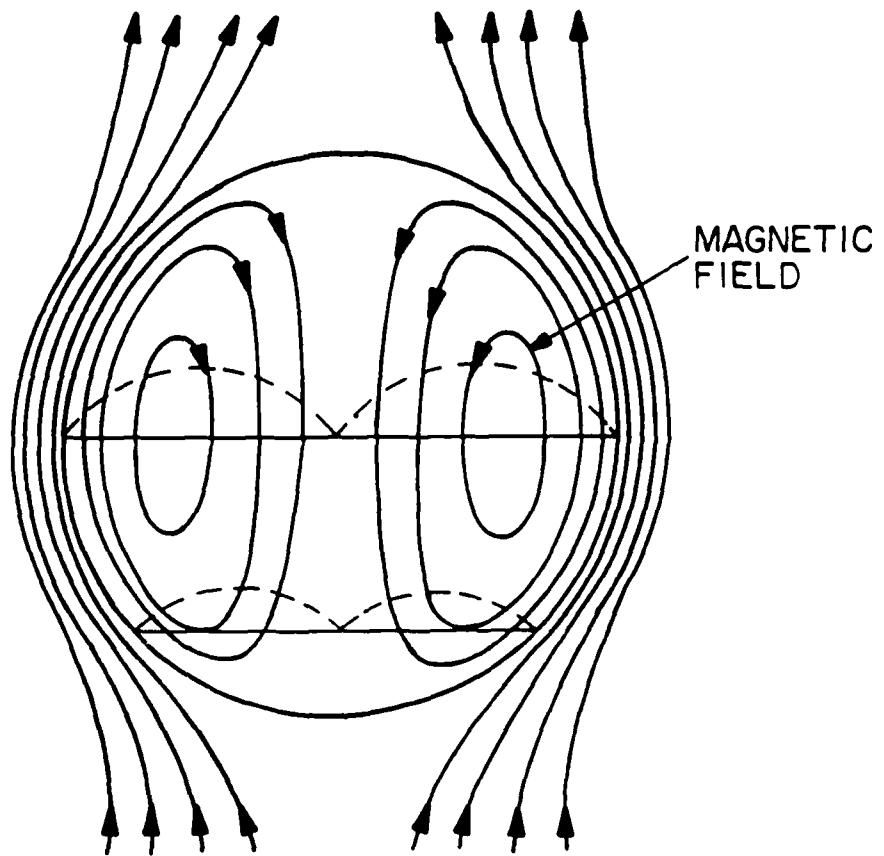
THE VORTEX PLASMOID SINGER (REF. 3)

FIGURE 5

FIELD

FIELD CONFIGURATION
WITH CLOSED FIELD

OPEN FIELD
LINES

DIAMAGNETIC PLASMA IN
ABSOLUTE – MIN – B REGION
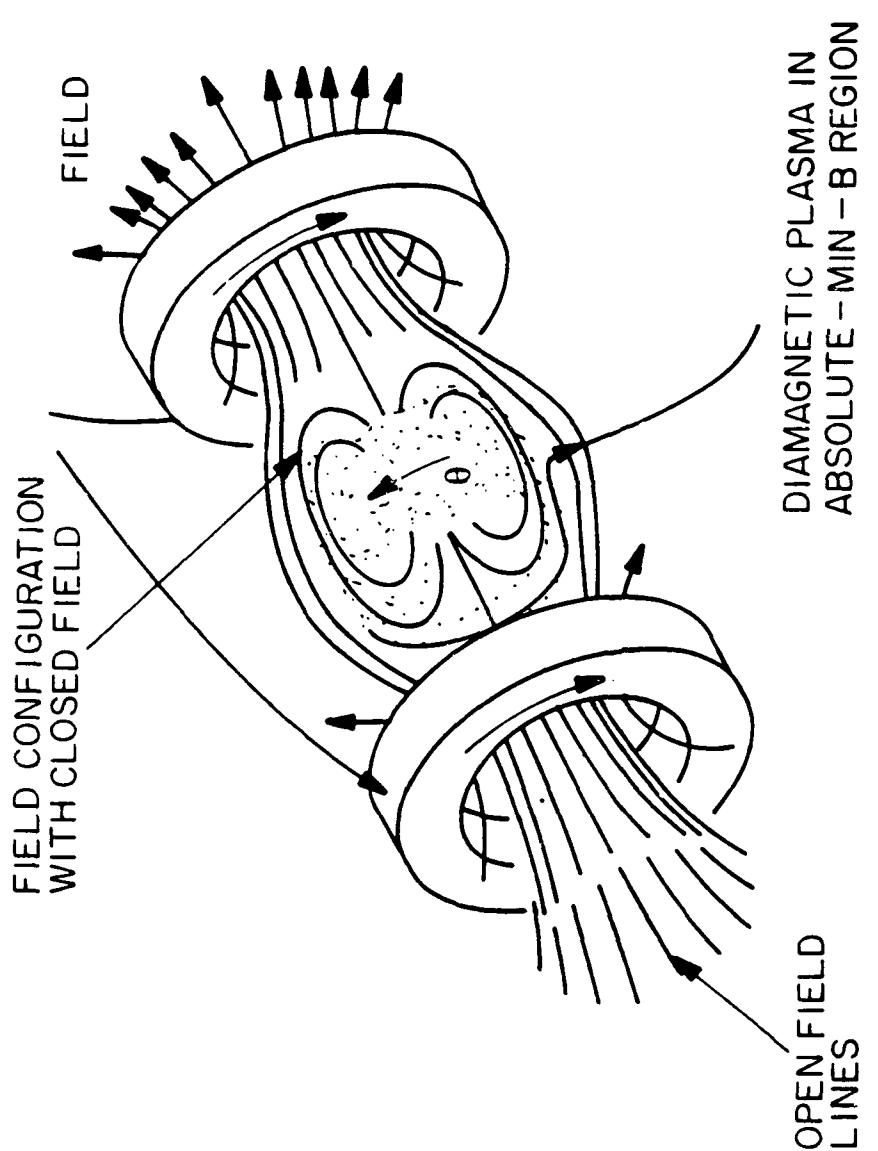
THE ASTRON/FIELD–REVERSED MIRROR ROTH (REF. 12)

FIGURE 6

A-136
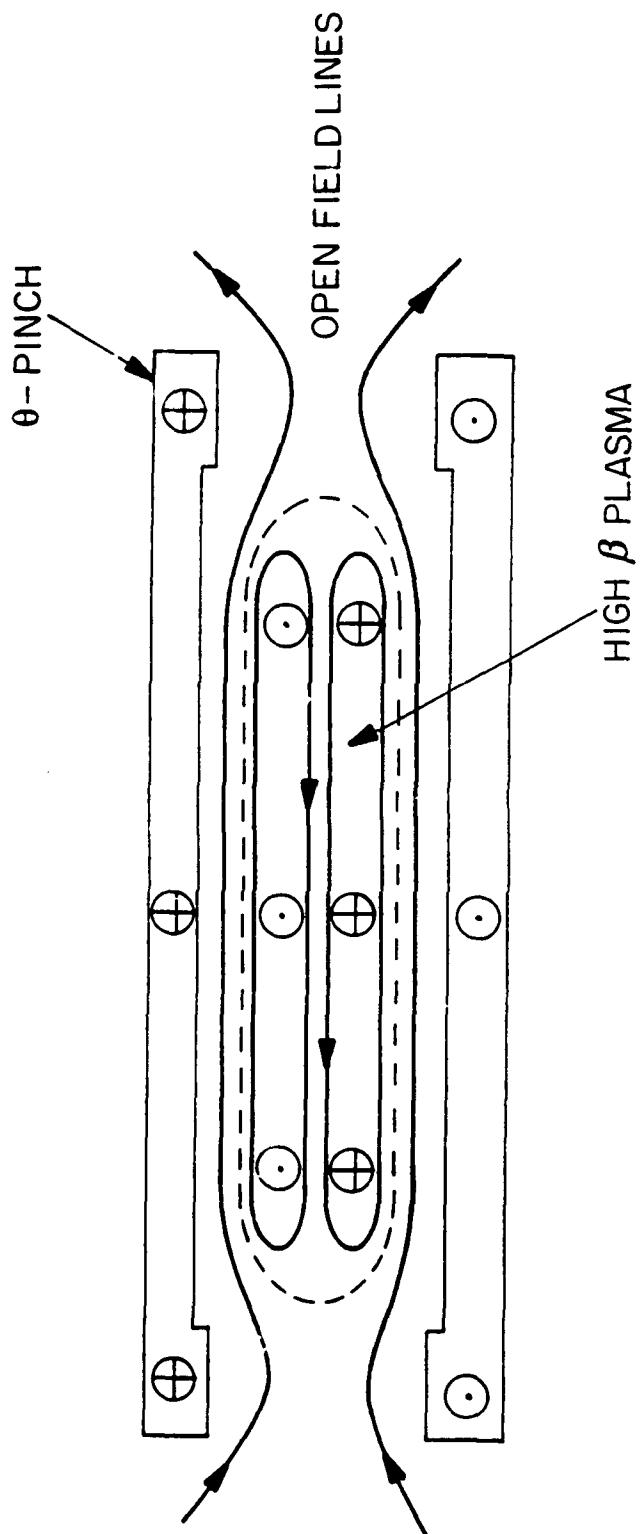
THE FIELD-REVERSED THETA PINCH ROTH (REF. 12)

FIGURE 7
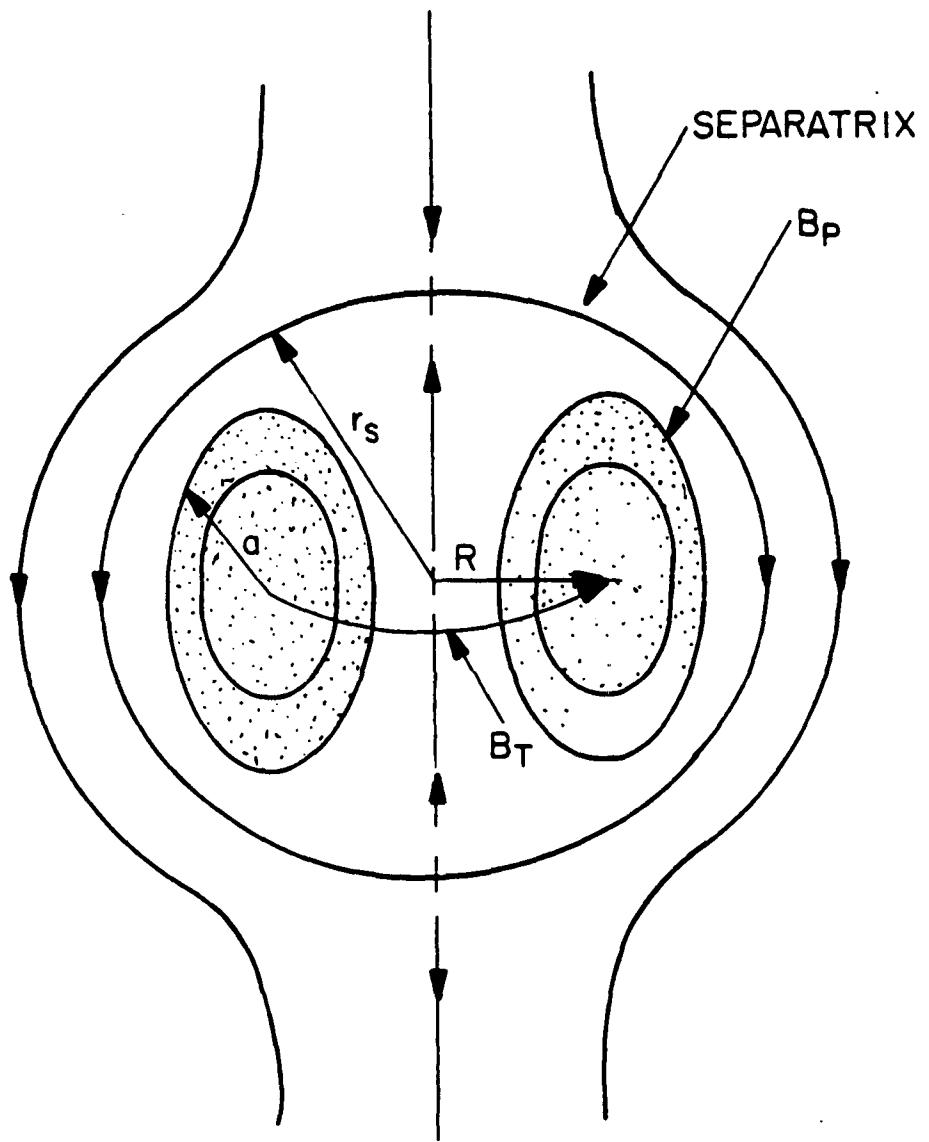
THE SPHEROMAK CONFIGURATION. ROTH (REF. 12)

FIGURE 8

LIGHTNING CHANNEL

⊙ MAGNETIC FIELD
OUT OF PAGE

⊗ MAGNETIC FIELD
INTO PAGE
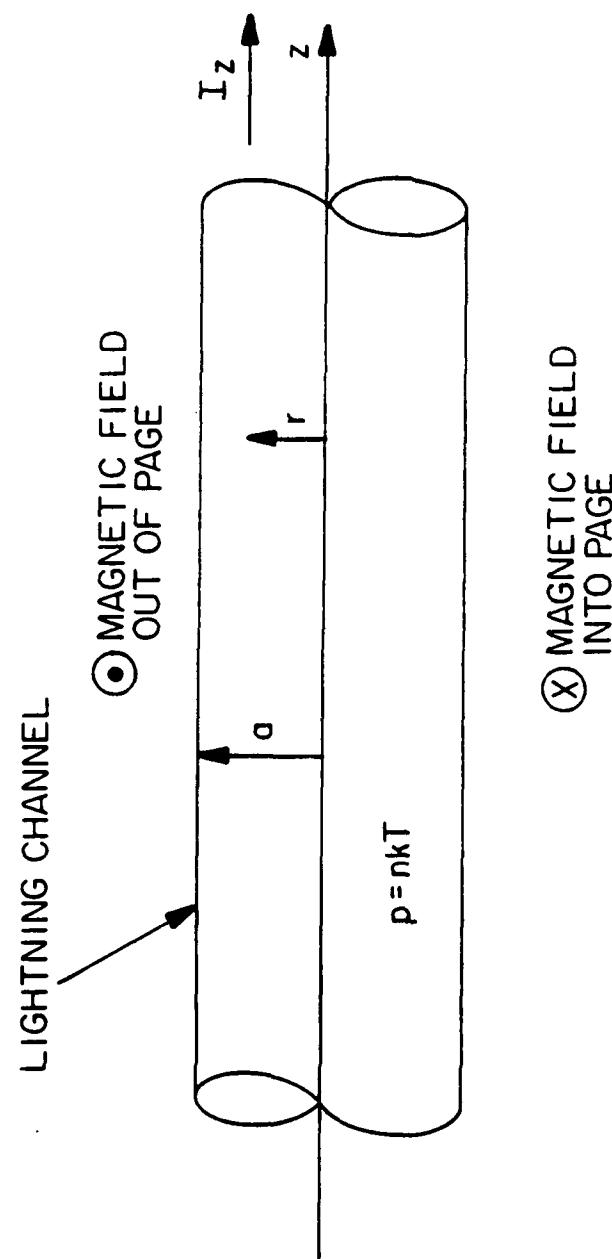
LIGHTNING CHANNEL AS A BENNETT PINCH.

FIGURE 9

$p = nkT$

I_z

z

a

r

FORMATION OF THE HELICAL KINK INSTABILITY (ROTH REF. 12)
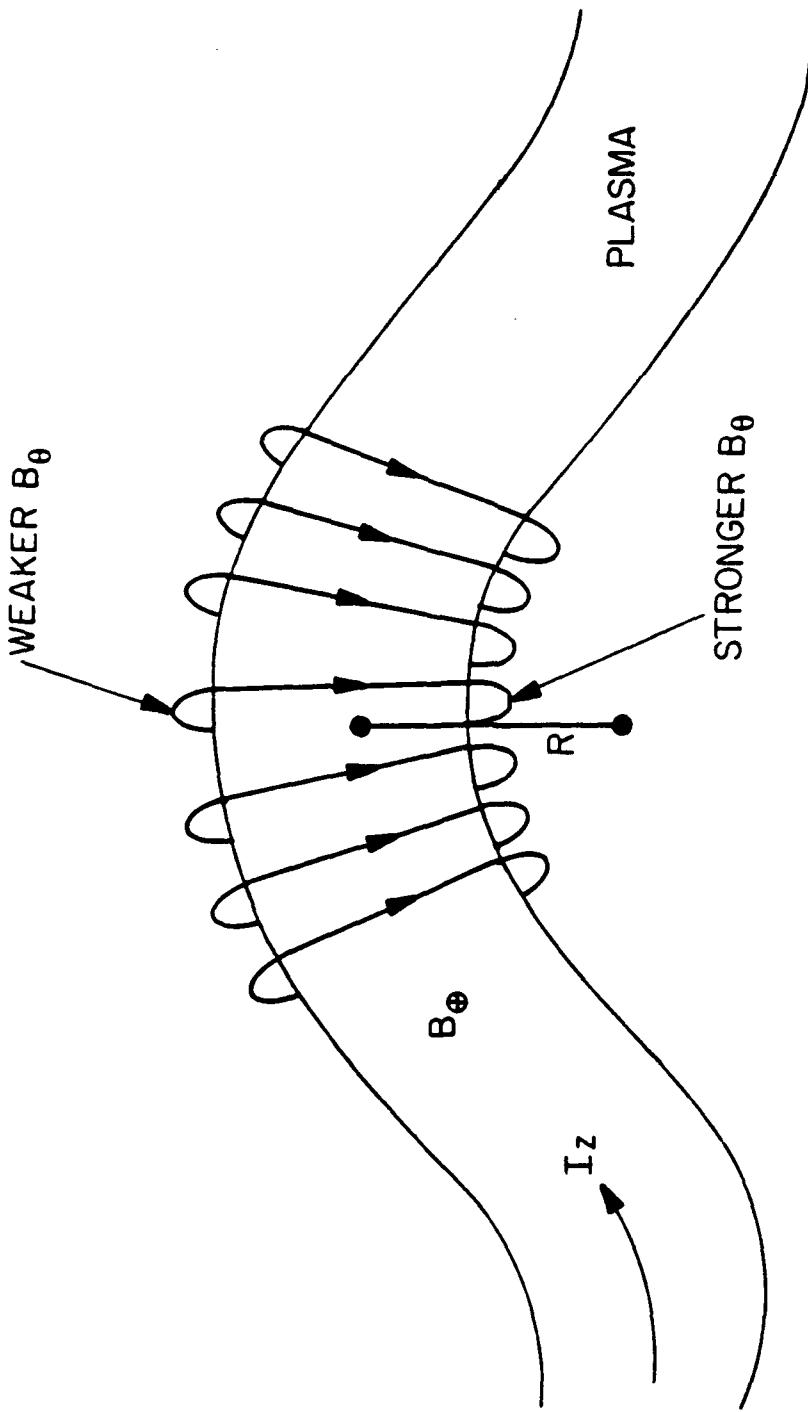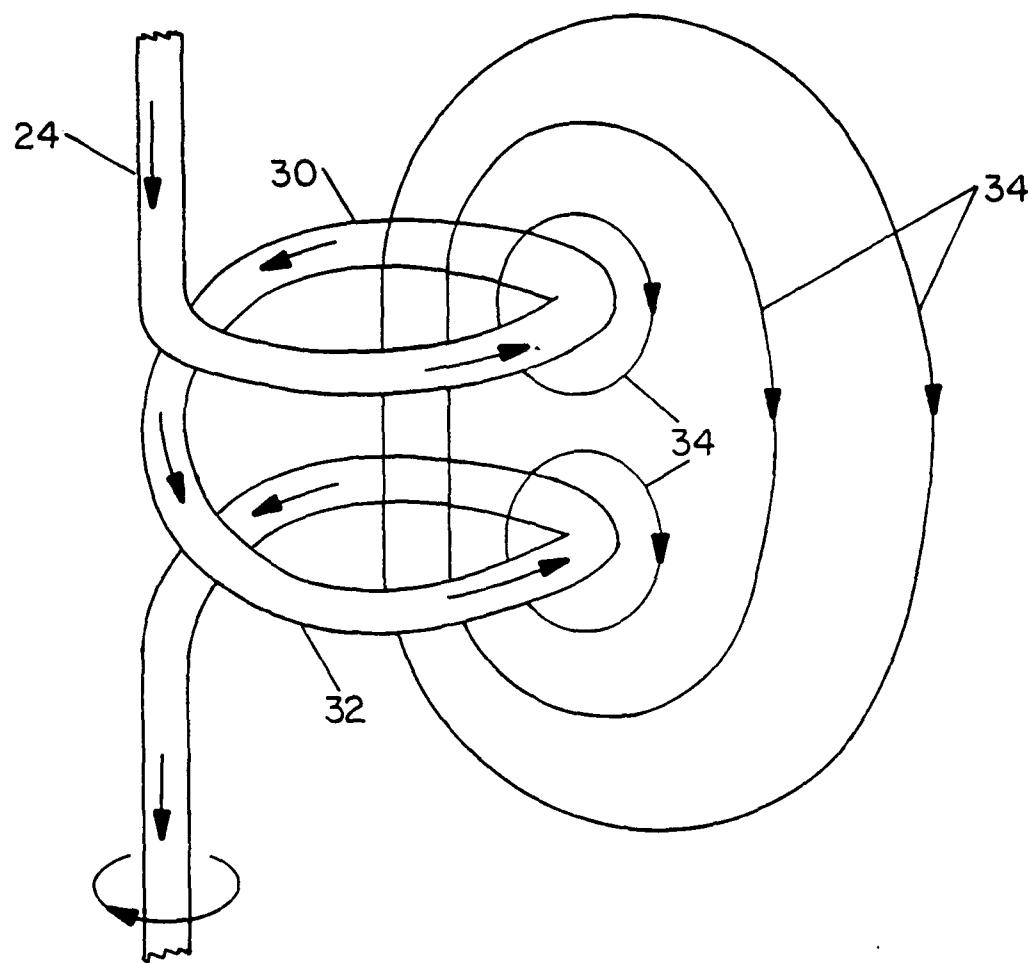
FIGURE 10

NONLINEAR EVOLUTION OF
THE KINK INSTABILITY. KOLOK (REF. 19)

FIGURE II

FIGURE 12

SMALLER
B

LARGER
B

PLASMA

I_z
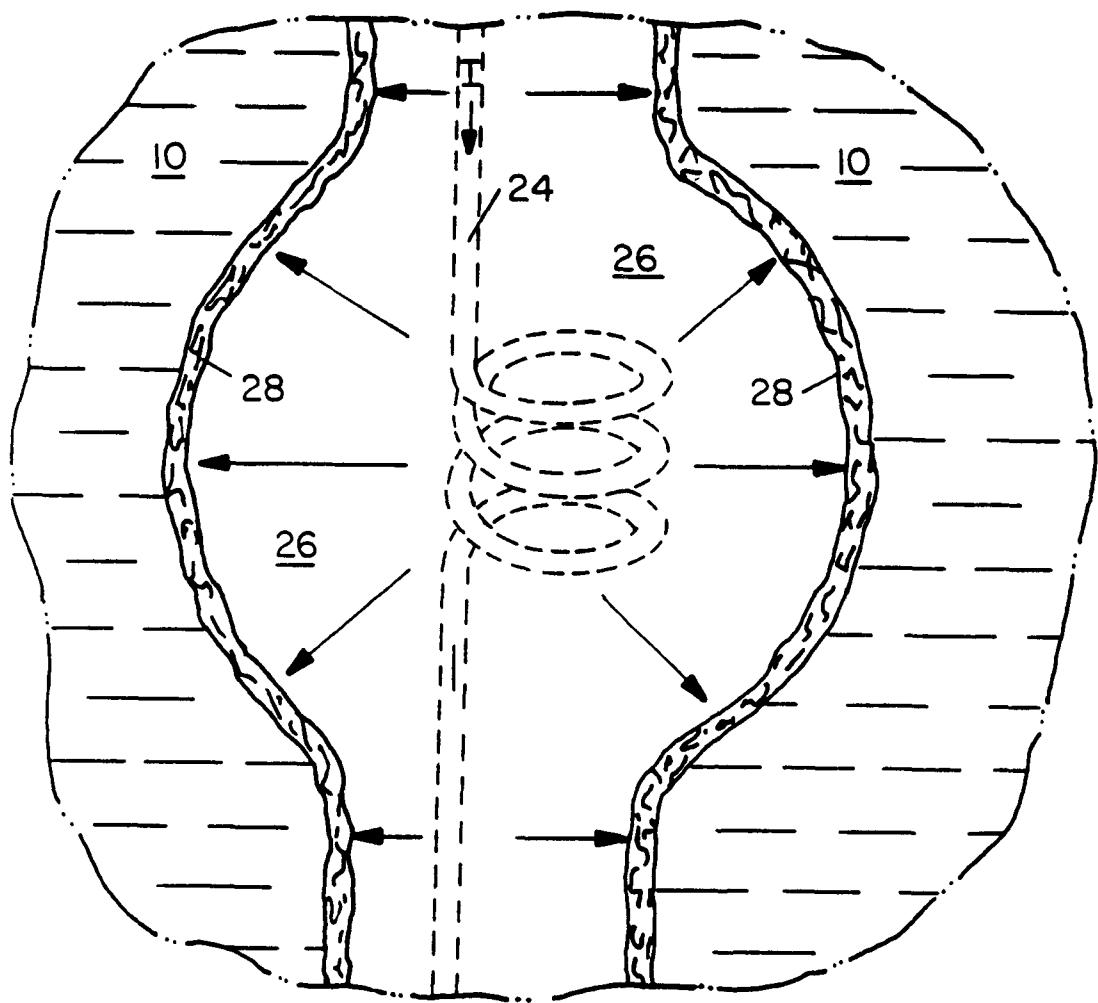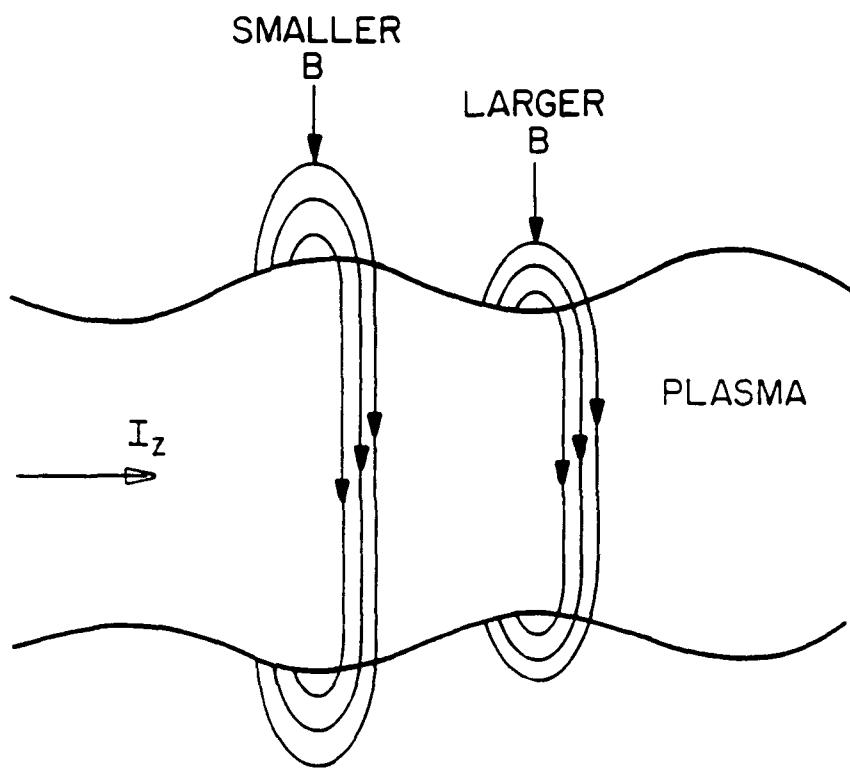
THE DEVELOPMENT OF A SAUSAGE OR
PINCH INSTABILITY. ROTH (REF. 12)

FIGURE 13

THE KOLOC MODEL OF BALL LIGHTNING. KOLOC (REF. 18)

FIGURE 14

ELECTRON ENERGY (eV)

R. GELLER AND J. HOSEA
EUR – CEA – FC – 459
MARCH 1968

FIGURE 15

TOTAL ELECTRON–NEUTRAL COLLISION FREQUENCY ν/P_0 (sec^{-1} – TORR^{-1})
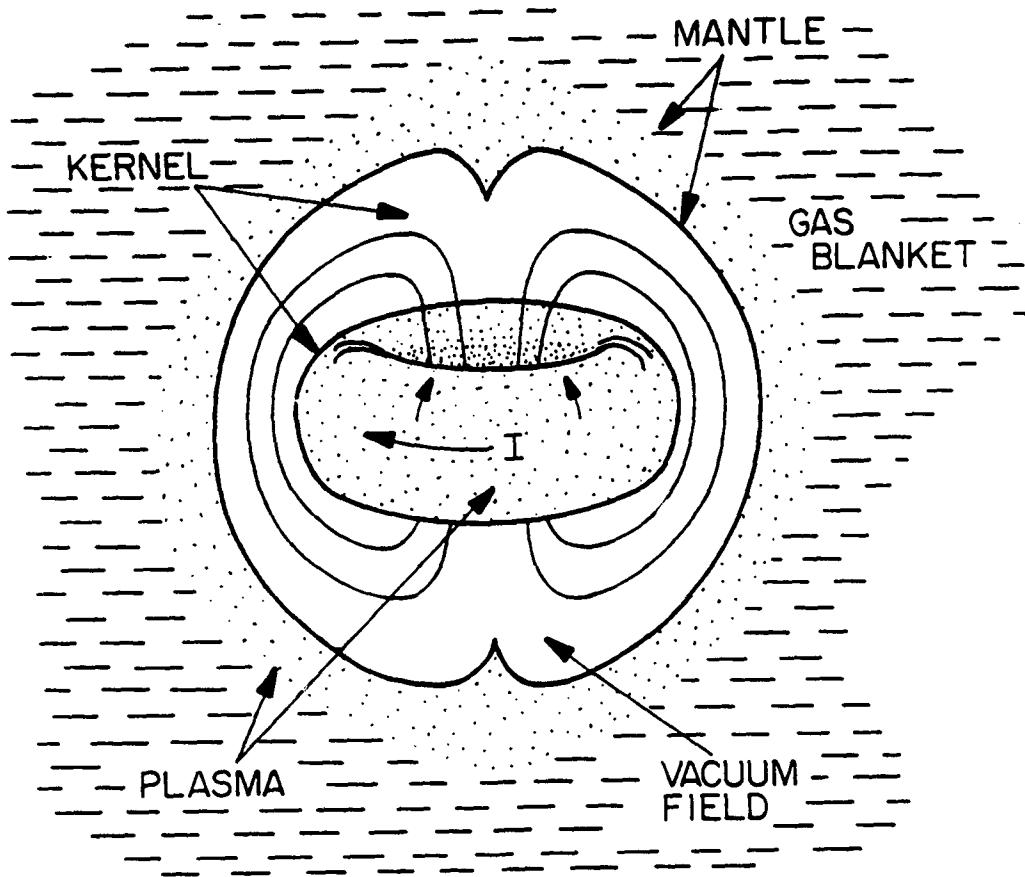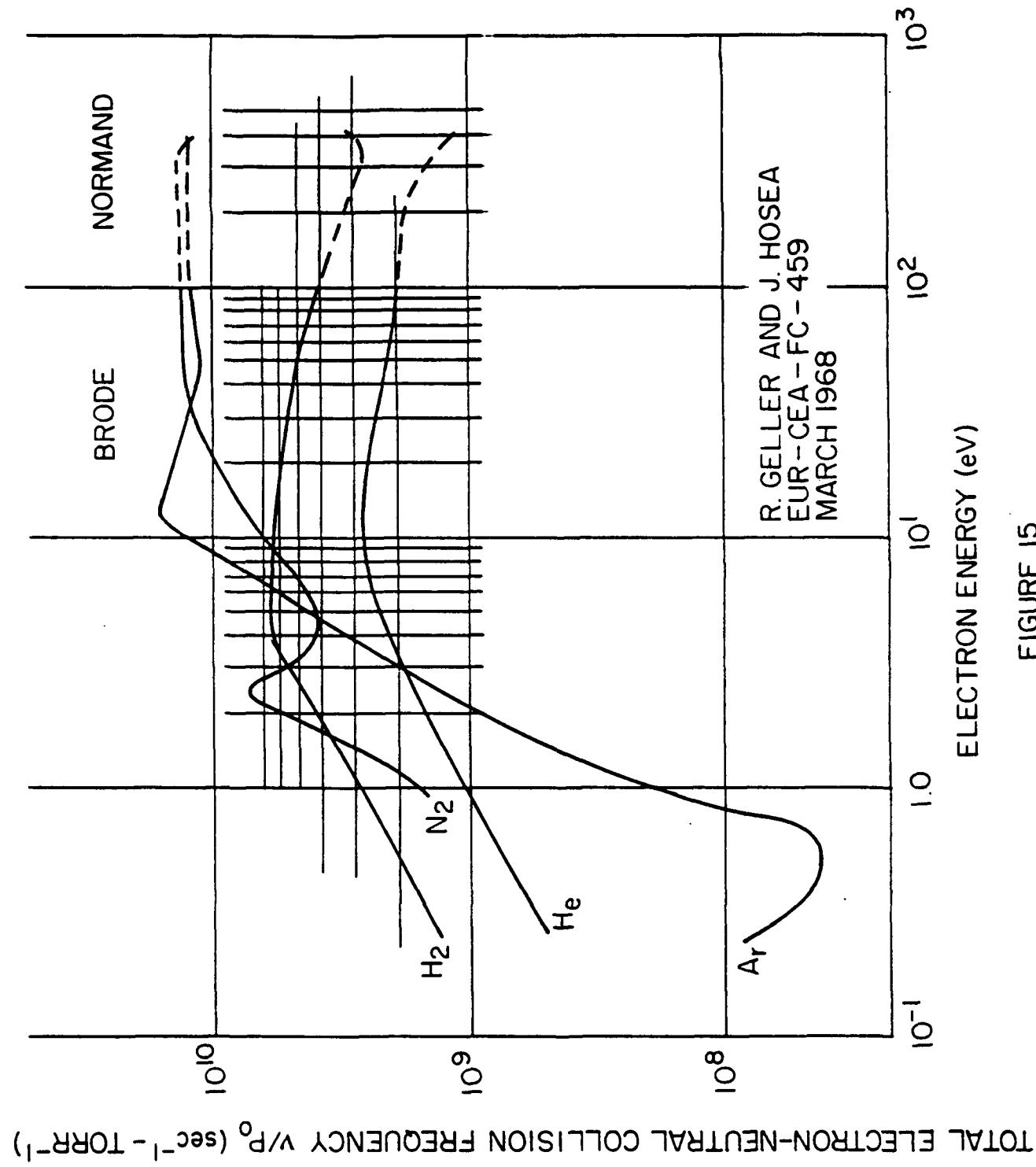
APPENDIX B

ABSTRACTS OF CONFERENCE PRESENTATIONS

Plasma Heating by Collisional Magnetic Pumping in a Steady-State Modified Penning Discharge*

Min Wu and J. Reece Roth

UTK Plasma Science Laboratory
Department of Electrical and Computer Engineering
University of Tennessee
Knoxville, Tennessee 37996-2100

This paper describes the experimental application of collisional magnetic pumping to heat a plasma by a sawtooth magnetic perturbation[1], and provides new results relating to the energy transfer process between the perturbed magnetic field and the parallel and perpendicular energy components of the heated species in a steady-state modified Penning discharge apparatus with a magnetic mirror configuration.

The general equation relating the change in total energy of a particle to the change of the magnetic field is

$$\frac{d^2E}{dt^2} - \left[-\frac{3}{2} v_c + \frac{d^2B/dt^2}{dB/dt} \left(\frac{dB}{dt} \right)^{-1} \right] \frac{dE}{dt} - \frac{v_c}{B} \frac{dB}{dt} E = 0$$

Using Floquet's theory and a perturbation treatment, Burger[2] et al. derived the energy increase rate when a sinusoidal perturbation is applied. The energy increase rate (or heating rate) is

$$\frac{dE}{dt} = \frac{\delta^2}{6} \frac{v_c \omega^2}{\frac{9}{4} v_c^2 + \omega^2} E_o$$

In later work,[3] it was found that a sawtooth perturbation satisfies the condition for first order (in δ) heating, and the heating rate for this case (sawtooth) is

$$\frac{dE}{dt} = \frac{\delta \omega}{3\pi} E_o$$

This can be an improvement of two or three orders of magnitude on the sinusoidal case. Small values of δ are also easier to achieve experimentally.

Experimental data, including such plasma characteristics as P_o, T_e, T_i, n_e and type of gas will be discussed, and heating of ions and electrons as functions of magnetic induction, electron number density, and neutral gas pressure will be presented. The detailed design of the above apparatus will also be presented and discussed.

1. Min Wu, L. Jiang and J. R. Roth, "Experimental Results on Collisional Magnetic Pumping in a Modified Penning Discharge with Magnetic Mirror Configuration", APS Bulletin Vol. 33, No. 9, p2019 (1988).

2. J. M. Berger, et al., "Heating of a Confined Plasma by Oscillating Electromagnetic Fields", Phys Fluids, Vol. 1, No. 4. pp 301-307, (1958).

3. M. Laroussi and J. R. Roth, "Analytical, Computational, and Experimental Results on Plasma Heating by Collisional Magnetic Pumping", APS Bulletin 32, No. 9. p. 1950. (1987).

Wu, M. and Roth, J. R.: "Plasma Heating by Collisional Magnetic Pumping in a Steady-State Modified Penning Discharge", Proceedings of the IEEE International Conference on Plasma Science, May 22-24, 1989, Buffalo, NY IEEE Catalog No. 89CH2760-7 (1989) pp. 73-74.

B-1

Real Plasma Effects of Microwave Radiation
Propagating Perpendicular to a Magnetized Plasma*

Lili Jiang and J. Reece Roth

UTK Plasma Science Laboratory
Department of Electrical and Computer Engineering
University of Tennessee
Knoxville, TN 37996-2100

Microwave absorbtion near electron cyclotron resonance has been investigated in a magnetized plasma over a wide range of frequencies, from 2 to 18 GHz. We have used a Hewlett Packard 8510 network analyzer, which is capable of swept frequency measurements, and of measuring reflection and transmission coefficients over these frequencies with 80 dB dynamic range. In previous work[1], a microwave beam was made to propagate along the axis of a magnetic mirror field. This radiation in the plasma column was attenuated up to 20 dB as it propagated along the axis of the magnetic mirror field at frequencies between 4 and 10 GHz[1]. This result suggests the feasibility of making targets disappear from radar screens by absorbing radar pulses in a n..ignetized plasma.

New experimental investigations have been undertaken on the attenuation of a microwave beam propagating across a uniform magnetic field with extraordinary and ordinary modes. The experimentally measured level of attenuation, absorption peak half-width, and phase angle are compared with the predictions of the Appleton equation[2].

The classical Penning discharge used to generate the plasma consists of a uniform magnetic field with a maximum value of 0.195T. An approximately 12 cm diameter and 118 cm long steady state plasma column is generated with a characteristic density of a few times 10^9 electrons/cm^3, and electron kinetic temperatures of a few tens of electron volts. Axial and radial Langmuir probes are used to measure electron number density and kinetic temperature.

1. L. Jiang and J. R. Roth, "Experimental Results of Microwave Absorption with Varying Magnetic Field in a Modified Penning Discharge", <u>APS Bulletin</u>, Vol. 25, No. 27, p. 1900, (1988).

2. M. A. Heald and C. B. Wharton, <u>Plasma Diagnostics with Microwaves</u>, (1978) New York.

<u>A Data Handling and Reduction System for Langmuir Probes.</u> F. GHANNADIAN, J. E. CROWLEY, and J. R. ROTH, <u>University of Tennessee, Knoxville.</u>*--Having a computer-aided data acquisition system with high accuracy and on-line data reduction for a Langmuir probe is a desirable feature in a plasma laboratory. For this purpose, a data acquisition system was designed, built, and tested to be applied to a Langmuir probe. The system consists of a IBM- PC/ AT, digital to analog and analog to digital converter card (DASCON-1), a transmitting and receiving network, and a voltage amplifier. The transmitting and receiving network consist of low voltage to frequency and frequency to voltage converters, and high voltage to frequency and frequency to voltage converters. These two parts are connected by fiber optic cables to eliminate the risk of arc to the low voltage part of the system. A computer program has been developed in QUICK BASIC to read the data, and by interaction with the user calculates the plasma potential, floating potential, electron temperature, ion temperature, and electron number density.

Ghannadian, F.; Crowley, J. E.; and Roth, J. R.: "A Data Handling and Reduction System for Langmuir Probes", <u>APS Bulletin</u>, Vol. 34, No. 9 (1989) pp. 2109.

Plasma Heating by Collisional Magnetic Pumping in a Magnetic Mirror Configuration.[*] MIN WU and J. REECE ROTH, University of Tennessee, Knoxville, TN 37996-2100 -- This paper presents results from the experimental application of collisional magnetic pumping to plasma heating. This heating is accomplished by superimposing a sawtooth magnetic perturbation on a DC magnetic field in a steady-state Penning discharge plasma in a magnetic mirror configuration[1-2]. Experimental data relating the electron kinetic temperature to such plasma parameters as the electron kinetic temperature, the electron number density, and the background steady-state confining magnetic field will be presented. In addition, the effects of two primary variables of the collisional magnetic pumping driving circuit, the rf driving frequency and the maximum exciter coil current, on the electron kinetic temperature will be reported. The diagnostic used to measure the change in electron kinetic temperature during collisional magnetic pumping is a Langmuir probe.

1. Wu, Min, L. Jiang, and J. R. Roth, APS Bulletin Vol. 33, No. 9, p2019, (1988).
2. Wu, Min, P. F. Keebler, and J. Reece Roth, Proceedings of the 1989 IEEE International Conference on Plasma Science, May 22-24, 1989, Buffalo, NY, IEEE Catalog #89CH2760-7 (1989) pp. 73-4.

Wu, M. and Roth, J. R.: "Plasma Heating by Collisional Magnetic Pumping in a Magnetic Mirror Configuration", APS Bulletin, Vol. 34, No. 9 (1989) pp. 2132-33.

MICROWAVE INTERACTIONS WITH A MAGNETIZED PLASMA NEAR THE ELECTRON CYCLOTRON FREQUENCY*

L. Henry Combs, Chaoyu Liu, and J. Reece Roth

UTK Plasma Science Laboratory
Department of Electrical and Computer Engineering
University of Tennessee
Knoxville, Tennessee 37996-2100

ABSTRACT

Microwave absorption and reflection is being investigated near electron cyclotron resonance of a hot, magnetized plasma for the ordinary and extraodinary modes of propagation, and over a range from 2 to 18 GHz. In an initial study[1], a microwave beam was made to propagate along the axis of a magnetic mirror field at frequencies between 4 and 10 GHz. These studies revealed broad-band absorption of up to 20 dB over most of this range, in plasma with densities of no more than 10^{11} per cubic centimeter. In later work[2], a microwave beam propagating across a uniform magnetic field in the ordinary mode was investigated. This study revealed what are presumed to be hot plasma effects not predicted by the Appleton equation, including an asymmetric absorption resonance, secondary absorption peaks, and an unaccounted for degree of attenuation away from the resonance peak.

This paper will describe new experimental investigations on the attenuation and reflection of a microwave beam propagating across a magnetic field uniform to within 1% in the plasma volume, in the ordinary and extraordinary modes. These attenuation and reflection measurements are made with a Hewlett-Packard model 8510 high frequency network analyzer, which is capable of operating over frequencies from 45 MHz to 18 GHz. Experimental data such as the plasma attenuation and reflection, absorption peak half-width, and phase angle will be measured as functions of the plasma parameters, and compared with the predictions of cold plasma theory as described by the Appleton equation. The classical Penning discharge used to generate the plasma consists of an approximately uniform magnetic field with a maximum value of 0.32 Tesla, corresponding to electron cyclotron resonance at approximately 9 GHz. The plasma is steady state, approximately 12 cm in diameter, and has densities ranging up to 10^{11} per cubic centimeter.

1. L. Jiang, Min Wu and J. Reece Roth, APS Bulletin, Vol. 25, No. 27, p. 1900, (1988).
2. L. Jiang, Min Wu and J. Reece Roth, Proceedings of The 16th IEEE International Conference on Plasma Science, IEEE Catalog #9CH2760-7 (1989) pp. 145-46.

6R 20 **Studies of Microwave Absorption by a Plasma Near the Electron Cyclotron Frequency**[*] L. HENRY COMBS, CHAOYU LIU, and J. REECE ROTH, University of Tennessee, Knoxville, TN 37996-2100. -- We report experimental measurements on the absorption of microwave radiation near the electron cyclotron frequency which propagates in the extraordinary mode, in a single pass, through a weakly ionized, turbulent, Penning discharge plasma. The plasma number density was on the order of $10^9/cm^3$, and the plasma diameter was approximately 12 centimeters. We report the absorption in dB as a function of the electron number density, the level of turbulence, and of other plasma parameters. Our results are compared with a cold plasma theory based on Appleton's equation, and are based on propagation between specially designed horns connected to a HP 8510 microwave network analyzer. We find that a single pass through such a plasma is sufficient to provide several tens of dB of attenuation, and that this agrees with cold plasma theory.

Space-Charge Wave Theory of FEL*

Liu, Shenggang

University of Tennessee, Knoxville

Abstract

The linear theory of Free Electron Laser (FEL) is provided from the point of view of space-charge waves. It is shown that this formulation is helpful in understanding the beam-wave interaction physics in FELs. To enhance the interaction efficiency by taking advantage of the space-charge wave, a new kind of hybrid free electron laser with a periodic structure is proposed.

A Special Quasi-Optical High Power Combiner System[*]

Xie Wengkai[*]; Liu Shenggang[**]

Abstract

A high power millimeter and submillimeter combiner by means of a special axisymmetric three-mirror Quasi-optical system is presented, and its theoretical analysis is given in this paper. Experimental verification has been carried out and the results are discussed.

[*]China University of Electronic Science and Technology, Chengdu. P.R.C.

[**]University of Tennessee, Knoxville. Visiting Distinguished Professor.

RELATIVISTIC THEORY OF THE TWO INTERPENETRATING BEAM - PLASMA INTERACTION*

by

Shenggang Liu, Senior Member, IEEE
Visiting Distinguished Professor
and
J. Reece Roth, Fellow, IEEE
Professor of Electrical Engineering

Plasma Science Laboratory
Department of Electrical and Computer Engineering
University of Tennessee, Knoxville   37996-2100

ABSTRACT

The beam-plasma interaction resulting from two equal density, oppositely directed electron beams interacting with heavy background ions has been studied both theoretically and experimentally in previous work (1,2). The nature of the interaction mechanism considered in this paper is illustrated schematically in Figure 1, a less constricted version of the model considered in references 1 and 2. We use perturbation theory to
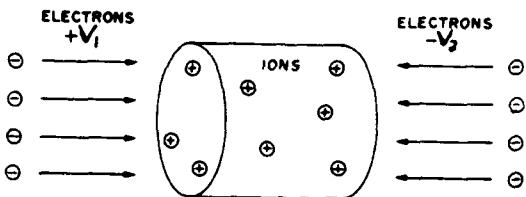
extend the previous non-relativistic model to include relativistic electron beams and the influence of relativistic effects on the beam-plasma interaction. In addition, the previous model was restricted to oppositely-directed electron beams with equal speeds interacting in a heavy-ion plasma. We generalize this model to include, along with relativistic effects, two beams of unequal velocity which are either parallel or anti-parallel. This generalized theory not only exhibits relativistic effects explicitly, but also facilitates comparison with familiar devices and processes such as the traveling wave tube, the Buneman instability, and the Pierce instability. A general relativistic dispersion equation has been obtained, and a new class of FEL based on this relativistic interaction is proposed (3).

1.   J. R. Roth, I. Alexeff, and R. Mallavarpu, Phys. Rev. Letters, Vol. 43, No. 6 (1979) pp. 445-49.

2.   I. Alexeff, J. R. Roth, J. D. Birdwell, and R. Mallavarpu, Physics of Fluids, Vol. 24, No. 7 (1981) pp. 1348-57.

3.   Shenggang Liu, Nuclear Instr. and Methods, Vol. A296, (1990) pp. 403-.

REFLECTION OF ELECTROMAGNETIC RADIATION FROM A NON-UNIFORM PLASMA SLAB AT AN ARBITRARY ANGLE OF INCIDENCE*

Mounir Laroussi and J. Reece Roth

UTK Plasma Science Laboratory
Department of Electrical and Computer Engineering
University of Tennessee
Knoxville, Tennessee 37996-2100

In this paper, we study the transmission, reflection, and absorption of microwave radiation near the electron cyclotron frequency by a non-uniform plasma slab. The wave is launched at an arbitrary angle of incidence (Fig. 1).
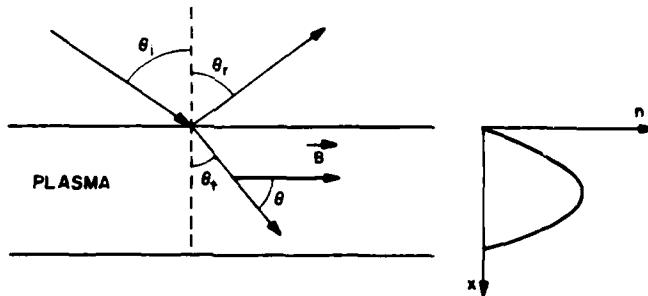

Fig. 1. Microwaves incident on a non-uniform plasma

Our plasma model is a cold, steady state, weakly ionized slab with a uniform background magnetic field parallel to the surface. The plasma density profile is parabolic with a maximum at the center. This geometry is intended to approximate the cylindrical plasma column which is the subject of our experimental measurements. We find that a single pass through such a plasma provides several tens of dB of attenuation across the slab diameter, and in the reflected signal. The transmission, reflection, and absorption depend on the magnetic field, number density, collision frequency, and the angle of incidence. These parametric dependences are calculated for our model from cold plasma theory (Ref. 1). These computer simulations are compared with experimental measurements made previously (Ref. 2), and more recently, on a plasma generated by a classical Penning discharge, using a network analyzer as a diagnostic instrument.

(1) M. A. Heald and C. B. Wharton, Plasma Diagnostics With Microwaves, Krieger Pub., Huntington, NY, 1978.

(2) P. D. Spence, "A Study of the Effective Electron Collision Frequency in a Weakly Ionized Turbulent Penning Discharge Plasma", Ph.D. Dissertation, University of Tennessee, Knoxville, August 1990, University Microfilms, Ann Arbor, MI.

Kinetic Theory of Electron Cyclotron Maser with Azimuthal Standing Wave[*]

Liu Shenggang

University of Tennessee, Knoxville

Abstract

The Kinetic theory of the Electron cyclotron maser and gyrotron with azimuthal standing wave has been carried out in this paper. The dispersion equation of ECRM and the starting current of the gyromonotron are given. The analysis shows that the right-hand rotating waves produce the right-hand cyclotron harmonics and the left-hand rotating waves give the left-hand cyclotron harmonics. It turns out that the beam-waves interactions of the two rotating wave are different from each other. The standing wave pattern in the azimuthal direction, therefore, may not remain during the interaction process and mode competition may take place.

Kinetic Theory of the Electron Cyclotron Maser with Asymmetry Between Electron Beam and Cavity*

Liu Shenggang

University of Tennessee, Knoxville

Abstract

The kinetic theory of Electron Cyclotron Maser (ECM) with asymmetry between theelectron beam and cavity is given in the paper. The dispersion equation of ECM and the expressions for starting current and frequency shift of the gyromonotron with asymmetry between beam and cavity have been derived and discussed.

Numerical and Experimental Investigations of the Attenuation of Microwaves by a Non-Uniform Plasma*

MOUNIR LAROUSSI, CHAOYU LIU, and J. REECE ROTH, University of Tennessee, Knoxville, TN 37996-2100 -- Experimental measurements have been made on the attenuation of microwave radiation by an axisymmetric, cylindrical, non-uniform magnetized plasma generated in a classical Penning discharge. The wave is launched in the extraordinary mode. The transmitting and receiving horns are connected to an S-parameter test set of a HP 8510 network analyzer which measures the transmission and reflection of the wave[1]. The radial number density profile is measured by a Langmuir probe and may be hollow, flat, or peaked on the plasma axis. The experimentally determined radial profile is entered into our computer simulation and a comparison between the experimentally measured attenuation and the simulation results is accomplished. Our simulation is based on cold plasma theory[2] and has been improved from a slab model to a cylindrical one.

(1)   M. Laroussi and J. Reece Roth, Proceedings of the 1991 IEEE International Conference on Plasma Science, Williamsburg, VA, CAT #91CH3037-9 (1991), p. 146.
(2)   M. A. Heald and C. B. Wharton, Plasma Diagnostics with Microwaves, Krieger Pub. Huntington, N. Y., 1978.

EXPERIMENTAL GENERATION OF A
STEADY-STATE GLOW DISCHARGE
AT ATMOSPHERIC PRESSURE*

J. Reece Roth, Mounir Laroussi, and Chaoyu Liu
UTK Plasma Science Laboratory
Department of Electrical and Computer Engineering
University of Tennessee
Knoxville, Tennessee 37996-2100

ABSTRACT

In industrial plasma engineering, a steady-state atmospheric glow discharge would allow many surface modification and other plasma processing operations to be carried out under atmospheric conditions, rather than in expensive vacuum systems which enforce batch processing. In this paper, we report some encouraging results of an experimental program conceived independently of the work reported by Kanda, et al. (Ref. 1). Our experiments were conducted on an experimental apparatus shown schematically in Figure 1. A parallel plate plasma reactor with square electrodes 25 cm on a side, covered with an insulating surface (rubber or glass), and with variable spacing, was set up in an enclosed box which made it possible to control the type of working gas used. This reactor was energized by a very specialized RF power supply capable of supplying up to 5 kilowatts of RF power at rms voltages up to 5 kilovolts, and over a frequency range from 1 kHz to 100 kHz.
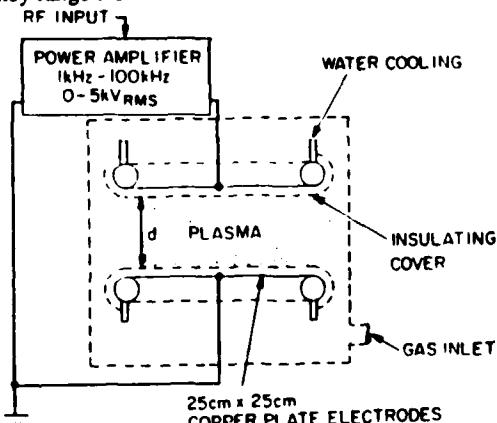
Figure 1. Atmospheric Plasma Reactor

We performed experiments at one atmosphere in helium, a mixture of helium and air, and, after Kanda, et al., argon with an admixture of acetone. We have been able to generate a steady state glow discharge in one atmosphere of helium at an electrode separation of 4.5 cm, yielding a 2.8 liter volume of helium plasma at one atmosphere. The power levels appeared to be low, no more than a few hundred watts. The largest volume helium plasma was achieved with 5 kV rms applied to the electrodes with a frequency in the vicinity of 4 kHz. Higher and lower frequencies were less effective. With electrode separations less than 4.5 cm in helium, the plasma was uniform. Similar volumes of plasma have been produced at one atmosphere in argon with acetone vapor. Work is continuing to maintain a steady-state glow discharge in atmospheric air.

1) N. Kanda, M. Kogoma, H. Jinno, H. Uchiyama, and S. Okazaki, Paper 3.2-20, Proc. 10th Intl. Symposium on Plasma Chemistry, Vol. 3 (1991).

2B3

A Plasma Filled Tunable Notch Absorber Microwave Filter*

Mounir Laroussi

Plasma Science Laboratory
University of Tennessee
Knoxville, Tennessee 37996-2100

At the Plasma Science Laboratory of the University of Tennessee,Knoxville,we have built and operated a compact,tunable microwave filter. This device is a direct spin-off of our plasma cloaking research[1]. It is basically a magnetized cylindrical plasma column(see Fig.1).
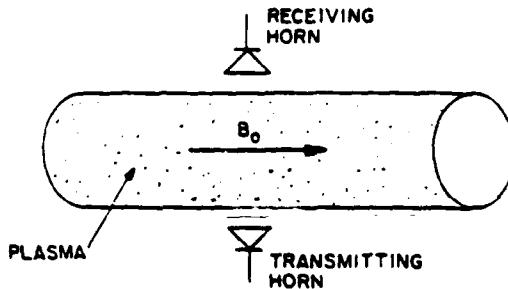
Fig.1 Cylindrical-shaped filter

When a microwave propagating in the extraordinary mode traverses the plasma column,it is attenuated if its frequency is near the electron cyclotron frequency. This attenuation occurs according to the Appleton equation [2],[3]. The bandwidth and depth of the attenuated band are functions of the collision frequency and the plasma number density. The center frequency of the attenuated band can be preselected by adjusting the applied axial magnetic field strength. This filter could have various applications in broadband microwave measurement systems, by removing aliasing,unwanted harmonics,and spurious signals. Performance data will be reported.

[1]   J.R.Roth,"Microwave Absorption System",United States Patent #4,989,006,Jan.29,1991.

[2] M.A. Heald and C.B. Wharton,Plasma Diagnostics with Microwaves,Krieger Pub.,Huntington,N.Y.,1978.

[3] M.Laroussi,C.Liu,and J.R.Roth,"Numerical and Experimental Investigations of the Attenuation of Microwaves by a Non-Uniform Plasma",APS Bulletin,Vol.36,No.9,p.2485, October 1991.

M. Laroussi: "A Plasma-Filled Tunable Notch Absorber Microwave Filter", Proc. 1992 IEEE International Conference on Plasma Science, Tampa, FL, June 1-3, 1992 IEEE Cat. #92TH0460-6 Paper 2B3, p. 106 (1992).

8P 27 <u>Characteristics of a Steady-State, Low Power Glow Discharge at Atmospheric Pressure.</u>* C. LIU and J. R. ROTH, <u>UTK Plasma Science Laboratory, University of Tennessee, Knoxville, TN 37996-2100</u>.

We have generated a steady-state, low power glow discharge at one atmosphere pressure in helium, a mixture of helium and air, and, after Kanda, et al. (ref. 1), argon with a mixture of acetone. The plasma·can be made uniform, and occupy volumes as large as 2.8 liters. Power inputs have ranged from below 60 watts to as much as 180 watts, and are proportional to the excitation frequency. Our plasma reactor consists of two plane parallel plates 25 cm on a side, covered by an insulating layer, and separated by up to 5 cm. The plates are energized by an RF power supply which can deliver up to 5 kV rms over the frequency range from 1 kHz to 100 kHz. The glow discharge is resistive at low frequency, and capacitive at high frequency. We will report on the phase angle between the voltage and current waveforms as a function of frequency, and the behavior of the power input as a function of frequency and of the type of gas.

1. N. Kanda, M. Kogoma, H. Jinno, H. Uchiyama, and S. Okazaki: Paper 3.2-20, Proc. 10th Intl. Symposium on Plasma Chemistry, Vol. 3 (1991).

Liu, C.; Chen, D.; and Roth, J. R.: Characteristics of a Steady-State, Low Power Glow Discharge at Atmospheric Pressure. <u>APS Bulletin</u> Vol. 37 (1992) p. 1563.

PLASMA-RELATED CHARACTERISTICS OF A STEADY-STATE GLOW DISCHARGE AT ATMOSPHERIC PRESSURE*

C.Liu, and J.R.Roth
UTK Plasma Science Laboratory
University of Tennessee
Knoxville, TN 37996-2100.

ABSTRACT

Following Kanda, et al.(ref.1), We have generated a large volume (up to 2.8 liters), low power (less than 200w), steady-state glow discharge plasma (ref.2) which allows many surface modification and other plasma processing operations to be carried out at one atmosphere, rather than in expensive vacuum systems which enforce batch processing. We have shown that the phase angle between the maximum of the voltage waveform and current breakdown is a function of frequency (1KHz to 100KHz) as well as voltage (up to 5KV(RMS)). Also the power increases with RF frequency as well as voltage (ref. 2).

The present study concentrates on the plasma-related characteristics and surface-treatment applications of this atmospheric pressure, steady-state glow discharge. The plasma floating potential will be measured as a function of RF frequency, RF voltage, and type of working gas. Helium, a mixture of helium and air, and argon will be used as working gases. The results of surface treatment of organic materials also will be reported. This plasma can modify the physical, chemical and electrical surface properties of the materials. We will show some correlations between the type and extent of the surface modifications and the plasma discharge parameters.
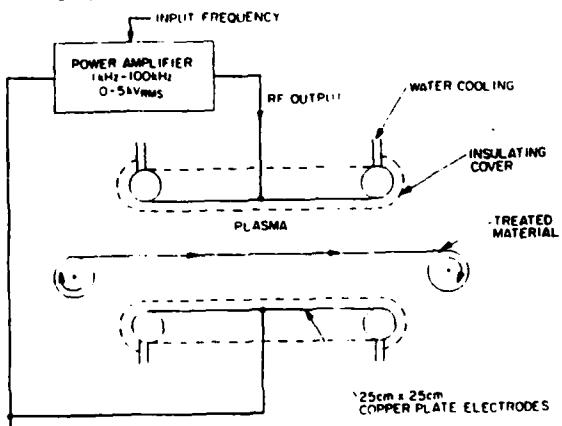
Fig.1 The experimental set up.

1. N.Kanda, M.Kogoma, H.Jinno, H.Uchiyama, and S.Okazaki: Paper 3.2-20, Proc. 10th Intl. Symposium on Plasma Chemistry, Vol.3 (1991). pp 3.2-20-1 to 3.2-20-4
2. C.Liu, and J.R.Roth: Paper 8P-27, 34th Annual Meeting of the APS Division of Plasma Physics, Seattle. Series II, Vol. 37, No.6 (1992). p 563

1S 18 <u>Preliminary Measurements of the Plasma Properties of a One Atmosphere Glow Discharge Plasma</u>* J. REECE ROTH, PAUL D. SPENCE, and CHAOYU LIU, <u>University of Tennessee, Knoxville, TN 37996-2100</u>.-- We have recently generated a uniform glow discharge at one atmosphere in helium, argon , and other gases. The active species from the plasma are useful for various forms of plasma surface treatment, such as improving the wettabiity, wickability, and printability. of fabrics made of PPL, nylon, and other normally non wettable materials. This superficial treatment can be done without batch processing, or the capital and energy costs of a vacuum system. In this paper we will report on the plasma related characteristics of the glow discharge plasma, and measurements designed to experimentally check a theory which predicts the range of frequencies which produce a positive space charge build-up, and hence the regime which produces uniform discharge.

(1)   C. Liu, P. Tsai and J. R. Roth: Paper 2P18, 20th IEEE Intl. Conference on Plasma Science, 93CH3334-0, p. 129 (1993).

1P26

AN ATMOSPHERIC GLOW DISCHARGE PLASMA FOR AERODYNAMIC BOUNDARY LAYER CONTROL*

Chaoyu Liu and J. Reece Roth
Dept. of Electrical and Computer Engineering
University of Tennessee
Knoxville, Tennessee 37996 USA

Abstract

A steady-state uniform glow discharge plasma has been generated between two insulated, parallel electrodes at one atmosphere pressure in helium, air, and other gases in the UTK Plasma Science Laboratory[1]. Preliminary measurements of this plasma have been reported.[2] Industrial applications of the atmospheric glow discharge plasma have been studied[3]. Exploratory research to extend this mechanism to the formation of a plasma layer on the surface of aircraft is underway in our lab. We intend to use the plasma layer to effect boundary layer control, using the electric field body force to reduce drag, minimize turbulence, and accelerate or decelerate the boundary layer on the surface of an aircraft. In this paper, we will report recent experimental results from our exploratory research program, aimed at creating a layer of uniform glow discharge plasma on the skin of a model aircraft at one atmosphere in several working gases, including air. The characteristics of this surface layer of uniform glow discharge plasma also will be reported.

[1] Roth, J. R.; Liu, C.; and Laroussi, M.: Experimental Generation of a Steady-State Glow Discharge at Atmospheric Pressure. 1992 IEEE International Conference on Plasma Science, Tampa, FL, June 1-3, 1992. IEEE Cat. #92TH0460-6, (1992) pp.170-171.

[2] Roth, J. R.; Spence, P. D.; and Liu, C.: Preliminary Measurements of the Plasma Properties of a One Atmosphere Glow Discharge Plasma. APS Bulletin Vol. 38 (1993) p.1901.

[3] Roth, J. R.; Wadsworth, L. C.; Spence, P. D.; Tsai, P. P.-Y.; and Liu, C.: One Atmosphere Glow Discharge Plasma for Surface Treatment of Nonwoven Textiles. Proc. 3rd Annual TANDEC Conference, Nov. 1-3, 1993, Knoxville, TN (1993).

APPENDIX C

AIR FORCE SPONSORED PATENTS AND PATENT FILINGS

United States Patent [19]

Roth

[54] MICROWAVE ABSORPTION SYSTEM

[75] Inventor: John R. Roth, Knoxville, Tenn.

[73] Assignee: The United States of America as represented by the Secretary of the Air Force, Washington, D.C.

[21] Appl. No.: 425,141

[22] Filed: Oct. 17, 1989

[51] Int. Cl.⁵ H01Q 17/00
[52] U.S. Cl. 342/1; 342/2
[58] Field of Search 342/1, 2

[56] References Cited

U.S. PATENT DOCUMENTS

3,127,608   3/1964   Eldredge 343/18
3,713,157   1/1973   August 343/18
3,773,684 11/1973   Marks 252/309
4,030,098   6/1977   Roth .
4,791,419 12/1988   Eubanks 342/1

OTHER PUBLICATIONS

L. Jiang et al, "Experimental Results of Microwave Absorption with Varying Magnetic Field in A Modified Penning Discharge", Presented at the Thirtieth Annual Meeting of the APS Division of Plasma Physics, Hollywood, Fla. Oct. 31–Nov. 4, 1988, APS Bulletin, vol. 33, No. 9, p. 1900 (1988).

Primary Examiner—Nelson Moskowitz
Assistant Examiner—Mark Hellner
Attorney, Agent, or Firm—William G. Auton; Donald J Singer

[57] ABSTRACT

Microwave absorption in a varying magnetic field is investigated near electron cyclotron resonance with a network analyzer which is capable of swept frequency measurements, and of measuring reflection and transmission coefficients from 0.045 to 18 GHz, with greater than 80 dB dynamic range. The experimental conditions are such that the plasma is generated in a modified Penning discharge in a magnetic mirror configuration. A microwave beam is caused to propagate along the axis of the magnetic mirror field in the plasma column. The microwave beam is attenuated near the electron cyclotron resonance frequency, providing microwave absorption over a range of frequencies spanning the electron cyclotron frequencies present in the axially varying magnetic field. The attenuation, along with hot-plasma effects, are measured as a function of frequency by the network analyzer.

14 Claims, 7 Drawing Sheets
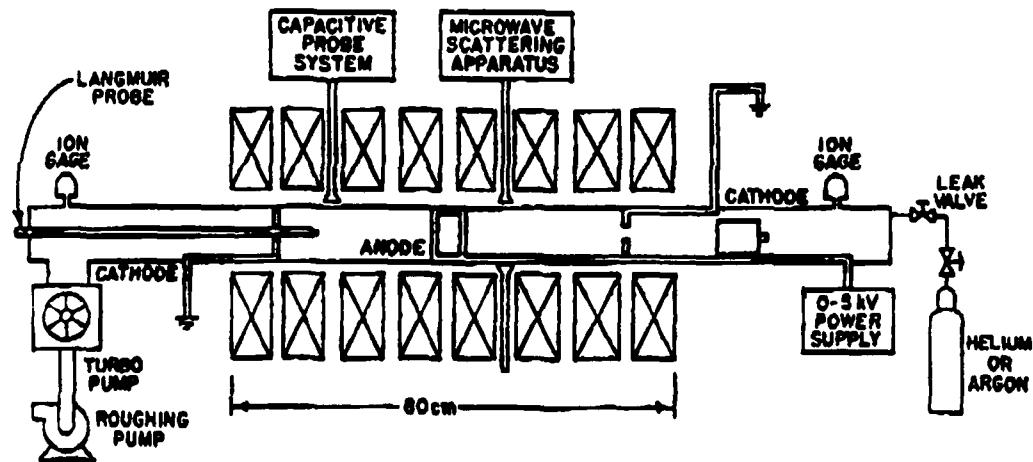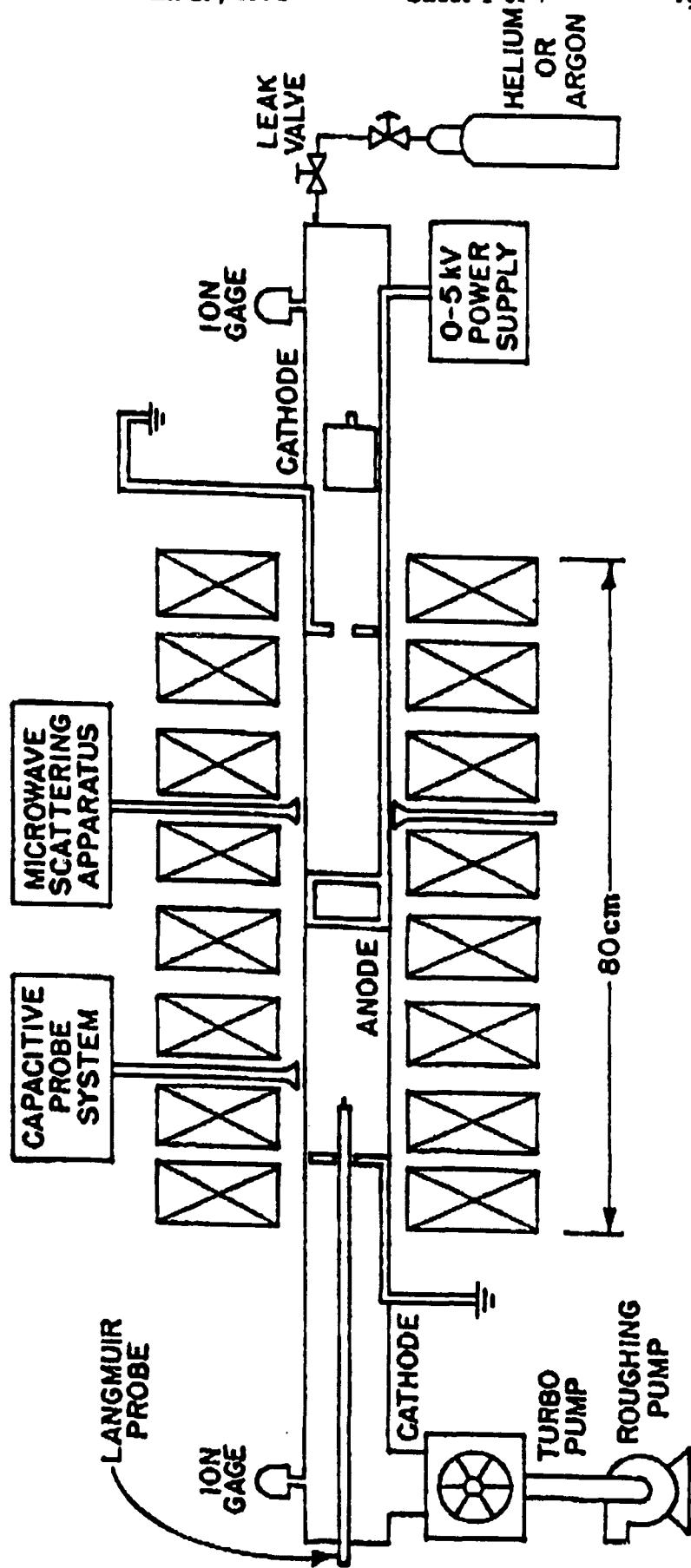
FIG. 1

FIG. 2

$\bar{n} = 1.5 \times 10^9 /cm^3$

NUMBER DENSITY (cm^3)

ANODE

DISTANCE FROM CATHODE (cm)

FIG. 3

Te=9.5eV

ELECTRON KINETIC TEMPERATURE (eV)

ANODE

DISTANCE FROM CATHODE (CM)

FIG. 4

TRANSMITTING HORN   RECEIVING HORN

B

PLASMA

NETWORK ANALYZER

S-PARAMETER TEST SET

FIG. 5

ATTENUATION (dB)

12

0

-12

-24

-36

-48

9.5   9.6   9.7   9.8   9.9   10

FREQUENCY (GHz)

FIG. 6

WAVE GUIDE

CATHODE 110

CATHODE

ANODE RING 120

PLASMA 150

MAGNET COILS 161-164

CATHODE 100

WAVE GUIDE 190

FIG. 7

ATTENUATION, dB

FREQUENCY, GHz

FIG. 8

FREQUENCY, GHz

FIG. 9

REFLECTED POWER, dB

SCALE
10.0 dB/div

FREQUENCY, GHz
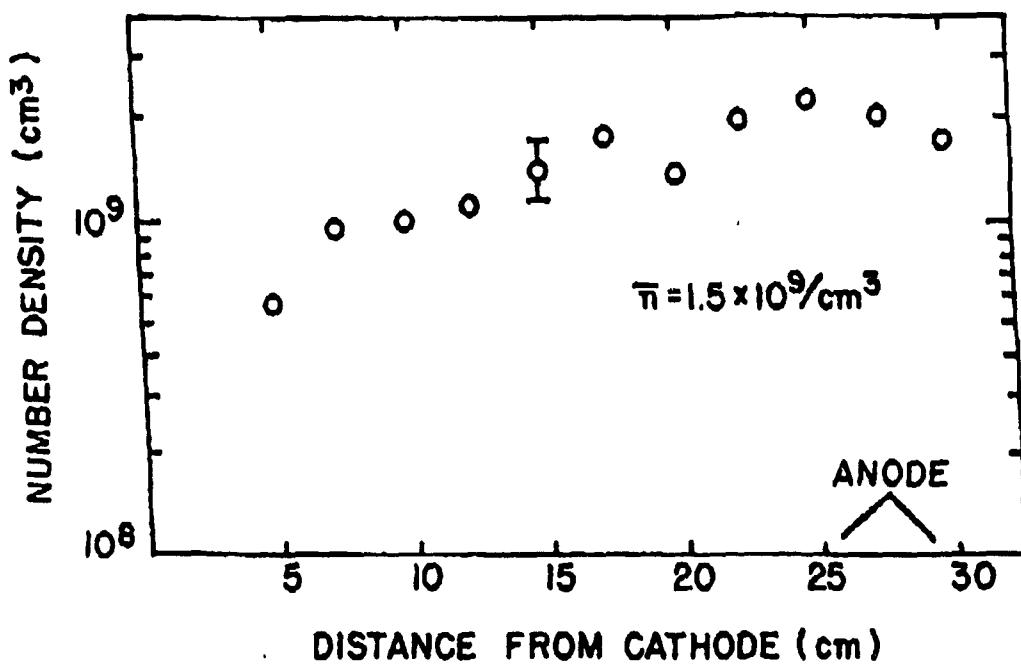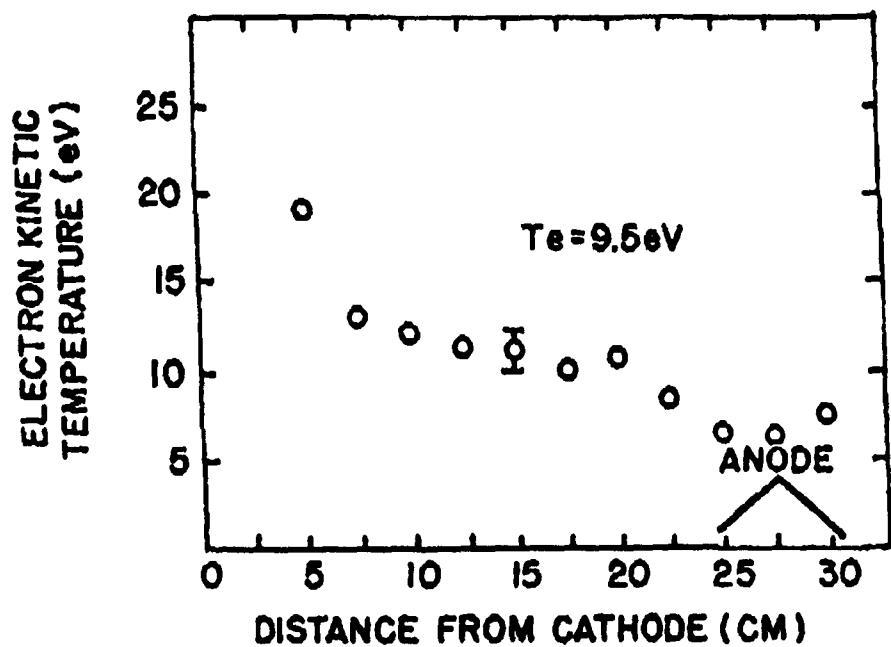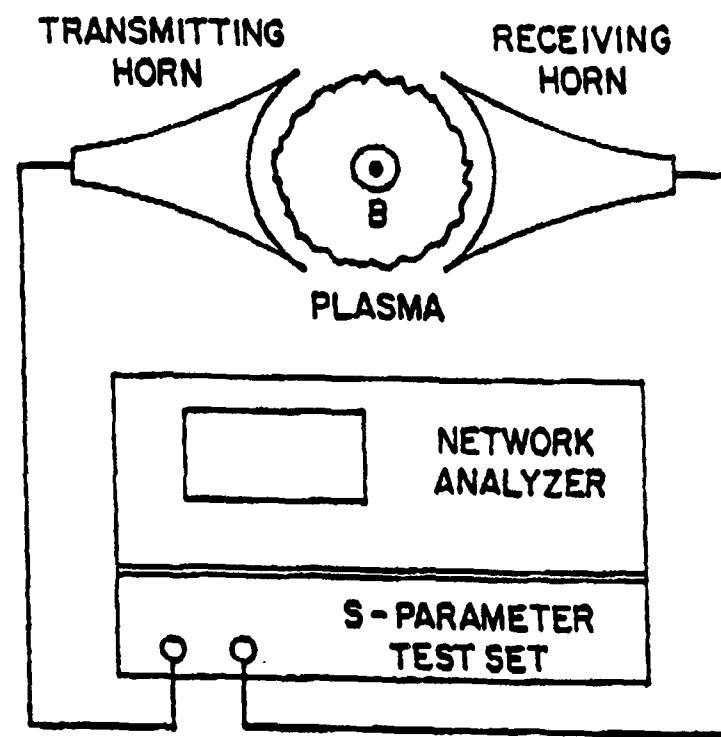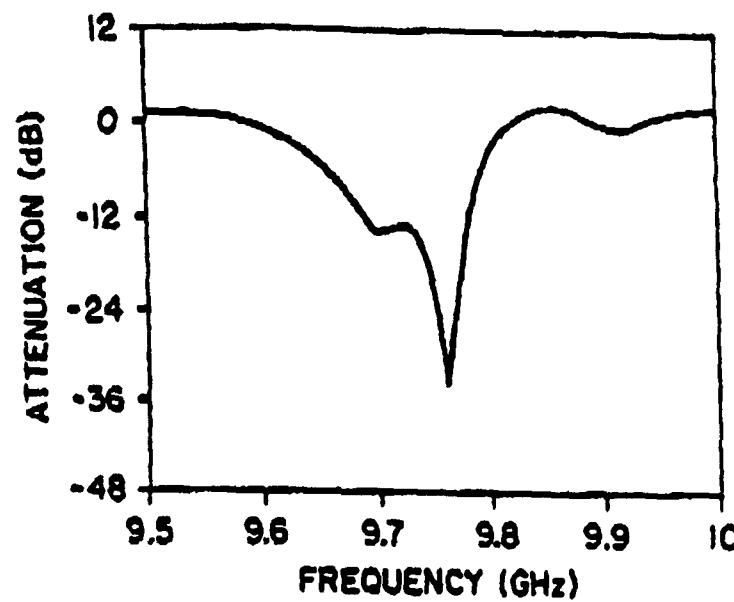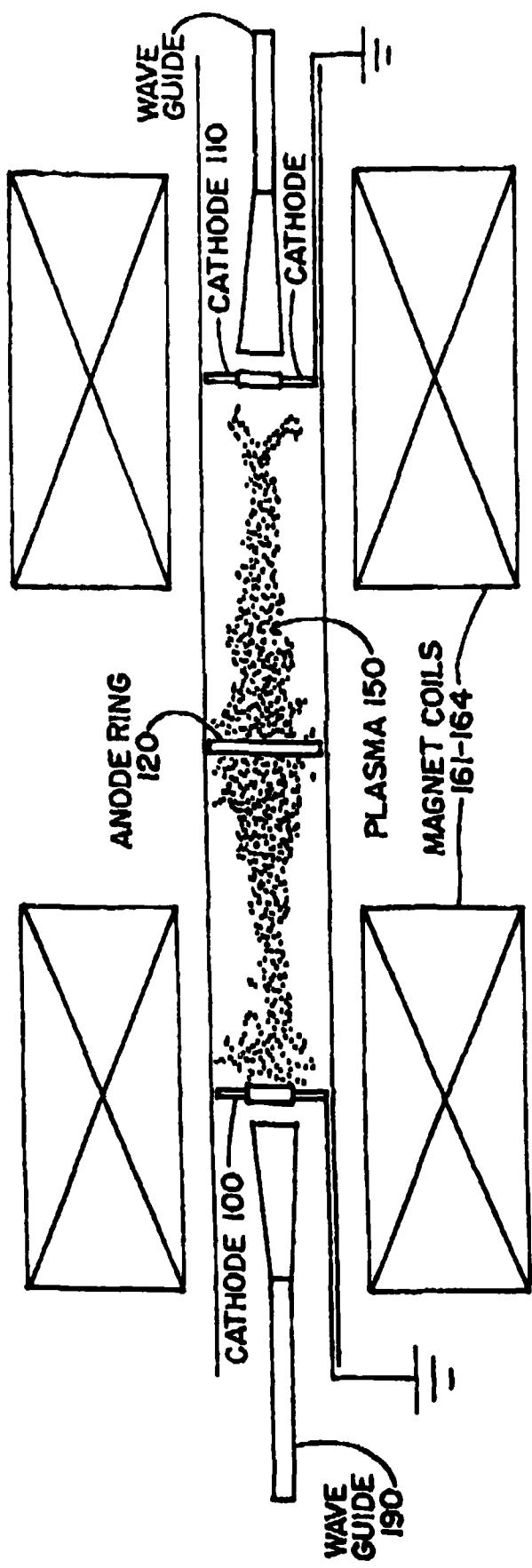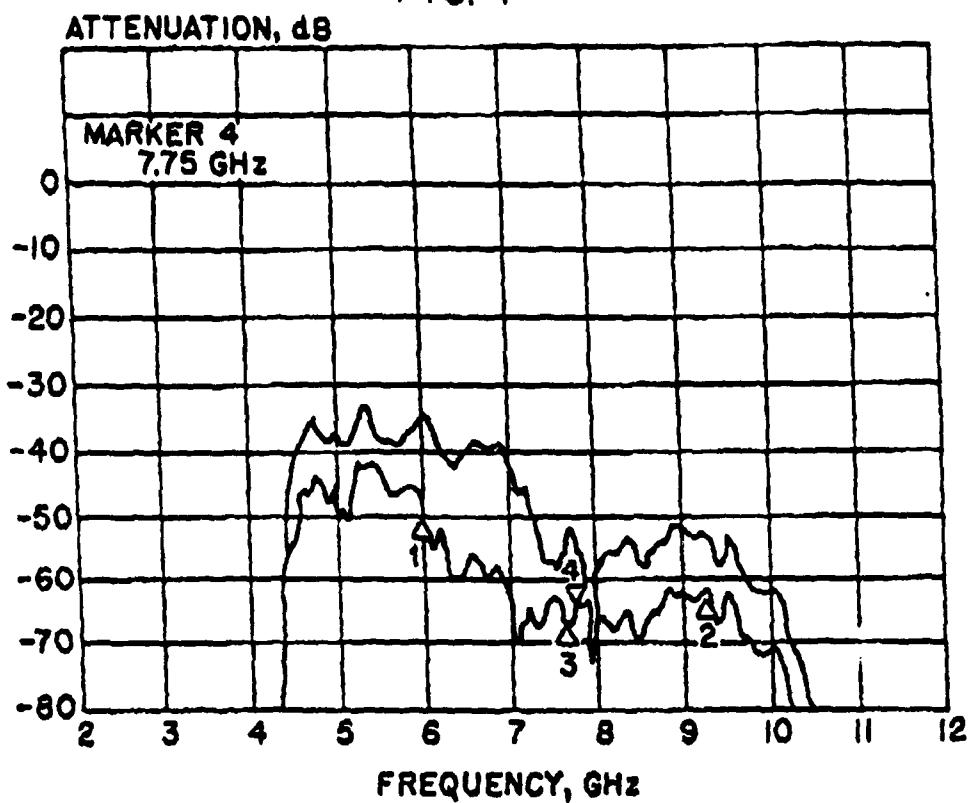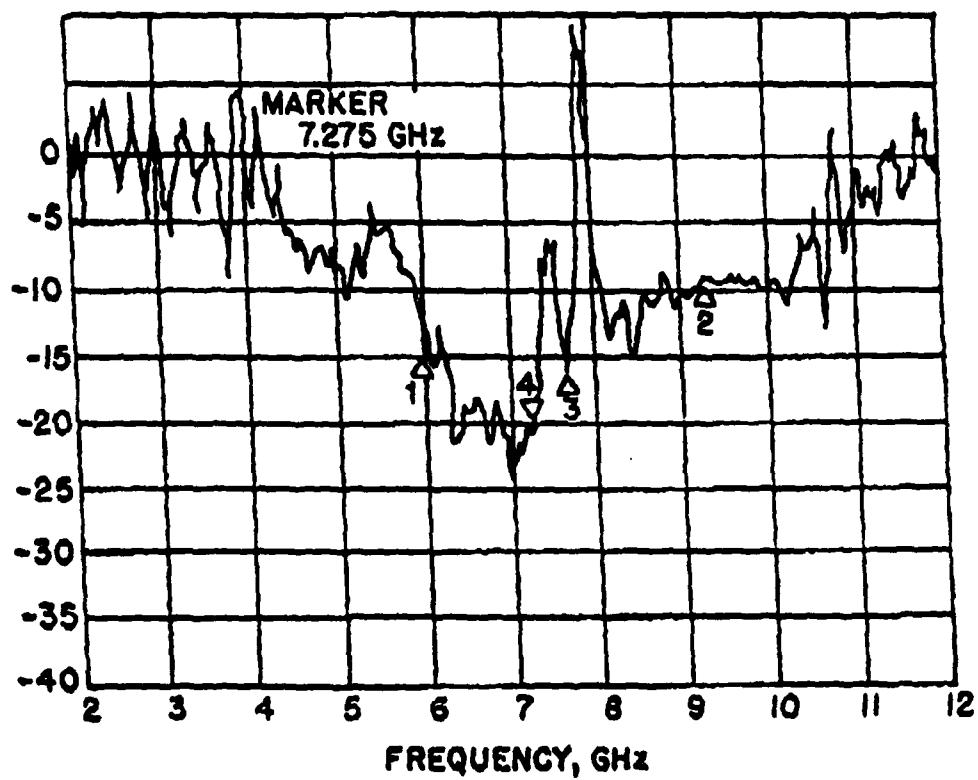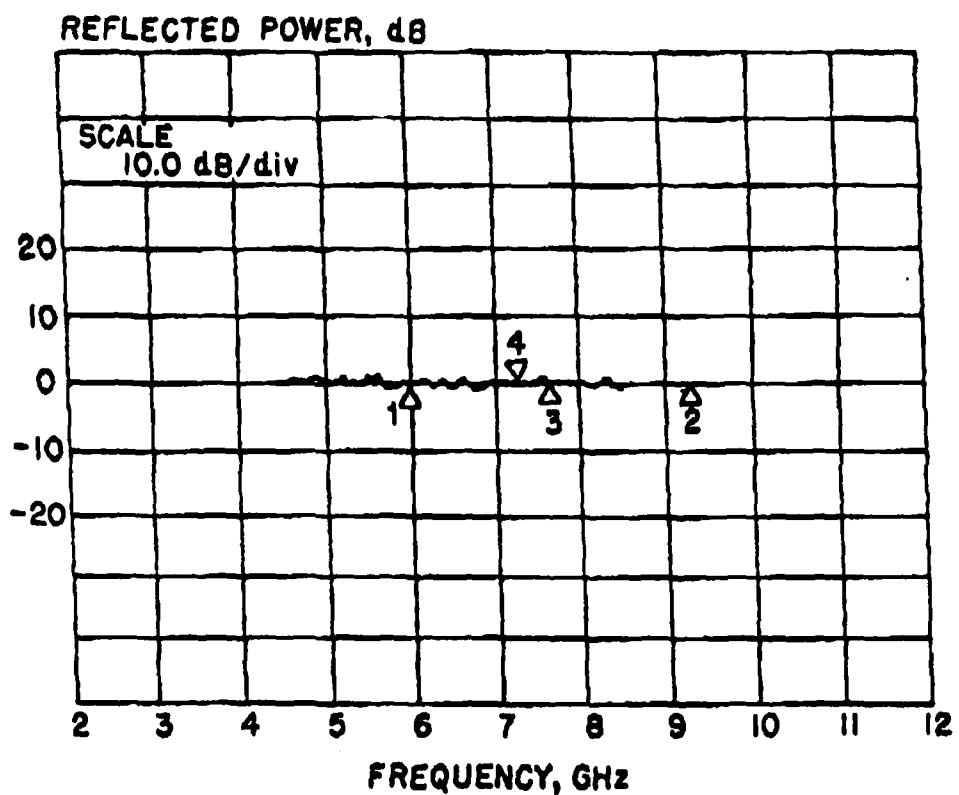
FIG. 10

ATTENUATION VS. ANODE CURRENT

- I_{coll} = 550 A
- X I_{coll} = 600 A
- + I_{coll} = 700 A
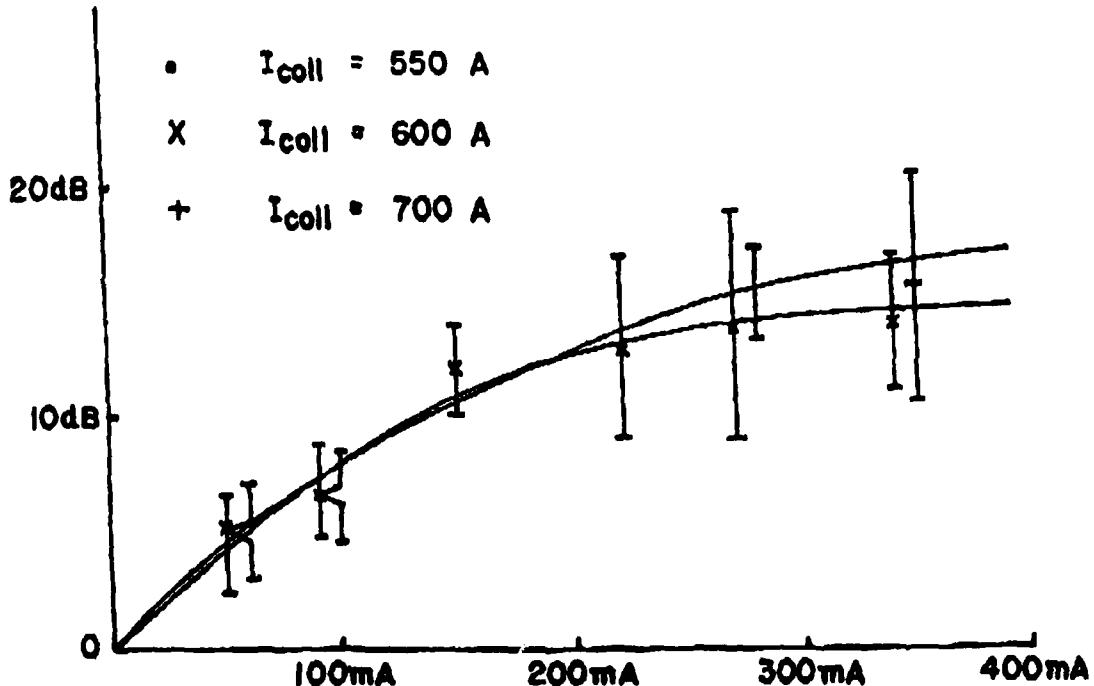
FIG. 11
(PRIOR ART)
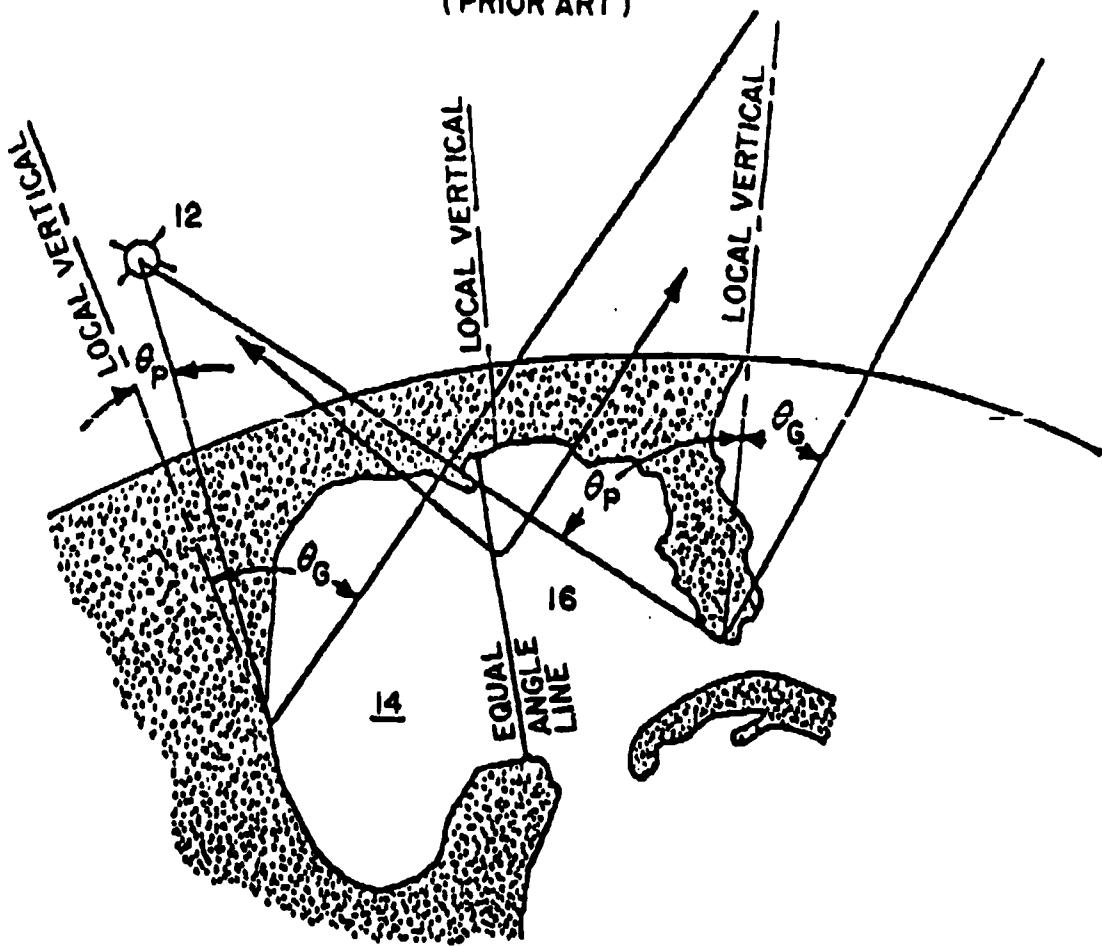
FIG. 12
(PRIOR ART)

4,989,006

1
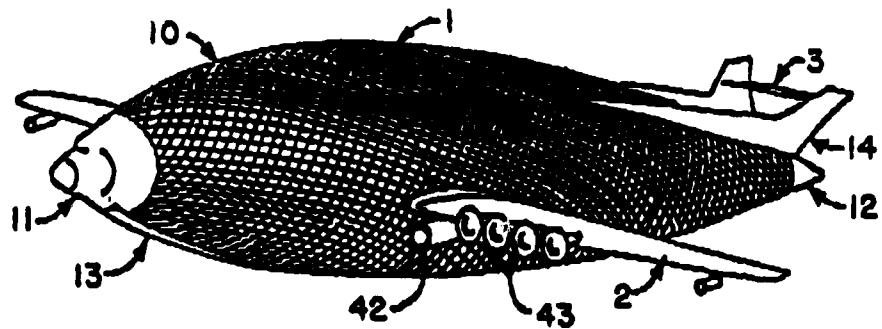
MICROWAVE ABSORPTION SYSTEM

STATEMENT OF GOVERNMENT INTEREST

The invention described herein may be manufactured and used by or for the Government for governmental purposes without the payment of any royalty thereon.

BACKGROUND OF THE INVENTION

The present invention relates generally to aircraft protection and antidetection systems and more specifically the invention pertains to a plasma cloaking device which provides microwave absorption using a varying magnetic field.

Traditional aircraft antidetection systems are divided into two broad categories: active systems (which generate radar jamming signals); and passive systems, which rely on some characteristics of the vehicle to reduce the radar return. When the radar jamming transmitter is located on the target aircraft, the jamming signal transmitted by the aircraft can sometimes act as a beacon to the radar tracking system. Passive systems, which include the use of radar absorbing materials on the vehicle's surface, are limited in their ability to reduce the vehicle's radar cross section.

The task of providing a microwave absorption system which can reduce the detectability of satellites and aircraft, and which can protect targets from directed energy weapons is alleviated, to some extent, by the systems disclosed by the following U.S. Patents, the disclosures of which are incorporated herein by reference:

U.S. Pat. No. 3,127,608, A. L. Eldridge, Object Camouflage Method and Apparatus;

U.S. Pat. No. 3,713,157, Henry August, Energy Absorption by a Radioisotope Produced Plasma;

U.S. Pat. No. 3,773,684, Alvin M. Marks, Dipolar Electro-Optic Compositions and Method of Preparation; and

U.S. Pat. No. 4,791,419, Gary R. Eubanks, Microwave Absorbing Means.

The August patent, Energy Absorption by a Radioisotope Produce Plasma, which describes a means of attenuating electromagnetic radiation passing through an ionized gas plasma adjacent to a body, teaches placing a radioisotope material on a surface of the body in contact with the gaseous medium surrounding the object. Such radioisotope material ejects energetic particles and quanta into the medium and causes ionization of the gas, forming an ionized gas plasma sheath around the object. This plasma sheath would absorb any electromagnetic energy entering it or would so distort any incoming signal that it would be unrecognized as a radar signal upon its return to its source. This patent also suggests superimposing a DC magnetic field upon the plasma in order to enhance attenuation.

The plasma around the object is constantly replaced by the continuous release of energetic particles and quanta into the gaseous medium surrounding the object. Additionally, this patent predicts a decrease in the plasma density as the distance from the object increases, providing impedance matching and a resulting decrease in the reflectivity of the plasma sheath.

The Eldridge Patent, Object Camouflage and Apparatus, teaches rendering an object invisible to radar by use of an ionized gas cloud surrounding the object. A particle accelerator is used to continuously ionize the gas immediately in front of the object and the object's

2

forward progress through the ionized gas cloud provides the necessary coverage of the object. This patent teaches that the ionized gas cloud will attenuate and refract any incident electromagnetic waves, which effectively makes the object invisible to radar.

The Marks Patent, Dipolar Electro-optic Compositions and Method of Preparation, teaches using a suspension of dipolar particles as a light-controlling means. The particles are in suspension and are oriented by the application of an external electric or magnetic field. This patent teaches a method for creating such a device in which the particles are evenly distributed throughout the suspension, have a fast orientation response upon application of the appropriate exterior field, and are sufficiently transparent or reflective to electromagnetic radiation, depending upon orientation, to allow use of the device as a practical light-controlling device.

The Eubanks Patent, Microwave Absorbing Means, defines a device which is designed to absorb the microwave radiation used in traffic control radar by using a microwave antenna connected to a microwave absorbing means. This patent teaches winding a wire around a fluorescent light bulb as a helical microwave antenna. Each end of the antenna is then electrically coupled to the absorbing tube (fluorescent light bulb) so that the microwave radiation received by the antenna is transmitted to the absorbing tube where it is then absorbed by the gas contained within the tube.

While the above-cited references are instructive, they do not acknowledge that a varying magnetic field in proximity with a plasma produces dramatic microwave absorption. More specifically, microwave absorption is enhanced when the varying magnetic field is produced near electron cycloton resonance.

The August reference discussed above teaches the use of a plasma to attenuate radar signals and suggests superimposing a DC magnetic field on the plasma as a means of enhancing attenuation. The Eldridge reference teaches using an ionized gas cloud to cloak an object, but fails to disclose or predict the use of a magnetic field with the ionized gas cloud to increase attenuation of the incident radar signals.

The Eubanks reference teaches the absorption of radar signals so as to reduce or negate any reflected signal, but this reference neither claims nor predicts the use of a dipolar magnetic field supplied with a weak plasma to absorb incoming radar signals. There are no plasmas in this reference.

The Marks reference is not concerned with the absorption of radar signals at all, but is a light-controlling device. There is no plasma present in this reference and a magnetic field, if present, is used for the sole purpose of controlling the orientation of dipolar particles in suspension.

While the above-cited references are instructive, there remains the need to provide a system capable of cloaking a target using a dipolar magnetic field supplied with a weak plasma to absorb probing radar signals. The present invention is intended to satisfy that need.

SUMMARY OF THE INVENTION

The present invention includes a method and apparatus for the plasma cloaking of military targets, such as space satellites or aircraft. This invention includes a superconducting magnetic coil, which will generate a dipole magnetic field, in a target. A weak plasma is supplied to this magnetic field; at orbital altitudes the

4,989,006

<div style="columns:2">

3

field will fill up with plasma as does the earth's magnetosphere, but in the atmosphere a plasma generating means is needed. Incoming radar signals will then enter this plasma and be absorbed.

In an embodiment which has been demeonstrated in the inventor's laboratory, a modified Penning discharge system is used to generate plasma by ionizing helium using: two cathodes, a ring anode and an electrical power source. The two cathodes are on opposite sides of the helium with the ring anode in the middle such that they ionize the helium into the plasma. Note that in such Penning discharge systems, the electrons are forced to oscillate between the two opposed cathodes, and are prevented from going into the ring anode by the presence of a magnetic field. Accordingly, a plurality of magnetic coils surround the cathodes and generate a varying magnetic field with a mirror configuration. As mentioned above, when microwave signals enter the magnetized plasma, they are attenuated, particularly when they reach a magnetic induction which corresponds the electron cycloton resonance frequency.

In operation, the system described above provides a plasma cloaking means by which military targets could be made to disappear from radar screens by surrounding them with a suitable magnetized plasma. These targets include both endoatmospheric aircraft, and exoatmospheric satellites and spacecraft. However, it is important to note that the attenuation of microwave signals is a protective measure against directed energy weapons as well as an antidetection device. More specifically, there exist a category of weapons which directs a powerful electromagnetic pulse (EMP) to disrupt the computer, control and communication system of targets. The present invention provides a magnetized plasma which can attenuate the effects of such threats. In a test configuration, the system described above includes: a radio frequency (RF) transmitter; a transmitting waveguide which conducts the RF signal to radiate near one cathode; a collecting waveguide placed at the opposing cathode; a feed horn receiver which collects and measures the attenuated microwave signals; a computer and a network analyzer which records the attenuation as a measured function of frequency.

As described above, it is an object of the present invention to provide a plasma cloaking system which can hide satellites and aircraft from radar tracking systems.

It is another object of the invention to provide a microwave attenuation system which protects targets from directed energy weapons.

It is another object of the present invention to provide a general purpose microwave signal antidetection system.

These objects together with other objects, features and advantages of the invention will become more readily apparent from the following detailed description when taken in conjunction with the accompanying drawings wherein like elements are given like reference numerals throughout.

DESCRIPTION OF THE DRAWINGS

FIG. 1 is a schematic of a complete Penning discharge system;

FIGS. 2 and 3 are charts of data produced by operation of the system of FIG. 1;

FIG. 2 is a chart of the axial profile of the number density at $V_A = 1.5$ kV, $I_A = 40$ mA, $P = 100$ Torr, $B = 0.255$ T, while FIG. 3 depicts the axial profile

4

of the electron kinetic temperature at $V_A = 1.5$ kV, $I_A = 40$ mA, $P = 100$ Torr, $B = 0.255$ T.

FIG. 4 is an illustration of the test configuration approach to the present invention to measure microwave attenuation produced by a varying magnetized plasma;

FIG. 5 is a chart of attenuation vs. Frequency;

FIG. 6 is a schematic of an embodiment of the present invention;

FIG. 7 is a chart of plasma attenuation, the upper curve is with the plasma off while the lower curve is with the plasma on;

FIG. 8 is a chart of normalized plasma accentuation;

FIG. 9 is a chart of normalized plasma reflection;

FIG. 10 is a chart of attenuation vs. anode current; and

FIGS. 11 and 12 are illustrations of two potential radar targets that can use the present invention as a plasma cloaking system.

DETAILED DESCRIPTION OF THE PREFERRED EMBODIMENT

The present invention includes a system which provides plasma protection by the interaction of electromagnetic radiation with magnetized plasma. The resulting absorption and attenuation of microwave signals allows the present invention to serve as a plasma cloaking device, or a protection system which attenuates the output signals of directed energy weapons.

Plasma cloaking can be effected by surrounding the object to be shielded with a plasma which is capable of either reflecting, scattering, or absorbing the incoming radiation. Approaches to plasma cloaking based on reflection and scattering must be handled with a great deal of caution lest the net effect be to increase the apparent size of the radar image of the object to be cloaked. It seems fairly clear that the safest of these three approaches is to absorb the radiation used to detect the target. A consideration of the basic principles of interaction of electromagnetic waves with plasmas indicates that it is relatively difficult to absorb microwave power in unmagnetized plasmas. Experience in the field of fusion research indicates that RF plasma heating (and therefore absorption) is most effectively done at three major frequencies; ion cyclotron resonance heating, lower hybrid heating, and electron cyclotron heating.

Ion and electron cyclotron heating are done at the gyro frequency of the ions or electrons, given by:

$$\omega = \frac{eB}{m} \qquad (1)$$

These frequencies are a function only of the charge to mass ratio and the magnetic induction. At magnetic inductions likely to be encountered in plasma cloaking applications, the ion cyclotron frequency is likely to be too low to be of interest, in view of the normal operating frequencies of systems of interest. Microwave frequencies in the electromagnetic spectrum range between 300 Mc and 300 Gc. A subset of these frequencies of special interest include the VHF, UHF and HF radar frequencies listed below in Table 1:

TABLE 1

Radar frequency band	Frequency
UHF ...	300–1,000 Mc
L ...	1,000–2,000 Mc
S ...	2,000–4,000 Mc
C ...	4,000–8,000 Mc
X ...	8,000–12,500 Mc

</div>

4,989,006

5

TABLE 1-continued

Radar frequency band	Frequency
K . . .	12.5–18 Gc
K . . .	18–26.5 Gc
K . . .	26.5–40 Gc
Millimeter . .	>40 Gc

In magnetic inductions of a few tenths of a Tesla, the electronic cyclotron frequency is comparable to the frequencies used by many radar systems. The third possibility, absorbing rf power at the lower hybrid frequency, is not likely to be of interest for plasma cloaking applications. The lower hybrid frequency is electron number density dependent, and it could be very difficult, in operational terms, to match the plasma number density to frequency. Consideration of the Appleton equation, which describes the interaction of electromagnetic radiation with a magnetized plasma, indicates that significant absorption should occur in the vicinity of the electron cyclotron frequency. For magnetic inductions between 0.010 and 0.42 Tesla (typical of our experiment), the electron cyclotron frequency ranges from 1.76 gigahertz to 70 gigahertz, the range of interest for radar systems. Some experimental data generated on the absorption of 9.75 gigahertz radiation at the electron cyclotron frequency, obtained at the UTK Plasma Science Laboratory, will now be described.

FIG. 1 is a schematic of a Penning discharge system whose components are usable in this invention. The FIG. 1 system can generate a uniform axial magnetic field, which produced the data of FIG. 5 which will be discussed below. The Penning discharge is operated in the steady state, and at magnetic inductions that vary between 0.10 Tesla and 0.42 Tesla. Pertinent features of this discharge are that it is electric field dominated, with strong axial and radial electric fields, sometimes exceeding several hundred volts per centimeter, and it has high levels of plasma turbulence, maintained by the energy input from the applied electric fields. The ions and electrons are heated by E/B rotation, which gives rise to an ion population that is hotter than the electron population. This Penning discharge system was used in a plasma heating experiment involving collisional magnetic pumping, in which plasma heating from collisional magnetic pumping was demonstrated for the first time.

On FIGS. 2 and 3 are shown some characteristic data taken along the axis of the discharge. The electron number density was typically 10⁹ per cubic centimeter, and the electron temperature was about 10 eV. This classical Penning discharge was instrumented with a variety of diagnostics, including the axial Langmuir probe that produced the data on FIGS. 2 and 3. Also included was the experimental setup shown on FIG. 4 in which a transmitting horn and a receiving horn were put on either side of the cylindrical plasma, and connected to a microwave network analyzer. This network analyzer makes it possible for us to irradiate the plasma with a microwave signal of variable frequency over the range from 0.2 to 18 gigahertz. After passing through the plasma, the signal is picked up by the receiving horn and analyzed by the network analyzer.

The purpose of the instrumentation shown in FIG. 4 was to implement a new diagnostic, intended to measure experimentally the effective electron collision frequency in the plasma. The dielectric constant of a plasma is given by the Appleton equation, below. This equation contains the electron cyclotron frequency ω_{cy}, the electron plasma frequency ω_p, and the collision

6

frequency ω. It can be shown that the full width of the absorption peak, at half-maximum amplitude at the electron cyclotron frequency is related to the effective electron collision frequency appearing in the Appleton equation. Thus, a measurement of the resonant absorption peak at the electron cyclotron frequency with the microwave network analyzer will allow a measurement of the effective collision frequency.

$$\epsilon(\omega) = \mu_{PR}^2 - 1 = \frac{\frac{\omega_p^2}{\omega^2}}{1 - j\frac{V_e}{\omega} - \frac{\omega_{cy}^2/\omega^2}{1 - \frac{\omega_p^2}{\omega^2} - j\frac{V_e}{\omega}}} \tag{2}$$

where

$$\alpha = \frac{\omega}{c}\chi \qquad \mu = \frac{\omega}{c}\mu$$

and

ω_p = plasma frequency,
ω = wave frequency, and
v = collision frequency
ω_{cy} = the electron cyclotron frequency

The parameters and are the wave propagation constants. Consideration of the Appleton equation indicates that significant absorption (several ten's of dB) should occur in the vicinity of the electron cyclotron frequency for plasmas of only moderate number densities (10⁸ and 10⁹ electrons per cubic centimeter). For magnetic inductions between about 0.010 and 0.42 Tesla (typical of our experiments), the electron cyclotron frequency ranges from 0.28 gigahertz to 11.8 gigahertz, the range of interest for many radar systems.

Some characteristic data are shown on FIG. 5. Here, the electron cyclotron frequency was approximately 9.75 gigahertz. At this frequency, the absorption of the power was about 36 dB. The full width at half maximum of this curve yields an effective electron collision frequency of 7.5 megahertz, more than a factor 30 higher than the binary electron-neutral collision frequency shown in Table 2 below. The value of the effective collision frequency, and the fact that it is usually much higher than the binary collision frequency in this turbulent plasma, is of great interest.

TABLE 2

COLLISION	COLLISION FREQUENCY, Hz
Electron-Neutral	255.10⁴
Ion-Neutral	27.10³
Electron-Electron	1.9.10³
Electron-Ion	950
Neutral-Neutral	137
Ion-Electron	0.5
Effective Collision Frequency (FIG. 6)	7.5.10⁹

For the present discussion of plasma cloaking, the point of interest in FIG. 5 is the very large attenuation achieved in the vicinity of the electron cyclotron frequency, 36 dB in FIG. 5. This large attenuation was in no way unusual, and even higher attenuations were observed. The process occurring in the plasma are relatively complicated, and are not fully described by the Appleton equation, which is based on the cold plasma approximation. The minor peak in FIG. 6 to the left

4,989,006

7

(lower frequency) of the electron cyclotron frequency represents a hot plasma effect. The fact that only a single such peak is seen, on one side of the electron cyclotron frequency, strongly indicates a nonlinear interaction. The general magnitude of the observed attenuation is consistent with the predictions of the Appleton equation, however, since this equation predicts attenuations that are typically 10's of dB for plasmas such as those in this classical Penning discharge. The average plasma density was approximately 1.5×10^9 particles per cubic centimeter. The plasma diameter was typically 12 or 15 centimeters, thus making the columnar density of the plasma no more than about 2×10^{10} electrons per square centimeter. Thus, at the electron cyclotron frequency in a magnetized plasma, the electrons can very effectively absorb microwave power in the gigahertz range. FIG. 6 is an example of absorption at 9.75 gigahertz; in the experiments on the classical Penning discharge absorption was observed from approximately 5 Gigahertz up to about 15 Gigahertz during the course of these experiments.

It appears that very large attenuations of microwave power are possible in rarified plasmas and plasmas with relatively small columnar densities, provided only that they are in a magnetic field. The data referred to thus far and shown in FIG. 5 were taken for the extraordinary mode, in which the electric field vector of the wave is perpendicular to the magnetic field. Similarly large absorptions are not necessarily to be expected in the ordinary mode, with E parallel to B.

In exploiting the resonance at the electron cyclotron frequency as a cloaking mechanism, one probably should use a magnetic dipole as the magnetic containment configuration. If one were to have an earth satellite containing a large superconducting coil with generates a dipolar magnetic field, one may reasonably expect this dipole to accumulate from its surroundings at orbital altitudes, enough plasma to be useful for cloaking purposes, just as the earth's magnetic field accumulates particles in the magnetosphere. Electromagnetic radiation approaching such a plasma-charged dipole would first enter relatively weak magnetic fields with low electron cyclotron frequencies of a few megahertz, and would be absorbed by electron cyclotron resonance. In traveling toward the dipole, the electromagnetic radiation would progressively go through magnetic fields corresponding to electron cyclotron resonance at higher and higher frequencies until, before it reached the surface of the spacecraft, the radiation traveled through a magnetic field sufficiently strong that it was above all expected radar frequencies. Any radiation in the ordinary mode which is not absorbed by its passage through the plasma would be scattered or reflected by the interaction with the complicated dipolar magnetic field.

The implementation of this plasma cloaking concept aboard aircraft and in the atmosphere might be considerably more difficult, because of the necessity of generating a plasma in the dipolar magnetic field to absorb the incoming radiation.

Returning to FIG. 5, note that microwave absorption at the electron cyclotron resonance frequency in plasma was measured in the modified Penning discharge with uniform configuration. The measurement was taken by a model 8510 Hewlett Packard network analyzer which is capable of swept frequency from 0.045 to 18 GHz with 80 dB dynamic range.

8

The reader's attention is now directed towards FIG. 6 which is a schematic which presents a plan view of a modified Penning discharge system of the present invention. The system of FIG. 6 generates a plasma 150 by ionizing helium or argon into a plasma using two opposed cathodes 100, 110 with an anode ring fixed between 21cm. A typical anode voltage would be 1,400 volts with a current of 50-500 mA. In one experiment, helium was used with a pressure of 1.1×10^{-3} Torr, but these parameters will be varied depending upon the application of the invention. The magnetic field was varied between 0.167 and 0.261 Tesla, but this parameter can also be varied.

In FIG. 6, a waveguide 190 is shown to conduct a microwave signal into the magnetized plasma. This waveguide 190 is depicted because it is part of a test system which can be used to test the effectiveness of the invention in damping and absorbing microwave signals.

The modified Penning discharge used for generating plasma consists of a magnetic field with a mirror configuration. The mirror ratio is 1.6 ($B_{max}/B_{min}=1.6$). A steady-state plasma is generated between two cathodes where the magnetic field is a maximum. The density used was a few times $10^9/cm^3$, with electron temperature about 10 eV. A microwave beam is caused to propagate along the axis of a magnetic mirror field in the plasma column. Two radiation antennas (horns) were mounted behind the cathodes. A microwave beam propagates through an aperture at the center of each cathode and is received at the other end. The measurement of transmission and reflection coefficients from 2 GHz to 12 GHz were taken with the network analyzer. The system was normalized so that the normalized attenuation and absolute attenuation of microwave absorption in the plasma were measured by the network analyzer.

Multiple runs of the test were made of the configuration show on FIG. 6 under the conditions described below in Table 3.

TABLE 3

OPERATING CONDITIONS

Run A	
B field (max)	0.261 Tesla
B field (min)	0.167 Tesla
1. Anode Voltage	1400 Volts
Anode Current	50 mA
HePressure	1.1×10^{-3} Torr
2. Anode Voltage	1550 volts
Anode Current	90 mA
HePressure	1.1×10^{-3} Torr
3. Anode Voltage	1400 volts
Anode Current	280 mA
HePressure	1.8×10^{-3} Torr
Run B	
B field (max)	0.084 Tesla
B field (min)	0.182 Tesla
1. Anode Voltage	1500 volts
Anode Current	50 mA
HePressure	1.1×10^{-3} Torr
2. Anode Voltage	1600 volts
Anode Current	90 mA
HePressure	1.1×10^{-3} Torr
3. Anode Voltage	1700 volts
Anode Current	150 mA
HePressure	1.1×10^{-3} Torr
4. Anode Voltage	2000 volts
Anode Current	270 mA
HePressure	1.5×10^{-3} Torr
5. Anode Voltage	2000 volts
Anode Current	340 mA
HePressure	1.7×10^{-3} Torr

4,989,006

9

TABLE 3-continued

OPERATING CONDITIONS	
6. Anode Voltage	1400 volts
Anode Current	350 mA
He Pressure	1.8×10^{-1} Torr
Run C	
B field (max)	0.329 Tesla
B field (min)	0.212 Tesla
1. Anode Voltage	1400 volts
Anode Current	350 mA
He Pressure	1.8×10^{-3} Torr

Some characteristic data are shown on FIG. 5. Here, the electron cyclotron frequency was approximately 9.75 gigahertz. At this frequency, the absorption of the power was about 36 dB. For the present discussion of plasma cloaking, the point of interest in FIG. 5 is the very large attenuation achieved in the vicinity of the electron cyclotron frequency, 36 dB. This large attenuation was in no way unusual, and even higher attenuations were sometimes observed. The general magnitude of the observed attenuation is consistent with the predictions of the Appleton equation, since it predicts attenuations that are typically 10's of dB for plasmas such as those in this classical Penning discharge. The average plasma density was approximately 1.5×10^9 particles per cubic centimeter. The plasma diameter was typically 12 or 15 centimeters, thus making the columnar density of the plasma no more than about 2×10^{10} electrons per square centimeter. Thus, at the electron cyclotron frequency in a magnetized plasma, the electrons can very effectively absorb microwave power in the gigahertz range. FIG. 5 is an example of absorption at 9.75 gigahertz. In the experiments on the classical Penning discharge, absorption was observed from approximately 5 gigahertz up to about 15 gigahertz during the course of these experiments.

It appears that very large attenuations of microwave power are possible in rarified plasmas and plasmas with relatively small columnar densities, provided only that they are in a varying magnetic field. The data referred to thus far and shown in FIG. 5 were taken for the extraordinary mode, in which the electric field vector of the wave is perpendicular to the magnetic field. Similarly large absorptions are not necessarily to be expected in the ordinary mode, with E parallel to B.

More data was taken using the system of FIG. 6, which is a modified Penning discharge with a magnetic mirror configuration having a ratio of maximum to minimum magnetic field of 1.6 to 1 along the axis. The geometry is shown schematically in FIG. 6, the cathodes of the Penning discharge were located at the magnetic field maximum, and immediately behind each was located a microwave horn which was screened from the plasma by horizontal grid wires aligned parallel to the electric field of the microwave radiation. This allowed microwave radiation from approximately 4 to 10 gigahertz to propagate along this magnetized plasma, with a magnetic field variation of at least 1.6 to 1 along the path of microwave propagation. The microwave horns were hooked up to our Hewlett Packard Model 8510 microwave network analyzer, which was swept over frequencies from 2 to 12 gigahertz. It was expected that attempting to propagate the microwave signal through a plasma embedded in a variable magnetic field would greatly broaden the bandwidth over which electron cyclotron resonance absorption occurred. This expectation was observed.

10

On FIG. 8 is shown the absolute attenuation of the microwave signal from approximately 4.3 GHz to 10.5 GHz. Beyond these frequency limits, the microwave waveguide and other circuit components cut off. The upper curve is the attenuation of the system with the plasma off. The lower curve shows the transmission through the system with the plasma on. In this case, there is up to approximately 20 dB of attenuation at frequencies which have an ion cyclotron resonance in the plasma volume.

The normalized attenuation is shown on FIG. 8, which shows the attenuation curve normalized to the signal received without the plasma. Here the attenuation is at least 5 dB over the entire range, and a maximum of more than 20 dB. Markers No. 2 and 1 on this plot indicate, respectively, the electron cyclotron resonance frequencies corresponding to the maximum and minimum of the magnetic induction in the plasma volume. It is interesting to note that significant attenuation occurs even at frequencies for which there is no electron cyclotron resonance in the plasma containment volume. FIG. 9 shows the normalized reflection of microwave signal from the plasma. In all cases, including this one, the reflected signal was within the noise limits of the system, and no more than one or two dB. These data are very encouraging indication that magnetized plasmas can not only absorb, but also not reflect any significant signal when the incoming radiation is in the extraordinary mode, and in electron cyclotron resonance. Finally, FIG. 10 shows the attenuation in dB as a function of the Penning anode current, which is proportional to the electron number density in the plasma. This shows a monotone increase of attenuation with electron number density, a dependence which is to be expected on the basis of the Appleton equation and elementary physical consideration.

Tests on the present invention have indicated that magnetized plasmas could absorb several tens of dB of incoming microwave energy in the extraordinary mode, using relatively low density plasmas (no more than 10^8 to 10^9 per cubic centimeter) and at frequencies ranging from 2 to 12 gigahertz, which spans the range used by many military radar systems.

Many variations of the present invention as generally described above are possible. For example, the plasma cloaking system can use a superconducting coil, which would generate a dipole magnetic field, in a target such as an aircraft or a space satellite. The dipolar magnetic field could be supplied with a weak plasma to form a "magnetosphere" surrounding the target. In this system, probing radar signals of a wide range of frequencies would enter this artificial magnetosphere surrounding the target, and be absorbed when they reached a magnetic induction corresponding to the electron cyclotron frequency.

FIGS. 11 and 12 are illustrations of potential radar targets that may use the present invention as a plasma cloaking device. FIG. 11 is an illustration of a satellite 12 that is being tracked by multiple ground-based radar systems. When this satellite 12 is equipped with a superconducting coil, a dipole magnetic field will surround the satellite. In orbital attitudes, the dipolar field will fill up with plasma, much as the earth's magnetosphere does from its surroundings. When the coil introduces a varying magnetic field in this plasma, it will attenuate the radar signals as described above.

Endoatmospheric aircraft will be difficult to surround with plasma since their forward velocity may

4,989,006

11

allow the wind to strip away the plasma cloud around
the craft. FIG. 12 is an illustration of an aircraft taken
from U.S. Pat. No. 4,052,025, which is incorporated by
reference, and which shows an aircraft encompassed by
a buoyant envelope. When the gas inside the envelope is 5
ionized He, the present invention can be used to cloak
the aircraft without the danger of the plasma cloud
being left behind. Alternative to this approach include
the generation of a steady released flow of ionized gas
around the aircraft which is replenished as it is left 10
behind.

While the invention has been described in its pres-
ently preferred embodiment it is understood that the
words which have been used are words of description
rather than words of limitation and that changes within 15
the purview of the appended claims may be made with-
out departing from the scope and spirit of the invention
in its broader aspects.

What is claimed is:

1. A microwave absorption system which protects a 20
target from microwave electromagnetic radiation, said
microwave absorption system comprising:

a means of producing a plasma which will circum-
scribe said target; and

a means for generating a varying magnetic field in 25
said plasma to produce thereby a varying magne-
tized plasma which interacts with said microwave
electromagnetic radiation to absorb and attenuate it
before it reaches said target; where said generating
means comprises a plurality of magnetic coils 30
which are fixed in proximity with said producing
means, and which collectively output said varying
magnetic field with a variation factor in magnetic
induction, said variation factor being a ratio of a
maximum of said varying magnetic field in Tesla, 35
divided by a minimum of said varying magnetic
field in Tesla, as produced by said plurality of mag-
netic coils.

2. A microwave absorption system which protects a
target from microwave electromagnetic radiation, said 40
microwave absorption system comprising:

a source of gas which may be converted into plasma
when subjected to an electric arc, said source of
gas outputting a gas cloud in proximity with said
target; 45

a means for generating a varying magnetic field in
said plasma to produce thereby a varying magne-
tized plasma which interacts with said microwave
electromagnetic radiation to absorb and attenuate it
before it reaches said target; 50

first and second cathodes which are fixed on opposite
sides of said gas cloud; and

a ring anode which is fixed between said first and
second cathodes to conduct said electric arc there-
between and produce thereby said plasma so that it 55
may be magnetized by said generating means with
said varying magnetic field and absorb said micro-
wave electromagnetic radiation before it reaches
said target.

3. A microwave absorption system which protects a 60
target from microwave electromagnetic radiation, said
microwave absorption system comprising;

a means of producing a plasma which will circum-
scribe said target; and

a means for generating a varying magnetic field in 65
said plasma to produce thereby a varying magne-
tized plasma which interacts with said microwave
electromagnetic radiation to absorb and attenuate it

12

before it reaches said target, wherein said micro-
wave electromagnetic radiation comprises trans-
mitted radar signals which have a radar frequency
that ranges between 300 megahertz and 300 giga-
hertz, and wherein said generating means generates
said varying magnetic field with a plasma fre-
quency which has a value near that of said radar
frequency in order to enhance absorption and at-
tenuation of said microwave electromagnetic radi-
ation as it interacts with said varying magnetized
plasma.

4. A microwave absorption which protects a target
from microwave electromagnetic radiation, said micro-
wave absorption system comprising:

a means of producing a plasma which will circum-
scribe said target; and

a means for generating a varying magnetic field in
said plasma to produce thereby a varying magne-
tized plasma which interacts with said microwave
electromagnetic radiation to absorb and attenuate it
before it reaches said target, wherein said micro-
wave electromagnetic radiation comprises an elec-
tromagnetic pulse signal directed at said target by a
directed energy weapon with a pulse frequency
that ranges between 300 megahertz and 300 giga-
hertz, and wherein said generating means generates
said varying magnetic field with a plasma fre-
quency which has a value near that of said pulse
frequency in order to enhance absorption and at-
tenuation of said microwave electromagnetic radi-
ation as it interacts with said varying magnetized
plasma.

5. A microwave absorption system, as defined in
claim 1, wherein said producing means comprises:

a source of gas which may be converted into plasma
when subjected to an electric arc, said source of
gas outputting a gas cloud in proximity with said
target;

first and second cathodes which are fixed on opposite
sides of said gas cloud; and

a ring anode which is fixed between said first and
second cathodes to conduct said electric arc there-
between and produce thereby said plasma so that it
may be magnetized by said generating means with
said varying magnetic field and absorb said micro-
wave electromagnetic radiation before it reaches
said target.

6. A microwave absorption system, as defined in
claim 1, wherein said microwave electromagnetic radia-
tion comprises transmitted radar signals which have a
radar frequency that ranges between 300 megahertz and
300 gigahertz, and wherein said generating means gen-
erates said varying magnetic field with a plasma fre-
quency which has a value near that of said radar fre-
quency in order to enhance absorption and attenuation
of said microwave electromagnetic radiation as it inter-
acts with said varying magnetized plasma.

7. A microwave absorption system, as defined in
claim 2, wherein said microwave electromagnetic radia-
tion comprises transmitted radar signals which have a
radar frequency that ranges between 300 megahertz and
300 gigahertz, and wherein said generating means gen-
erates said varying magnetic field with a plasma fre-
quency which has a value near that of said radar fre-
quency in order to enhance absorption and attenuation
of said microwave electromagnetic radiation as it inter-
acts with said varying magnetized plasma.

4,989,006

13

8. A microwave absorption system, as defined in claim 1, wherein said microwave electromagnetic radiation comprises an electromagnetic pulse signal directed at said target by a directed energy weapon with a pulse frequency that ranges between 300 megahertz and 300 gigahertz, and wherein said generating means generates said varying magnetic field with a plasma frequency which has a value near that of said pulse frequency in order to enhance absorption and attenuation of said microwave electromagnetic radiation as it interacts with said varying magnetized plasma.

9. A microwave absorption system, as defined in claim 2, wherein said microwave electromagnetic radiation comprises an electromagnetic pulse signal directed at said target by a directed energy weapon with a pulse frequency that ranges between 300 megahertz and 300 gigahertz, and wherein said generating means generates said varying magnetic field with a plasma frequency which has a value near that of said pulse frequency in order to enhance absorption and attenuation of said microwave electromagnetic radiation as it interacts with said varying magnetized plasma.

10. A plasma cloaking system which protects targets from being detected by radar systems that emit microwave electromagnetic radiation, said plasma cloaking system comprising:

a means for producing a plasma which will circumscribe said target; and

a means for generating a varying magnetic field in said plasma to produce thereby a varying magnetized plasma which interacts with said microwave electromagnetic radiation to absorb and attenuate it before it reaches said target; wherein said generating means comprises a plurality of magnetic coils which are fixed in proximity with said producing means, and which collectively output said varying magnetic field with a variation factor in magnetic induction, said variation factor being a ratio of a maximum of said varying magnetic field in Tesla, divided by a minimum of said varying field in Tesla, as produced by said plurality of magnetic coils.

11. A plasma cloaking system which protects targets from being detected by radar systems that emit microwave electromagnetic radiation, said plasma cloaking system comprising:

a source of gas which may be converted into plasma when subjected to an electric arc, said source of gas outputting a gas cloud in proximity with said target;

14

a means for generating a varying magnetic field in said plasma to produce thereby a varying magnetized plasma which interacts with said microwave electromagnetic radiation to absorb and attenuate it before it reaches said target;

first and second cathodes which are fixed on opposite sides of said gas cloud; and

a ring anode which is fixed between said first and second cathodes to conduct said electric arc therebetween and produce thereby said plasma so that it may be magnetized by said generating means with said varying magnetic field and absorb said microwave electromagnetic radiation before it reaches said target.

12. A plasma cloaking system which protects targets from being detected by radar systems that emit microwave electromagnetic radiation, said plasma cloaking system comprising:

a means for producing a plasma which will circumscribe said target; and

a means for generating a varying magnetic field in said plasma to produce thereby a varying magnetized plasma which interacts with said microwave electromagnetic radiation to absorb and attenuate it before it reaches said target, wherein said microwave electromagnetic radiation comprises transmitted rear signals which have a radar frequency, and wherein said generating means generates said varying magnetic field with a plasma frequency which has a value near that of said radar frequency in order to enhance absorption and attenuation of said microwave electromagnetic radiation as it interacts with said varying magnetized plasma.

13. A microwave absorption system, as defined in claim 10, wherein said microwave electromagnetic radiation comprises transmitted radar signals which have a radar frequency, and wherein said generating means generates said varying magnetic field with a plasma frequency which has a value near that of said radar frequency in order to enhance absorption and attenuation of said microwave electromagnetic radiation as it interacts with said varying magnetized plasma.

14. A microwave absorption system, as defined in claim 13, wherein said microwave electromagnetic radiation comprises transmitted radar signals which have a radar frequency, and wherein said generating means generates said varying magnetic field with a plasma frequency which has a value near that of said radar frequency in order to enhance absorption and attenuation of said microwave electromagnetic radiation as it interacts with said varying magnetized plasma.

* * * * *

FINAL

A ONE ATMOSPHERE, UNIFORM GLOW DISCHARGE PLASMA

ABSTRACT

A steady-state, glow discharge plasma is generated at one atmosphere of pressure within the volume between a pair of insulated metal plate electrodes spaced up to 5 cm apart and R.F. energized with an rms potential of 1 to 5 KV at 1 to 100 KHz. Space between the electrodes is occupied by air, nitrous oxide, a noble gas such as helium, neon, argon, etc. or mixtures thereof. The electrodes are charged by an impedance matching network adjusted to produce the most stable, uniform glow discharge.

License Rights

The U.S. Government has a paid-up license in this invention and the right in limited circumstances to require the patent owner to license others on reasonable terms as provided for by the terms of contract No. AFOSR 89-0319 awarded by The U.S. Air Force.

CROSS-REFERENCES TO RELATED APPLICATIONS

This application is a Continuation-In-Part of U.S. Patent Application Serial No. 08/068,508 filed May 28, 1993.

BACKGROUND OF THE INVENTION

Field of Invention

The present invention relates to methods and apparatus for generating low power density glow discharge plasmas at atmospheric pressure.

Description of the Prior Art

In the discipline of physics, the term "plasma" describes a partially ionized gas composed of ions, electrons and neutral species. This state of matter may be produced by the action of either very high temperatures, strong constant electric fields or radio frequency (R.F.) electromagnetic fields. High temperature or "hot" plasmas are represented by celestial light bodies, nuclear explosions and electric arcs. Glow discharge plasmas are produced by free electrons which are energized by imposed direct current (DC) or R.F. electric fields, and then collide with neutral molecules. These neutral molecule collisions transfer energy to the molecules and form a variety of active species which may include photons, metastables, atomic species, free radicals, molecular fragments, monomers, electrons and ions. These active species are chemically active and/or physically modify the surface of materials and may therefore serve as the basis of new surface properties of chemical compounds and property modifications of existing compounds.

Very low power plasmas known as dark discharge coronas have been widely used in the surface treatment of thermally sensitive materials such as paper, wool and synthetic polymers such as polyethylene, polypropylene, polyolefin, nylon and poly(ethylene terephthalate). Because of their relatively low energy content, corona discharge plasmas can alter the properties of a material surface without damaging the surface.

Glow discharge plasmas represent another type of relatively low power density plasma useful for non-destructive material surface modification. These glow discharge plasmas can produce useful amounts of visible and ultraviolet radiation. Glow discharge plasmas have the additional advantage therefore of producing visible and UV radiation in the simultaneous presence of active species. However, glow discharge plasmas have heretofore been successfully generated typically in low pressure or partial vacuum environments below 10 torr, necessitating batch processing and the use of expensive vacuum systems.

Conversely, the generation of low power density plasmas at one atmosphere is not entirely new. Filamentary discharges between parallel plates in air at one atmosphere have been used in Europe to generate ozone in large quantities for the treatment of public water supplies since the late 19th century. Filamentary discharge plasmas are dramatically distinguished from uniform glow discharge plasmas. Such filamentary discharges, while useful for ozone production, are of limited utility for the surface treatment of materials, since the plasma filaments tend to puncture or treat the surface unevenly.

It is, therefore, an object of the present invention to teach the construction and operating parameters of a continuous glow discharge plasma sustained at a gas pressure of about one atmosphere or slightly greater.

INVENTION SUMMARY

This and other objects of the invention to be subsequently explained or made apparent are accomplished with an apparatus based upon a pair of electrically insulated metallic

5 plate electrodes. These plates are mounted in face-to-face parallel or uniformly spaced alignment with means for reciprocatory position adjustment up to at least 5 cm of separation. Preferably, the plates are water cooled and covered with a dielectric insulation.

10 To broaden the range of operating frequency and other parameters over which the desirable uniform (as opposed to filamentary) glow discharge is observed, an impedance matching network is added to the circuit for charging the electrodes. The parameters of such a matching network are adjusted for the most

15 stable, uniform operation of the glow discharge. This condition can occur when the reactive power of the plasma reactor is minimized.

A radio frequency power amplifier connected to both plates delivers up to several hundred watts of power at a working

20 voltage of 1 to at least 5 KV rms and at 1 to 100 KHz. To assist the starting of the plasma, the electrical discharge from a standard commercial Tesla coil may be briefly applied to the volume between the R.F. energized plates. An electric field established between the metallic plate electrodes must be strong enough to

25 electrically break down the gas used, and is much lower for helium and argon than for atmospheric air. The RF frequency must be in the right range, discussed below, since if it is too low, the discharge will not initiate, and if it is too high, the plasma forms filamentary discharges between the plates. Only in a

30 relatively limited frequency band will the atmospheric glow discharge plasma reactor form a uniform plasma without filamentary discharges.

To stabilize the plasma and discourage the formation of plasma filaments, an inductor may be connected from the median plane to ground.

At least in the volume between the plates wherein the glow discharge plasma is established, a one atmosphere charge of helium, argon or other gas or mixture of gases is established and maintained.

The median plane between two parallel electrodes may or may not contain an insulating or electrically conductive screen or plate which may be used to support exposed materials in the glow discharge plasma environment. If electrically conductive, the median screen or plate may be electrically floating or grounded.

BRIEF DESCRIPTION OF THE DRAWINGS

Relative to the drawings wherein like reference characters designate like or similar elements throughout the several figures of the drawings:

Figure 1 is a schematic of the present invention component assembly.

Figure 2 represents a preferred embodiment of the electrical circuit, including an impedance matching network and a grounded midplane screen connected to ground through an inductor.

Figure 3, 4 and 5 represent alternative power supply output stage circuits.

Figure 6 schematically represents the upper chamber of a one atmosphere glow discharge plasma reactor having a median grid plate.

Figure 7 represents a graph of voltage, current and power waveforms for a uniform glow discharge plasma.

Figure 8 represents a graph of voltage, current and power waveforms for a filamentary discharge plasma.

Figure 9 is a log-log graph of total and plasma power density in milliwatts per cubic centimeter as a function of RMS

voltage applied to the electrodes.

Figure 10 is a log-log graph of total and plasma power density in milliwatts per cubic centimeter, as a function of R.F. frequency.

5   Figure 11 is a graph of amplifier frequency and corresponding breakdown current phase angles respective to a particular operating example of the invention.

Figure 12 is a graph of amplifier frequency and corresponding total reactor power consumption respective to a
10   particular operating example of the invention.

DESCRIPTION OF THE PREFERRED EMBODIMENT

Referring to the invention schematic illustrated by Figure 1, the electrodes 10 are fabricated of copper plate having a representative square plan dimension of 21.6 cm x 21.6 cm.
15   Silver soldered to the plates 10 are closed loops 11 of 0.95 cm copper tubing having hose nipples 12 and 13 connected therewith on opposite sides of the closed tubing loop. The edges of the electrode plates should have a radius of curvature comparable to the separation between the electrode plates and median plate to
20   discourage electrical breakdown at the edge of the electrodes. Not shown are fluid flow conduits connected to the inlet nipples 12 for delivering coolant fluid to the loop 11 and to the outlet nipples 13 for recovering such coolant fluid.

The integral metallic units comprising plates 10 and
25   tubing 11 are covered with a high dielectric insulation material 14 on all sides to discourage electrical arcing from the edges or back side of the electrode plates.

Preferably, some mechanism should be provided for adjusting the distance s between plates 10 up to at least 5 cm
30   separation while maintaining relative parallelism. Such a mechanism is represented schematically in Figure 1 by the rod adjusters 15 secured to the upper and lower plates 10. This

arrangement anticipates a positionally fixed median screen or plate 30. Although parallelism is used here in the context of parallel planes, it should be understood that the term also comprises non-planar surfaces that are substantially equidistant. Also

5   included are the geometry characteristics of a cylinder having an axis parallel :o another cylinder or to a plate.

Energizing the plates 10 is a low impedance, high voltage, R.F. power amplifier 20 having independently variable voltage and frequency capacities over the respective ranges of 1 to

10   at least 9 KV and 1 to 100 KHz. An impedance matching network 31 is connected between the R.F. power amplifier and the electrode plates.

Surrounding the plate assembly is an environmental isolation barrier 21 such as a structural enclosure suitable for

15   maintaining a controlled gas atmosphere in the projected plan volume between the plates 10. Inlet port 22 is provided to receive an appropriate gas such as air, helium or argon, mixtures of either with air or a mixture of argon with helium. Ambient air may also be used. In any case, gas pressure within the isolation barrier 21

20   is substantially ambient thereby obviating or reducing the need for gas tight seals. Normally, it is sufficient to maintain a low flow rate of the modified one atmosphere gas through the inlet port 22 that is sufficient to equal the leakage rate. Since the pressure within the isolation barrier 21 is essentially the same as that

25   outside the barrier, no great pressure differential drives the leakage rate. A vent conduit 28 controlled by valve 29 is provided as an air escape channel during initial flushing of the enclosure. Thereafter, the valve 29 may be closed for normal operation.

To broaden the range of operating frequency and other

30   parameters over which the desirable uniform (as opposed to filamentary) glow discharge occurs, an impedance matching network, one embodiment of which is illustrated schematically by Figure 2,

is added to the power circuit for charging the electrodes 10. The parameters of this impedance matching network are adjusted for the most stable, uniform operation of the glow discharge. This condition can occur when the reactive power of the plasma reactor

5   is minimized.

Figures 3 through 5 represent alternative power supply options having respective attractions. Figures 3 corresponds to a configuration wherein the bottom electrode terminal T_1 is connected to ground potential and the top terminal T_2 is charged at the full

10   working potential. Figures 4 and 5 are electrical equivalents wherein the T_1 and T_2 voltages are $180°$ out of phase but at only half the maximum potential. Figure 4 represents a grounded center tap transformer whereas Figure 5 represents a solid state power circuit embodiment.

15   Electric fields employed in a one atmosphere, uniform glow discharge plasma reactor are only a few kilovolts per centimeter, values which if D.C. would usually be too low to electrically break down the background gas. Gases such as helium and air will break down under such low electric fields, however, if

20   the positive ion population is trapped between the two parallel or uniformly spaced electrodes, thus greatly increasing their lifetime in the plasma while at the same time the electrons are free to travel to the insulated electrode plates where they recombine or build up a surface charge. The most desirable uniform one

25   atmosphere glow discharge plasma is therefore created when the applied frequency of the RF electric field is high enough to trap the ions between the median screen and an electrode plate, but not so high that the electrons are also trapped during a half cycle of the R.F. voltage. The electrons may be trapped by bipolar

30   electrostatis forces.

If the RF frequency is so low that both the ions and the electrons can reach the boundaries and recombine, the particle

lifetimes will be short and the plasma will either not initiate or form a few coarse filamentary discharges between the plates. If the applied frequency is in a narrow band in which the ions oscillate between the median screen and an electrode plate, they do

5   not have time to reach either boundary during a half period of oscillation and are carried for long times. If the more mobile electrons are still able to leave the plasma volume and impinge on the boundary surfaces, then the desirable uniform plasma is produced. If the applied RF frequency is still higher so that both

10   electrons and ions are trapped in the discharge, then the discharge forms a filamentary plasma.

Without limiting our invention to any particular theory, we are disposed to a relationship between the electrode spacing, the RMS electrode voltage, and the applied frequency which results

15   in trapping ions but not electrons between the two plates, and produces the desired uniform one atmosphere glow discharge plasma. On Figure 7 is a schematic of the upper chamber of the one atmosphere glow discharge plasma reactor. The lower boundary of this space is the midplane screen or plate, the floating potential

20   of which should remain near ground if the RF power supply output is connected as a push-pull circuit to the two electrodes with a grounded center tap. In the data reported herein, the median screen was grounded through an inductive current choke. In the configuration of Figure 7, a Cartesian coordinate system is applied

25   as shown, with the applied electric field in the x-direction. The maximum amplitude of the electric field between the grounded median screen and the upper electrode is E_o, and the separation of the screen from the electrodes is the distance d. The median screen, with an exposed sample on it, is assumed not to allow ions through

30   the median plane from the upper chamber to the lower, or vice-versa.

The electric field between the electrodes shown on Figure

C-24

7 is given by

$$E=(E_o\sin\omega t, O, O).$$

(1)

It is assumed that the one atmosphere glow discharge operates in a magnetic field free plasma. The equation of motion for the ions or electrons between the two plates is given by a Lorentzian model, in which the electrons and ions collide only with the neutral background gas and, on each collision, give up all the energy they acquired from the RF electric field since the last collision to the neutral gas. The equation of motion for the ions or electrons in the Lorentzian model is given by

$$F=ma=-mv_cv-eE,$$

(2)

where the first term on the right hand side is the Lorentzian collision term, according to which the momentum mv is lost with each collision that occurs with a collision frequency v_c. The x component of Eq. 2 is given by

$$m\frac{d^2x}{dt^2}+mv_c\frac{dx}{dt}=eE_o\sin\omega t,$$

(3)

where the electric field E from Eq. 1 has been substituted into the right hand side of Eq. 2. The general solution to Eq. 3 is

$$x=C_1\sin\omega t=C_2\cos\omega t,$$

(4)

where the constants C_1 and C_2 are given by

$$C_1 = -\frac{eE_o}{m} \frac{1}{(\omega^2 + v_c^2)},$$

(5)

and

$$C_2 = -\frac{v_c eE_o}{\omega m} \frac{1}{(\omega^2 + v_c^2)}$$

(6)

The one atmosphere helium glow discharge is operated at
5   frequencies between $\omega/2\pi$ = 1 and 30 KHz, where, for helium at one
atmosphere,

$$v_{ci} \approx 6.8 \times 10^9 \ ion \ collisions/sec.,$$

(7a)

and

$$v_{ce} \approx 1.8 \times 10^{12} electron \ coll./sec.$$

(7b)

10   The collision frequency for ions and electrons given by Eqs. 7a and
7b is much greater than the RF frequency, $V_c \gg \omega$. The relation $v_c \gg \omega$
for ions and electrons, implies that C_2 is much greater than the
constant C_1, or

$$C_2 \approx \frac{eE_o}{m\omega v_c} \gg C_1$$

(8)

15   The time dependent position of an ion or an electron in the
electric field between the plates is given by substituting Eq. 8
into Eq. 4, to obtain

$$x(t) = -\frac{eE_o}{m\omega v_c}\cos\omega t.$$

(9)

The RMS displacement of the ion or electron during a half cycle is given by

$$x_{rms} = \frac{2}{\pi}\frac{eE_o}{m\omega v_c}\,meters.$$

(10)

5   If V_o is the driving frequency, in Hertz, then the radian RF frequency is given by

$$\omega = 2\pi v_o,$$

(11)

and the maximum electric field between the plates can be approximated by the maximum voltage V_o appearing between them,

$$E_o = \frac{V_o}{d} = \frac{\pi V_{rms}}{2d}.$$

10   (12)

If the charge in question moves across the discharge width from the median plane to one of the electrode plates during one full cycle, then we may write

$$x_{rms} \leq \frac{d}{2}.$$

(13)

15   Equation 13 states that the RMS displacement of the particle has to be less than half the clear spacing in order to have a buildup of charge between the plates. In the geometry shown in Figure 7, the distance d is identified with the distance between the grounded median screen and the energized electrode. Substituting Eqs. 11 to

C-27

13 into Eq. 10 yields the relationship

$$\frac{d}{2} \approx \frac{eV_{rms}}{2\pi m v_o v_c d}.$$

(14)

If we now solve for the critical frequency v_o above which charge buildup should occur in the plasma volume, we have

$$v_o \approx \frac{eV_{rms}}{\pi m v_c d^2} Hz.$$

5

(15)

In Eq. 15, the collision frequency v_c is approximately given by Eqs. 7a or 7b for ions or electrons, respectively, at one atmosphere, and the RMS voltage is that which bounds the upper and lower limit of the uniform discharge regime.

10   The range of parameters over which we have operated a one atmosphere, uniform glow discharge plasma reactor is given in Table I. The nominal pressure at which this discharge has been operated is one atmosphere. The variation of several torr shown in Table I is not intended to represent the day-to-day fluctuations of

15   barometric pressure, but the pressure differential across the midplane screen which is intended to drive active species from the upper plasma through the fabric being exposed. The RMS power shown in Table I is the net power delivered to the plasma, less the reactive power which does not appear in the plasma. The total

20   volume of plasma between the two electrode plates is given by

C-28

$$S = 0.93 \ d(cm) \ liters,$$

(16)

where d is the separation of a plate from the median screen in centimeters.

The power densities shown in Table I are far below those

5   of electrical arcs or plasma torches, but also are several orders of magnitude higher than the power densities associated with some other forms of plasma treatment such as corona discharges. The power densities of the one atmosphere glow discharge plasma are generally low enough not to damage exposed fabrics, but are also

10   enough higher than coronal plasmas used for surface treatment that they should provide far more active species than the latter. The plasma parameters, such as electron kinetic temperature and number density are somewhat speculative at this early stage in the development of our invention. A few results from probing the

15   plasma midplane with a floating Langmuir probe indicates that the plasma, without grounding the midplane screen, will float to positive potentials of several hundred volts. The ion kinetic temperatures are very likely close to that of the room temperature atoms with which they frequently collide at these high pressures;

20   the electrons apparently remain numerous and energetic enough to excite the neutral background atoms, hence making this a glow discharge. The existence of excited states which emit visible photons implies that the electron population has a kinetic temperature of at least an electron volt. The diagnostic

25   difficulties of measuring plasma parameters at this high pressure are very severe, since ordinary Langmuir probing technique cannot be applied due to the short mean free paths of the electrons compared to a Debye distance. Electron number densities, however, may be measured by microwave interferometric techniques.

TABLE I

OPERATING CHARACTERISTICS OF THE ONE

ATMOSPHERE GLOW DISCHARGE PLASMA REACTOR

5   working gas = He, He + 1-7% O_2, Ar, Ar + He, Ar + 1-7% O_2, $N2O$ and atmospheric air

frequency = 1 KHz to 100 KHz

voltage = 1.5 - 9.5 kV_{rms} plate to plate

electrode gap d = 0.8 -3.2cm

pressure = 760 +15, -5 torr

10   RMS power = 10 watts to 150 watts

power density = 4 - 120 mW/cm^3

plasma volume = 0.7 - 3.1 liters

On Figures 8 and 9 are shown two waveforms of voltage and
15   current taken in helium at the same electrode separation and gas
flow conditions, but at two different frequencies. Figure 8 was
taken in the uniform glow discharge regime at a frequency of 2.0
kHz, and Figure 9 was taken in the filamentary discharge regime at
a frequency above the uniform plasma operating band at 8.0 kHz.
20   The high output impedance of our RF power supply results in a
voltage waveform (trace B) that is very close to sinusoidal. The
reactive current waveform (trace C) is interrupted by a breakdown
of the plasma twice each cycle, once when the voltage is positive,
and once when the voltage is negative. Trace A shows the reactive
25   current waveform at the same voltage and operating conditions, but
in air, rather than helium. There was no perceptible plasma
present in air under these conditions, and the power is completely
reactive. This purely reactive current of trace A was subtracted
from the total plasma current in trace C, to yield trace D. The
30   instantaneous power deposited in the plasma (trace E) is found by
multiplying the excess plasma current above the reactive current

(trace D) by the voltage at that point (trace B). The average power is found by integrating over the duration of the pulses shown, and dividing by this duration. It is in this manner that the power and power density into the plasma were calculated for

5   these highly nonsinusoidal current waveforms. Figures 8 for the uniform discharge and 9 for the filamentary discharge show characteristically different power waveforms in trace E; this is a method of distinguishing the uniform from the filamentary discharge.

10   The plasma power is of interest because it is proportional to the production rate of active species in the plasma; the reactive power is significant because it determines the required power handling rating of the plasma power supply and associated equipment. The total power is the sum of plasma and

15   reactive power. On Figure 10 is shown a log-log plot of the plasma and total power density in milliwatts per cubic centimeter, as functions of the RMS voltage applied to the parallel plates. The active plasma volume in Figure 10 was 1.63 liters, with a separation between the median screen and each plate of d = 1.75

20   centimeters in a plasma of helium gas. On Figure 11 is a similar presentation of the power density plotted on log-log coordinates as a function of the frequency. The approximate bound of the uniform plasma discharge regime is shown by the arrow. These data were taken in helium gas for the same plasma volume and electrode

25   separation as Figure 10.

EXAMPLE 1

     In a first operational example of the invention, the above described physical apparatus sustained a glow discharge plasma in one atmosphere of helium at standard temperature with a

30   separation distance s of 3.0 cm between plates 10. The plates were charged with a 4.4 KV working potential. Holding these parameters constant, the R.F. frequency was increased as an independent

variable. As the dependent variable, Figure 11 charts the corresponding breakdown current phase angle. Similarly, Figure 12 charts the total power, reactive and plasma, used to sustain the plasma at the respective R.F. frequencies.

5   **EXAMPLE 2**

In a second operational example of the invention, the above described physical apparatus is used to sustain a glow discharge plasma in one atmosphere of helium at standard temperature with a separation distance s of 1.0 cm between plates

10   10. In this example, the frequency was held constant at 30 KHz while plate potential was manipulated as the independent variable and current breakdown phase angle, θ, (Table 2) and total power, P, (Table 3) measured as dependent variables.

Table 2

V(KV)	1	1.5	2	2.5	3	3.5
θ(deg)	28	40	61	46	65	76.5

Table 3

V(KV)	1	1.5	2	2.5	3	3.5
P(W)	7	13	22	57	50	44.9

20   **EXAMPLE 3**

A third operational example of the invention included a one atmosphere environment of helium between a 1 cm separation distance s between plate electrodes 10 charged at 1.5 KV rms potential. R.F. frequency was manipulated as the independent

25   variable. As a measured dependent variable, Table 4 reports the corresponding phase angle θ of breakdown current. The measured dependent variable of Table 5 reports the corresponding total power consumption data, both reactive and plasma.

<center>**Table 4**</center>

f(KHz)	10	20	30	40	50	60	70	80	90	100
θ(deg)	43	32	43	52	54	61	60	56	45	22.5

<center>**Table 5**</center>

f(KHz)	10	20	30	40	50	60	70	80	90	100
P(W)	5	8	11	19	35	43	47	57	89	124

EXAMPLE 4

The largest volume helium plasma of 3.1 liters was achieved with the above described apparatus at a 3.2 cm plate separation having a 5 KV potential charged at 4 KHz.

It will be understood by those of ordinary skill in the art that the present invention is capable of numerous arrangements, modifications and substitutions of parts without departing from the scope of the invention. In particular, Figures 3, 4 and 5 represent respective power supply options having respective attractions.

Figures 3, 4 and 5 are electrical equivalents wherein the T_1 and T_2 voltages are $180°$ out of phase but at only half the maximum potential. Figure 4 represents a grounded center top transformer whereas Figure 5 represents a solid state power circuit embodiment with or without a provision for a grounded center tap of the output.

Although expansive data is not presently available, it is to be noted that a uniform glow discharge plasma has been sustained by the Figure 1 apparatus with a one atmosphere ambient air environment and 8KV/cm R.F. electric field.

Having fully disclosed our invention, the presently preferred embodiments and best modes of practice,

WE CLAIM:

Claim 1. A glow discharge plasma generation apparatus comprising a pair of electrically insulated electrodes energized by radio frequency amplifier means for energizing said electrodes with an impedance matching network having a potential of 1 to at least 5 KV rms at 1 to 100 KHz, said electrodes being aligned and secured in equidistant opposition with means to charge a volumetric space between said electrodes with a glow discharge plasma sustaining gas at a pressure of about 1 atmosphere.

Claim 2. An apparatus as described by Claim 1 wherein said means to charge said volumetric space between said plates comprises a gas barrier envelope surrounding said plates and the volumetric space therebetween.

Claim 3. An apparatus as described by Claim 2 comprising gas supply means to maintain about one atmosphere of pressure within said envelope by a substantially steady supply flow of said gas.

Claim 4. An apparatus as described by claim 3 wherein said gas is helium.

Claim 5. An apparatus as described by claim 2 wherein said gas is a mixture of helium and air.

Claim 6. An apparatus as described by Claim 3 wherein said gas is argon.

Claim 7. An apparatus as described by claim 3 wherein said gas is a mixture of argon and air.

Claim 8. An apparatus as described by Claim 3 wherein said gas is a mixture of argon and helium.

Claim 9. An apparatus as described by Claim 1 wherein said gas is atmospheric air.

Claim 10. An apparatus as described by Claim 3 wherein said gas is nitrous oxide.

Claim 11. An apparatus as described by Claim 1 wherein said plates are fluid cooled.

C-34

Claim 12. An apparatus as described by Claim 11 wherein fluid flow conduits are bonded to said plates to extract heat from said plates.

Claim 13. A method of generating a glow discharge plasma within a volumetric space between two electrodes energized by radio frequency amplifier means having an impedance matching network, said method comprising the steps of operating said amplifier means to energize said electrodes with a potential of 1 to at least 5 KV rms at 1 to 100 KHz frequency and charging the volumetric space between said electrodes with a glow discharge plasma sustaining gas at approximately 1 atmosphere of pressure.

Claim 14. A method as described by Claim 13 wherein said electrodes are enclosed by an environmental gas barrier internally charged by a substantially continuous flow of said gas.

Claim 15. A method as described by Claim 14 wherein said gas is helium.

Claim 16. A method as described by claim 14 wherein said gas is a mixture of helium and air.

Claim 17. A method as described by Claim 14 wherein said gas is argon.

Claim 18. A method as described by claim 14 wherein said gas is a mixture of argon and air.

Claim 19. A method as described by Claim 14 wherein said gas is a mixture comprising helium and argon.

Claim 20. A method as described by Claim 13 wherein said gas is atmospheric air.

Claim 21. A method as described by Claim 14 wherein said gas is nitrous oxide.

Claim 22. A method as described by Claim 13 wherein lectrodes are positioned at a separation distance therebetween of 5 cm or less.

FIGURE 1

FIGURE 2

C-37
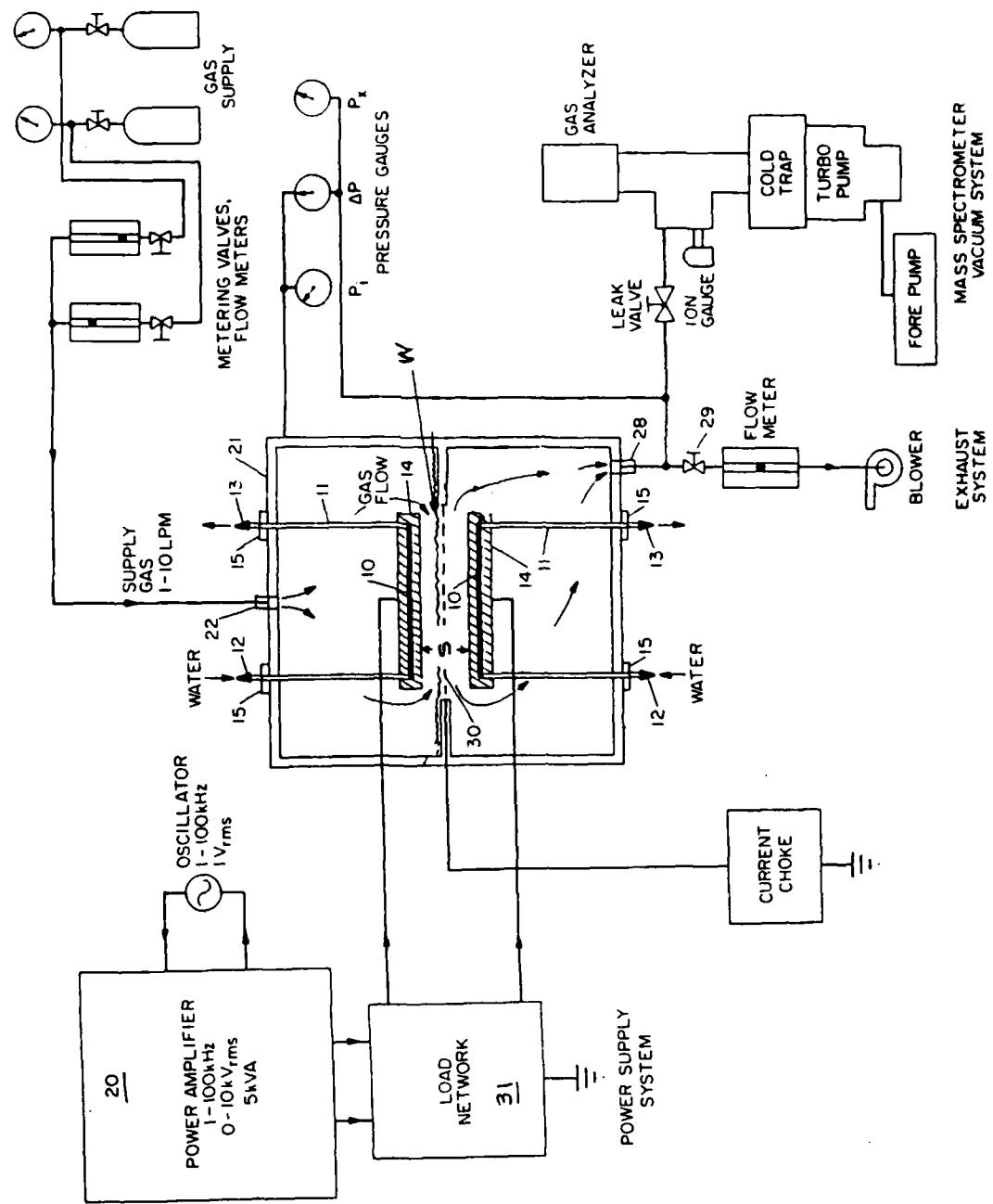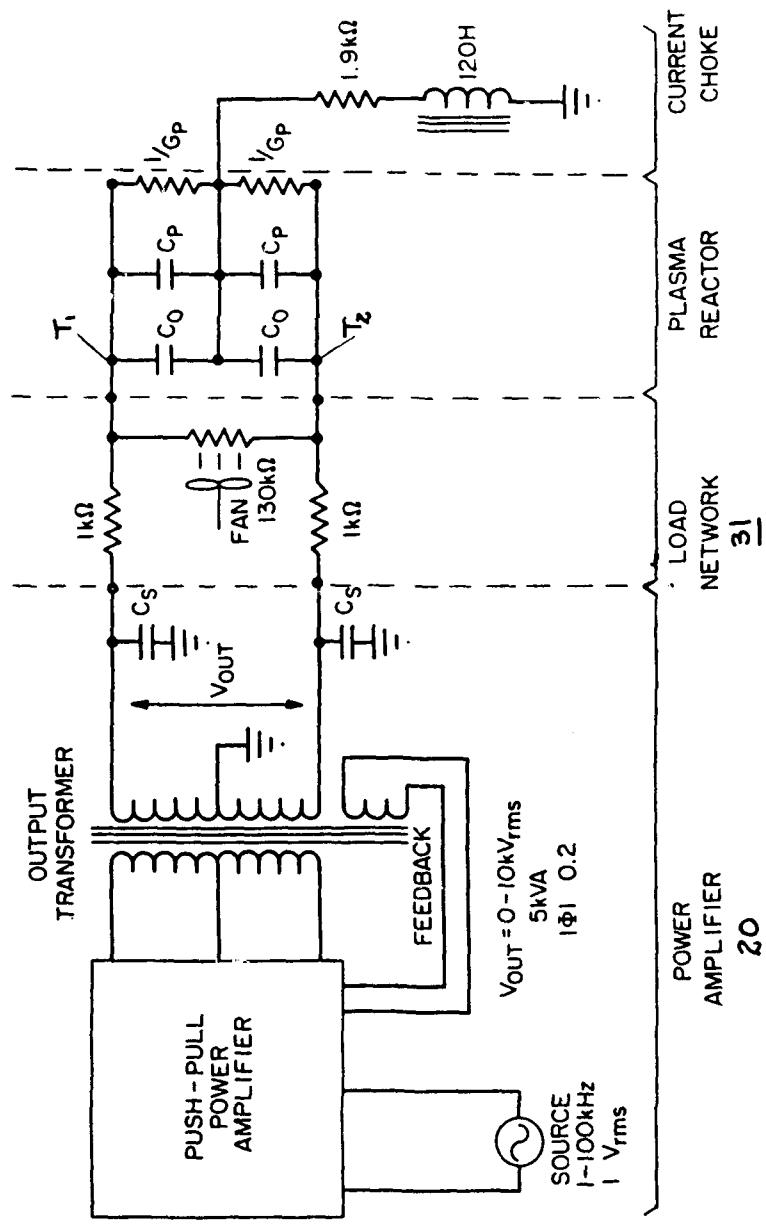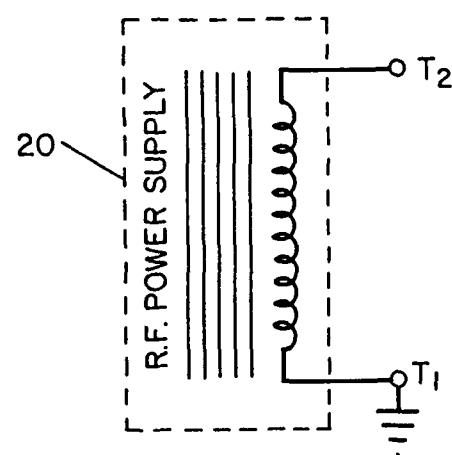
FIGURE 3

FIGURE 4

FIGURE 5

C-38

FIGURE 6

Reactive Current
$I_r = 1.3 \text{ mA}_{rms}$

Plate Voltage
$V = 1012 \text{ V}_{rms}$
(2 kHz)

1 mA/div

1150 V/div

200 μsec/div

10 mA/div

Total Current
$I_t = 9.6 \text{ mA}_{rms}$

200 μsec/div

11.5 watts/div

Plasma Power
$P_p = 8.3 \text{ watts}$

Plasma Current
$I = 8.8 \text{ mA}_{rms}$

Plate Voltage
$V_p = 1012 \text{ V}_{rms}$

200 μsec/div

FIGURE 7

C-40

Reactive Current
$I_r = 8.0$ mA$_{rms}$

10 mA/div

1150 V/div

Plate Voltage
$V = 920$ V$_{rms}$
(8 kHz)

50 μsec/div

Total Current
$I_t = 56$ mA$_{rms}$

50 mA/div

Plasma Current
$I = 52$ mA$_{rms}$

50 μsec/div

115 watts/div

Plasma Power
$P_p = 18.4$ watts

Plasma Current
$I = 52$ mA$_{rms}$

Plate Voltage
$V = 920$ V$_{rms}$

50 μsec/div

FIGURE 8
C-41

FIGURE 9

FIGURE 10

FIGURE 11

C-44
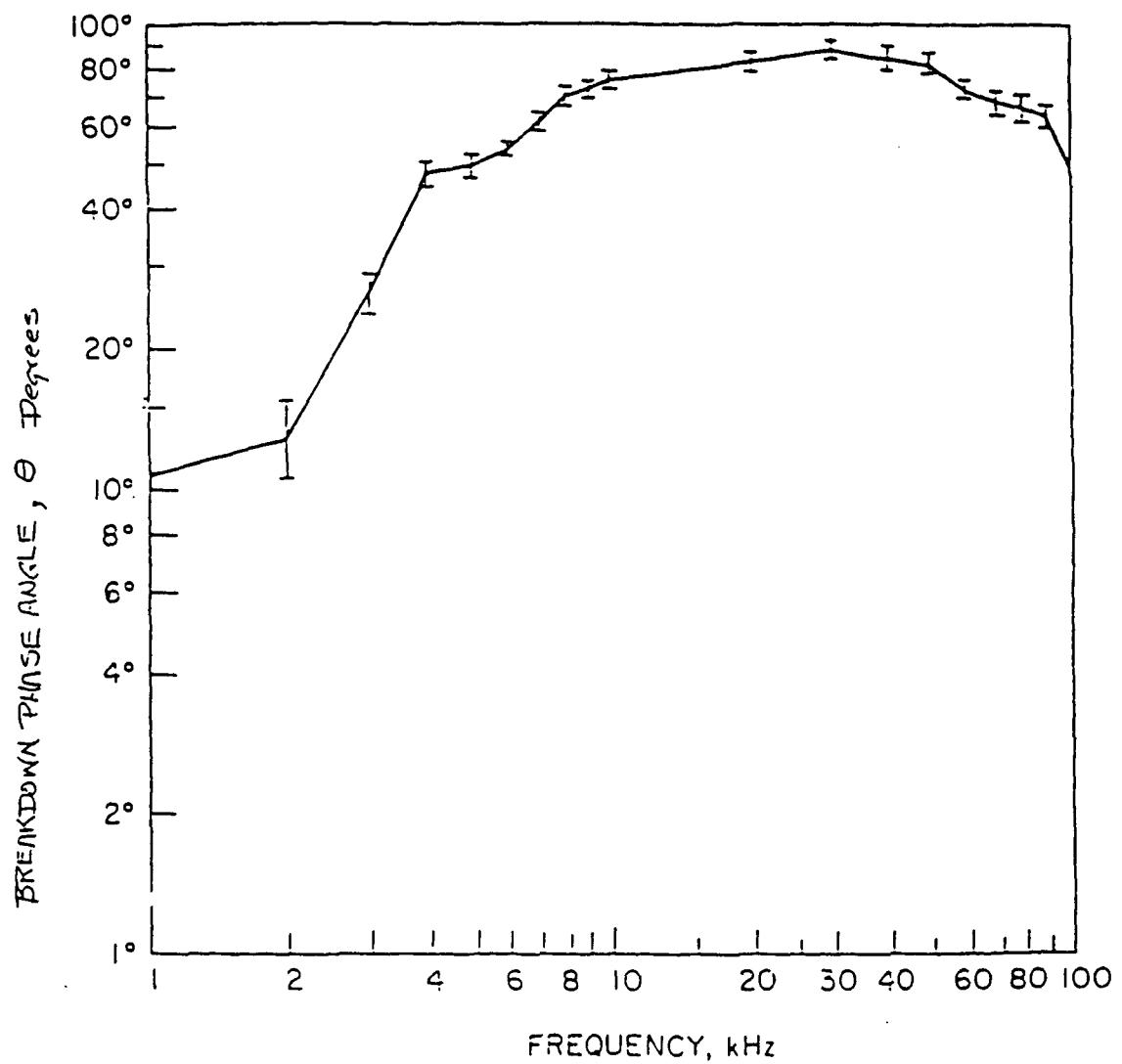
METHOD AND APPARATUS FOR COVERING BODIES
WITH A UNIFORM GLOW DISCHARGE PLASMA
AND APPLICATIONS THEREOF

STATEMENT OF GOVERNMENT INTEREST

5   This invention was made with Government support under

AFOSR Grant 89-0319 awarded by the Air Force. The Government has

certain rights in this invention.

BACKGROUND OF THE INVENTION

        The present invention relates to a method and apparatus

10   for covering the surface of a free-standing body, particularly a

vehicle such as an aircraft or a ship, with a uniform glow

discharge plasma, and for the use of such plasma covering for

various applications, including affecting the aerodynamic

properties of the body by decreasing or increasing the drag of the

15   body in the atmosphere. The invention also relates to methods and

apparatus for treating a workpiece with such a plasma.

        The term "plasma" usually describes a partially ionized

gas composed of ions, electrons and neutral species. This state of

matter may be produced by the action of either very high

20   temperatures, or strong direct current (DC) or radio frequency (RF)

electric fields. High temperature or "hot" plasmas are represented

by stars, nuclear explosions and electric arcs. Glow discharge

plasmas are produced by free electrons which are energized by an

imposed DC or RF electric field and then collide with neutral

C-45

molecules. These neutral molecule collisions transfer energy to the molecules and form a variety of active species which may include photons, excited atoms, metastables, individual atoms, free radicals, molecular fragments, monomers, electrons and ions.

5   Low power plasmas, such as dark discharges and coronas, have been used in the surface treatment of various materials. Because of their relatively low energy content, corona discharge plasmas can alter the properties of a material surface without damaging the surface.

10   Glow discharge plasmas represent another type of relatively low power density plasma. These glow discharge plasmas can produce useful amounts of visible and ultraviolet (UV) radiation. Glow discharge plasmas have the additional advantage therefore of producing visible and UV radiation in the simultaneous

15   presence of active species. However, glow discharge plasmas have heretofore been successfully generated typically in low pressure or partial vacuum environments below 10 torr which may necessitate batch processing and the use of expensive vacuum systems.

          The generation of low power density plasmas at one

20   atmosphere is not new. Filamentary discharges between parallel plates in air at one atmosphere have been used in Europe to generate ozone in large quantities for the treatment of public water supplies since the late 19th century. Such filamentary discharges, while useful for ozone production, are of limited

25   utility because the filaments are indicative of a non-uniform plasma with uneven properties and effects on exposed materials.

SUMMARY OF THE INVENTION

The present invention includes methods and apparatus for covering a body with a uniform glow discharge plasma. The invention also includes methods for treating a workpiece with such

5   a glow discharge plasma. The invention further includes bodies which are covered with a glow discharge plasma.

The plasma may be formed in atmospheric air or in other gases at about one atmosphere of pressure, or at pressures below or above one atmosphere. The plasma may also be formed in the

10 atmosphere above ground level, provided there is sufficient atmospheric gas in which to generate the plasma, or may be generated in other gases of such reduced pressures.

In accordance with the method of the present invention a steady-state one atmosphere glow discharge plasma is generated

15 above the surface of a body in a gas. The body may have disposed thereon a first electrode terminal and a second electrode terminal, wherein the first electrode terminal is connected to a first pole of a radio frequency (RF) power source which has first and second opposite poles, and wherein the second electrode terminal is either

20 connected to the second pole of said RF power source or is grounded. As used herein, the term "electrode terminal" is intended to encompass any suitable electrode means for use in generating an electric field. The plasma is generated by utilizing the RF power source to energize the first electrode terminal
relative to the second electrode terminal with an RF driving

voltage, wherein the voltage is high enough to generate an electric field above the surface of the body, and the applied frequency of the RF electric field is high enough to trap the positive ions of the plasma on electric field lines between the two electrode

5   terminals, but not so high that the electrons of the plasma are also trapped during a half cycle of oscillation of the RF voltage. In this manner, plasma is produced in the gas above the surface of the body.

Many different types of bodies may be covered with a

10   plasma glow discharge in accordance with the present invention. The body may be a vehicle designed for movement in the air (such as an aircraft) on the water (such as a ship) or on the ground (such as a car or truck).

The body may also be industrial equipment used for

15   applying the glow discharge plasma to a workpiece being processed by the industrial equipment.

The method and apparatus of the present invention are suitable for use in atmospheric air. Such air may be at one atmosphere sea level pressure (760 torr), or at the greatly reduced

20   pressures found higher in the atmosphere. Other gases in which a glow discharge plasma can form may also be used. These include, but are not limited to, the noble gases, such as helium, neon and argon, as well as carbon dioxide and nitrogen, or mixtures thereof.

In one embodiment of the present invention a steady-state

25   uniform one atmosphere glow discharge plasma is generated on the
surface of a body in the atmosphere. The body has an insulated

metallic skin on which are disposed strip electrodes which are

spaced from and generally parallel to each other. The adjacent

strip electrodes are connected to opposite poles of a radio

frequency (RF) power source. To generate the plasma, one or more

5   of the strip electrodes connected to one pole of the RF power

source are energized relative to one or more adjacent strip

electrodes connected to the other pole. The driving current is of

high enough voltage to generate the glow discharge above the

surface of the body. A voltage of more than about 10 kV RMS per cm

10   is suitable in one atmosphere of air. The current is of relatively

low frequency. The frequency should be sufficiently high such that

the ions generated in the plasma between the electrodes do not have

time during a half cycle of oscillation along electric field lines

to impact either electrode. On the other hand, the frequency

15   should be sufficiently low such that the electrons of the plasma

are not also trapped in the plasma, but have time to impact the

body or otherwise leave the plasma during a half cycle of

oscillation. A frequency in the range of about 100 Hz to about 30

kHz, depending on electric field and geometry as well as other

20   factors discussed below has been found suitable. In this manner,

the positive ion content of the plasma builds up, while the

electrons can impact the body to build up a charge on the body.

This acts to allow a steady state uniform glow discharge plasma to

form above the body.

25   In another embodiment of the invention, at least a

portion of the insulated metallic skin of the body is used as one

of the electrodes for generating the plasma. That is, the skin of the body, or a portion of the skin, is connected to one pole of the RF power source, and thus acts as the first electrode. A second electrode is provided spaced from the first electrode, such that

5   the plasma is generated between the electrodes. The second electrode may either be connected to the second pole of the RF power source, or may be grounded.

In a particular embodiment of the present invention, such a layer of plasma is applied to a moving vehicle, such as an

10   aircraft, ship or car, to reduce the drag and otherwise improve the aerodynamic characteristics of the atmospheric boundary layer on the vehicles. This is accomplished by reducing the level of boundary layer turbulence and by suppressing the formation of turbulent vortices.

15   In another embodiment of the invention, the plasma is generated on the surface of a vehicle, such as an aircraft, in a peristaltic fashion to alter the speed of the vehicle in relation to the surrounding atmosphere.

In a\.dition, the plasma may be generated on the surface

20   of a body, such as an aircraft, to prevent the formation of ice and to remove ice present on the body.

The glow discharge plasma may also be generated on the surface of a body, such as a vehicle at night or in low visibility conditions, to make the body more visible.

BRIEF DESCRIPTION OF THE DRAWINGS

Figure 1 is a schematic representation of apparatus for generating a plasma glow discharge between two plate electrodes.

Figure 2 is a schematic representation of a tubular body with apparatus for generating a uniform glow discharge plasma on the tubular body in accordance with the present invention.

Figure 3 is a photograph of an apparatus corresponding to that depicted schematically in Figure 2

Figure 4 is a photograph of the apparatus shown in Figure 3 under power, showing the body of the apparatus coated with a plasma in accordance with the present invention.

DESCRIPTION OF THE PREFERRED EMBODIMENT

The present invention includes methods and apparatus for covering a body with a uniform glow discharge plasma. The invention also includes methods for treating a workpiece with such a glow discharge plasma. The invention further includes bodies which are covered with a glow discharge plasma.

The plasma may be formed in atmospheric air or in other gases at about one atmosphere of pressure or below or above atmospheric pressure. The plasma may also be formed in the atmosphere above ground level, provided there is sufficient atmospheric gas in which to generate the plasma, or may be generated in other gases of such reduced pressures.

The methods and apparatus of the present invention are suitable for use in atmospheric air. Such air may be at one atmosphere sea level pressure (760 torr), or at the greatly reduced pressures found higher in the atmosphere. Other gases in which a glow discharge plasma can form may also be used. These include, but are not limited to, the noble gases, such as helium, neon and argon, as well as carbon dioxide and nitrogen, or mixtures thereof.

Many different types of bodies may be covered with a plasma glow discharge in accordance with the present invention. The body may be a vehicle designed for movement in the air (such as an aircraft) on the water (such as a ship) or on the ground (such as a car or truck).

The body may also be equipment used for applying the glow discharge plasma to a workpiece. The electrodes may be in the open when the plasma is to be generated in air. In those situations where an environmental risk may come about by exposure to the gases generated or otherwise, the apparatus and the work piece treated in accordance with the invention will advisedly be appropriately surrounded by a protective barrier. For instance, an enclosure of material like PLEXIGLAS can readily be provided for the equipment, with suitable inlet and outlet for the workpiece to be plasma treated. In cases in which the plasma gas is other than ambient air, the enclosure may be designed to also retain the treatment gas and prevent the surrounding air from entering the treatment zone.

In one embodiment of the present invention a steady-state uniform one atmosphere glow discharge is generated on the surface

of a body in the atmosphere. The body can have the plasma generated on its outer surface or on an inner surface, as in a hollow tube. The body has an insulated metallic skin on which are disposed strip electrodes which are spaced from and generally

5   parallel to each other. The adjacent strip electrodes are connected to opposite poles of a radio frequency (RF) power source. To generate the plasma, one or more of the strip electrodes connected to one pole of the RF power source are energized relative to one or more adjacent strip electrodes connected to the other

10   pole. The driving current is of high enough voltage to generate electric fields above the surface of the vehicle, suitably of more than about 10 kV RMS per cm. The current is of relatively low frequency, suitably within the range of about 100 Hz to about 30 kHz. On one hand, the frequency should be sufficiently high such

15   that the ions generated in the plasma above the insulated skin of the body and trapped on electric field lines do not have time during a half cycle of oscillation to impact the electrodes. On the other hand, the frequency should be sufficiently low such that the electrons of the plasma are not also trapped in the plasma, but

20   have time to impact the electrode or skin or otherwise leave the plasma during a half cycle of oscillation. In this manner, the positive ion content of the plasma builds up, while the electrons can impact the insulated skin to build up a charge on the skin. This acts to allow a steady quasi-neutral state uniform glow

25   discharge plasma to form above the insulated skin.

This embodiment of the invention could be used on a vehicular body, such as an aircraft, ship or terrestrial vehicle, in which the strip electrodes would be applied to the outer skin of the vehicle to generate a glow discharge plasma on the exterior of

5   the vehicle. This embodiment could also be used on various types of industrial equipment.

In another embodiment of the invention, at least a portion of the insulated metallic skin of the body is used as one of the electrodes for generating the plasma. That is, the skin of

10 the body, or a portion of the skin, is connected to one pole of the RF power source, and thus acts as the first electrode. A second electrode is provided spaced from the first electrode, such that the plasma is generated between the electrodes. The second electrode may either be connected to the second pole of the RF

15 power source, or may be grounded.

In accordance with this embodiment, the first electrode may be a first portion of the insulated skin of the body, and the second electrode may be a second portion of the metallic skin which is electrically isolated from the first portion. In such an

20 embodiment, the RF driving voltage is applied between the two portions of the skin. When the body is a vehicle such as an aircraft, there are any number of configurations that may be used. The first electrode could comprise the fuselage, with the second electrode comprising the wings. Alternatively, the first electrode

25 could comprise the skin on a forward portion of the aircraft, with

the second electrode comprising the skin of an aft portion.

C-54

Likewise, the first electrode could comprise the skin of a ventral (lower) portion of the aircraft and with the second electrode comprising a dorsal (upper) portion.

In another embodiment in which a portion of the skin is used as the first electrode, a separate second electrode may be provided. In such instances, the entire skin may act as the first electrode. When the body is a vehicle, such as an aircraft or ship, the second electrode may be grounded to the atmosphere or sea, respectively, or may be connected to the second pole of the RF power source. In one such embodiment for a vehicle or other body, the second electrode comprises a high porosity screen generally parallel to and between the skin and the screen. Suitably a spacing of at least one centimeter is used. Alternatively, such a screen can be essentially coextensive with the insulated skin of the vehicle which is acting as the first electrode.

An alternative particularly applicable to aircraft is to use essentially the entire metallic skin of the aircraft as the first electrode, with the second electrode comprising a conductive wire which is insulated from the metallic skin and is trailed in the atmosphere behind the aircraft. In this manner, the surrounding atmosphere is established as a grounded reference plane.

Another embodiment is applicable when the vehicle is an aircraft powered by one or more jet engines. The engines are electrically insulated from the rest of the aircraft. Such jet engines generally have an exhaust containing partially ionized

gases when under power. In this case, the metallic skin of the rest of the aircraft is used as the first electrode and the partially ionized gases of the exhaust are used as the second electrode. Again, as discussed above, the surrounding atmosphere is thus established as a grounded reference plane. In addition, the exhaust portion of the jet engines can be surrounded with a suitable circular biasing electrode.

In like manner, when the body to which the plasma is being applied is a ship in water, the water can be utilized as the grounded second electrode. In such a case, at least a portion of the superstructure above the water line would be connected to the RF power source and used as the first electrode. This works particularly well when the surrounding water is highly conductive salt water. If the ship is in fresh water which is not sufficiently conductive to maintain the plasma, then the wake of the ship can be seeded with a suitable salt, such as an alkali metal salt, to increase the conductivity and allow the utilization of the high conductivity wake as the second electrode.

In a particular embodiment of the present invention, such a layer of plasma is applied to a moving vehicle, such as an aircraft, ship or car, to reduce the drag and otherwise improve the aerodynamic characteristics of the atmosphere boundary layer on the vehicles. This is accomplished by reducing the level of boundary layer turbulence and by suppressing the formation of turbulent vortices.

By turning the plasma on and off, and varying the intensity of the plasma through the input power density and the applied RF voltage, it is possible to vary the drag coefficient of an aircraft from the normal value without the plasma layer, to

5 values which may be much lower than those normally encountered. The plasma would tend to be swept along with the aerodynamic boundary layer flow, and would tend to accumulate in areas of stagnation or in vortices, thus making these aerodynamically drag-producing structures subject to an electric field, which may be

10 manipulated by auxiliary or control electrodes on the surface of the aircraft.

In addition to reducing the drag and manipulating the geometry and position of vortices and areas of stagnant air flow, the boundary layer may be either speeded up or slowed down by

15 producing traveling electrostatic peristaltic waves along the direction of movement of the aircraft. To accomplish this, the surface of the aircraft is covered with a series of insulated strip electrodes, oriented perpendicular to the normal aerodynamic flow of the boundary layer gases over the aircraft. These strip

20 electrodes can then be energized in sequence, to induce the generation of peristaltic plasma waves along the surface of the aircraft. When such peristaltic waves are generated from front to back on the aircraft, they exert an acceleration of the plasma in the boundary layer, thus making the flow more laminar, and

25 discouraging the formation of vorticity. On the other hand, if such waves are generated from back to front on t'   ircraft, then

the action would work against the aerodynamic flow and could increase the drag on the aircraft, thus producing a braking effect on the motion of the aircraft though the atmosphere. Thus, the peristaltic waves can be used to either accelerate or decelerate

5   the aircraft.

Various elaborations of this plasma-related boundary layer control are also possible. For example, the surface of the aircraft or vehicle can be fitted with a series of parallel insulated electrodes, the contours of which are perpendicular to

10 the most laminar and least turbulence-producing boundary layer flow over the aircraft, as determined by wind tunnel tests. Phased excitation of these contoured parallel insulated electrodes could provide a body force accelerating the boundary layer flow over the aircraft in a direction which is least likely to lead to turbulence

15 and vortex formation. Such manipulation of the boundary layer by electrostatic body forces may, in addition, have the effect of raising the Reynolds number for transition to turbulent flow both locally, and for the aircraft or vehicle as a whole.

If no peristaltic effect is desired, then the electrodes

20 can be oriented in any suitable direction on the aircraft, and all powered simultaneously to create a uniform steady-state plasma.

The electrodes should be arranged in parallel strips on the surface of the aircraft or other vehicle with adjacent strips being operated at radio frequency voltages 180° out of phase with

25 each other. The RF voltages should be sufficiently high such that RMS electric fields of 10 kilovolts per centimeter (kV/cm) or

higher ar generated above the surface of the vehicle suitably to a height of about one centimeter or more. The width of the individual strip electrodes should be wide enough to create a uniform plasma layer over the surface of the vehicle. The strip

5   electrodes can be oriented on the surface of the vehicle as a matter of convenience, in a quasi-parallel pattern, or the electrodes can be placed parallel or perpendicular to the velocity vector of the gas in the boundary layer flowing over the surface of the vehicle. The width of the individual strip electrodes can be

10 adjusted over the surface of the aircraft, in such a way as to produce dense plasma where it is most needed, and more rarified plasma where that is satisfactory for the intended application of the plasma layer.

In addition, the plasma may be generated on the surface

15 of a body, such as an aircraft, to prevent the formation of ice and to remove ice present on the body.

The glow discharge plasma may also be generated on the surface of a body, such as a vehicle at night or in low visibility conditions, to make the body more visible.

20 The apparatus required to generate a one atmosphere glow discharge plasma around a body includes a low-frequency RF power supply capable of operating from below about 500 Hz up to at least about 10 kHz, or even up to about 30 kHz, at RMS voltages up to about 20 kV. One pole of the power supply is connected to the

25 first electrode, and the other is connected to the second electrode, or grounded, as discussed above.

These connections should be made through an impedance matching network, the function of which is to minimize the reactive power in the RF circuit. Such an impedance matching network can broaden the range of operating frequency and other parameters over

5   which the desirable uniform (as opposed to filamentary) glow discharge is observed. The parameters of such a matching network are adjusted for the most stable, uniform operation of the glow discharge. This condition can occur when the reactive power of the plasma reactor is minimized.

10   Tests conducted on a parallel plate uniform glow discharge plasma reactor operating at atmospheric pressure indicated that such glow discharges could be maintained by average power densities ranging from below 10 milliwatts per cubic centimeter to values higher than 100 milliwatts per cubic

15   centimeter. On the basis of these experiments, it is reasonable to suppose that a power density of about 50 milliwatts per cubic centimeter may be required to maintain a layer of plasma surrounding an aircraft. If the aircraft has a total surface area of 500 square meters, and if the layer of plasma is two centimeters

20   thick, 10 cubic meters of plasma would need to be generated at 50 milliwatts per cubic centimeter. This would require an energy input to generate such a plasma of 500 kW, a power level about one percent of the total shaft horsepower generated by the jet engines of typical aircraft. Thus, there appears to be no reason, on

25   energetic grounds, why full-scale aircraft should not be able to supply the power requirements for generating such a uniform plasma

over their surface, at an energy cost in shaft horsepower that is only a few percent of that developed for their flight requirements. Even in an extreme case, the mass of the electrical power generator and power supplies required to produce the high voltage RF needed

5   to produce the plasma should require no more than about 1 kilogram per kilowatt, thus burdening the aircraft in the example above with no more than about 500 kilograms of additional equipment. In practice, this is likely to be a very generous overestimate of the mass of a single unit generating half a megawatt of electrical and

10   RF power.

An electric field established between the metallic electrodes must be strong enough to electrically break down the gas used, and is much lower for helium and argon than for atmospheric air. The RF frequency should be within a suitable range, as

15   discussed above, since if it is too low, the discharge will not initiate, and if it is too high, the plasma will form filamentary discharges between the electrodes. Within this suitable frequency band a uniform slow discharge plasma forms without filamentary discharges.

20   Electric fields employed in a one atmosphere, uniform glow discharge plasma reactor are only a few kilovolts per centimeter, values which, if D.C., would usually be too low to electrically break down the background gas. Gases such as helium and air will break down under such low electric fields, however, if

25   the positive ion population is trapped between the two parallel or uniformly spaced electrodes. This greatly increases the ions'

lifetime in the plasma, while at the same time the electrons are free to travel to the insulated electrode plates where they recombine or build up a surface charge. The most desirable uniform one atmosphere glow discharge plasma is therefore created when the

5   applied frequency of the RF electric field is high enough to trap the ions between the electrodes, but not so high that the electrons are also trapped during a half cycle of the R.F. voltage. The electrons may be trapped by ambipolar electrostatic forces.

If the RF frequency is so low that both the ions and the

10   electrons can reach the boundaries and recombine, the particle lifetimes will be short and the plasma will either not initiate or form a few coarse filamentary discharges between the plates. If the applied frequency is in a narrow band in which the ions oscillate between the electrodes, they do not have time to reach

15   either boundary during a half period of oscillation and be confined for long times. If the more mobile electrons are still able to leave the plasma volume and impinge on the boundary surfaces, then the desirable uniform plasma is produced. If the applied RF frequency is still higher so that both electrons and

20   ions are trapped in the discharge, then the discharge becomes electrically polarized and forms a filamentary plasma.

The following examples are illustrative of the invention but they should not in any way be considered as limiting the invention thereto.

EXAMPLE 1

Without being limited to any particular theory, it is believed that a relationship exists between the electrode spacing, the RMS electrode voltage, the ion mobility, and the applied frequency which results in trapping ions but not electrons between the two electrodes, and produces the desired uniform one atmosphere glow discharge plasma.

In accordance with this theory, Figure 1 presents a schematic of an atmospheric glow discharge plasma reactor in which the plasma is generated between upper plate electrode 50 and grounded lower plate electrode 52 connected to opposite poles of an R.F. source 54. In the configuration of Figure 1, a Cartesian coordinate system is applied as shown, with the applied electric field in the x-direction. The maximum amplitude of the electric field between the grounded lower electrode 52 and the upper electrode 52 is E_0, and the separation of the electrodes is the distance d.

The electric field between the electrodes shown on Figure 1 is given by

$$E = (E_0\sin\omega t, 0, 0). \qquad\qquad (1)$$

It is assumed that the one atmosphere glow discharge operates in a magnetic field free plasma. The equation of motion for the ions or electrons between the two plates is given by a Lorentzian model, in which the electrons and ions collide only with the neutral

background gas and, on each collision, give up all the momentum in the direction of the electric field they acquired from the RF electric field since the last collision with the neutral gas. The equation of motion for the ions or electrons in the Lorentzian

5   model is given by

$$F = ma = -m\nu_c v - eE, \qquad (2)$$

where the first term on the right hand side is the Lorentzian collision term, according to which the momentum mv is lost with each collision that occurs with a collision frequency ν_c. The x component of Eq. 2 is given by

$$m\frac{d^2X}{dt^2} + m\nu_c\frac{dx}{dt} = eE_0\sin\omega t, \qquad (3)$$

10   where the electric field E from Eq. 1 has been substituted into the right hand side of Eq. 2. The general solution to Eq. 3 is

$$x = C_1\sin\omega t = C_2\cos\omega t, \qquad (4)$$

where the constants C_1 and C_2 are given by

$$C_1 = -\frac{eE_0}{m}\frac{1}{(\omega^2+\nu_c^2)}, \qquad (5)$$

and

$$C_2 = -\frac{\nu_c e E_0}{\omega m}\frac{1}{(\omega^2 + \nu_c^2)} . \tag{6}$$

The one atmosphere helium glow discharge is operated at frequencies between $\omega/2\pi = 1$ and 30 kHz, where, for helium at one atmosphere,

$$\nu_{ci} \approx 6.8 \times 10^9 \text{ ion collisions/sec.,} \tag{7a}$$

and

$$\nu_{ce} \approx 1.8 \times 10^{12} \text{ electron coll./sec.} \tag{7b}$$

5   The collision frequency for ions and electrons given by Eqs. 7a and 7b is much greater than the RF frequency, $\nu_c \gg \omega$. The relation $\nu_c \gg \omega$ for ions and electrons, implies that C_2 is much greater than the constant C_1, or

$$C_2 \approx -\frac{e E_0}{m \omega \nu_c} \gg C_1 \tag{8}$$

The time dependent position of an ion or an electron in the
10   electric field between the plates is given by substituting Eq. 8 into Eq. 4, to obtain

$$x(t) \approx -\frac{e E_0}{m \omega \nu_c} \cos\omega t. \tag{9}$$

The RMS displacement of the ion or electron during a half cycle is given by

$$x_{rms} = \frac{2}{\pi}\frac{e E_0}{m \omega \nu_c} \text{ meters.} \tag{10}$$

C-65

If ν is the driving frequency, in hertz, and V_{rms} is the RMS voltage applied to the plate electrodes, then the radian RF frequency is given by

$$\omega = 2\pi\nu, \tag{11}$$

and the electric field between the plates can be approximated from the RMS voltage V_{rms} applied to the plate electrodes,

$$E_0 = \frac{V_{rms}}{d}. \tag{12}$$

If the charge in question moves across the entire discharge width d between the plates, on the average, during one full cycle, then this would provide

$$x_{rms} \approx \frac{d}{2}. \tag{13}$$

In accordance with Equation 13 the RMS displacement of the ions has to be less than half the clear spacing in order to have a buildup of charge between the plates, that is, $x_{rms} < d/2$ to have a charge buildup. Substituting Eqs. 11 to 13 into Eq. 10 yields the relationship

$$\frac{d}{2} \approx \frac{eV_{rms}}{\pi^2 m\nu\nu_c d}. \tag{14}$$

Solving for the critical frequency ν_0 above which charge buildup should occur in the plasma volume, gives

$$v_0 \approx \frac{2eV_{rms}}{\pi^2 m v_c d^2} \ Hz. \tag{15}$$

In Eq. 15, the collision frequency v_c for helium is approximately given by Eqs. 7a or 7b for ions or electrons, respectively, at one atmosphere, and the RMS voltage is that which bounds the upper and lower limit of the uniform discharge regime.

5   For helium ions, the following experimental conditions were used:

     $V_{rms} \approx 1000$ volts (threshold for discharge initiation)

     $d \quad \approx 1.25 \ x \ 10^{-2}$ meters

     $v_{ci} \quad = 6.8 \ x \ 10^9$/sec

10   This gives, for singly charged helium ions:

     $v_0 \quad > 4.6$ kHz, theoretical

This was in good agreement with the experiment which gave:

     $v_0 \quad \approx 3.0$ kHz, experimental.

For electrons,

15        $v_{ce} \quad = 1.8 \ x \ 10^{12}$/sec, and

     $V_{rms} \approx 1000$ volts.

The threshold for confinement of both species is:

     $v_0 \quad \approx 127$ kHz,

which is consistent with the observed formation of filamentary

20   discharges below 100 kHz.

          For helium, at one atmosphere pressure the voltage V_o should be greater than about 1.5 kV_{rms}, and the frequency v between about 1 kHz and about 3 kHz to produce an electric field E greater

than about 1 kV_{rms}/cm. Preferably, the minimum electric field E for helium is about 2 kV_{rms}/cm.

For air, at one atmosphere pressure, the voltage V_o should be greater than about 5 kV_{rms}, and the frequency v should be

5   between about 1 kHz and about 2.5 kHz. Preferably, the minimum electric field E for oxygen is about 8 kV_{rms}/cm.

The above formulae are applicable to air and other gases and mixtures thereof by substituting appropriate value for such gases from scientific published literature or standard reference

10   manuals, like the Handbook of Chemistry and Physics, CRC Press, 69th Edition, 1988-1989, or others. Publications from the American Institute of Electrical Engineers or the I.E.E.E. may also be useful sources for information.

EXAMPLE 2

15   A laboratory simulation of apparatus made in accordance with the present invention was prepared, as shown schematically in Figure 2. The body to be coated with a uniform glow discharge plasma was a length of 2-inch diameter copper pipe 60 which may be grounded as shown. Strip electrodes 62 and 64 were provided in the

20   form of wires surrounded by plastic insulation. Two parallel lengths of insulated wires were spiral wrapped side-by-side around the length of the copper pipe. To distinguish the two spirals in the drawing, electrode 64 is marked along its length with x's. In this case, the thickness of the insulation maintained a uniform

spacing between the copper wires. The two strip electrodes were connected to an RF power source 66. For purposes of this test, the test apparatus was placed inside a closed chamber filled with helium gas at one atmosphere pressure. As discussed above, helium

5   requires a lower voltage than air for generating a plasma, and it is for this reason that helium was used in this test. When power was applied to the circuit, a uniform violet glow discharge plasma was observed covering the coated copper body. It is the steady violet glow which shows that a uniform glow discharge plasma has

10   been established.

Figure 3 and 4 are photographs of an apparatus in accordance with that depicted schematically in Figure 2. Figure 3 shows the apparatus unpowered and Figure 4 shows the apparatus under power with a visible uniform violet glow discharge plasma

15   covering the body of the apparatus.

What is claimed is:

1. A method for generating a steady-state one atmosphere glow discharge plasma above the surface of a body in a gas, said body having disposed thereon a first electrode terminal and a second electrode terminal, wherein said first electrode terminal is connected to a first pole of a radio frequency (RF) power source which has first and second opposite poles, and wherein the second electrode terminal is either connected to the second pole of said RF power source or is grounded, the method comprising:

generating said plasma by utilizing said RF power source to energize said first electrode terminal relative to said second electrode terminal with an RF driving voltage, wherein the voltage is high enough to generate an electric field above the surface of the body, and the applied frequency of the RF electric field is high enough to trap the positive ions of the plasma on electric field lines between the two electrode terminals; but not so high that the electrons of the plasma are also trapped during a half cycle of oscillation of the RF voltage,

whereby a glow discharge plasma is produced in the gas above the surface of the body.

2. The method of claim 1 wherein said body has a skin on which are disposed insulated strip electrodes which are spaced

from and generally parallel to each other, wherein adjacent strip electrodes are connected to the opposite first and second poles of the RF power source, and wherein the strip electrodes connected to the first pole comprise the first electrode terminal and the strip

5   electrodes connected to the second pole comprise the second electrode terminal.

3.   The method of claim 2 wherein said body is a vehicle.

4.   The method of claim 3 wherein the vehicle is moving and said strip electrodes are oriented generally parallel to the velocity vector of the movement of the vehicle.

5.   The method of claim 3 wherein the vehicle is moving and said strip electrodes are oriented generally perpendicular to the velocity vector of the movement of the vehicle.

6.   The method of any one of claims 2 to 5 wherein said strip electrodes are all energized simultaneously to generate said plasma.

7.   The method of any one of claims 2 to 5 wherein said strip electrodes are energized in a predetermined sequence to generate said plasma.

LAW OFFICES
EISER & ASSOCIATES
SUITE 500
30 SO FIFTEENTH ST
PHILADELPHIA, PA 19102
(215) 6383
ECC   (5) 875-6384

8. The method of claim 1 wherein said body has a metallic skin covered with an insulating layer,

wherein at least a portion of the insulated metallic skin is used as the first electrode terminal,

and wherein the second electrode terminal is provided spaced from said first electrode terminal with the insulating layer on said first electrode terminal interposed between said first and second electrodes.

9. The method of claim 8 wherein essentially the entire metallic skin of the body is used as the first electrode.

10. The method of claim 8 wherein said body is a vehicle.

11. The method of claim 8 wherein a first portion of said metallic skin is electrically isolated from a second portion of said metallic skin, said first portion being used as the first electrode terminal and said second portion being used as the second electrode terminal.

12. The method of claim 11 wherein the body is an aircraft.

13. The method of claim 8 wherein the body is a ship having a metallic skin in water wherein a portion of the skin of

C-72

the ship above the water level is utilized as the first electrode terminal and the water is utilized as the second electrode terminal.

14. A method for decreasing the drag coefficient and the production of vorticity on a vehicle moving through the atmosphere comprising generating a steady-state one atmosphere glow discharge plasma above the surface of said vehicle.

15. A method of affecting the speed of a vehicle relative to a surrounding atmosphere in which the vehicle is moving, the method comprising generating a steady-state one atmosphere glow discharge plasma on the surface of said vehicle by
5   the method of claim 5, and energizing said strip electrodes in a peristaltic sequence which affects the speed of said vehicle relative to said surrounding atmosphere.

16. Apparatus for generating a steady-state one atmosphere glow discharge plasma above the surface of a body in a gas, the apparatus comprising:
   a radio frequency (RF) power source which has first and
5   second opposite poles,
   a first electrode terminal which is connected to the first pole of the RF power source, and
   a second electrode terminal which is either connected to

the second pole of the RF power source or is grounded,

wherein said RF power source comprises means to energize said first electrode terminal relative to said second electrode terminal with an RF driving voltage, wherein the voltage is high enough to generate an electric field above the surface of the body,

5   and the applied frequency of the RF electric field is high enough to trap the positive ions of the plasma on electric field lines between the two electrode terminals, but not so high that the electrons of the plasma are also trapped during a half cycle of oscillation of the RF voltage.

17.   The apparatus of claim 16 wherein said body has a skin and wherein said first and second electrode terminals comprise insulated strip electrodes disposed on said skin, wherein said electrodes are spaced from and generally parallel to each other,

5   wherein adjacent strip electrodes are connected to the opposite first and second poles of the RF power source, and wherein the strip electrodes connected to the first pole comprise the first electrode terminal and the strip electrodes connected to the second pole comprise the second electrode terminal.

18.   The apparatus of claim 17 further comprising means to energize said strip electrodes in a predetermined sequence.

19.   The apparatus of claim 16 wherein said body comprises a metallic skin covered with an insulating layer,

and wherein the first electrode terminal comprises at least a portion of said insulated metallic skin,

and wherein the second electrode terminal is spaced from the first electrode terminal with the insulating layer on the first

5 electrode terminal interposed between said first and second electrode terminals.

ABSTRACT OF THE DISCLOSURE

Method and apparatus for covering a free-standing body with a uniform glow discharge plasma, particularly at atmospheric pressure. The method may be used to provide a body coated with

5   such a plasma, and also to treat a workpiece.

FIGURE 1

54

R.F. SOURCE

ω

PLASMA

$E_0 \sin \omega t$

y

x

z

50

52

d

C-77
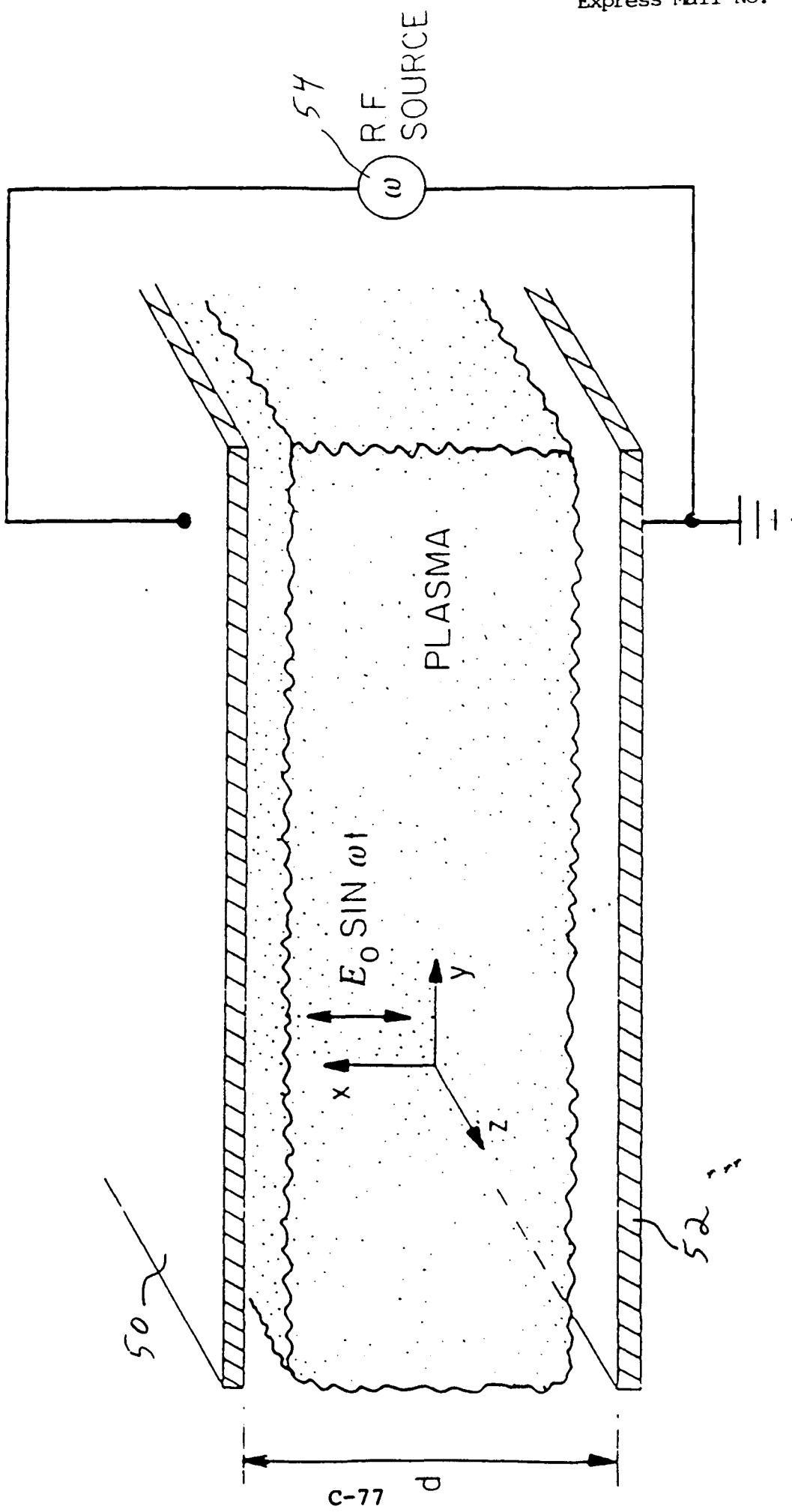
SCHEMATIC OF THE ONE ATMOSPHERE GLOW DISCHARGE PLASMA REACTOR
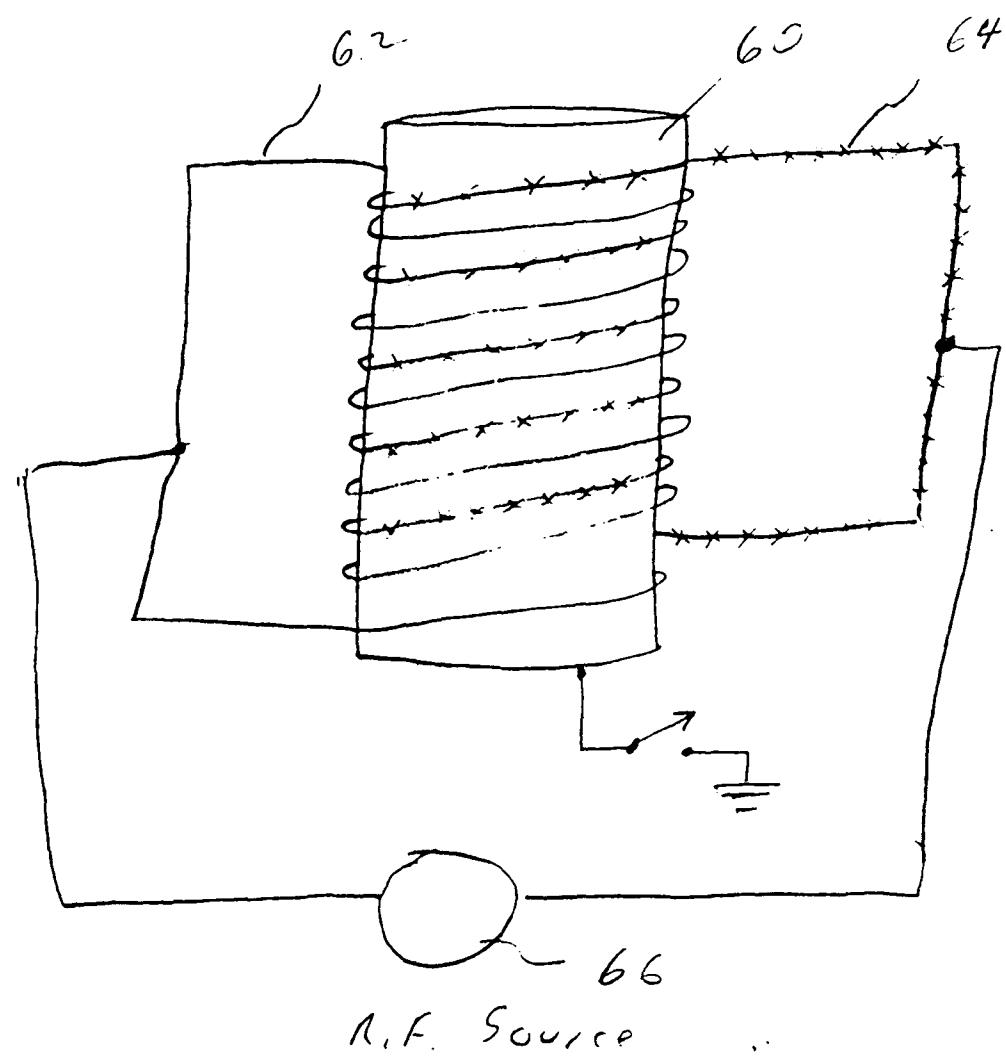
FIGURE 2
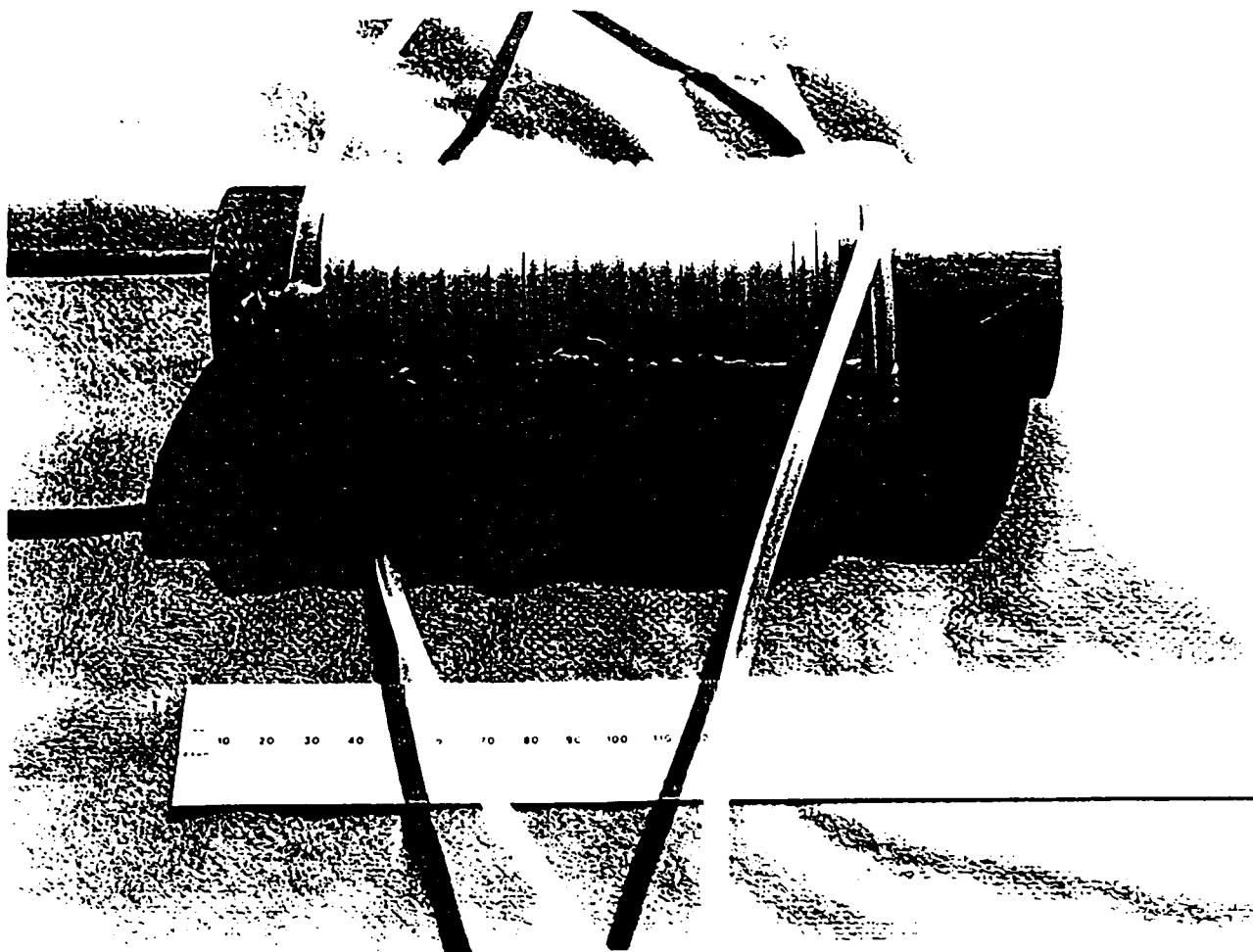
FIGURE 3
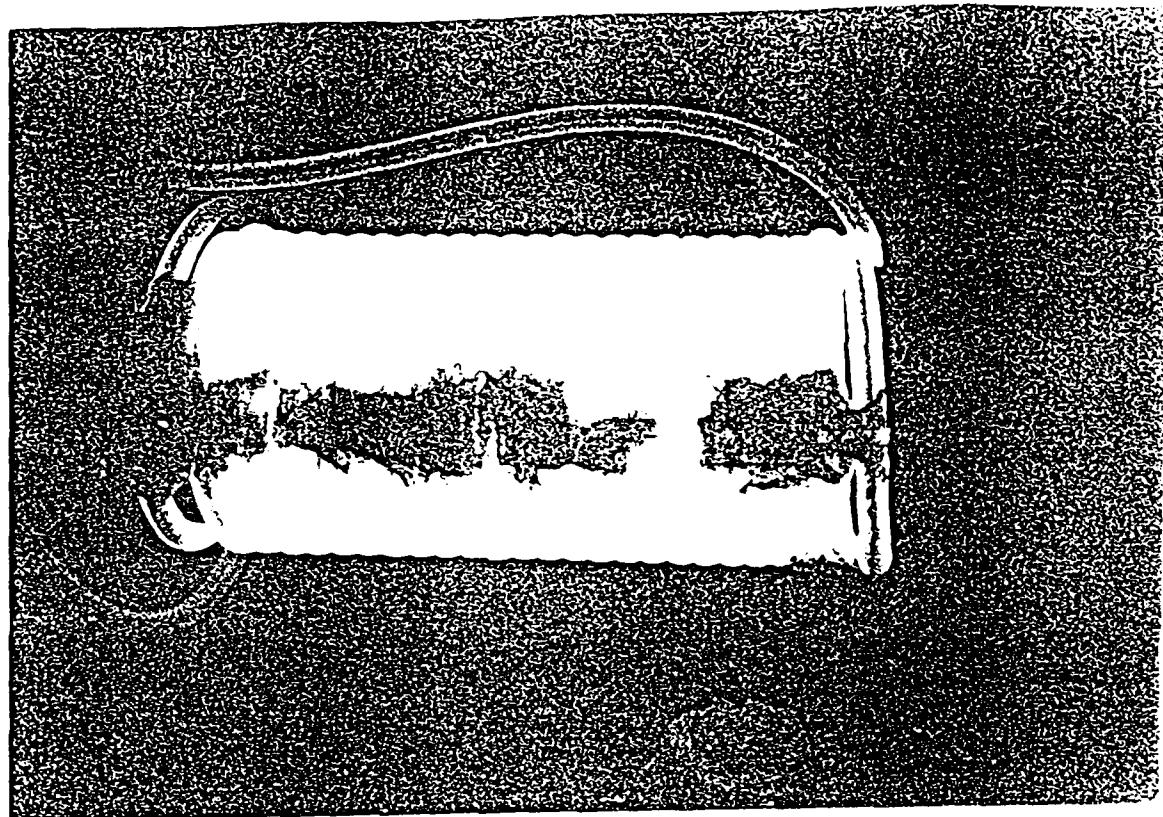
FIGURE 4

APPENDIX D

PUBLICITY GENERATED BY CONTRACT AFOSR 89-0319

International classroom

Prof gets peek at Chinese life

By CINDY SHEA
Daily Beacon Research Editor

Just three weeks after the Beijing turmoil this summer, a UT professor traveled to China to exchange knowledge about fusion energy research and industrial plasma engineering with the Chinese.

Reece Roth, professor of electrical engineering, left for Beijing on June 25 for a three-week trip that turned into an education in Chinese technology and culture, he said.

"By the time I reached Beijing all signs of the destruction had been removed," Roth said, except that the city was under martial law. "The people I encountered felt the current government was a passing phase and would soon leave the scene."

In Beijing, he met with Professor Xinz Zhong Li of Tsinghua University, leader of a team that is translating Roth's textbook into Chinese. Tsinghua University press will publish his book, Introduction to Fusion Energy.

"Everybody was very friendly and very eager to interact with the United States," he said. Most Chinese scholars had spent a year or so in the states as part of their education, so the language barrier was not as bad as Roth had feared.

The Chinese are interested in fusion-related research because they are concerned about long-term energy needs and the growing air-pollution problem in China, he said.

As part of his trip, Roth gave 34 lectures at two universities, three research institutes and a microwave tube factory.

"I lectured in English and only once needed a translator," he said. They were interested in my lecture on industrial plasma engineering and in the work we are *doing at UT on plasma ion plantation*, a process for improving the corrosive resistance of metals.

When asked to give a talk about cold fusion, Roth refused on the grounds that the entire subject was a blunder and an embarrassment to American science, he said.

Roth saw firsthand industrial plasma and fusion-related research underway in China. He toured a microwave tube factory in Chengdu, which several years ago was off limits to foreigners such as himself, Roth said.

He was allowed to photograph an architect's scale model of the entire tube works. "I was even allowed to photograph products still under development," which most U.S. companies would have forbidden.

All over China, government entities were being pressured to convert from purely government functions to consumer or industrial functions, he said. For instance, five years ago the tube factory's business was 80 percent military and in four years the figure is expected to fall to 20 percent.

The components made in this factory are probably used in electronic warfare, and the decrease in military business could signal a trend toward demilitarization, Roth said.

When Roth ventured outside the *labs and universities*, what he saw was frantic construction. The government has been forced to slow the pace because the annual growth rate was approaching 15 percent, causing runaway inflation, he said.

In addition to exchanging technical knowledge, his hosts insisted Roth spend time visiting cultural monuments. "I brought back a much broader appreciation of the Chinese culture," he said.

"I found out how inadequate our public education is with respect to China," Roth said, referring to his discovery of DuFu, the Chinese equivalent of Shakespeare.

"It was particularly annoying for me to realize how little I knew about a major power like China," he said.

Nevertheless, the Chinese education system is not without problems, Roth said. He expected to find technical education and graduate programs thriving, but this was not the case.

What Roth saw were incredibly run-down campus buildings. Faculty pay was grossly inadequate, and students complained of living four to six in a single room, he said.

But the Chinese displayed a strong desire for contact with other countries, with the exception of Japan, Roth said. Yet Japan leads the world in industrial plasma engineering, an area of interest to the Chinese, he said. The people were reluctant to interact or deal with the Japanese, perhaps because of residual bitterness after World War II, Roth suggested.

The United States made a mistake as well. After the Beijing turmoil, officials discouraged scientists and business people from traveling to China, Roth said.

"It was a fluke of funding that I went," he said. The U.S. Air Force paid his way to and from Beijing while his Chinese hosts paid all other expenses.

"The United States is going to make a serious blunder in terms of long-range foreign policy if they continue to isolate this country from China," Roth said.

Nevertheless, the United States seems to be the destination of choice for Chinese, he said.

Context

THE UNIVERSITY OF TENNESSEE, KNOXVILLE

TRAVELS

J. Reece Roth, Professor of Electrical and Computer Engineering. Destination: China, June 25-July 15.

Roth arrived in Beijing just three weeks after what the Chinese government called "the turmoil." He spent the following three weeks travelling through China, giving lectures and observing the state of industrial plasma and fusion related research. His travel expenses to and from China were paid by the U.S. Air Force, and his Chinese hosts paid all other expenses.

Roth was surprised by his hosts' openness in discussing technical matters and allowing him to observe technical developments, even after he told them that his trip was sponsored by the U.S. Air Force. For example, he was allowed to photograph everything he wanted to inside the Guoguang Electron Tube Works in Chengdu, including products still under development. Most U.S. companies would not have allowed this on grounds of commercial secrecy, he notes. In fact, the only restriction placed on photographs was in Beijing, where he was told not to photograph the soldiers.

Roth's memories of the soldiers are as good as any photograph, however. He describes them as mostly "extremely young" and not particularly seasoned. "Twice, while driving through Beijing, I found myself staring down the barrel of a casually handled assault rifle," he writes.

While in Beijing, Roth met with Professor Li, Xingzhong of the Tsinghua University Physics Department, leader of the team translating Roth's *Introduction to Fusion Energy* textbook into Chinese and visited the Tsinghua University Institute of Nuclear Energy Technology. He also presented a lecture on "Ball Lightning as a Route to Fusion Energy." He presented two lectures at the Beijing Institute of Physics and visited their tokamak (a device for producing controlled thermonuclear power) laboratory.

On the 18-hour train ride to Hefei, Roth had plenty of time to observe the frantic construction that he says is taking place all over China. He toured the Institute of Plasma Physics, which has two tokamaks in operation and one planned. The government has asked the Institute to begin tying its work to industrial applications, so officials were very interested in Roth's recommendations for branching out into industrial applications.

Roth also discussed the UT Knoxville Plasma Science Laboratory's work on plasma ion implantation as a way to improve the corrosion resistance of metals, and lectured on long-range energy issues, industrial plasma engineering, and the theory of plasma ion implantation.

In Chengdu, Roth visited the University of Electronic Science and Technology (UESTC). This university, like others Roth visited, showed signs of inadequate financial support—dirty buildings, overcrowded dormitories, and poorly paid faculty and staff. The only bright spot was the UESTC's state-of-the-art equipment, funded by World Bank loans.

In between a busy lecture schedule, he toured the antenna laboratory, the laser laboratory, and the materials science laboratories.

He was most impressed by the Microwave Measurements Laboratory, which occupied an entire floor of a building and contained top-of-the-line Hewlett Packard microwave test equipment worth more than $2 million. The staff are using the equipment to develop new microwave devices, Roth says.

Roth also asked for, and got, an extensive tour of the Guoguang Electron Tube Works. Some of the new applications for microwave power developed there include sterilizing and preserving foods and artificially aging wines and liquors.

The last stop was the Southwestern Institute of Physics in Leshan. Facilities there include the H-1 tokamak, the largest in China. Roth presented lectures on many topics, including the physics and engineering issues of tokamaks, and also showed slides of major tokamak experiments.

Roth left China with the impression that basic fusion research in China is in danger of falling by the wayside, since the Chinese government is pushing universities and research institutes to enter the industrial marketplace with products. If researchers are made to concentrate on plasma industrial engineering instead of, rather than in addition to, fusion research, the government may lose its capability to participate in the development of fusion energy.

Chinese Engineer First
Visiting Distinguished Professor

An internationally-known researcher from China is the first visiting Distinguished Professor at UT-Knoxville, Chancellor John Quinn has announced.

Dr. Shenggang Liu will spend one year conducting research and teaching for the Department of Electrical and Computer Engineering in the UT College of Engineering.

Liu, a specialist in microwave electronics, is on leave of absence from the China Institute of Electronic Science and Technology, where he serves as professor and president. The Institute, located in Southwest China 1,500 miles from Beijing, has about 8,000 students.

Liu also is a member of the Chinese Association of Science and Technology, the Permanent Committee of Chinese Electronics, the Chinese Institute for Electronics and the Ministry of the Electronic Industry of China.

"We are especially grateful that an international scholar of such eminence is willing to join our faculty in a visiting capacity," Quinn says. "We hope that his presence will help spark an exchange of knowledge between UT-Knoxville and the Institute of Electronic Science and Technology in China."

The title of Distinguished Professor is held by eight UT-Knoxville faculty members. Liu is the first visiting scholar to have the title.

Liu was at UT for two weeks in 1987 as a visiting lecturer. He has been a guest at several U.S. research universities, including the Massachusetts Institute of Technology and the University of California-Berkeley.

In addition to promoting student and faculty exchanges, Liu hopes to learn about the U.S. educational system, environmental policies and applications for microwave research while at UT.

"After a year here, we will be able to understand our common interests more deeply, and that will be a basis for finding common projects," Liu says. "When I return to China, I hope to show my colleagues things about this educational system that will help us make beneficial changes to our educational system."—*Mike Bradley*

FOR IMMEDIATE USE
Radar (360)
Feb. 21, 1991

KNOXVILLE, Tenn. -- A new radar evasion system developed at the University of Tennessee-Knoxville eventually may replace stealth technology now used to shield U.S. warplanes from radar, a UT electrical engineer said Thursday.

Dr. J. Reece Roth said the magnetized plasma cloaking system he invented has several advantages over stealth technology.

Magnetized plasma cloaking traps intensely heated, electrically charged gases -- known as plasmas -- in a magnetic field around the intended target, Roth said. He said the plasmas:

* Render radar ineffective by absorbing the radar signals.

* Shield the target from microwave energy weapons which can disable electronic systems or cause structural damage.

Current stealth technology offers little protection against microwave energy weapons, Roth said.

If used in military aircraft, magnetized plasma cloaking would be effective regardless of the aircraft's shape, Roth said. The shape of stealth planes inhibits radar detection but compromises maneuverability and performance, he said.

Roth's system absorbs such a wide band of radar frequencies that military personnel using it would not need to know the exact frequency of enemy radar, he said. Some conventional radar jamming devices are ineffective without incoming radar frequencies, he said.

Roth said magnetized plasma cloaking is ideal for spy satellites and space stations that orbit high above the Earth's atmosphere, where generation of plasmas around the aircraft is relatively simple to achieve.

But inside the Earth's atmosphere, neutral molecules would collide with electrically charged ions in the plasma, Roth said. Creating a magnetized plasma in the Earth's atmosphere by conventional methods would require too much onboard electrical power to be practical, he said. Roth is searching for a more feasible means of creating plasma within the atmosphere.

''It may be difficult to find a practical way to create a magnetic field in the Earth's atmosphere,'' Roth said. ''But with the cost of a single stealth bomber at about $600 million, I think we will be able to find a better, cheaper way to evade enemy radar through magnetized plasma cloaking.''

Roth's system, which was patented in January, is financed by the Air Force Office of Scientific Research.

FILED BY UT NEWS CENTER (615-974-2225)-MKB
###
==

UT-developed radar may replace stealth

A new radar evasion system developed at the University of Tennessee eventually may replace stealth technology now used to shield U.S. warplanes from radar, according to a UT electrical engineer.

Dr. J. Reece Roth said the magnetized plasma cloaking system he invented has several advantages over stealth technology.

Magnetized plasma cloaking traps intensely heated, electrically charged gases — known as plasmas — in a magnetic field around the intended target, Roth said. He said the plasmas:

■ Render radar ineffective by absorbing the radar signals.

■ Shield the target from microwave energy weapons which can disable electronic systems or cause structural damage.

Current stealth technology offers little protection against microwave energy weapons, Roth said.

If used in military aircraft, magnetized plasma cloaking would be effective regardless of the aircraft's shape, Roth said.

Roth's system absorbs such a wide band of radar frequencies that military personnel using it would not need to know the exact frequency of enemy radar, he said. Some conventional radar jamming devices are ineffective without incoming radar frequencies, he said.

Roth said magnetized plasma cloaking is ideal for spy satellites and space stations that orbit high above Earth's atmosphere, where generation of plasmas around the aircraft is relatively simple to achieve.

But inside Earth's atmosphere, neutral molecules would collide with electrically charged ions in the plasma, Roth said. Creating a magnetized plasma in Earth's atmosphere by conventional methods would require too much on-board electrical power to be practical, he said. Roth is searching for a more feasible means of creating plasma within the atmosphere.

"It may be difficult to find a practical way to create a magnetic field in the Earth's atmosphere," Roth said. "But with the cost of a single stealth bomber at about $600 million, I think we will be able to find a better, cheaper way to evade enemy radar through magnetized plasma cloaking."

Roth's system, which was patented in January, is financed by the Air Force Office of Scientific Research.

UT Radar Development May Replace Stealth Technology

BY MIKE BRADLEY

A new radar evasion system developed at UT-Knoxville eventually may replace stealth technology now used to shield U.S. warplanes from radar, a UT electrical engineer says.

Dr. J. Reece Roth says the magnetized plasma cloaking system he invented has several advantages over stealth technology.

Magnetized plasma cloaking traps intensely heated, electrically charged gases—known as plasmas—in a magnetic field around the intended target, Roth says. He says the plasmas:

•Render radar ineffective by absorbing the radar signals.

•Shield the target from microwave energy weapons which can disable electronic systems or cause structural damage.

Current stealth technology offers little protection against microwave energy weapons, Roth says.

If used in military aircraft, magnetized plasma cloaking would be effective regardless of the aircraft's shape, Roth says. The shape of stealth planes inhibits radar detection but compromises maneuverability and performance, he says.

Roth's system absorbs such a wide band of radar frequencies that military personnel using it would not need to know the exact frequency of enemy radar, he says. Some conventional radar jamming devices are ineffective without incoming radar frequencies, he says.

Roth says magnetized plasma cloaking is ideal for spy satellites and space stations that orbit high above the Earth's atmosphere, where generation of plasmas around the aircraft is relatively simple to achieve.

But inside the Earth's atmosphere, neutral molecules would collide with electrically charged ions in the plasma, Roth says. Creating a magnetized plasma in the Earth's atmosphere by conventional methods would require too much onboard electrical power to be practical, he says. Roth is searching for a more feasible means of

---

With the cost of a single stealth bomber at about $600 million, I think we will be able to find a better, cheaper way to evade enemy radar through magnetized plasma cloaking.

---

creating plasma within the atmosphere.

"It may be difficult to find a practical way to create a magnetic field in the Earth's atmosphere," Roth says, "But with the cost of a single stealth bomber at about $600 million, I think we will be able to find a better, cheaper way to evade enemy radar through magnetized plasma cloaking."

Roth's system, which was patented in January, is financed by the Air Force Office of Scientific Research.

Faculty and Departmental

N E W S

ELECTRICAL AND COMPUTER ENGINEERING
Joseph M. Googe
Head

Prof Patents New Stealth Technology

"I invented Star Trek's energy shield," *Dr. Reece Roth* tells his students. And the electrical and computer engineering professor has the patent to prove that he did, a patent issued Jan. 29, 1991, and assigned to the Air Force.

"You can take any spacecraft and, if you provide it with a dipolar magnetic field, it will act like the earth's magnetosphere and trap a plasma. It will protect you from directed-microwave energy weapons and hostile probing," he says. That's Star Trek stuff, all right.

A couple years ago, Roth was meeting with an advisory committee of the Air Force's Geophysical Laboratory. There, Dr. Robert Barker, a staffer with the AF's Office

of Scientific Research and Roth's program manager for the past eight years, originated the idea of using plasma as a cloaking device for aircraft and satellites.

It intrigued Roth, doubly so when he read one of his graduate student's dissertations and found in it data that, while not targeted at the cloaking concept, nonetheless supports it.

He made a proposal that everyone on the advisory committee thought so simple that surely someone else had long ago written it up in the professional journals. A colleague made a literature search but found nothing.

"This is an entirely new approach to the stealth problem, to making targets disappear from radar screens," Roth says.

Barker's office committed $80,000 a year to Roth and told him to proceed. Roth is convinced the technology will be a lot cheaper than the $600 million required to build a single copy of today's stealth bomber.

"What we're proposing—the math calculations prove it will work and our experiments in the plasma lab confirm it—is to absorb incoming radar signals as well as protect satellites from beams of intense radiation shot from directed-microwave energy weapons.

"Conventional stealth technology makes targets small either by using dielectric materials that permit radar signals to pass through them or by using designs that bounce signals away from the radar receiver. In current electronic warfare, they use active strategies to jam radar or give false signals to fool the enemy's receiver so it thinks the target is elsewhere.

"This method is passive. We surround the object with a plasma—the energy shield. Plasma is the fourth state of matter in which matter becomes electrically charged electrons and ions that can be trapped in magnetic fields. By putting a magnetic field around the target, we can rely on the fact that at a particular frequency, microwaves, and radar signals will be very strongly absorbed by the plasma

"And it doesn't take a very dense plasma. We've got a large absorption in our laboratory experiments."

The patent came through quickly—in less than 15 months—because the Patent Office found nothing in the patent literature like Roth's proposal. He didn't even have to go to Washington and argue for his proposal, an action that's standard procedure.

Mounir Laroussi (PhD/EE '88) got Roth's work going with his dissertation data. He returned to UTK last August and is now working on cloaking research with Roth.

"We've produced enough data to show this is an interesting approach. It absorbs a lot of energy and in fact can make a target disappear from a radar screen. The concept should work well in space. We're now working on a way to apply the concept to targets in the atmosphere—to airplanes."

ELECTRICAL AND COMPUTER ENGINEERING

Distinguished Professor Liu Visiting College

An internationally known researcher from China is the first visiting Distinguished Professor at the University of Tennessee, Knoxville.

Dr. Shenggang Liu will spend one year conducting research and teaching for the Department of Electrical and Computer Engineering in the College of Engineering.

Liu, a specialist in microwave electronics, is on leave of absence from the China Institute of Electronic Science and Technology where he serves as professor and president. The institute, located in Southwest China 1,500 miles from Beijing, has about 8,000 students.

The title of Distinguished Professor is held by eight UT, Knoxville faculty members. Liu is the first visiting scholar to have the title.

Liu was at UT for two weeks in 1987 as a visiting lecturer. He has been a guest at several U.S. research universities, including the Massachusetts Institute of Technology and the University of California-Berkeley.

In addition to promoting student and faculty exchanges, Liu hopes to learn about the U.S. educational system, environmental policies, and applications for microwave research during his visit.

*

From the UTK Engineering School's Alumni Newsletter, Fall, 1991

The Daily Beacon

Radar filter built from scrap

Campus-designed device funded by Air Force

By BRIAN WINFREY
Daily Beacon Government Editor

The UT Electrical Engineering Department has developed a new radar filter that will cut back on interference in radar systems.

"It filters out whatever frequency we select. Whenever you deal with small signals you have to deal with things like background noise and imaging," said Mounir Laroussi, research associate in electrical engineering, who developed the project.

"The Air Force funded us to develop a prototype. The results so far look very promising."

"Some of the filters you can buy off the shelf cost in the thousands of dollars," Laroussi said. "The prototype was built from scrap around the lab. I guess it cost around $20."

Radar works on a process of emitting microwaves that bounce off an intended target back to a receiving

> 'The prototype was built from scrap around the lab. I guess it cost around $20.'
>
> **Mounir Laroussi**

unit. The filter allows for clearer reception of microwaves by eliminating problems such as background noise.

UT Research Corp will apply for a patent next week. Laroussi said The patent will be in his name.

"We already have several companies who have expressed interest in the design. We're close to signing a confidentiality agreement with one company, so we can discuss specific

details," he said.

The filter uses plasma (superheated gas) in its construction.

"Plasma is the fourth state of matter," Laroussi said. "It's what you get when you heat a gas. Ninety-nine percent of the universe is composed of plasma in one form or another."

The idea for the filter was spun off from an earlier project funded by the Air Force, which involved making aircraft radar invisible.

Before we did the filter, we were working on a project called plasma cloaking," Laroussi said. "The idea was that by surrounding an object in plasma, you could make it disappear from a radar screen. You could also hide things such as satellites from detection. The Air Force was very satisfied with the results.

"That was a project which was very hot in the media during the Gulf War, as you can imagine," he said.

"The TV crews were here to do interviews, etc."

Research associate Mounir Laroussi's new radar filter attenuates signals by passing them through plasma energy, the fourth state of matter, which is contained within a vacuum by magnets.
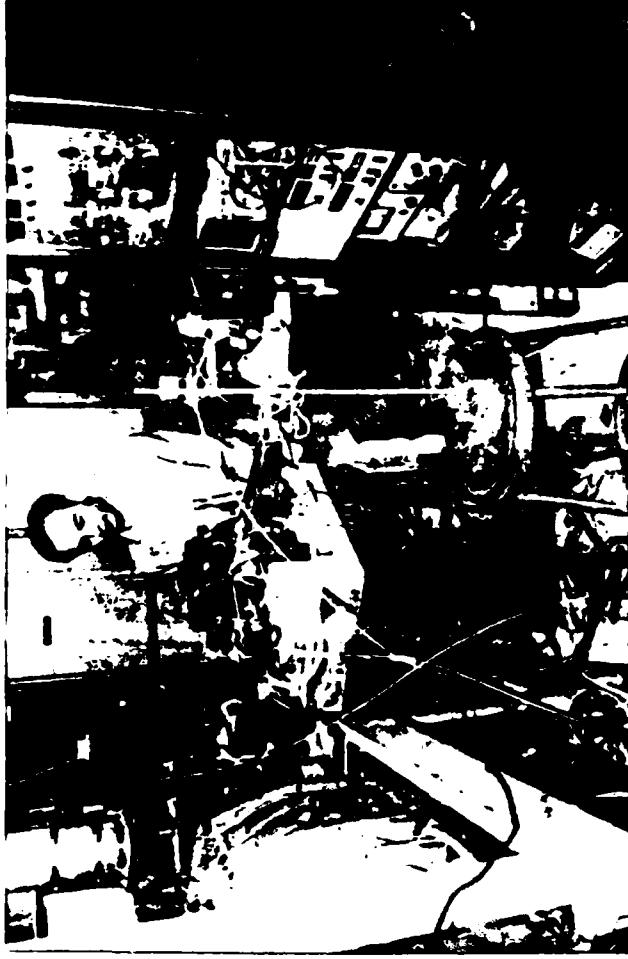
HEALTH & SCIENCE
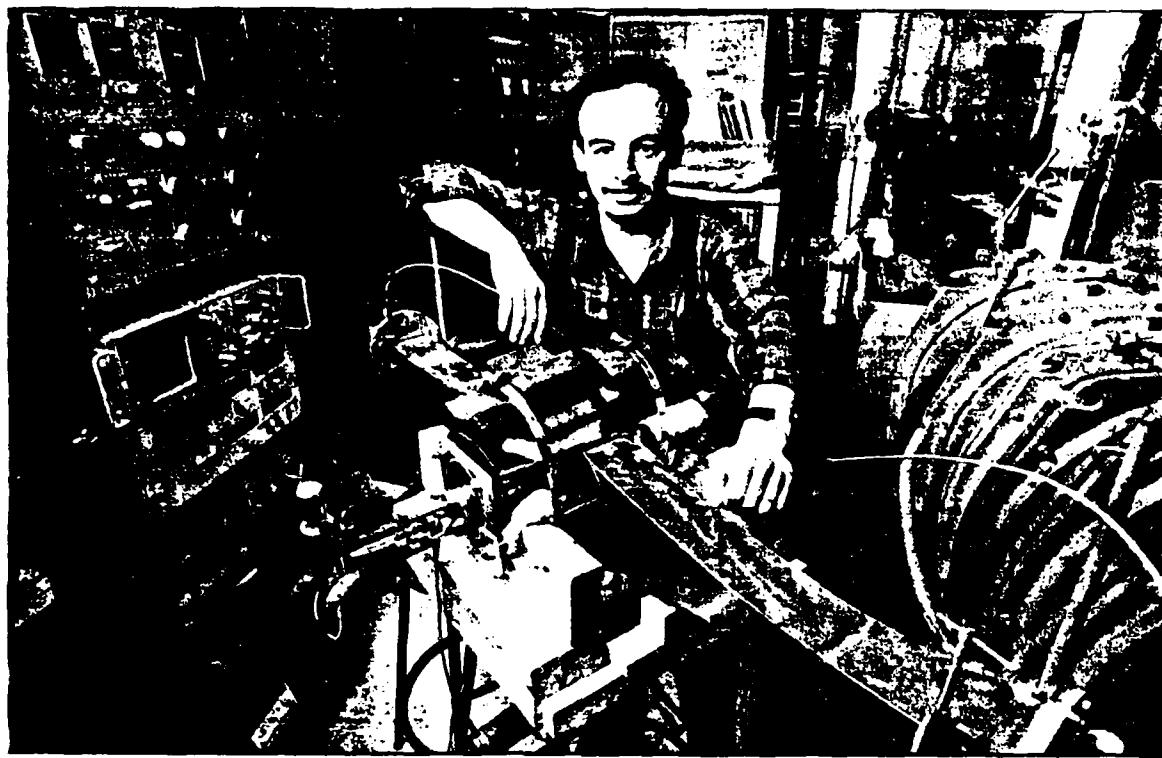
Dr. Mounir Larouss's tunable microwave filter is a "radar garbage collector" that clears radar screens

Radar Garbage Collector
UT professor invents tunable microwave filter

By Marti Davis
News-Sentinel staff writer

Using fast-custom into much different basement laboratories, a researcher assistant at the University of Tennessee has built a better way to give the university a measure of fame it probably seems likely to follow.

Dr. Mounir Laroussi, an electrical engineer, his invention a tunable microwave filter. The device is a kind of high-tech garbage collector that disposes of the invisible junk that clutters a radar screen with blips and bleeps.

Laroussi's invention came to mind while he was working with Professor Reece Roth on a radar-blocking system for the U.S. Air Force.

"I was driving around in the city one day and all of a sudden I thought if we can block radar we can probably also use the same method to make it cleaner."

He set to work in the basement of Ferris Hall, welding bits of copper sheeting into law-like shields that surround a seemingly empty glass beaker. On top of the glass beaker are a few scarred black magnets.

In truth, it doesn't look like much.

That's until you turn the lights out the lights. Then the device emits a bright fluorescent light — a sci-fi fantasy vision come true.

The light is actually extremely excited gas that is traveling in a spiral, shaped by the force of the magnets.

Microwave radar signals are transmitted through the copper laws. Any that are traveling at the same frequency as the spiral of excited gas are sucked into that path and destroyed.

The radar signals traveling at a different frequency than the air spiral passes through the device unsullied. The result is a clear, garbage-free image on the radar screen.

In the radar-blocking project shared by Roth and Laroussi, the same principle is being developed to conceal U.S. jets and satellites from detection by the enemy. Invisible signals of air tuned to the same frequency as enemy radar, will surround planes and satellites, soaking up signals and protecting them from detection.

The Air Force has issued patents and continues to fund the research of Roth and Laroussi.

"The Air Force is extremely excited about the project, but it's years from implementation," says Laroussi.

"Not so with the radar garbage collector. Its implementation appears imminent."

An Atlanta-based company that produces microwave signals has already signed a agreement with UT to discuss developing the device.

Meanwhile, the UT Research Corporation group set up to market the discoveries of UT scientists, is applying for a patent.

Laroussi is named as inventor. If the microwave filter is commercially successful, he will reap part of the profit.

Says Laroussi, "We will share the royalties."

TUTORIAL MINI COURSE

[text illegible]

Faculty and Departmental

NEWS

ELECTRICAL AND COMPUTER ENGINEERING
Joseph M. Googe
Head

Reece Roth in China

[text largely illegible]

... faculty and graduate students headed by

... Professor Xiazhong Li began translating Roth's 650-page textbook four years ago ...

... between Roth's textbook and China ...

... Tennessee when they worked over ...

Even before the Tsinghua linkage agreement was signed last year, Roth provided videotapes of his industrial plasma engineering courses, ECE 565-566, so Li could jump start an industrial plasma engineering graduate course at Tsinghua. Last September, a colleague of Li's, Professor Chuntong Ying, came to UTK and presented a seminar on China's isotope separation program.

Roth went back to China last July. He visited Tsinghua in Beijing, the Institute of Plasma Physics in Hefei, the University of Electronic Science and Technology of China in Chengdu, the Guoguang Electron Tube Works also in Chengdu, and Fudan University in Shanghai. Not only did Roth tour and consult, he delivered 20 lectures on various phases of industrial plasma engineering and fusion energy.

Cooperation between UTK and the University of Electronic Science and Technology of China dates back to 1985 when UESTC president, Professor Shenggang Liu visited UTK and the College of Engineering. Liu, also a member of the Chinese Academy of Sciences, returned for a week in 1987 and then for the full school year in 1990-91 as UTK's first Visiting Distinguished Professor. In 1991, Liu signed an agreement that created a formal linkage between his university and UTK.

ESM professor, Dr. Igor Alexeff made reciprocal visits to UESTC in the summers of 1988 and 1991; Roth in July of 1989 and 1992.

China sent Chaoyu Liu to UTK for doctoral studies in the electrical and computer engineering department, and visiting Professor Shan-Fu Yu just completed six months of research in microwave-generated plasmas at UTK's Plasma Science Laboratory.

UESTC furnished $3,000 worth of microwave equipment to UTK's plasma lab which Yu used to isolate the microwave power supply from the plasma-filled vacuum tank he could simplify the tuning and improve the stability of the system.

As another consequence of linkage, a translation team headed by Professor Shenggang Liu began translating a two-volume textbook on industrial plasma engineering Roth is now writing. The Chinese and English editions should be published by the end of this year.

Liu has asked the Chinese National Science Foundation to fund a broad-scale, five-year effort in industrial plasma engineering. If the foundation comes through, UTK-UESTC linkage activities and exchanges will expand, Roth says.

Liu has asked Roth to return to China in 1994 to lecture again in an industrial plasma engineering summer school.

Liu surprised Roth when he was preparing to go to China last summer. He informed Roth that he, Roth, had been awarded the title of Honorary Professor by the UESTC faculty and administration, an action that had been approved by the Chinese Ministry of Education.

"I felt a little strange about being an honorary professor at a university whose working language I could not speak," Roth says, "but it was pointed out to me that I was shortly to be the author of a Chinese textbook I could not read!"

Liu conferred the title on July 10, the first day of the summer school at which Roth was to deliver a series of lectures. For his lecture on that opening day, Roth spoke about the historical and cultural roots of Western science and technology.

"I thought a discussion of the Western academic tradition might be of interest to an audience most of whom had never been outside of China and were about as far away physically from Western institutions as it is possible to get. This lecture seemed to be well received."

Seventy people, including Tsinghua's administrators, the current and a former president of the university, and two members of the Chinese Academy of Sciences, attended the lecture and the award ceremony.

THE DAILY BEACON

UNIVERSITY & WORLD

UT researcher gets recognition

STEPHANIE PORTER
Daily Beacon Staff

Mounir Laroussi, a research associate in the Plasma Science Lab, was recently named to Who's Who in America in Science and Engineering for his studies of plasma and his invention of a microwave filter.

"I was surprised by the selection. I felt I needed to get a little older and do more things, but somehow, they selected me," Laroussi said.

"The universe in which we live is 99 percent plasma. To study plasma is like to study the universe. It is a very important subject," he said.

Laroussi has worked on many different studies, but the project that brought him the most recognition was his invention of a microwave filter which is used in communications, radar and other systems.

"The project that I think probably made anyone list me in there (Who's Who in America) is my invention of a microwave filter that makes scattering of waves more simple and neater. It's like having a TV set and making the picture clearer. It takes out all the garbage," Laroussi said.

Laroussi did an earlier study with Professor Reece Roth on the interaction of waves with plasma in general. The interaction with electromagnetic waves with plasma is very important because when we communicate over the horizon we always rely on the waves being reflected from the ionosphere which is a layer filled with plasma, he said.

This interaction is very important in communication systems and radar systems, Laroussi said.

"Out of that study, I had an idea and used what I learned to design a microwave filter that worked with the same principal. The idea, the invention and the prototype were all done here at UT. I guess this invention is my claim to fame."

Besides being named to Who's Who in America, Laroussi was also named an assistant editor of international journal "Physics Essays."

"I was lucky this year. I have had many things happen to me. They put me in Who's Who and I became an assistant editor of an international journal," Laroussi said.

The editoral board of this journal has many recognized people. There are two or three Nobel prize winners on the editoral board.

Laroussi is currently working with Professor Roth on a method to harden metals and improve their corrosion resistance. He is trying to make a theory to explain what is happening during the experiment.

Laroussi is originally from Tunisia. He earned his doctoral degree in electrical engineering at UT in June 1988.

APPENDIX E

ABSTRACTS OF TWO MASTERS THESES AND
ONE PH.D. DISSERTATION COMPLETED
UNDER AFOSR SPONSORSHIP

INVESTIGATION OF THE NONLINEAR BEHAVIOR
OF A WEAKLY-IONIZED PLASMA

A Thesis

Presented for the

Master of Science

Degree

The University of Tennessee, Knoxville

Scott Allen Stafford

May 1989

ACKNOWLEDGMENTS

The author wishes to express his sincere appreciation to Dr. J. R. Roth for his patience, financial support, and helpful advice throughout the course of this research.

The author also extends his gratitude to the remaining members of his committee, Dr. Mark Kot and Dr. Igor Alexeff. Dr. Kot's input was especially helpful in gaining a better understanding of the mathematics involved.

A special thanks is also extended to Roberta L. Campbell and Jenny Daniel for their help with the typing and figure preparation of this thesis.

Finally, the author wishes to express his appreciation to his family and friends for their support and encouragement throughout his academic career.

ABSTRACT

The nonlinear behavior of plasmas has been studied by conventional time series methods for many years. Since the advent of the concept of chaotic dynamics in the early 1960's, many new theoretical approaches to turbulence have been developed. In the past ten years these methods have been applied to plasma fluctuations. In the last two or three years, commercial computer software has become available which allows the ready application of a wide range of analytical methods from nonlinear dynamics to laboratory plasmas. Most applications thus far have been to pulsed or unmagnetized plasmas. This report will describe the application of chaos theory to a steady-state, magnetized plasma.

TABLE OF CONTENTS

CHAPTER I

INTRODUCTION

In the past twenty-five years, research in nonlinear dynamics has flourished. In particular, new concepts have been developed to quantify chaotic behavior. Many of these concepts had their origin in the work of Edward Lorenz, a meteorologist interested in the behavior of a simplified set of equations which model convection in the atmosphere (Lorenz, 1963). Since then these concepts have been applied to fluid flow (Brandstater et al., 1983), chemical reactions (Simoyi et al., 1982), the spreading of diseases (Schaffer, 1985), and biological rhythms (Glass, 1983).

The purpose of this thesis research is to apply the various tools of nonlinear dynamics to potential fluctuations measured in a steady-state, magnetized plasma. The plasmas generated in the UTK Plasma Science Laboratory do not allow us to examine a well-defined transition from coherence to turbulence. Therefore, this leaves two main goals: to look for evidence of low-dimensional chaos; and to look for a trend, or lack of trend, in the parameters which describe the state of turbulence. Chaos-related concepts which were used in this study are reconstructed phase portraits, Poincare sections, correlation dimensions and Lyapunov exponents.

This report will consist of eleven chapters, including this one. Chapter II is a general overview of chaotic dynamics. Chapters III and IV are an introduction to the fundamental mathematical concepts of chaotic dynamics for those readers new to this topic. In Chapter V a brief discussion of the effects of noise is given. Chapter VI is for those readers wanting to learn more about previous applications of nonlinear dynamics to plasmas. In Chapter VII

the experimental apparatus and data handling system are described. Chapter VIII gives a brief description of the software package that was used to study the nonlinear behavior of the plasma fluctuations. Chapter IX consists of a comparison of two known reference cases to a particularly interesting set of plasma data. Chapter X is comprised of the results of parametric variation on the state of turbulence. Finally, conclusions and suggestions for future work are discussed in Chapter XI.

PLASMA HEATING
BY COLLISIONAL MAGNETIC PUMPING
IN A MODIFIED PENNING DISCHARGE

A Thesis
Presented for the
Master of Science
Degree
The University of Tennessee, Knoxville

Min Wu
August 1989

ABSTRACT

Collisional magnetic pumping as a plasma heating method in a modified Penning discharge set up as a magnetic mirror configuration was experimentally investigated. The heating rate as a function of rf driving circuit frequency, rf maximum exciter coil current, Penning discharge current, and background steady-state confining magnetic field was experimentally verified according to the heating rate equation. The Penning discharge electrode and magnetic field arrangement resulted in the formation of two electron populations in a helium plasma. It was found that the primary electrons were heated more than the secondary electrons. More importantly, it was found that these four parameters had a functional dependence consistent with the heating rate equation in most cases, although the magnitude of the heating was as much as 100 times more than theoretically predicted.

ACKNOWLEDGEMENTS

The author wishes to express his sincere appreciation to his major professor, Dr. J. Reece Roth, for his encouragement, patience, good advice, and continuous help throughout the course of this research.

Special thanks go to Dr. Igor Alexeff and Dr. Marshall O. Pace, the members of his committee, for review of this thesis.

Appreciation is also extended to my good friend and co-worker, Philip F. Keebler, for typing some of this very early manuscript with infinite patience.

Special appreciation is also extended to the University of Tennessee Plasma Science Laboratory and supporting staff, Dr. J. Reece Roth, Dr. Igor Alexeff, Fred Dyer, Mark Rader, and Philip F. Keebler. I would also like to express my appreciation to the Department of Electrical and Computer Engineering, especially Jenny L. Daniel for figure preparation.

The author wishes to recognize the financial support given by the Air Force Office of Scientific Research, especially Dr. Robert J. Barker, Program Manager, under contracts AFOSR-86-0100 and AFOSR-89-0319 which have made my graduate studies and research possible.

Finally, the author would like to express his deepest appreciation and gratitude to his parents for their constant support, patience, understanding, and encouragement throughout his graduate education.

TABLE OF CONTENTS

CHAPTER I

INTRODUCTION

In fusion reactors, it is necessary to heat a magnetically-contained plasma (ionized gas) to a kinetic temperature high enough so that the plasma ions are sufficiently hot to overcome the Coulomb barrier and fuse. In addition, the plasma must be dense enough, and the containment time long enough so that a net power output is achieved. The amount of power produced by a plasma is proportional to the number of fusion reactions that can occur in a given time. Thus, if more reactions are forced to occur by sufficiently heating the plasma, more net power can be produced. The concepts, understanding, and technique of plasma heating can be extended to applications to high power lasers, military weapons, aerospace power and propulsion systems, and industrial applications of plasma.

Only a limited number of plasma heating methods are available, and so alternate methods are of interest. Because the different plasma particle species give rise to a limited number of different characteristic resonance frequencies, many options are available for heating a plasma. Heating methods recently adopted by the international fusion research community are ohmic heating by binary Coulomb collisions and Spitzer resistivity; neutral beam injection heating; and radio frequency heating, including ion cyclotron resonant heating, electron cyclotron resonant heating, lower hybrid heating, and collisional magnetic pumping (Roth, 1986), which is the subject of interest in this thesis.

The goal of supplementing the plasma heating of fusion reactors by magnetic pumping is to deliver radio frequency power at high efficiencies to the plasma interior.

The "magnetic pumping" plasma heating concept orginated with Spitzer in 1953 (Spitzer et al., 1953), to heat a plasma confined in a Stellarator magnetic containment device. About five years later, Berger (Berger et al., 1958) carried out the theoretical analysis necessary to show that a confined plasma could be efficiently heated by oscillating electromagnetic fields. Until recently, the literature on this subject was limited owing to the fact that it was initially a classified project, and the low heating rates possible with the mechanism initially proposed.

In previous work carried out by Laroussi in 1988, it was shown both theoretically, computationally, and experimentally that plasma heating was possible by first-order collisional magnetic pumping. In that research, magnetic pumping was applied to a straight, cylindrical plasma, confined by an axially uniform steady-state magnetic field, B_o. The magnetic perturbation is achieved by wrapping an exciter coil of length, l, inductance, L, and number of turns, N, around a cylindrical section of plasma and perturbing the confining magnetic field given by

$$B = B_o(1 + \delta f(t))$$,

where B_o is the uniform steady state background magnetic field, and δ is the magnetic field modulation factor defined by

2

$$\delta = \frac{\Delta B}{B_o}$$

which is much less than unity, and f(t) is a periodic function of time for the current which is applied to the exciter coil. Figure I.1 on the following page depicts how the exciter coil is wrapped around the cylindrical plasma containment vessel and then driven by the periodic current waveform, f(t). Laroussi showed experimentally that a sawtooth-shaped function produced an energy increase rate that is directly proportional to the magnetic field modulation factor δ, compared to a sinusoidal function, f(t), which produced an energy increase rate that is directly proportional to the square of this factor. The factor δ is less than unity and when squared, becomes a small number. Thus the potential improvement in the heating rate is evident. Throughout the present research, this function, f(t), is a periodic sawtooth-shaped waveform.

In magnetic pumping, the oscillating electric field is produced by variation of the axial magnetic field and is thus perpendicular to it. This type of heating was called "magnetic pumping" due to the existence of a compressional wave propagating perpendicular to the background magnetic field, causing the plasma to be cylically compressed and relaxed by an alternating E x B force. The compression and relaxation phases are illustrated below in Figure I.2.

Raising the temperature of a potentially unstable plasma requires that energy inputs occur on a time scale less than the particle confinement time, while energy inefficiency is held to a minimum. Consequently, the heating rate and energy confinement time are fundamental parameters to be considered in establishing bulk plasma heating requirements. The heating

3
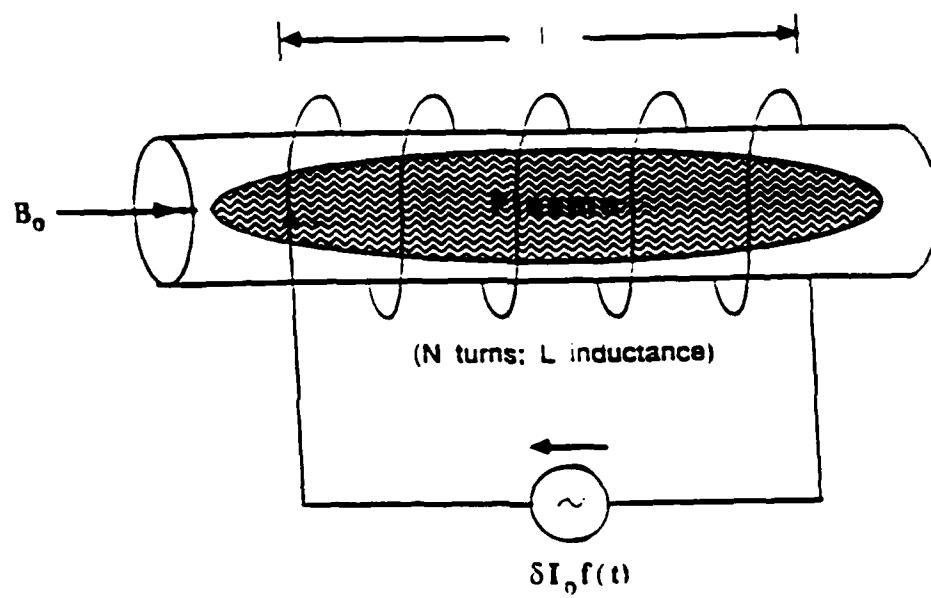
Figure I.1: Exciter coil arrangement around a cylindrical plasma.

4
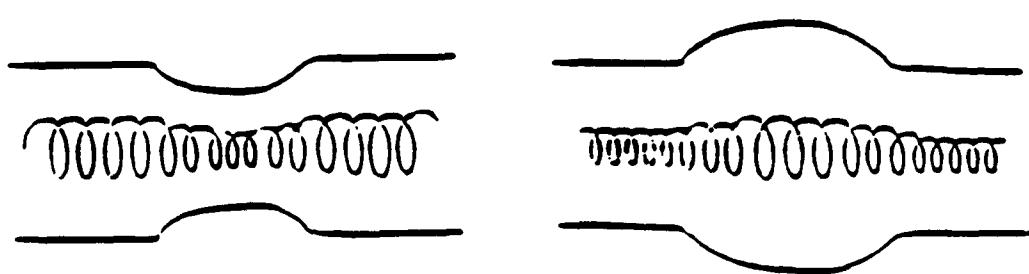
Figure I.2: Plasma compression phase on left during positive half cycle of f(t); plasma relaxation phase on right during negative half cycle of f(t).

rate is limited by the technological limitations of the heating system, which includes the external circuitry generating the periodic current waveform, $f(t)$. The energy confinement time can be enhanced by energy deposition deep within the plasma. The functional dependence of the heating rate on such parameters as the Penning discharge anode current, the maximum exciter coil driving current, the frequency of the current in the exciter coil, and the background steady-state confining magnetic field are experimentally investigated and are compared to the equation describing the relative energy change of the particles.

6

A STUDY OF THE EFFECTIVE ELECTRON COLLISION FREQUENCY IN A WEAKLY IONIZED TURBULENT PENNING DISCHARGE PLASMA

A Dissertation

Presented for the

Doctor of Philosophy

Degree

The University of Tennessee. Knoxville

PAUL D. SPENCE

AUGUST 1990

E-19

ACKNOWLEDGEMENT

ABSTRACT

The effective electron collision frequency is studied on a weakly ionized, turbulent Penning discharge plasma. The magnetized plasma of this discharge is radially inhomogeneous and subject to a high level of low frequency electrostatic fluctuations due to drift wave turbulence. An effective electron collision frequency is determined from collision broadened absorption spectra of the extraordinary mode wave near the electron gyro frequency resonance. When the level of electrostatic turbulence is excited above the level of thermal fluctuations, the collision frequency is significantly greater than the electron-neutral collision frequency. The scaling of this collision frequency as a function of the absolute rms level of electrostatic fluctuations is investigated.

TABLE OF CONTENTS